An investigation into Cocaine and amphetamine regulated transcript (CART) peptide in the rat cerebellum

by

Daniel A. Press

A thesis submitted for the degree of Doctor of Philosophy

University of Warwick, Department of Biological Sciences

September 2007

Contents:

Chapter 1: Introduction

Chapter 2: Materials and Methods.

Chapter 3: Distribution of CART peptide in the Cerebellum.

Chapter 4: Electrophysiological Measurement of CART peptide actions in the vestibular cerebellum.

Chapter 5: Determination of Purkinje cell firing patterns

Tables:

Figures:

Acknowledgements:

I would like to thank my supervisor, Dr. Mark Wall, for his support, perseverance and guidance. I would like to thank my PhD committee members for their input and guidance, Prof. Nicholas Dale, Prof. Dave Spanswick, Dr. Paul Squires and Prof. John Davie. Thanks to all the members of the Neuroscience group at the University of Warwick that have helped me over the years and a special thanks to Dr. Rachid Id Bihi for keeping me sane through writing up this thesis. I would like to thank the BBSRC for my funding.

I would like to thank the menagerie of characters from Leamington Spa that have provided moral support over the years and would like to thank İnci and my family for always believing in me.

Declaration:

I, Daniel A Press, hereby declare that all the work reported in this thesis is my own unless stated otherwise in the text or figure legends. None of this work has been previously submitted for any degree at this or any other institution. All sources of information used in the preparation of this thesis are indicated by references. Parts of chapter 3 and 4 have been published in poster form (**British Neurosci. Assoc. Abstr., Vol 19, P72, 2007**).

Abstract:

Cocaine and Amphetamine Regulated Transcript (CART) peptide is a putative neuropeptide, which has been implicated in a variety of physiological processes including feeding, reward and reinforcement and locomotion. However, CART peptide receptors have not yet been identified and CART peptide's mechanism of action still remains unclear.

Using immunohistochemistry, I have confirmed the presence of CART peptide in fibres in the vestibular cerebellum (lobes IX and X and the paraflocculus) and have shown that the CART peptide has a banded distribution. Co-localisation with Vesicle Glutamate Transporter 2 (vGluT2) demonstrated CART peptide expression at climbing fibre-Purkinje cell synapses. Thus CART peptide may act as a neurotransmitter.

Application of CART peptide (fragment amino acids 55-102), significantly increased the firing rate of vestibular Purkinje cells, an effect that persisted when synaptic inputs were blocked. CART peptide appeared to directly depolarise the membrane potential of Purkinje cells, and this may underlie the observed increase in firing rate. CART peptide did not modulate excitatory or inhibitory inputs onto Purkinje cells, and did not appear to have a role in synaptic plasticity.

I have investigated what controls the firing rate and pattern of firing of Purkinje cells *in vitro*. The major factor is the activity of inhibitory interneurones whereas excitatory inputs have little effect. I have identified 7 different firing patterns and have shown that blocking synaptic inhibition not only changes the firing rate, but also the firing pattern. I have also demonstrated that the AMPA receptor antagonist, 6-cyano-7-nitroquinoxaline-2,3-dione (CNQX) has a direct excitatory effect on Purkinje cells, increasing the firing rate and depolarising the membrane potential.

Abbreviations:

aa – Amino acid

Ach – Acetylcholine

ACTH – Adrenocorticotrophic hormone

aCSF – Artificial cerebrospinal fluid

AHP – Afterhyperpolarisation

AMPAR – Alpha-amino-3-hydroxy-5-methyl-4-isoxazolepropionic acid receptor

ANS – Antonomic nervous system

Arc – Accurate nucleus

Arg - Arginine

ATP – Adenosine 5'-triphosphate

cAMP – cylic adenosine monophosphate

CART – Cocaine and amphetamine regulated transcript

ChAT – Choline acetyltransferase

CNS – Central nervous system

CNQX - 6-cyano-7-nitroquinoxaline-2,3-dione

CRE – cAMP responsive element

CREB - cAMP responsive element-binding

p-CREB - cAMP responsive element-binding, phosphorylated

CRF/CRH - Corticotrophin releasing factor/hormone

Cys - Cysteine

DCN – Deep cerebellar nuclei

DS – Dorsal striatum

DSE – Depolarization-induced suppression of excitation

DSI – Depolarization-induced suppression of inhibition

EC_{50} – Half maximal effective concentration

EPSC – Excitatory postsynaptic current

EPSP – Excitatory postsynaptic potential

ERK/MAPK – Extracellular signal-regulated kinase/mitogen-activated protein kinase

GABA – Gamma-aminobutyric acid

GIRK – G-protein coupled inward rectifier

GPCR – G-protein coupled receptors

GHRH – Growth hormone releasing hormone

HPA - Hypothalamic-pituitary-adrenal (axis)

I_h – Hyperpolarisation activated current

IPSC – Inhibitory postsynaptic current

IPSP – Inhibitory postsynaptic potential

LDCV – Large dense core vesicles

Leu - Leucine

LTD – Long term depression

LTP – Long term potentiation

Lys - Lysine

MEK - MAPK/ERK kinase

mGluR - Metabotropic glutamate receptors

mRNA – Messenger ribonucleic acid

MAO – Medial accessory olive

α-MSH – α-melanocyte-stimulating hormone

NO – Nitric oxide

NPY - Neuropeptide Y

PC1/3 – Prohormone convertase 1/3

PC2 – Prohormone convertase 2

Pef/LH – Lateral hypothalamus perifornical area

PKA – Protein kinase A

PNS – Peripheral nervous system

POMC – Pro-opiomelancortin

PVDF – Polyvinylidene fluoride

SDHB – Mitochondrial succinate dehydrogenase, subunit B

SNc – Substantia nigra pars compacta

SNr – Substantia nigra pars recticula

SPN – Sympathetic preganglionic neurones

SSV – Small synaptic vesicles

TTX - Tetrodotoxin

VGluT2 – Vesicular glutamate transporter 2

VTA – Ventral tegmental area

Chapter 1: Introduction

1.1 – Neuropeptides

Cocaine and amphetamine regulated transcript (CART) peptide is a putative neuropeptide. Neuropeptides can be defined as "peptides that have direct synaptic effects or indirect modulatory effects on the nervous system" (http://www.biology-online.org/dictionary.asp, 17/09/07). Many neuropeptides were originally identified in non-neural tissue such as the gut and then later discovered in the brain. They vary in size from 2 amino acids up to around 50 (above 50 they are often classified as proteins). Neuropeptides represent the largest group of neurotransmitter molecules but differ in a number of significant ways from classical or fast neurotransmitters (Mains and Eipper, 2006).

Neuropeptides can be classified either on the area of the brain where they are expressed (hypothalamic releasing factors: CRH (corticotropin releasing hormone), GHRH (growth hormone releasing hormone) and somatostatin) or on structural similarities (Opiate peptides: β-endorphin, Leu-enkephalin, Met-enkephalin). However, structurally similar neuropeptides can have very different functions, for example the 9 amino acid peptides vasopressin and oxytocin are only different at 2 positions, but their functions in the body are very different. For example, in the amygdala, both vasopressin and oxytocin have an excitatory effect on the neurones they innervate, however vasopressin increases the fear response whereas oxytocin reduces the fear response (Debiec, 2005).

An important difference between classical neurotransmitters and neuropeptides is their synthesis and processing. For example, the neurotransmitter acetylcholine (ACh)

is synthesised at the nerve terminal by the enzyme choline acetyltransferance (ChAT) and after release the ACh is broken down to choline and acetic acid, the choline being transported back into the cell to be used again to synthesise more ACh (Bear et al., 2007). In contrast, neuropeptides are initially synthesised as a large preprohormone (100-250 residues) by ribosomes in the cell body. This preprohormone contains a signal sequence which facilitates trafficking to the Golgi apparatus/endoplasmic reticulum (Figure 1.1). The preprohormone is then cleaved to form a smaller prohormone in the Golgi apparatus and the active neuropeptides are produced by the action of a prohormone convertase, packaged into vesicles and transported to the nerve terminals by axonal transport (Seidah and Chrétien, 1999).

A single prohormone can give raise to multiple copies of the same neuropeptide, as with FMRFamide precursors (Li et al., 1999) or multiple different neuropeptides, as with pro-opiomelancortin (POMC) (Zhou et al., 1999a). In cases where multiple neuropeptides can be generated from a single prohormone then it is the different prohormone convertases that give rise to the different neuropeptides. For example the action of prohormone convertase 1 on POMC gives adrenocorticotropic hormone (ACTH) and β-endorphin but further action of prohormone convertase 2 converts ACTH into the neuropeptide α-melanocyte-stimulating hormone (α-MSH). Diversity of members of a neuropeptide family can also be increased by gene splicing.

Neuropeptides are packed into large dense core vesicles (LDCV). The concentration of neurotransmitter inside these vesicles is generally lower than found in the small synaptic vesicles containing classical neurotransmitters (3-10 mM compared to 100-500 mM). In many neurones both LDCV and vesicles containing classical neurotransmitters are in the same terminals; however LDCV are usually at a lower density and located further from the synaptic cleft. Thus many neurones signal by the

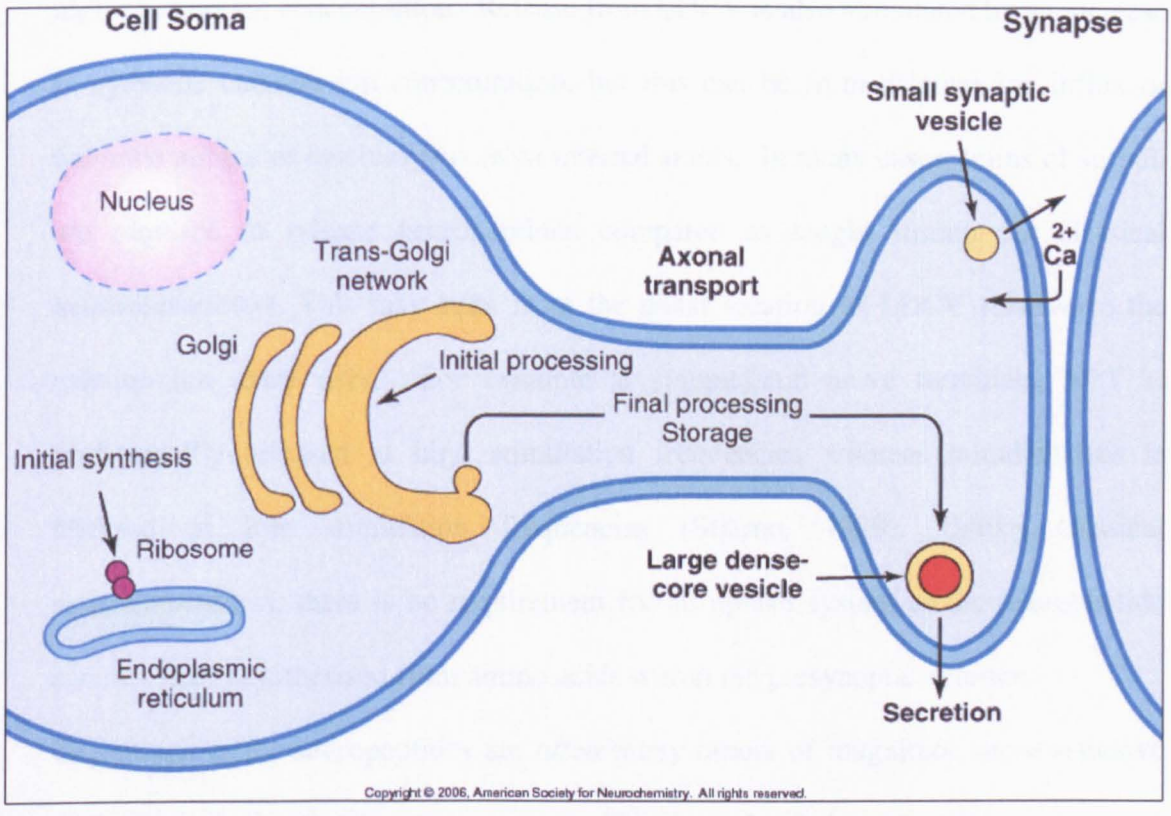

Figure 1.1 – The intracellular pathway for synthesis, storage and secretion of neuropeptides. Neuropetide precursors are synthesised in ribosome on the endoplasmic reticulum, transported to the Golgi apparatus where they are processed before being packed into large dense core vesicle and transported to synapses. Taken from Siegal, G. J., R. W. Albers, S. T. Brady and D. L. Price (2006). Basic Neurochemistry: Molecular, Cellular and Medical Aspects, Elsevier Acemdemic Press.

co-transmission of a fast classical neurotransmitter and a neuropeptide. The release of neuropeptides from LDCV is different from neurotransmitter release from small synaptic vesicles (SSV). Release from SSV is stimulated by a transient increase in calcium ion concentration in the pre-synaptic density; release is local and requires a high calcium ion concentration. Release from LDCV is also stimulated by an increase in cytosolic calcium ion concentration, but this can be from calcium ion influx or from the release of calcium ions from internal stores. In many cases, trains of stimuli are required to release neuropeptides compared to single stimuli for classical neurotransmitters. This may stem from the distal location of LDCV relative to the calcium ion entry sites. For example at sympathetic nerve terminals, NPY is preferentially released at high stimulation frequencies whereas noradrenaline is released at low stimulation frequencies (Stjärne, 1989). Unlike classical neurotransmitters, there is no requirement for an uptake system as the neuropeptide can be readily synthesised from amino acids within the presynaptic neurone.

The receptors for neuropeptides are often many orders of magnitude more sensitive than classical neurotransmitter receptors. This is probably because the concentration of peptide released is often much less than that for classical neurotransmitters. The receptors for neuropeptides are most commonly G-protein coupled receptors (Hille, 2001) with no evidence for neuropeptides directly activating ligand gated ion channels. G-protein coupled receptors (GPCR) can have a large number of post-synaptic effects, and these are determined by the G-protein to which they are coupled. G-proteins can exert an effect by directly modulating ion channels, either by opening them directly, as with GIRK the potassium ion channel (Yi et al., 2001) or by changing the probability of opening, as with L-type calcium channels (Dolphin, 2003). G-proteins also influence the levels of secondary messengers; this can then affect ion

channels directly, for example activation of I_h current by cAMP (DiFrancesco and Tortora, 1991) or activation of a signal cascade which can result in the phosphorylation/dephosphorylation of ion channels, altering their gating properties. In addition signal cascades, initiated by activation of G-proteins, can result in changes to receptor density either via phosphorylation or changes in gene expression. In general, the effects of neuropeptides are often much longer lasting than the action of classical neurotransmitters.

1.2 – Cocaine and amphetamine regulated transcript

Cocaine and amphetamine regulated transcript (CART) was first identified by Douglass *et. al.* (1995) as an mRNA upregulated in the striatum after application of the psychostimulants, amphetamine and cocaine. Using the method of PCR differential display (Liang and Pardee, 1992) a transcript was identified which was upregulated in the striatum, present but not regulated by psychostimulants in the hippocampus and absent from the cerebellum (Douglass et al., 1995). Northern blots revealed that there were in fact two transcripts, approximately 700 and 900 base pairs long. The gene sequence was determined (ascension number U10071, Genebank); the CART gene contains 2 introns and 3 exons, and was predicted to code for an 116 or 129 amino acid (aa) long peptide (Douglass et al., 1995). The peptide sequence shows no sequence similarity to any known peptides, however it did show sequence homology to an acid extract peptide fragment from ovine hypothalamus (Spiess et al., 1981). Further to this work the human CART gene (ascension number U20325, Genebank) was identified (Douglass and Daoud, 1996) and showed to have

approximately 80 % sequence identity and 92 % sequence similarity in the protein coding region. The human CART gene maps to chromosome 5q13-14, a region which has been previously associated with obesity and energy homeostasis in humans (Dominguez, 2006). To date, CART type genes have been identified in at least 12 different species (human, monkey, chimp, cow, pig, mouse, rat, chicken, frog, puffer fish, zebra fish and goldfish) and the protein coding region of these genes appears tightly conserved. Interestingly no homologous genes have been identified in invertebrates.

Analysis of the upstream region of the CART gene in mouse identified a number of binding motifs (Dominguez et al., 2002), including TATA box, STAT, cAMP responsive element (CRE), AP1, SP1, AP2, E-box and Pit-1 sites. Of these sites two have received attention. CART peptide levels show diurnal variation in blood and in brain (hypothalamus, nucleus accumbens, amygdala and midbrain) and this maybe via the E-box and a circadian transcription factor (Vicentic, 2006). It has also been shown that p-CREB binds to the CRE binding site upstream of the CART gene (Lakatos et al., 2002) and increases CART peptide levels in GH3 and CATH cells (Domingez and Kuhar, 2004). It has been shown *in vivo* that CART expression in the nucleus accumbens is regulated by the cAMP/PKA/CREB pathway (Jones and Kuhar, 2005).

The CART gene codes for a 129 or 116 aa long peptide (rat long below):

MESSRLRLLPVLGAALLLLLPLLGAGAQEDAELQPRALDIYSAVDDASHEKE
LPRRQLRAPGAVLQIEALQEVLKKLKSKRIPIYEKKYGQVPMCDAGEQCAVR
KGARIGKLCDCPRGTSCNSFLLKCL

The first 27 aa (in red) are a signal sequence that aids trafficking and peptide secretion and are removed to give the proCART peptide. In rat, both the long (including the aa shown in green) and short form are expressed, however in human only the short form is found. There are 6 cysteine resides and these form 3 disulphide bridges: CysI(55)-CysIII(73), CysII(61)-CysV(81) and CysIV(75)-CysVI(88). There are a number of pairs of basic residues (putative sites for the action of prohormone convertases) on the CART peptide, however only 3 of these lie before the first cysteine residue: Lys(48)Lys(49), Lys(53)Arg(54) and Lys(60)Lys(61). The peptide fragments that have been observed will be addressed in the next section.

1.3 – CART peptides

1.3.1 – What CART peptide fragments are present in the brain and where are they expressed?

In situ hybridisation studies revealed that CART mRNA is expressed all over the mammalian central nervous system (CNS) (Couceyro et al., 1997) and peripheral nervous system (PNS) (Ekblad, 2006; Wierup and Sundler, 2006), including: the hypothalamus, striatum, retina, spinal cord, pituitary, medulla, adrenal gland, gut and pancreas. Although CART mRNA is widely expressed, it is not ubiquitous.

There are very few studies that look at the ontogeny of CART. As early as prenatal day 11 (E11) CART positive cells have been observed from the mesencephalon to the ventral brainstem and by E13 cells in the diencephalon are observed (Risold et al., 2006). CART positive cells are not observed in the telencephalon until the late stages

of gestation (E18) and continues after birth reaching a maximum between 5 and 8 days postnatal (P5-8) and decrease after that reaching the low adult expression level by P22 (Dun et al., 2001). The only PNS area where developmental changes in CART peptide have been explored is the pancreas. It would seem plausible that CART peptide fragments may have roles in neurogenesis or synaptagenesis but as of yet there is no experimental evidence to support this.

In the hypothalamus, CART mRNA expression is regulated by leptin (a feeding factor which inhibits feeding) and injection of a recombinant CART peptide fragment (corresponding to the amino acids residues 55-102 of the long CART peptide) into rat brain results in a decrease in feeding (Kristensen et al., 1998). In addition, an antibody against the CART peptide 55-102 fragment, when injected into the rat brain, increases feeding. These three observations led to the proposition that CART peptide is anorectic and provided the first test of CART peptide function: the inhibition of feeding. The CART peptide fragment 55-102 was isolated from yeast expression (Thim et al., 1998) and the presence of 3 disulphide bridges confirmed. Disruption of the disulphide bridges results in the loss of peptide function (it no longer inhibits feeding). The N-terminus fragments (from amino acid 1-53) are inactive (having no effect on feeding). The fragment aa 55-102 is considered by most investigators to be the longest physiologically active CART peptide fragment. Because the yeast expression system includes intrinsic prohormone convertases it was not possible to isolate the full length proCART peptide. However expression in *Escherichia coli* resulted in the isolation of a full length peptide, which also inhibited feeding upon central administration (Couceryro and Fitz, 2003). The other major CART peptide fragment which has received attention is the fragment 62-102 which also inhibits feeding (Dylag et al., 2006).

A full immunohistochemical study of the distribution of CART peptide showed that it has a wide distribution of expression in the rat brain (Koylu et al., 1998). CART peptide is found either in neuronal cell bodies or in fibres (axons) systems in many areas of the CNS and PNS. To my knowledge there is no evidence of CART peptide in glia. In the monkey hypothalamus CART peptide has been shown by electron microscopy to be present in LDCV (Smith et al., 1997).

The CART peptide fragments are generated *in vivo* by prohormone convertase 1/3 (PC1/3) and 2 (PC2) (Dey et al., 2003). The longer fragment (55-102) can be generated by either PC1/3 or PC2, but the shorter fragment (62-102) is only generated by PC2. This gives a mechanism to differentially produce these two CART peptides: convertase expression.

Because modulation of CART mRNA levels is associated with stimulant drugs, areas of the brain associated with reward and reinforcement (ventral tegmental area, substania nigra, nucleus accumbens, lateral hypothalamus and prefrontal cortex) have been intensively studied. The identification of CART peptide as anorectic has also led to intensive study of the distribution and role of CART peptides in the area of the brain which controls feeding: the hypothalamus. CART peptide is also found in areas of the brain associated with stress (hypothalamic-pituitary-adrenal axis and sympathetic division of the autonomic nervous system). Finally the presence of CART peptide in the areas of the brain associated with emotional states (amygdala and hippocampus) has led to research into a possible role for CART peptides in fear and anxiety.

There are currently two CART gene knockout mice strains (Asnicar et al., 2001) (Wierup et al., 2005). Both of these mice strain strains show a mild obese phenotype and have altered responses to psychostimulants compared to wild-type mice (Moffett

et al., 2006). In addition these mice have altered pancreatic function, have slightly reduced bone mass and show high levels of anxiety.

1.3.2 – CART peptides and reward/reinforcement.

As previously mentioned, CART was identified after administration of the psychostimulants cocaine and amphetamine (Douglass et al., 1995). However these results proved to be controversial as other groups were unable to repeat this observation (Vrang et al., 2002; Marie-Claire et al., 2003). It appears that to get a reliable increase in CART mRNA and CART peptide expression levels requires a binge-dosing regime rather than acute administration (Hunter et al., 2005). The increase in CART mRNA in the nucleus accumbens is due to an increase in intracellular levels of cAMP (Jones and Kuhar, 2005). Elevated levels of cAMP have also been found in this area of the brain in human cocaine overdose victims (Tang et al., 2003).

Although the neurochemistry of drug abuse is highly complex, one of the key pathways that is activated during drug use and facilities drug addiction is the mesolimbic dopamine system (Figure 1.2). The mesolimbic dopamine system can simply be thought of as 4 interconnected areas of the brain: the striatum (dorsal striatum (DS) and nucleus accumbens (NA)), substantia nigra (- pars compacta (SNc) and - pars recticula (SNr)), lateral hypothalamus (perifornical area (Pef/LH)) and ventral tegmental area (VTA). All of these areas contain CART peptide positive fibres and the NA and Pef/LH contain CART positive cell bodies.

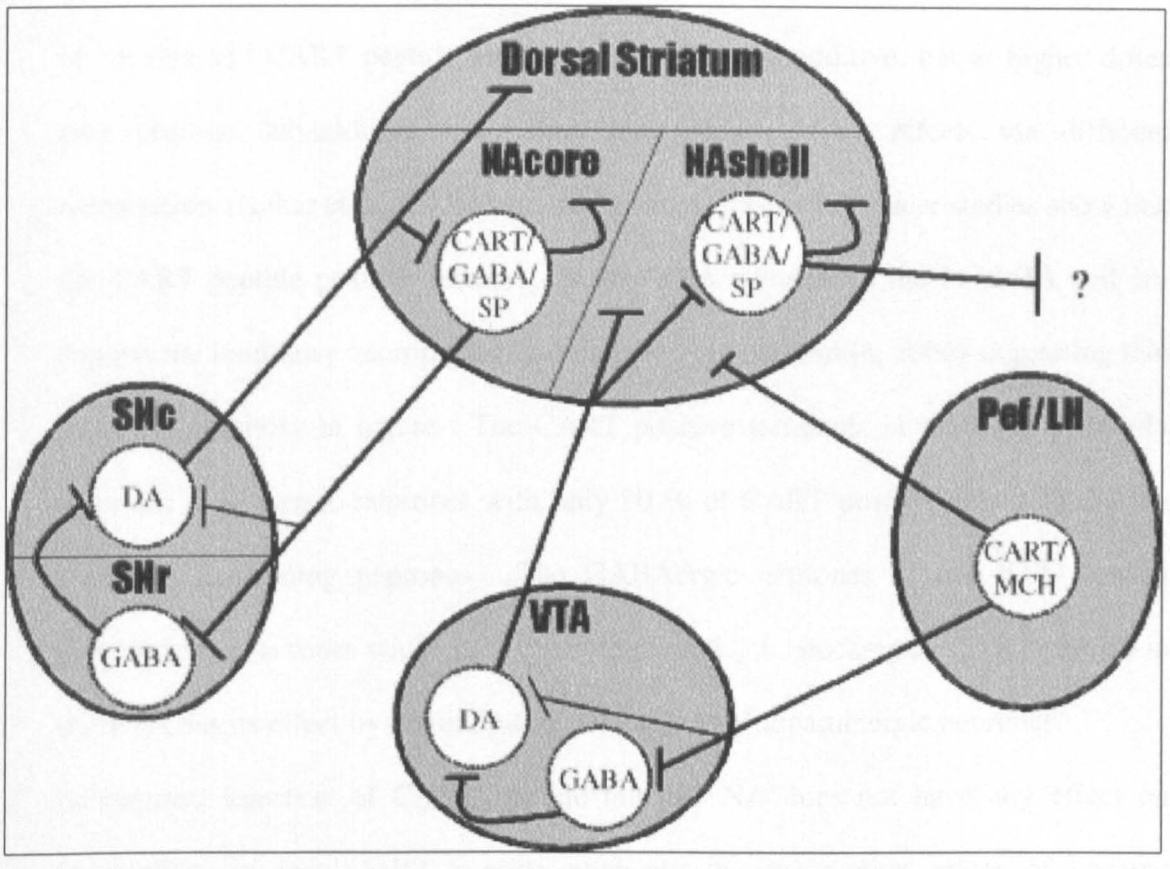

Figure 1.2 – The mesolimbic dopamine system. Four interconnected brain areas with the final output being from the nucleus accumbens . CART, cocaine-and-amphetamine regulated transcript; DA, dopamine; MCH, melanin-concentrating hormone; NA, nucleus accumbens; Pef/LH, perifornical area of the lateral hypothalamus; SNc, substantia nigra pars compacta; SNr, substantia nigra pars reticulata; SP, substance P; VTA, ventral tegmental area. . Taken from Philpot, K. B. and Y. Smith (2006). "CART peptide and the mesolimbic dopamine system." Peptide **27**(8): 1987-1992.

Direct injection of CART peptide (unless otherwise stated CART peptide refers to the fragment 55-102) into the VTA results in an increase in locomotive activity and induces conditional placement preference (the animal spends more time in the area associated with injection of CART peptide) (Kimmel et al., 2000). This effect is similar to direct cocaine administration, although somewhat smaller. When low doses of cocaine and CART peptide are co-injected they are additive, but at higher doses they become sub-additive, suggesting they may mediate effects via different mechanisms (Kuhar et al., 2005). Immunohistochemistry and tracer studies show that the CART peptide positive terminals in the VTA come from the Pef/LHA and co-express the inhibitory neuropeptide α-MSH (Philpot and Smith, 2006) suggesting that they are inhibitory in nature. The CART positive terminals in the VTA primarily innervate GABAergic neurones with only 30 % of CART positive fibres contacting dopamine containing neurones. The GABAergic neurones of the VTA contact dopaminergic neurones which project out to the NA. It appears that CART peptide in the VTA has its effect by dis-inhibiting the excitatory dopaminergic neurones.

In contrast, injection of CART peptide into the NA does not have any effect on locomotion, in fact CART peptide attenuate the locomotive effect of cocaine (Jaworski et al., 2003). The CART positive cells in the NA receive dopaminergic inputs from the VTA and the Pef/LH and project out of the NA into various brain regions associated with reward behaviour. Inside the NA there are local interneurons which are positive for CART peptide and GABA, and also for other neuropeptides such as substance P (Hubert and Kuhar, 2005) and dynorphin (Dallvechia-Adams et al., 2002). In addition there is a CART peptidergic output from the NA to SNr and SNc areas.

The substantia nigra is the final part of the reward and reinforcement CART puzzle. The synaptic terminals of CART peptide containing fibres from the NA in the SN also contain GABA and are almost exclusively found in the substantia nigra pars reticula (SNr) (Dallvechia-Adams et al., 2001). These neurones are inhibitory in nature and project to the dopaminergic neurones of the substantia nigra pars compacta (SNc), which in turn project out of the SN back to the NA and the DS.

Finally CART knockout mice still show typical behaviour when given psychostimulant drugs but different labs give conflicting results on how much the knockout effects locomotor activity and conditioned place preference (Moffett et al., 2006). What is clear is that CART knockout mice self administers less cocaine than wild type mice (Couceyro et al., 2005). It appears that CART peptide mediates the reward and reinforcement mechanisms in the brain by dis-inhibition of the dopaminergic neurones of the mesolimbic system. This suggests that the CART peptide receptor(s) are inhibitory, at least in the VTA, NA and SN. As of yet there has been no direct electrophysiological evidences of effect of CART peptide on neurones in mesolimbic dopamine system.

1.3.3 – CART peptides and feeding/energy homeostasis

The initial suggestion that CART peptide was involved in feeding and energy homeostasis came from the observation that injection of CART peptide into the fourth or lateral ventricles resulted in reduction of food intake, primarily by reduction of meal size rather than meal number (Aja et al., 2002). This reduction in food intake translated into a reduction in body fat and was seen in both lean and obese rats

(Larsen et al., 2000). It was expected that the CART knockout mice would have a strong obese phenotype, but this was not observed. The mild obesity phenotype seen in the CART knockout mice may in fact be due to a pancreatic dysfunction rather than central effects (CART knockout mice are hypoinsulinemic). It is clear that the involvement of CART peptides in feeding and energy homeostasis is not simple, and this may reflect the complexity of the neuronal circuits involved.

When thinking about food intake and energy expenditure it has become clear that the accurate nucleus (Arc) is central. The Arc is located in the hypothalamus adjacent to the third ventricle. Neurones of the Arc respond to circulating leptin. Leptin is produced by adipose tissue, crosses the blood brain barrier at the median eminence, and inhibits feeding. Neurones of the Arc can (in simple terms) be classified as either anabolic or catabolic; the anabolic neurones of the Arc contain CART peptide and POMC, are stimulated by leptin, increase energy expenditure and reduce feeding. The catabolic neurones contain neuropeptide Y (NPY) and agouti-related peptide (AGRP), are inhibited by leptin, decrease energy expenditure and increase feeding. Thus it appears that in the Arc, CART peptides partially mediate the anabolic homeostatic signal, and this explains the decrease in feeding observed when CART peptide is injected in the rat brain. In humans a point mutation in the CART gene (resulting in a change from Leu to Phe at position 34) leads to an obese phenotype (Yanik et al., 2006). This mutation interferes with the processing of proCART into the active CART peptide fragments, therefore reducing the available active CART peptide. This would seem to add more weight to the argument that CART's role in the hypothalamus is anabolic. However more recent immunohistochemical studies have demonstrated that in humans, CART peptide is not co-localised with POMC, but is expressed in a subset of NPY containing neurones (Menyhért et al., 2007) which

are usually considered catabolic. These conflicting results demonstrate that the role of CART peptide in energy homeostasis is still not clear.

1.3.4 – CART peptides and stress.

Stress can be defined as something perceived, real or imagined, which threatens homeostasis. It is a very general term, as many things, especially in higher mammals, can be thought of as stressors. What is clearer is how the body responds to stress. There is a three phase response to stress; firstly signals are send out to prepare muscle for activity. Secondly the sympathetic division of the ANS become activated; this increases heart rate, relaxes airways, inhibits digestion and increases available energy. Finally stress hormones are released, these are chemical such as adrenaline and noradrenaline and glucocorticoids.

The stress response is mediated by the hypothalamic-pituitary-adrenal (HPA) axis. Under stressful situation the hypothalamus releases the neuropeptide/horomone corticotrophin releasing hormone (CRF) which then stimulates the release of ACTH from the pituitary gland into the blood stream. ACTH travels to the adrenal gland where it stimulates the release of corticosterone (in rodents, or cortisol in humans) which in turn stimulates the release of energy from energy stores. Corticosterone also inhibits the CRF producing neurones in the hypothalamus, creating a negative feedback loop. CART peptide is found at all level of the HPA axis as well as in the sympathetic division of the ANS (Dun et al., 2006).

Intracerebroventricular injection of CART peptide increases expression of CRF in the hypothalamus (Stanley et al., 2001) which in term leads to an increase in circulating

ACTH and corticosterone. In turn, levels of CART peptide in the hypothalamus appear to be regulated by CRF and corticosterone (Stanley et al., 2004). CART peptide is found in the blood and passes freely across the blood brain barrier (Kastin and Akerstrom, 1999), the source of CART peptide in the blood is unknown but its levels are under the control of corticosterone (Vicentic et al., 2004). What role CART peptide plays in the blood is unknown, but its link to corticosterone suggests a role in energy release.

Intracerebroventricular injection of CART peptide into conscious rabbits results in an increase in heart rate, arterial blood flow, renal sympathetic nerve activity and increases the plasma concentration of epinephrine and norepinephrine (Matsumura et al., 2001). This is most likely due to activation of the sympathetic division of the ANS. In the spinal cord, sympathetic preganglionic neurones (SPNs) contain CART peptide, with SPN terminals onto postganglionic neurones also positive for CART peptide (Dun et al., 2000). The SPNs are one of only a few sites were there is data on the electrophysiological effects of CART peptide. Application of 100-300 nM CART peptide increased the amplitude of NMDA receptor mediated currents without directly depolarising the SPNs suggesting a possible increase in the number of functional NMDA receptors. The frequency of miniature postsynaptic excitatory currents was also increased which suggests an action on the presynaptic neurone (Dun et al., 2006).

1.3.5 – CART peptides and fear/anxiety

There is increasing evidence that appetite regulating peptides have a role in the regulation of anxiety and in most cases anorectic peptides act as anxiogenic factors

(Stanek, 2006). This appears true for CART peptide as application of CART peptide (55-102) increases anxiety in mice. Interestingly, application of CART peptide (63-102) has no such effect on anxiety, even at doses which inhibit feeding (Chaki et al., 2003). This suggests that the mechanism (or receptor) by which CART peptide modulates anxiety is different from that modulating energy homeostasis. It has also been demonstrated that humans with a point mutation in the CART gene (Leu changed to Phe at position 34) have increased anxiety as compared to weight matched controls (Miraglia del Giudice et al., 2006).

The amygdala is the centre of emotion in the brain, and as previously mentioned CART is expressed in the amygdala, but mRNA levels of CART are not altered by chronic stress (Hunter et al., 2007). This suggests that CART peptide has a different mechanism in anxiety than in responding to stress.

1.3.6 – Other putative roles of CART peptide

CART peptide has been implicated in the regulation of lactation as the levels of CART peptide are increased in the hypothalamus and pituitary during lactation (Smith et al., 2006). CART peptide also modulates the hypothalamic-pituitary-gonadal axis, as CART peptide decreases gonadotrophin-releasing hormone interpulse interval via a leptin-dependant mechanism (Lebrethon et al., 2000). CART peptide is implicated in pain transmission in the spinal cord; intrathecal injection of CART peptide produces hyperalgesia in mice (Ohsawa et al., 2000) and enhances the analgesic effect of morphine (Damaj et al., 2004). Female odours stimulate neurones in the premamillary nucleus which express CART peptide (Cavalcante et al., 2006),

suggesting a possible role in mating behaviour.In the pancreas CART peptide is expressed in δ-cells and also during development in α-cells, β-cells and PP-cells (Wierup et al., 2004). CART peptide levels in β-cells are upregulated in several type of type-2 diabetes (Wierup and Sundler, 2006).

Of the other areas of the CNS where CART peptide is expressed, the one of most interest to me is the cerebellum. Although no CART mRNA is found in the cerebellum, CART positive fibres have been observed in the vestibular cerebellum presumably from climbing fibres (Koylu et al., 1998). Climbing fibres originate in inferior olive, and this structure is positive for both CART mRNA and CART peptide. There are no reports in the literature of CART peptides in any other areas of the vestibular system, but this may reflect that no-one has studied CART peptide

CART peptide's diverse distribution in the CNS is reflected in the diversity of physiological effects which CART peptide has been implicated in. Much of the research into CART peptide has been focused on feeding/homeostasis, and this probably reflects the growing medical importance of obesity. However CART research has been hindered because of the lack of antagonists and the lack of an identified CART receptors. It seems that wherever you look in the brain you find CART peptide, but the roles of CART peptide in different areas appears to be very different. I'm certain that interest in CART peptide will continue, as if could reveal more about how some of the key pathways in the brain work, and CART receptor agonist/antagonist are interesting targets of medical pharmacology, for the treatment of obesity, stress related disorders and drug addiction.

1.4 – CART peptide receptor

Although the CART peptide receptor has yet to be identified, we do know that CART peptide shows no appreciable binding affinity to 60 different receptors including classical neurotransmitters receptors (for example $GABA_A$ receptor) and neuropeptide neurotransmitters receptors (such as NPY receptor) (Vicentic et al., 2006). It has been demonstrated that CART peptide can bind specifically to neuronal type cells. Using radiolabelled CART peptide AtT20 cells (mouse LAF1, pituitary tumour cells; http://www.biotech.ist.unige.it/cldb/cl296.html) were shown to bind CART peptide with a K_d value of 49.5 pM (Vicentic et al., 2005). It has also been demonstrated that CART peptide can bind to dissociated hypothalamic neurones and also HepG2 cells (human, hepatocellular carcinoma cells; http://en.wikipedia.org/wiki/Hep_G2, 17/09/07) suggesting that a specific receptor for CART peptide does exist (Keller et al., 2005). It has also been found that CART peptide increases ERK/MAPK (extracellular signal-regulated kinase/mitogen-activated protein kinase) activity in AtT20 cells in a dose-dependent manner, and this effect is blocked by both MEK (MAPK/ERK kinase) inhibitor and pertussis toxin (selective inhibitor of $G_{i/o}$). This suggests that CART peptide can bind to a receptor coupled to $G_{i/o}$ protein leading to the activation of the ERK/MAPK signalling cascade (Lakatos et al., 2005).

More recently, a binding study identified the first protein to show a direct binding affinity for CART peptide, however this protein was not a GPCR, or even a protein expressed in the outer cell membrane, but a mitochondrial protein (Mao et al., 2007). The protein which interacts with CART peptide is subunit B of the mitochondrial succinate dehydrogenase (SDHB). At a concentration between 0.2-4.0 nM, CART peptide significantly increased SDHB activity resulting in increased ATP generation.

This increase in ATP generation may underlie the apparent neuroprotective role of CART peptide during cerebral ischemia (Xu et al., 2006). If CART peptide is a modulator of mitochondrial activity then it may have a primary role in setting the basal metabolic rate of cells or could be associated with the flight or fight mechanism. There have been few studies investigating whether CART peptides have electrophysiological actions on neurones. Studies have shown that injection of CART into the brain can result in c-fos expression, which is a marker for increased neuronal activity (Vrang et al., 1999; Vrang et al., 2000).The first direct evidence for an action of CART peptide on neuronal electrophysiology comes from Yermolaieva *et al* (2001), who showed that CART peptide inhibits L-type voltage gated calcium channels in cultured hippocampal neurones. They showed using fura-2 AM (a calcium dependant fluorophore) filled neurones that 1 μM CART peptide reduced the cytosolic calcium increase elicited by potassium induced depolarisation by 48 ± 14 %. This reduction is similar to that seen with the L-type calcium channel antagonist, nifedipine (55 %). Furthermore the application of CART peptide and nifedipine was not significantly different from applying nifedipine alone. The calculated EC_{50} for CART peptide was 600 nM and the inhibitory effects of CART peptide were blocked by the $G_{i/o}$ inhibitor pertussis toxin and were not affected by other G-protein inhibitors. Using the patch-clamp method (barium ions as the charge carrier) they were able to show that CART peptide reduces the L-type calcium channel current by 80-90 % (Yermolaieva et al., 2001).

Wall and Spanswick (2004) showed that application of CART peptide (100-200 nM) either hyperpolarised or depolarised the membrane potential of rat sympathetic preganglionic neurones (SPNs) in spinal cord slices (Wall and Spanswick, 2004). The hyperpolarisation was abolished by bicuculline suggesting that the CART peptide was

via $GABA_A$ receptor activation. In contrast, Dun et al (2006) showed that CART peptide did not affect the resting membrane potential of SPNs, but their experiments were done in the presence of the sodium channel blocker, TTX. It would seem plausible that CART peptide could be modulating the activity of local (inhibitory) interneurones contacting SPN as well as directly affecting the SPNs via a GPCR.

The major problem with investigating CART peptide, using electrophysiology, is the lack of any CART receptor antagonists thus it is difficult to exclude any non-specific actions. This is further complicated by the diverse actions of CART peptide in different areas of the CNS. In addition it appears that CART peptide seems to have multiple effects on the same cellular target (for example SPNs). The identification of a single mechanism of CART peptide action in a discrete area of the brain could help narrow the possible targets of CART peptide and aid the identification of a CART peptide receptor. This is one of the main reasons I chose to investigate the role of CART peptide in the cerebellum, as it appears that CART peptide is expressed in a distinct region (vestibular cerebellum) and appears to be in a distinct subset of neurones (climbing fibres).

1.5 – Overview of cerebellum anatomy and function

The cerebellum is an area of the hindbrain located dorsal to the brainstem. It is connected to the brainstem via the three pairs of fibre bundles (peduncles) and the space between the brainstem and cerebellum forms the 4^{th} ventricle (Figure 1.3). It is unique within the brain as being the only area which is continuous across the midline

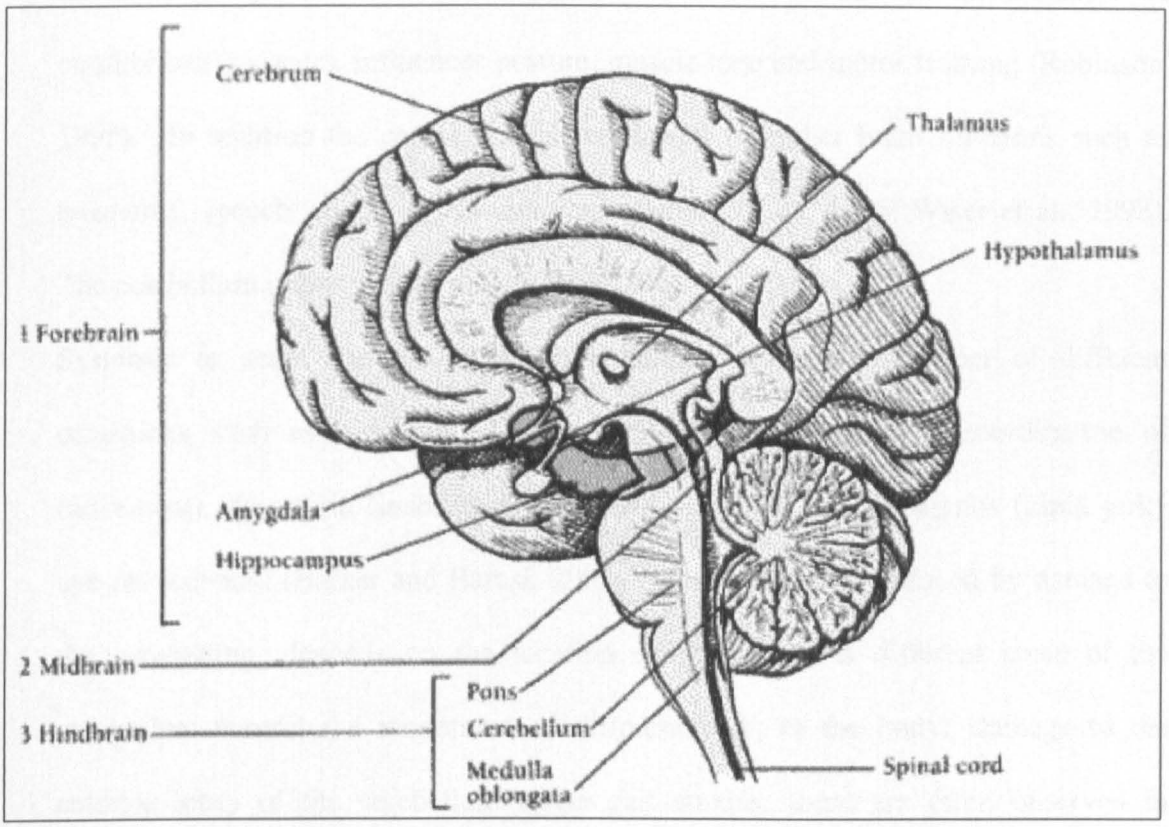

Figure 1.3 – Position of the cerebellum relative to other major brain structures. Taken from http://www.sfn.org/, 19/09/07.

of the brain. In humans, the cerebellum makes up approximately 10 % of the total brain volume and contains more than 50 % of the total neurons of the brain (Bear et al., 2007).

The main functions of the cerebellum are reasonably well understood, its primary function being in the coordination of complex movements, maintenance of equilibrium (balance), influences posture, muscle tone and motor learning (Robinson, 1995). In addition the cerebellum is implicated in higher brain functions such as reasoning, speech, spatial awareness, and memory (Fiez, 1996; Wiser et al., 1998). The cerebellum operates at an unconscious level.

Systemic or acute damage to the cerebellum results in a number of different conditions such as: hypotonia (reduced muscle tone), ataxia (incoordination of movement), dysarthria (inability to articulate properly) and nystagmus (rapid jerky eye movements) (Barker and Barasi, 2003). The symptoms produced by damage to the cerebellum, depends on the location of the lesion as different areas of the cerebellum control the movement of different parts of the body. Damage to the anterior lobes of the cerebellum cause gait ataxias; these are often observed in alcoholics and give a characteristic drunken walk, even when sober. Whereas damage to the midline of the cerebellum can cause a truncal ataxia (incoordination of muscles used to maintain upright posture) and nystagmus (FitzGerald and Folan-Curran, 2002). Ataxias can also result from genetically inherited diseases, such as Friedreich's ataxia (Pearce, 2004). Friedreich's ataxia is an autosomal recessive disease caused by a GAA triplet repeat expansion in the intron of the gene coding for a 210 amino acid protein, frataxin (Campuzano et al., 1996) and is characterised by a gait ataxia, dysarthria, variable nystagmus and eventually heart failure (due to cardiac hypertrophy).

1.5.1 – Anatomy

The outer surface of the cerebellum consists of a thin sheet of cortex which is repeatedly folded to give the cerebellum its characteristic appearance. When cut saggitally there are a number of deep fissures which divide the cerebellum into ten lobes (labelled I to X) (Figure 1.4). In the medial-lateral axis, the cerebellum can be divided into three regions; in the centre is the vermis (Latin worm) and on the outside are two hemispheres (Figure 1.5). There are two pairs of small additional structures on the edge of the hemispheres called the flocculus and paraflocculus. Between the brainstem and the cerebella cortex are the peduncles which carry all the fibres entering and leaving the cerebellum. Underneath the cerebellar cortex lies a layer of subcortical white matter composed of all afferent and efferent fibres and the deep cerebellar nuclei (DCN), which receive the output of the cerebellar cortex. The cortex of the cerebellum has three distinct layers; the outermost layer is the molecular layer, then there is the Purkinje cell layer, and the innermost layer is the granule cell layer. As the name suggests, the granule cell layer mainly contains the granule cells and also contains the mossy fibres and Golgi cells (inhibitory interneurones). Traversing the granule cell layer are the climbing fibres (on the way to the molecular layer) and Purkinje cell axons leaving the cortex. The Purkinje cell layer contains the cell bodies of the Purkinje cells and the cell bodies of Bergmann glia (cerebellar astrocytes). The molecular layer contains the axons of the granule cells (parallel fibres), the dendrites of the Purkinje cells, Golgi cell dendrites and the stellate cells and basket cells (inhibitory interneurones) (Figure 1.6). The processes of Bergmann glia extend into the molecular layer, terminating with bulbous endfeet at the pial surface.

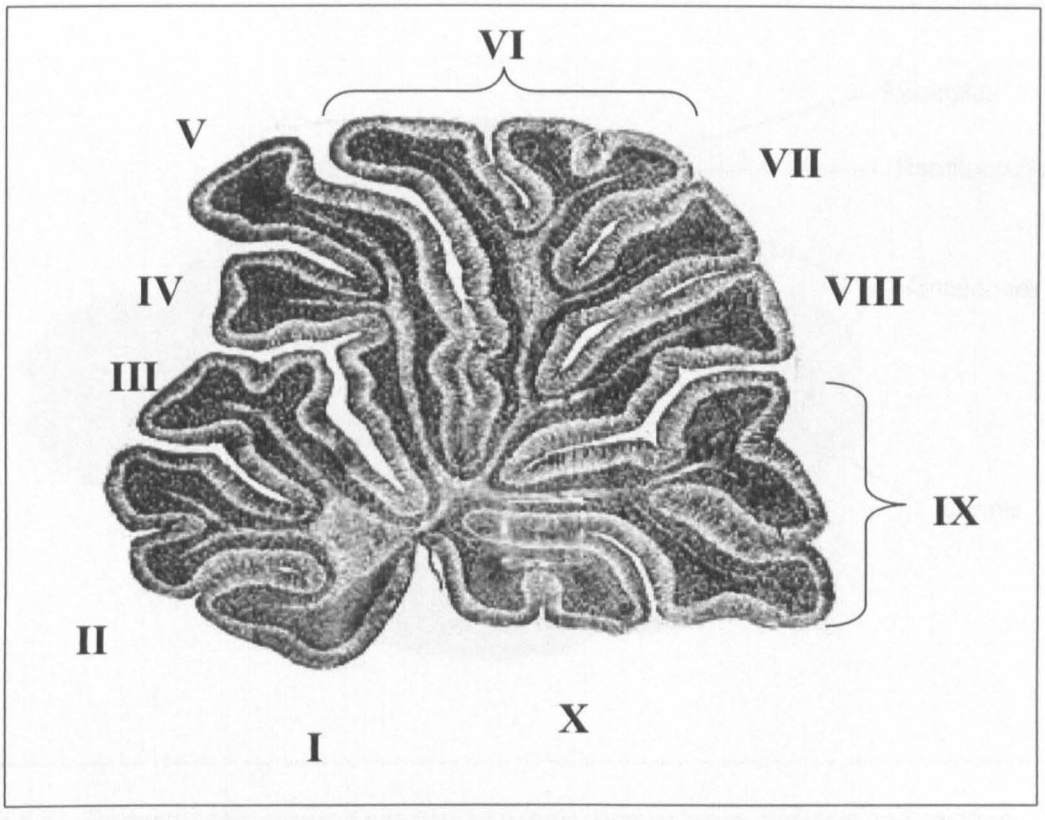

Figure 1.4 – Parasaggital slice showing relative positions of the 10 lobes. Taken from http://health.ucsd.edu/news/2002/11_07_Nikon2.html, 10/05/05.

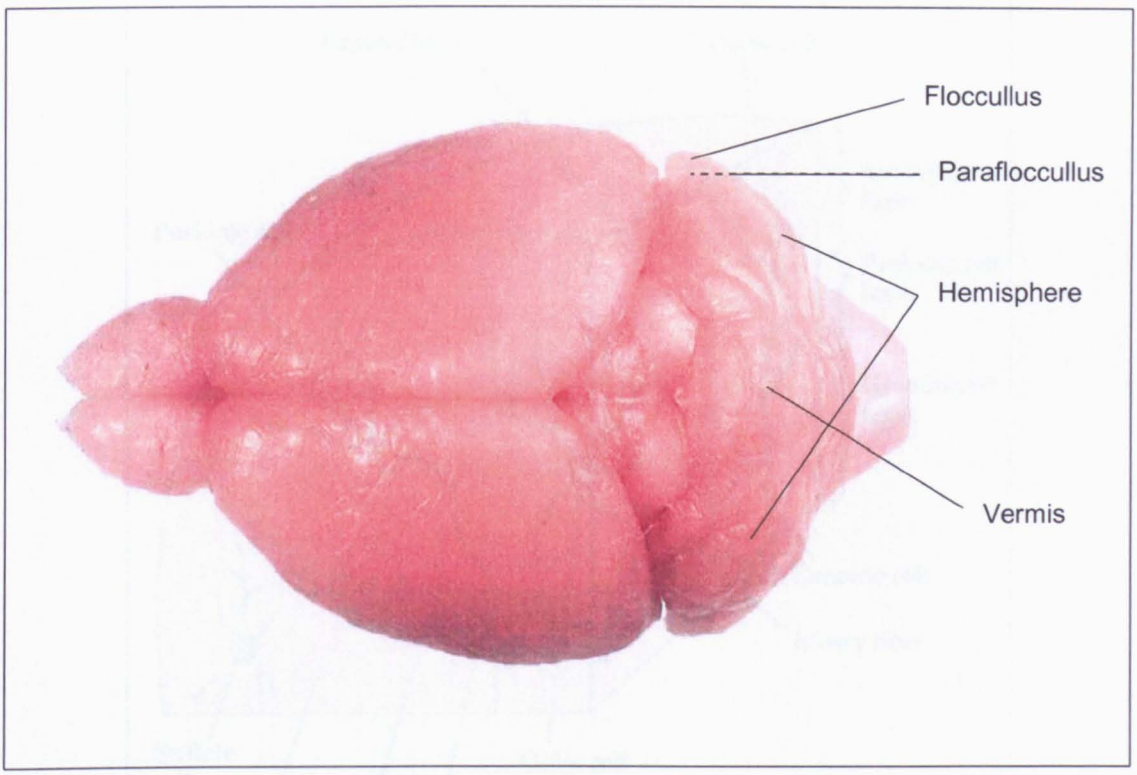

Figure 1.5 – Rodents brain showing position of vermis, hemispheres, flocullus and parafloculus (under the floccullus). Taken from http://www.nervenet.org/papers/cerebellum2000.html, 19/09/07.

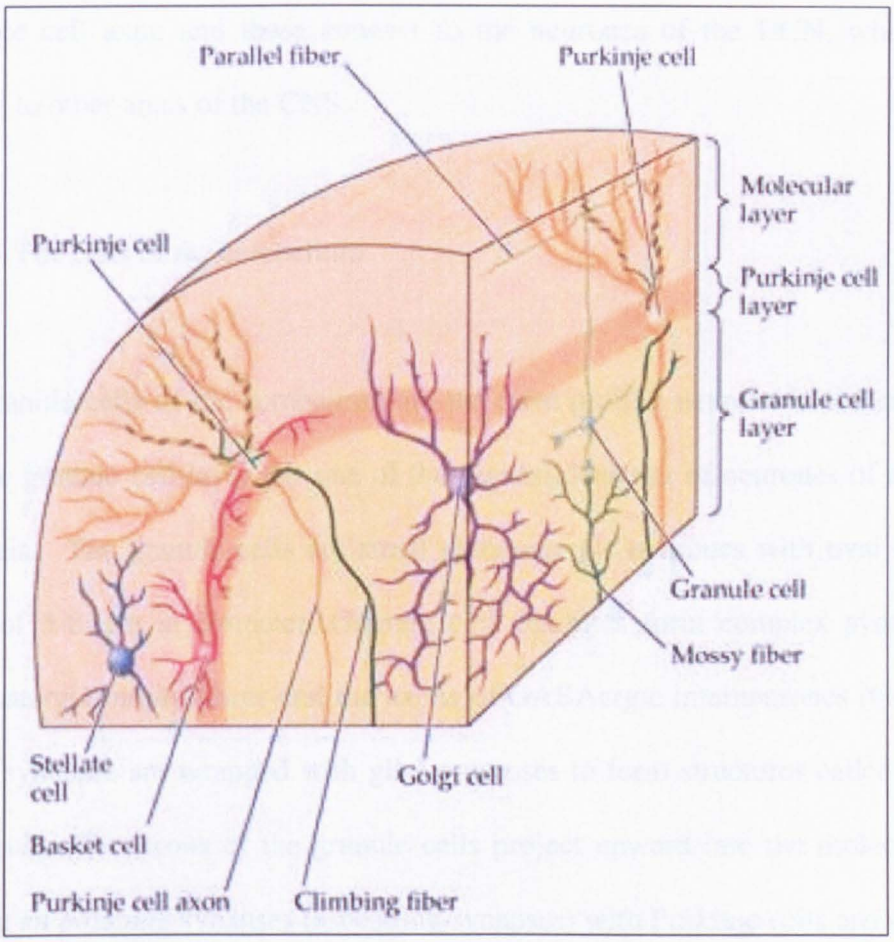

Figure 1.6 – Illustration of three layer of the cerebellar cotrex showing the relative positions and morphology of neurones. Taken from http://www.tnb.ua.ac.be/models/index.shtml, 10/05/05.

There are two major inputs into the cerebellum; the mossy fibres, which originate from many nuclei throughout the brainstem (such as the pontine nucleus) and from spinal cord, and the climbing fibres, which originate from the inferior olive (also in the brain stem). Both of these inputs are glutamatergic and also innervate neurones in the DCN via collaterals. There is only one output from the cerebella cortex, the Purkinje cell axon and these connect to the neurones of the DCN, which in turn project to other areas of the CNS.

1.5.2 – The cells of the cerebellum

The granule cells of the cerebellum are the most prolific neurone in the entire CNS, and the granule cell layer has one of the highest densities of neurones of any part of the brain. The granule cells are small glutamatergic neurones with oval or circular soma of 5-8 μm in diameter. Granule cell dendrites form complex synapses with glutamatergic mossy fibres and the axons of GABAergic interneurones (Golgi cells). These synapses are wrapped with glial processes to form structures called cerebellar glomeruli. The axons of the granule cells project upward into the molecular layer, making *en passante* synapses (ascending synapses) with Purkinje cells and Golgi cells before their axons bifurcate and become parallel fibres. Parallel fibres can run for several mm making multiple excitatory synaptic contacts onto Purkinje cells and Golgi cells.

The GABAergic interneurones, Golgi cells, have somas located in the granule cell layer and their axons form part of the granule cell glomeruli. Their dendrites are located in the molecular layer and also in the granule cell layer. They receive excitatory (glutamatergic) inputs from parallel fibres in the molecular layer, and also

from mossy fibres and climbing fibres. They are inhibited by axon collaterals from Purkinje cells (GABAergic). The Golgi cells provide feed-back inhibition to granule cells.

GABAergic Purkinje cells are the sole output of the cerebellar cortex and are located in a layer between the granule cell layer and molecular layer. They have a large soma (20-40 μm), a long axon which projects out of the cerebellar cortex and a single large and extensively arborised dendrite. The dendrites of Purkinje cells are planner in the dorsal-ventral axis (maintained in saggital slices) and neighbouring Purkinje cells' dendrites significantly overlap. Purkinje cells receive excitatory (glutmatergic) inputs from parallel fibres and from climbing fibres and inhibitory (GABAergic) inputs from stellate and basket cells.

Basket cells have their soma and dendrites in the molecular layer, but their axons project onto the Purkinje cell bodies. The basket cell dendrites contact parallel fibres, but also receive inputs from climbing fibres and Purkinje cell axon collaterals. The axons from a single basket cell can contact up to 150 Purkinje cells and a single Purkinje cell can receive inputs from as many as 50 different basket cells, this gives the basket cell-Purkinje cell synapse a dense mesh like appearance somewhat reminiscent of basket work, hence the name, basket cell.

Stellate cells are located in the outermost 1/3 of the molecular layer and are small cells with radial dendrites contacting parallel fibres. Their axons form inhibitory (GABAergic) synapses with Purkinje cell dendrites. Together the basket cells and stellate cells are thought to provide feed-forward inhibition of Purkinje cells.

1.5.3 – The neural circuits of the cerebellum

The cerebellum has two intrinsic circuits, both converging on the Purkinje cell (Figure 1.7):

- mossy fibres → granule cell / parallel fibres → Purkinje cells
- climbing fibres → Purkinje cell

A single glutamatergic mossy fibre forms synapses with 20-30 granule cells. The axons of the granules cells bifurcate to become the parallel fibres which make glutamatergic synaptic contacts on the most terminal dendrites of Purkinje cells, the so called spiny branchlets. The parallel fibres pass through the cerebella cortex orthogonal to the plane of the Purkinje cell dendrites (thus are cut in saggital sections), and a single parallel fibre will make a synaptic contact onto one in every 3-5 Purkinje cell it passes. Because of the very large number of parallel fibres, a Purkinje cell can receive up to 200,000 synaptic contacts from parallel fibres, each synapse being very weak, activation of approximately 50 parallel fibres are required to generate an action potential in a Purkinje cell (Barbour, 1993).

The climbing fibre-Purkinje cell synapse is a unique synapse in the CNS; each Purkinje cell is innervated by only one climbing fibre (although this is not the case in immature animals). The glutamatergic climbing fibre makes hundreds of individual synaptic contacts onto the stubby spines of the main dendrites and on the soma of the Purkinje cell. The shear number of synaptic contacts makes this the strongest single synapse in the whole nervous system. The activation of the climbing fibre produces a very large depolarisation of the Purkinje cell (called a complex spike).

There is also an extrinsic circuit which the cerebellum is part of; the mossy fibres and climbing fibres make excitatory (glutamatergic) inputs onto neurones of the DCN

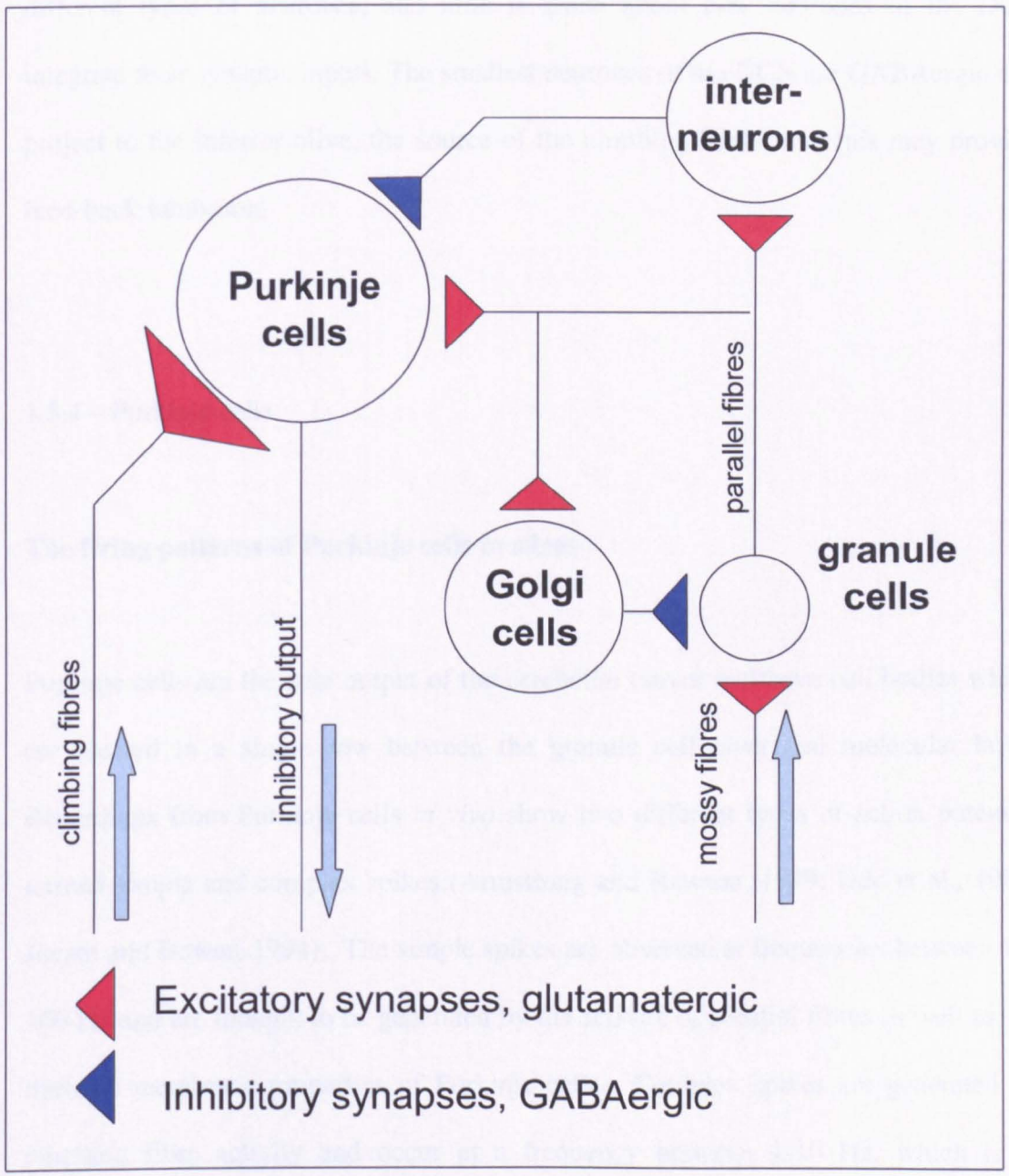

Figure 1.7 – Two intrinsic circuits of the cerebellum, with the interneurones shown.

before they pass into the cerebella cortex, the Purkinje cells make inhibitory (GABAergic) synapses onto neurones of the DCN. The DCN contains at least 3 different types of neurones, and little is know about how neurones of the DCN integrate their synaptic inputs. The smallest neurones of the DCN are GABAergic and project to the inferior olive, the source of the climbing fibres, and this may provide feed-back inhibition.

1.5.4 – Purkinje cells

The firing patterns of Purkinje cells in slices

Purkinje cells are the sole output of the cerebellar cortex and have cell bodies which are located in a single row between the granule cell layer and molecular layer. Recordings from Purkinje cells *in vivo* show two different types of action potential termed simple and complex spikes (Armstrong and Rawson, 1979; Udo et al., 1981; Jaeger and Bower, 1994). The simple spikes are observed at frequencies between 10-100 Hz and are thought to be generated by the activity of parallel fibres as well as the intrinsic membrane properties of Purkinje cells. Complex spikes are generated by climbing fibre activity and occur at a frequency between 1-10 Hz, which is in agreement with the observed firing rate of neurones in the inferior olive, the source of climbing fibres (Bal and McCormick, 1997).

In parasagittal cerebellar slices, the climbing fibre inputs are usually inactive (as their soma are in the inferior olive and thus their axons are cut) and therefore very few spontaneous complex spikes are observed. The majority of the parallel fibres are also

cut, with only a small number still intact and active. Despite this, Purkinje cells in slices are still constituently active, exhibiting a wide range of reported firing frequencies (1-150 Hz) (Llinás and Sugimori, 1980a; Häusser and Clark, 1997; Womack and Khodakhah, 2002; Smith and Otis, 2003; Cerminara and Rawson, 2004; Loewenstein et al., 2005). The firing frequency of Purkinje cells *in vitro* appears to be modulated by the activity of inhibitory interneurones (stellate and basket cells), since blocking these inputs significantly increases the firing frequency of Purkinje cells (Häusser and Clark, 1997). The firing frequency is also modulated by nitric oxide which is released by parallel fibres (Smith and Otis, 2003). Purkinje cells (*in-vitro*) exhibit a variety of firing patterns including tonic (continuous) and bursting (episodes of firing interspersed with periods of quiescence). An interesting firing pattern is the 'trimodal' firing pattern, first observed when the GABAergic synapse were blocked (Womack and Khodakhah, 2002). This pattern of firing consists of a fast tonic burst of action potentials, followed by a group of short fast bursts of firing, in which the interval between progressive spikes inside the bursts gets shorter and shorter, and finally a period of quiescence. This whole pattern lasts from tens of second to a few minutes (at 32°C) and then repeats. This trimodal firing has also been observed in slices without pharmacological modification (McKay et al., 2007) but as far as I know not *in vivo*.

The membrane properties of Purkinje cells are complex since they express a large number of different voltage and ligand gated ion channels and have a complex planar arborised dendrite. The tonic firing of Purkinje cells is thought to result from a complex interplay of the somatic resurgent sodium current, voltage gated calcium current and calcium-dependant potassium current, which are all active around the resting membrane potential of the active Purkinje cell (Raman and Bean, 1997; Jaeger

and Bower, 1999; Raman and Bean, 1999; Swensen and Bean, 2003). As well as firing tonically, Purkinje cells are sometimes observed to firing in long bursts of tonic activity interspersed with periods of quiescence. It is thought that activation of the hyperpolarisation-activated mixed cation current, (I_h), is required to produce this pattern (Williams et al., 2002). The firing pattern of Purkinje cells is also modulated by the dendrites. As early as 1980 it had been demonstrated that calcium spikes in the dendrites filtered down into the soma to give mixed sodium/calcium action potentials (Llinás and Sugimori, 1980b) and more recently it has been shown that it is the dendrites that control tonic and trimodal firing (Womack and Khodakhah, 2002) and also bursting behaviour (Womack and Khodakhah, 2004).

Purkinje cell inputs

Upon activation of a climbing fibre there is a very strong post synaptic Purkinje cell response (the complex spike). The complex spike consists of a sodium-dependent action potential followed by 2 or 3 calcium spikes and a long afterhyperpolarisation (AHP) in which the Purkinje cell is unable to generate simple spikes. The climbing fibres release glutamate to activate Purkinje cell alpha-amino-3-hydroxy-5-methyl-4-isoxazolepropionic acid receptors (AMPARs) and also release CRF onto CRF receptor type 1 (Primus et al., 1997; Chen et al., 2000). When recordings are made from Purkinje cells in voltage clamp, the stimulation of climbing fibres produces a large fast excitatory postsynaptic current (EPSC) which shows paired pulse depression (Llano et al., 1991b). The kinetics of the EPSC are determined by the glutamate transporters in the membranes of glia that surround the climbing fibre-

Purkinje synapse (Takayasu et al., 2004). CRF modulates the AHP of complex spikes (Fox and Gruol, 1993).

Parallel fibres also release glutamate, which activate Purkinje cell AMPA receptors and metabotropic glutamate receptors (mGluRs) and they also release nitric oxide (Kimura et al., 1998). However the activation of parallel fibres is different from climbing fibre activation as upwards of 50 parallel fibres need to be activated to push the Purkinje cell to threshold and fire an action potential (Barbour, 1993). When parallel fibre EPSCs are recorded in voltage clamp, paired stimulation results in facilitation, this is thought to be due to the residual pre-synaptic cytosolic calcium from the previous stimulation increasing the number of vesicles released (Atluri and Regehr, 1996). Parallel fibres influence Purkinje cells directly and indirectly via the activation of GABAergic interneurones.

The GABAergic stellate and basket cells (inhibitory interneurones) exert a strong influence on the properties of Purkinje cells. The Purkinje cell expresses $GABA_A$ receptors on it dendrites and on its soma, and in addition GABA released from inhibitory interneurones can act on $GABA_B$ auto receptors (Kulik et al., 2002). The GABA receptors of Purkinje cells are all of the form $\alpha 1\beta 1/2\gamma 2$ and thus are sensitive to benzodiazepine modulation (Laurie et al., 1992; Macdonald and Olsen, 1994). The classical model of the cerebellum suggests that the role of the inhibitory interneurones is to increase the temporal resolution of information through-put by inhibiting the Purkinje cells surrounding the Purkinje cells directly excited by parallel fibres (centre surround antagonism) (Dunbar et al., 2004). However, it is now becoming clear that the activation of the inhibitory interneurones by parallel fibres affect the integration of parallel fibre activity (Mittmann et al., 2005).

Plasticity

The cerebellum is thought to be one of the areas of the brain involved in the acquirement of motor learning: the increased efficiency of performing a motor task (such as walking or throwing a ball) produced through repeated trials. It has been suggested that plasticity of Purkinje cell synapses is the site of motor learning in the cerebellum (Ito, 2000) and that long term depression (LTD) of the parallel fibre-Purkinje cell synapse is key. LTD is produce by the repeated co-stimulation of parallel fibres and climbing fibres (for example 5 minutes at 1 Hz). The depression of the parallel fibre synapse requires calcium influx, activation of AMPAR and mGluRs (which are located outside of the synaptic cleft and are activated by glutamate spillover) (Hartell, 2002). The calcium influx is produced by the activation of climbing fibres which depolarise the Purkinje cell dendrites resulting in influx of calcium ions through voltage gated calcium channels. The activation of mGluRs activates protein kinase C, phospholipase C and phospholipase A_2, these combined with the increased cytolsolic calcium produce internalisation of AMPARs (Daniel et al., 1998). In addition to this mechanism, nitric oxide (NO) has also been implicated in the induction of LTD via protein kinase G (Hartell, 2002). The parallel fibre-Purkinje cell synapse has also been shown to undergo long term potentation (LTP), however this effects appear to be completely presynaptic, requiring only high frequency stimulation of parallel fibres, and interestingly is mediated by NO. It has been suggested that the LTP may reverse LTD, which is required if the system is not to become saturated. Another hypothesis is that LTD is not involved in motor learning, but is rather a form of neuroprotection (Kimura et al., 2005). High levels of

glutamatergic activity can lead to excititoxic cell death of Purkinje cells (O'Hearn and Molliver, 1993).

Another form of plasticity, which is observed at Purkinje cell synapses is the depolarization-induced suppression of inhibition (DSI) and depolarization-induced suppression of excitation (DSE) (Llano et al., 1991a; Kreitzer and Regehr, 2001). This is the short-term (several tens of seconds) inhibition of either inhibitory interneurones (in DSI) or parallel/climbing fibres (in DSE) after depolarisation of Purkinje cells. DSI/DSE is produced by the release of endocannabinoids from Purkinje cell dendrites, which then activate CB_1 receptors on interneurone axon, parallel fibre and climbing fibre terminals (Maejima et al., 2001; Yoshida et al., 2002; Brown et al., 2003; Diana and Marty, 2004). Endocannabinoid release from Purkinje cells is triggered by either calcium influx from a strong depolarisation (such as climbing fibre activity) (Brenowitz and Regehr, 2003), activation of mGluRs (produced by a train of parallel fibre EPSPs) (Maejima et al., 2001) or a combination of weak activation of mGluRs and mild depolarisation (Maejima et al., 2005). Although DSI/DSE is only a form of short-term plasticity, CB_1 knockout mice, where DSI/DSE is blocked (Wilson and Nicoll, 2002), show impaired motor learning (Kishimoto and Kano, 2006). This suggests that DSI/DSE and the endocannabioniods are involved in longer term plasticity in the cerebellum. It has recently demonstated another form of retrograde plasticity at the Purkinje cell. After termination of DSI (from stimulation of climbing fibres) a depolarization-induced potentiation of inhibition (DPI) can occur (Duguid and Smart, 2004). This increase in interneurone activity islonger lasting that DSE and is mediated my retrograde release of glutamate acting on NMDA receptors on interneurones.

1.6. – The vestibular cerebellum

As previously mentioned, CART peptide expression has been reported in the vestibular cerebellum (Koylu et al., 1998). The vestibular cerebellum is part of the vestibular system which is concerned with maintaining balance; it includes the otolith organs, the semicircular canals, cranial nerve VIII and the vestibular nuclei. The vestibular cerebellum is thought to be concerned primarily with maintaining balance. The vestibular cerebellum is made up to neurones in lobe IX and X as well as the paraflocculus (Bear et al., 2007). Neurones of the vestibular nucleus project to a subset of neurones on the inferior olive which project only into the vestibular cerebellum. Vestibular neurones also project directly to the cerebellar cortex in the form of mossy fibres (Fushiki and Barmack, 1997; Xiong and Matsushita, 2000). The granule cells of the vestibular cerebellum also receive inputs from other areas of the brainstem including brain stem nuclei relaying information from the visual system of the CNS as well as postural muscles via the spinal cord (Barmack et al., 1992b). The current model is that the vestibular cerebellum integrates information about the position of the head with information about the state of the postural muscles of the body to maintain balance.

The vestibular cerebellum is different in a number of ways from the rest of the cerebellum. All mossy fibres are glutamatergic, but in the vestibular cerebellum many of the fibres also contain acetylcholine and both granule cells and the deep cerebellar nuclei express both nicotinic and muscarinic acetylcholine receptors (Barmack et al., 1992a; Jaarsma et al., 1997; Takayasu et al., 2003). The firing frequency of Purkinje cells in the vestibular cerebellum appears lower than in other areas of the cerebellum (personal observation). Because of the position of the

vestibular cerebellum (lobe IX and X are located on the dorsal edge of the cerebellum, directly above the brainstem and the paraflocucllus in the rat is located in a small pocket of the temporal bone of the skull) if it very difficult to make *in vivo* recordings. However field recordings have shown that Purkinje cell activity (both simple and complex spike) is linked to head motion (Kano et al., 1991; Barmack and Shojaku, 1992).

Chapter 2: Materials and Methods.

2.1 - Immunohistochemistry

2.1.1 – Solutions for immunohistochemistry.

TST - Tris 1.21 g/l, NaCl 5.84 g/l and Tween 0.5 ml/l; adjusted to pH 7.5 with 1M HCl.

TST + Marvel - As TST but with 5 % Marvel milk powder.

Dissection aCSF - NaCl 124 mM, $MgSO_4$ 1.3 mM, KCl 5 mM, $CaCl_2$ 2.4 mM, KH_2PO_4 1.2 mM, $_D$-glucose 10 mM and $NaHCO_3$ 26 mM.

PBS - NaCl 8 g/l, KCl 0.2 g/l, Na_2HPO_2 1.15 and KH_2PO_4 0.2 g/l (made up by media prep, University of Warwick)

PFA - PBS with 4% paraformaldehyde (The paraformaldehyde was dissolved by heating the mixture to reflux whilst stirring).

Immuno PBS - PBS with 0.4% Triton 100 and 1% BSA

2.1.2 – Antibodies for immunohistochemistry

Rabbit anti-CART (55-102) (rat) serum - came as lyophilized powder (Phoenix Pharmaceuticals, Inc). Made up to 50µl with distilled water and then frozen (-20°C) as 1µl and 5µl aliquots until required.

Monoclonal anti-calbindin D-28K (mouse IgG1 isotype) – came as a solution in PBS with 15 mM sodium azide (Sigma). Stored frozen as 1 µl and 5 µl aliquots until required.

Rabbit anti-CRF(H-104) IgG – came as solution in PBS with <0.1% sodium azide and 0.1 % gelatine (Santa Cruz Biotechnology, Inc). Stored frozen as 1 µl and 5 µl aliquots until required.

Sheep anti-CRF(N-20) IgG – came as solution in PBS with <0.1% sodium azide and 0.1 % gelatine (Santa Cruz Biotechnology, Inc). Stored frozen as 1 µl and 5 µl aliquots until required.

Guinea-pig anti-VGluT2 (rat) IgG – (Chemicon). Stored frozen as 1 µl and 5 µl aliquots until required.

Goat anti-rabbit IgG, HRP conjugated – Stored frozen as 1 µl aliquots (Sigma Aldrich)

Donkey anti-goat IgG, HRP conjugated – Stored frozen as 1 µl aliquots (Sigma Aldrich)

Alexa Fluor® antibodies (Invitrogen) – The probes used were raised in goat and donkey. Probes used against CART peptide antibody were raised against rabbit. Probes used against Calbindin-D-28K antibody were raised against mouse. Probes used against CRF antibodies were raised against rabbit or goat (goat and sheep antibody are 100 % cross-reactive). Probes used against VGluT2 antibody were raised against guinea-pig. The wavelengths used were 405 nm, 488 nm, 594 nm and 633 nm. These secondary antibodies were stored frozen as 2-5 µl aliquots.

CART peptide - (Pheonix Pharmaceuticals), rat long CART peptide fragment 55-102, rl CART (55-102). Stored frozen as 10 µl vials (100 µM).

2.1.3 – CART peptide dot blot.

A strip of Polyvinylidene fluoride (PVDF) membrane was wetted with methanol, then distilled water and then allowed to dry. Four concentrations (100 μM, 10 μM, 1 μM and 100 nM) of CART peptide solution were dotted (2 μl drops) onto the membrane and allowed to completely dry. The PVDF membrane was placed in a tube with sufficient TST + Marvel to cover it and then agitated for 1 hour at room temperature. The solution in the tube was replaced with one containing the CART peptide antibody (1:5000 in TST + Marvel) and then the tube was agitated over night at room temperature. The membrane was washed 5 times with TST. The solution in the tube was then replaced with one containing the secondary antibody (Goat anti-rabbit IgG – HRP conjugated 1:2500 in TST + Marvel) and the tube was then agitated for 1 hour at room temperature. The membrane was washed 5 times with TST. The membrane was incubated in a 1:1 mixture of luminol and hydrogen peroxide from an enhanced chemiluminescence kit (EZ-ECL Chemiluminescence Detection Kit; Biological Industries Ltd.). The membrane was then dried, wrapped in cling film and under dark conditions, fixed to a photographic film (Kodak BioMax XAR) and exposed for 10 seconds, moved and exposed for 30 seconds. Finally, the photographic film was then developed.

2.1.4 – CRF dot blot.

A similar protocol was used for the CRF dot blots as for the CART peptide dot blots (section 2.1.3). Four squares of membrane were used, and onto each were dotted 4 drops (5 µl) of 100 µM CRF (Sigma Aldrich) onto the same spot. Two of the pieces of membrane were incubated in a solution of rabbit anti-CRF(H-104)(human) serum (1:500) and the other 2 pieces were incubated in a solution of goat anti-CRF(N-20)(human) serum (1:500). The secondary antibodies used were goat anti-rabbit IgG, HRP conjugated and donkey anti-goat IgG, HRP conjugated (1:2500). The membranes were treated in the same way with the EZ-ECL kit but exposed to the photographic film for 30 and 90 seconds

2.1.5 – Preparation of tissue for fluorescence immunohistochemistry.

In accordance with the Animals (Scientific Procedures) Act (1986) male Wistar rats were killed by cervical dislocation and decapitated. Either the whole brain or just the vermis of the cerebellum was rapidly dissected out while washing with ice-cold aCSF (bubbled with 95 % O_2/ 5 % CO_2). The block of brain was placed directly into ice cold PFA and fixed at 5°C over night. On the following day, the tissue was washed 3 times in PBS, and in the case of young animal brains (or when coronal sections were required), the block of tissue was mounted in 2 % agar (Sigma). The tissue or agar block (containing tissue) was trimmed and glued to a cutting chamber filled with ice cold dissection aCSF. Slices (100-125 µm) were cut using a vibratome (HM 650V;

Microm). Individual slices were placed into wells of a 24 well plate with approximately 1 ml of PBS in each well.

2.1.6 – Single antibody stain.

In some experiments, the tissue was only stained with one antibody: either CART peptide or calbindin D-28K. In this case, the PBS was removed from each well and replaced with 450µl of a 10 % solution of normal goat serum in immuno- PBS. This was incubated (with agitation) for one hour at room temperature. The solution was removed and the slices washed 3 times with PBS. Primary antibody (1:1000) in immuno-PBS (200 µl) was added to each well, agitated at room temperature for 1 hour, then incubated at 5°C overnight. The primary antibody solution was removed and kept at 5°C for a maximum of 14 days. The solution of primary antibody was used a maximum of 3 times with no loss of activity, although before use the solution was filtered to remove any particulate matter. The slices were washed 5 times with PBS. Secondary antibody solution (300 µl, 1:300 in immuno-PBS) was added to each well and agitated at room temperature for 4 hours. The secondary antibody solution was removed and discarded. The slices were washed 5 times with PBS. The slices were mounted on glass slides with glass coverslips in VectaShield mounting median (Vector laboratories) and then viewed.

2.1.7 – Double antibody stain.

Double stain experiments where carried out for: CART peptide and calbindin D-28K, CRF peptide and calbindin D-28K, and VGluT2 and calbindin D-28K. All primary antibodies were used at 1:1000 except the CRF antibody which was used at 1:100. In all experiments, calbindin D-28K staining was used as a positive control.

A similar protocol was followed as for the single stain experiments except that the solutions of primary antibodies contained two antibodies and the solutions of secondary antibodies contained two different secondary antibodies, raised against the animals used for the primary antibodies with different wavelength responses (488 nm and 594 nm). In the case of the experiment using the antibody against CRF, horse serum was used instead of normal goat serum.

2.1.8 – Triple antibody stain.

The triple stain protocol was only used for CART peptide, calbindin D-28K and VGluT2. A similar protocol to that of the single and double staining experiments was used, only all three antibodies were applied together. The wavelengths of the secondary antibodies used were 405 nm against the mouse (for calbindin D-28K), 488 nm against guinea-pig (for VGluT2) and 633 nm against rabbit (for CART peptide). For these experiments, the slices were mounted within 24 hours.

2.1.9 – Immunohistochemistry controls.

During the antibody staining experiments outlined above, one or two slices were always used as negative controls: the primary antibodies were omitted and replaced with immuno-PBS. I also carried out some additional controls: to eliminate the possibility of cross reaction between antibodies in multiple staining experiments and; tested the specificity of the CART peptide antibody, by preabsorbing it with CART peptide. Eighteen slices were taken, and placed in 6 columns of 3 wells. The same procedure was carried out for all the wells in each column, thus giving 3 repeats of each experiment. As a positive control, the triple stain protocol (CART peptide, calbindin and VGluT2) was applied to the slices in the first and sixth columns. The triple stain protocol was also carried out on the slices in the second column but 1μM CART peptide was present. The triple stain protocol was carried out on slices in the third, fourth and fifth columns but a single primary antibody was missing from each column, CART peptide (column 3), calbindin D-28K (column 4) and VGluT2 (column 5). The same secondary antibody solution was applied to all wells (as section 2.2.5). An additional control experiment was carried out to check that the fluorescence observed originated from the binding of secondary antibodies: primary antibodies were applied to six slices and the secondary antibody step was omitted.

2.1.10 – Fluorescence and Confocal microscopy

Lower magnification images showing distribution of staining were acquired with a Lecia MZ FIII upright microscope. Confocal images were acquired using the Lecia

SP2 confocal system linked to a Lecia DM RE7 upright microscope. For multiple stainings the response of the photodiodes was set to minimise cross contamination between signals. Most images were made from stacks for confocal sections; these were made by performing maximal averages of thin slices. The number of sections taken for a stack varied based on thickness of stack, but was chosen to be as close as possible to the maximum effective number (calculated as stack thickness divided by optical slice thickness). For very thick stacks were fine details was not necessarily required the number of sections in the stack was significantly lower than the maximum to reduce the time taken to acquire them. Figure were prepared using Adobe Photoshop CS.

2.2 - Electrophysiology

2.2.1 – Solutions for cell electrophysiology.

Dissection aCSF - NaCl 124 mM, $MgSO_4$ 1.3 mM, KCl 5 mM, $CaCl_2$ 2.4 mM, KH_2PO_4 1.2 mM, $_D$-glucose 10 mM and $NaHCO_3$ 26 mM.

aCSF - NaCl 124 mM, KCl 1.9 mM, KH_2PO_4 1.2 mM $CaCl_2$ 2.4 mM, $MgCl_2$ 1.3 mM , $_D$-glucose 10 mM and $NaHCO_3$ 26 mM. Osmolarity of 310-320 mOsm.

CsCl internal - CsCl 130 mM, $MgCl_2$ 2 mM, $CaCl_2$ 1 mM, Cs EGTA 10 mM, Cs HEPES 10 mM and Na_2 ATP; adjusted to pH 7.2 with 1M CsOH and the osmolarity was adjusted to 300 mOsm with sucrose.

KGluc internal - K D-gluconate 135 mM, NaCl 7 mM, HEPES 10 mM, EGTA 0.5 mM, Na_2 ATP 2 mM, Na_2 GTP 0.3 mM and 10 mM Na phosphocreatine; adjusted to pH 7.2 with KOH and the osmolarity was adjusted to 300 mOsm is sucrose.

KGluc/Cl internal - KCl 70 mM, K D-gluconate 60 mM, $MgCl_2$4 mM, Na_2 ATP 4 mM, Na_2 GTP 0.4 mM, and HEPES 10 mM; adjusted to pH 7.2 with KOH and the osmolarity was adjusted to 300 mOsm is sucrose.

2.2.2 – Slice preparation for electrophysiological recording

In accordance with the Animals (Scientific Procedures) Act (1986) male Wistar rats (postnatal days 20-35) were killed by cervical dislocation and then decapitated. The vermis of the cerebellum was rapidly removed into ice cold dissection aCSF (bubbled with 95 % O_2/ 5 % CO_2). The tissue was glued onto the cutting stage of a microtome (HM 650 V; Microm) and covered with ice cold dissection aCSF (bubbled with 95 % O_2/ 5 % CO_2). Typically 6-8 slices (250 μm) were cut from each adult rat. Slices were stored in recording aCSF (continually bubbled with 95 % O_2/ 5 % CO_2) at room temperature for a minimum of one hour before recording.

2.2.3 – Set up for recording of electrical properties of Purkinje cells.

Individual slices were viewed on a Zeiss FS Axioskop microscope with a 40X water immersion objective and Normaski differential interference optics at a total magnification of 640X. Slices were held down with a platinum harp, maintained at

either 22-24°C (room temperature) or 30-32°C and continually perfused with recording aCSF (bubbled with 95 % O_2/ 5 % CO_2). The perfusion system consisted of a heating element (controlled by a temperature regulator via a thermocouple in the bath), a dripper, flow regulator and a multi-tap array fitted with multiple syringe barrels. The aCSF entered the bath by gravity and was sucked out of the bath by a peristaltic pump (Watson Marlow) via a capillary tube. The perfusion rate was set to one drop every two seconds, which was approximately 1 ml/min. The bath volume was between 1 to 2 ml. Experiments using a dye (Fast Green) showed that the time taken for the aCSF to reach the bath from the multi-tap array was 2-3 minutes, and the aCSF in the bath was completely exchanged after 4 minutes. The bath temperature was recorded during experiments to ensure it stayed constant.

Recordings were made using either a Patch Clamp EPC8 (HEKA) or Axopatch 200A (Axon Instruments) amplifier. The signal from the amplifier was digitised on-line by a Digidata 1322A (Axon Instrument) controlled by Clampex 8.0 software (Axon Laboratories). Synaptic currents were evoked by a DS2A MKII stimulator (Digitimer Ltd.) controlled by a Master 8 stimulator (Intracel) via a thin walled patch-pipette filled with aCSF positioned on the surface of the slice.

2.2.4 – General procedures for patch clamp recordings.

Cell attached and whole cell patch clamp recordings were made from the soma of superficially located Purkinje cells (identified by position in the slice and characteristic morphology) in the vestibular cerebellum (lobes IX and X). Recording pipettes were pulled from thick-walled borosilicate glass capillaries (GC150F;

Harvard Apparatus) on a horizontal puller (P-97; Shutter Instruments) and then fire-polished. For stimulating synaptic currents, stimulating pipettes were pulled from thin-walled borosilicate glass capillaries (GC150TF; Harvard Apparatus), the tips broken and fire polished to remove sharp edges.

2.2.5 – Cell attached recording.

Patch pipettes were filled with aCSF and had resistances of 2-10 MΩ. After establishing a cell attached recording, if the seal resistance was less than 50 MΩ or greater than 1GΩ then the recording was discarded. Recordings with a seal resistance outside this range tended to be either unstable or the recorded action potentials had a low amplitude making analysis difficult. The data was filtered at 5 kHz and sampled at 5 kHz. Age of the rats used was 20-35 days postnatal (P20-35).

2.2.6 – Climbing fibre excitatory post synaptic currents (EPSCs)

Climbing fibre EPSCs were recorded with CsCl filled patch-pipettes which had resistances of 4-8 MΩ. The series resistance (5.7 ± 0.4 MΩ) and capacitance (35.8 ± 4.2 pF) were compensated by 70 %. The stimulation pipette was placed in the granule cell layer near to the Purkinje cell being recorded from. EPSCs were evoked with alternate and single pairs of square voltage pulses of 200 μs duration and 10-50 V amplitude. EPSCs were recorded using Clampex 8.0., with the stimulus artefact used to trigger acquisition. EPSCs were filtered at 5 kHz and sampled at 20 kHz. To isolate

climbing fibre EPSCs, recordings were made in the presence of 10 μM bicuculline. Age of the rats used was P15-21.

2.2.7 – Parallel fibre excitatory post synaptic currents (EPSCs)

Parallel fibre EPSCs were recorded with CsCl filled patch pipettes which had a resistance of between 4-8 MΩ. Resistance (4.7 ± 0.2 MΩ) and capacitance (9.7 ± 1.5 pF) were compensated by 70 %. The stimulation pipette was placed in the molecular layer near to the Purkinje cell being recorded from. EPSCs were evoked with alternate and single pairs of square voltage pulses of 200 μs duration and 10-50 V amplitude. EPSCs were filtered at 5 kHz and sampled at 20 Khz. EPSCs were recorded using Clampex 8.0., with the stimulus artefact used to trigger acquisition. To isolate parallel fibre EPSCs, recordings were made in the presence of 10 μM bicuculline. Age of the rats used was P15-21.

2.2.8 – GABAergic miniature inhibitory postsynaptic currents (mIPSCs).

GABAergic mIPSCs were recorded with patch pipettes filled with CsCl internal solution with resistances of 4-8 MΩ. Resistance (19.8 ± 2.6 MΩ) and capacitance (8.0 ± 0.9 pF) were compensated by 70 %. Miniature IPSCs were filtered at 5 kHz and sampled at 20 kHz and were continuously recorded using a roll mode protocol (Clampex 8.0). Miniature IPSCs were recorded in 0.5 μM tetrodotoxin and in the presence of the glutamate receptor antagonist kynurenic acid. Under these recording

conditions (symmetrical chloride, at a holding potential of -70 mV), mIPSCs were inward. Age of the rats used was P20-24.

2.2.9 – Current clamp roll mode.

Current clamp recordings from Purkinje cells were made using KGluc filled patch-pipettes with resistances of 4-8 MΩ. Data was sampled at 20 kHz using a roll mode protocol (Clampex 8.0). Routinely, 7 minute sessions of roll mode recording were interspersed with the periodic recording of current-voltage relationships. Age of the rats used was P20-26.

2.2.10 – Current clamp current-voltage relationships.

There were two different protocols for acquiring current voltage relationships. The method used for sections 4.6.1-2 was 10 current steps starting at -450 pA and increasing by 50 pA each successive step. The step length was 1 second and the interval between steps was 5 seconds. The current voltage relationship protocol used in section 4.6.3 was different because the 10 currents steps started at -300 pA and increased by 100 pA each time. Age of the rats used was P20-26.

2.2.11 – LTD protocol.

The same protocol was used as to acquire parallel fibre EPSCs with the modification that KGluc/Cl internal solution (Kimura et al., 2005) was used in the patch pipette. Resistance (14.4 ± 1.5 MΩ) and capacitance (15.1 ± 2.0 pF) were compensated by 70 %. Age of the rats used was P15-20.

2.2.12 – Drugs used in recordings

CART peptide - (Pheonix Pharmaceuticals), rat long CART peptide fragment 55-102, rl CART (55-102).

Bicucuclline - (Trocris), bicuculline methyiodide.

CNQX - (Trocris), 6-cyano-7-nitroquinoxaline-2,3-dione.

Kynurenic acid - (Sigma Aldrich)

Zolpidem - (Sigma Aldrich)

TTX - (Alomone), tetrodotoxin.

2.3 – Data Analysis

2.3.1 – Analysis of cell attached firing rate.

The initial analysis of Purkinje cell firing rates was carried out using Mini Analysis software (v 6. Synaptasoft Inc). Action potentials were recorded by the crossing of a manually set threshold. Analysis was semi-automatic with any detection of noise or missed action potentials corrected by the operator. The output of Mini Analysis

consisted of the time of occurrence of each action potential. This was converted to an Excel (Microsoft) file and imported into Excel. The data was first sorted so all the events were sequential (any missed events are added to the end of the Mini Analysis file and so are out of order). Then the time interval between successive action potentials and the instantaneous frequency (inverse of the event interval) were calculated. Events per second were calculated using the histogram function in Origin (v 6.1 Microcal). Once the instantaneous frequencies had been calculated they were sorted numerically and events with an instantaneous frequency of zero (double detection of the same event) or above 500 Hz (these events are too fast to be real) were deleted from the data. Histogram plots and cumulative frequency plots were all produced using Origin. The mean, standard deviation, number of events, standard error of the mean, coefficient of variance, 5 % value, 25 % value, median, 75 % value and 95 % value were all calculated with Excel. Statistical Significance, unless otherwise stated, was calculated with the student t-test (Excel).

2.3.2 – Analysis of EPSCs.

Both parallel fibre and climbing fibre EPSCs were analysed with Clampfit (v 8.0 Axon Laboratories). Amplitudes and 10-90 % rise times were measured from individual EPSCs and then averaged. Decay kinetics where calculated by fitting the decay of averaged EPSCs (aligned on stimulus artefact) with single or multiple exponentials. Minimising standard deviation (Clampfit) was used to determine whether the decay was best fitted by a single exponential or by the sum of two exponentials. The zero time point of the fitted exponentials was defined as the time at

the peak of the current. Weighted decays were calculated using the formula: tau(w) = (tau1xA1+tau2xA2)/(A1+A2), where tau1 and tau2 were decays constants and A1 and A2 were relative amplitudes. For paired EPSCs, the amplitude of the second EPSC was determined by subtracting the averaged and scaled single EPSC from each pair of EPSCs. The paired pulse ratio was then calculated as the ratio of the mean second and first EPSC amplitudes.

2.3.2 – Analysis of mIPSCs

Miniature IPSCs were semi-automatically detected (with a threshold of -20 pA) using Mini Analysis software. Events were identified as mIPSCs by a slower decay than rise. There was considerable heterogeneity in the time course of mIPSCs, with some having very slow rises (presumably because they arise from synapses on distal dendrites and undergo heavy filtering). Thus to simplify analysis, currents with a 10-90 % rise time longer than 3 ms were excluded from analysis (Wall, 2005).The time of mIPSC occurrence, mIPSC amplitude and 10-90 % rise time were measured for each individual mIPSC. Instantaneous frequency was calculated in the same way as for Purkinje cell firing.

2.3.3 – Analysis of current clamp current-voltage data.

The current voltage relationships (IVs) were analysed using Clampfit 8.0. Current voltage relationships for Purkinje cells have a characteristic shape: injection of

negative current produces a rapid hyperpolarisation followed by a slow "sag" back up towards the baseline (for example see figure 4.22C in chapter 4). This sag results from the slow activation of the hyperpolarisation activated current, I_h. Thus to fully describe this IV relationship, the membrane potential change in response to negative current injection has to be measured at two points: firstly, at the beginning of the current step (*initial*, before activation of I_h) and secondly at the end of the step (*steady state*, after I_h activation). It was necessary to adjust both these values to compensate for the voltage drop across the seal resistance. This was done by measuring the instantaneous jump in membrane potential at the end of the current step and deleting this value from the membrane potentials. The *initial* membrane potential was plotted against current injected to calculate the resting membrane potential and membrane resistance (intersect and gradient respectively). The *steady state* membrane potential was subtracted from the *initial* membrane potential to give the potential produced by activation of the hyperpolarisation activated current, I_h. Changes in the *initial, steady state* and I_h potential were used to investigate possible effects of CART peptide on Purkinje cell electrical properties. By plotting the I_h potential against injected current then the I_h conductance was calculated as the inverse of the gradient; the intersect with the y-axis gives the size of the I_h current at rest.

Injection of positive current steps causes the Purkinje cell to fire action potentials. By plotting the number of action potentials fired during each current step against the amount of current injected, the excitability of the Purkinje cell can be calculated. The gradient of this line gives the excitability: frequency of action potentials (Hz)/current injected (pA). By normalising this value to the membrane resistance it is possible to remove any effects of differences in membrane resistance between Purkinje cells. The X-intersect of this line gives the firing threshold (in pA), and this can be

converted to firing threshold in mV by multiplying by the membrane resistance and adding the resting membrane potential.

2.4 – Statistical methods.

Most of the statistical methods used were standards and were calculated in either excel, origin or graphpad instat. However the product moment correlation was calculated was calculated by hand using the equation:

$$r = \frac{\sum (x - \bar{x})(y - \bar{y})}{n\sigma_x \sigma_y}$$

The degrees of freedom were equal to n-2 and significance tested using statistical tables (Campbell, 1989).

Were median values were used (firing rate) then significance was calculated either using Wilcoxen t-test, for paired data, or Krustal-Wallis test, for unpaired data. For a worked example of Wilcoxen t-test on firing rate data see appendix 1. The upper and lower quartiles were used to indicate the confidence interval for the median and were tabulated after the median in the format (lower quartile, upper quartile).

Chapter 3: Distribution of CART peptide in the Cerebellum.

3.1 – Introduction.

The extensive study of CART peptide distribution by Koylu *et. al* in 1997 identified that a CART peptide fragment is present in the adult rat cerebellum. Their staining study showed that CART peptide was only present in fibres in the parafloccus and nodulus, areas of the vestibular cerebellum, no staining was observed in cell bodies and no CART mRNA was detectable in the cerebellum.

I have used an antibody against CART peptide to fully characterise the distribution and development of CART peptide expression in the cerebellum. By combining CART peptide antibody staining with other antibodies, I have investigated the specific cellular localisation of CART peptide. This has helped me to localise the regions of the cerebellum where CART peptide is most likely to have a signalling role and thus aided my physiological experiments.

3.2 – Reactivity of CART peptide antibody to CART peptide.

To check the effectiveness of the antibody against CART peptide, I performed a dot blot experiment using an antibody raised against rat long CART peptide fragment 55-102 (Phoenix Pharmaceuticals) together with the rat long CART peptide fragment 55-102 (Serotec) (fig 3.1). Four different concentrations of CART peptide where dotted onto a PVDF membrane and reacted with the CART peptide antibody (1:5000). Using Enhanced Chemo Luminescence the antigen was still detectable with a dot of 2

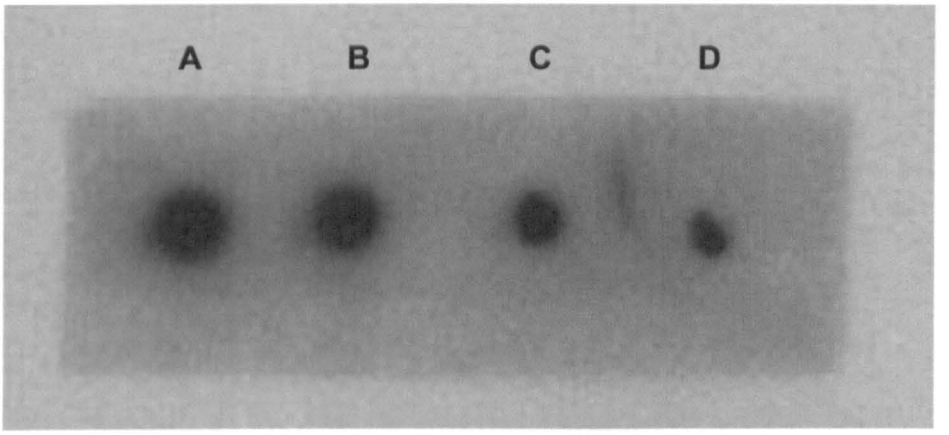

Figure 3.1 Dot blot illustrating sensitivity of CART peptide antibody. PVDF membrane dotted with 2µl of rlCART(55-102) peptide solution A-100µM, B-10µM, C-1µM and D-100nM. Treated with 1:5000 rabbit anti-rlCART(55-102). Membrane developed using ECL and exposed on photographic film for 10s. Figure twice actual size.

μl of 100 nM CART peptide. The dots were less than 2 mm across giving a lower detection limit of 64 nmol/m^2.

The membrane only required a 10 second exposure to visualise the CART peptide dots, longer exposures resulted in the development of the area outside the dot. This was probably due to a low level of non-specific antibody (primary or secondary) binding directly to the PVDF membrane.

3.3 – Localisation of CART peptide in parasaggital section of the cerebellum.

Having established that the CART peptide antibody is effective at detecting CART peptide, parasagittal vermal sections from 6 adult rats' (postnatal days 28-42) cerebella were stained for CART peptide (fig 3.2). As previously reported (Koylu et al., 1998) CART peptide had a distinct expression pattern being localised to distinct vermal lobes. By convention vermal lobes are numbered from 1 to 10 (I to X, see figure 3.2a). Slices showed densities of CART peptide positive staining only in lobe X and in the ventral region of lobe IX adjacent to lobe X. The CART peptide staining was in the molecular layer, in fibre like structures and not in cell bodies. Little or no staining was detected in the granule cell or Purkinje cell layers, or in any structures in the white matter of the cerebellum. Not all the parasagittal slices were positive for CART peptide (in some slices there was no CART peptide expression). The positive slices were grouped together in the lateral or medial regions of the vermis.

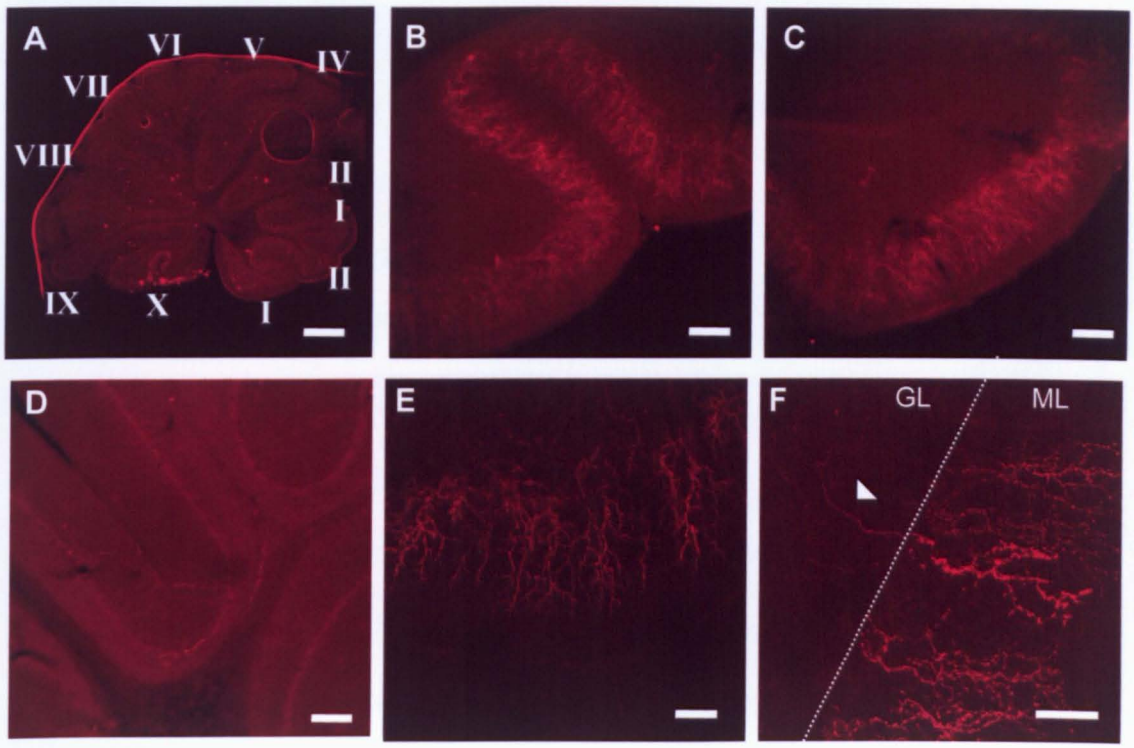

Figure 3.2 CART peptide staining in cerebellar parasaggital slice.
Parasaggital sections (125µm) from adult rat cerebella (A-D P32, E P48, and F P28) stained for CART peptide (red). A-D images aquired on Ziess upright fluorescence microscope E-F on Lieca confocal microscope. A- Low magnification image of a slice from the centre of the vermis. There was only staining in the molecular layer of lobe X (nodulus). B,C – Higher magnification of lobe X shows that the CART peptide positive structures were a dense matting of fibres and no cell bodies. D – Outside of lobe X, lobe VII, there were no CART peptide positive structures. E – Stack of confocal images (20µm) shows CART peptide was only present in fibres in the molecular layer. F - Stack of confocal images (10µm) shows the fibres containing CART peptide (white triangle) originate outside of the molecular layer (ML) and pass through the granule cell layer (GC). Scale bar A 400µm, B-F 40µm

3.4 – Banded distribution of CART peptide in coronal sections of the cerebellum.

In the cerebellum some peptides are found in parasagittal bands (Leclerc et al., 1992); the observation that CART peptide is not present in all the parasagittal sections could be the result of such a banded distribution. To investigate this, coronal sections from 4 adult rats (postnatal day 30-42) cerebella were stained for CART peptide (fig 3.3). CART peptide positive structures were only found in the centre of the vermis or at the lateral edges, forming 3 distinct bands of CART peptide positive fibres within lobes IX and X. This banding of CART peptide is consistent with my previous observation that CART peptide is only expressed in either the medial of the lateral regions of the vermis. There was no CART peptide staining observed in the cerebellar hemispheres. Lobes IX and X of the cerebellum, together with the paraflocculus (two small lobes on the posterior border of the cerebellum) make up the vestibular cerebellum. To investigate whether CART peptide is expressed in the paraflocculus coronal sections of the paraflocculus from 2 adult rats (postnatal day 30-42) cerebella were stained for CART peptide (fig 3.4). CART peptide containing fibres were observed in the molecular layer of the paraflocculus, suggesting that CART peptide is expressed in all regions of the vestibular cerebellum.

3.5 – CART peptide is not expressed in Purkinje cell dendrites.

Since the majority of the CART peptide staining was observed in the molecular layer, the cellular element expressing CART peptide must be within this layer. There are a number of different cellular components in the molecular layer: the dendrites of the

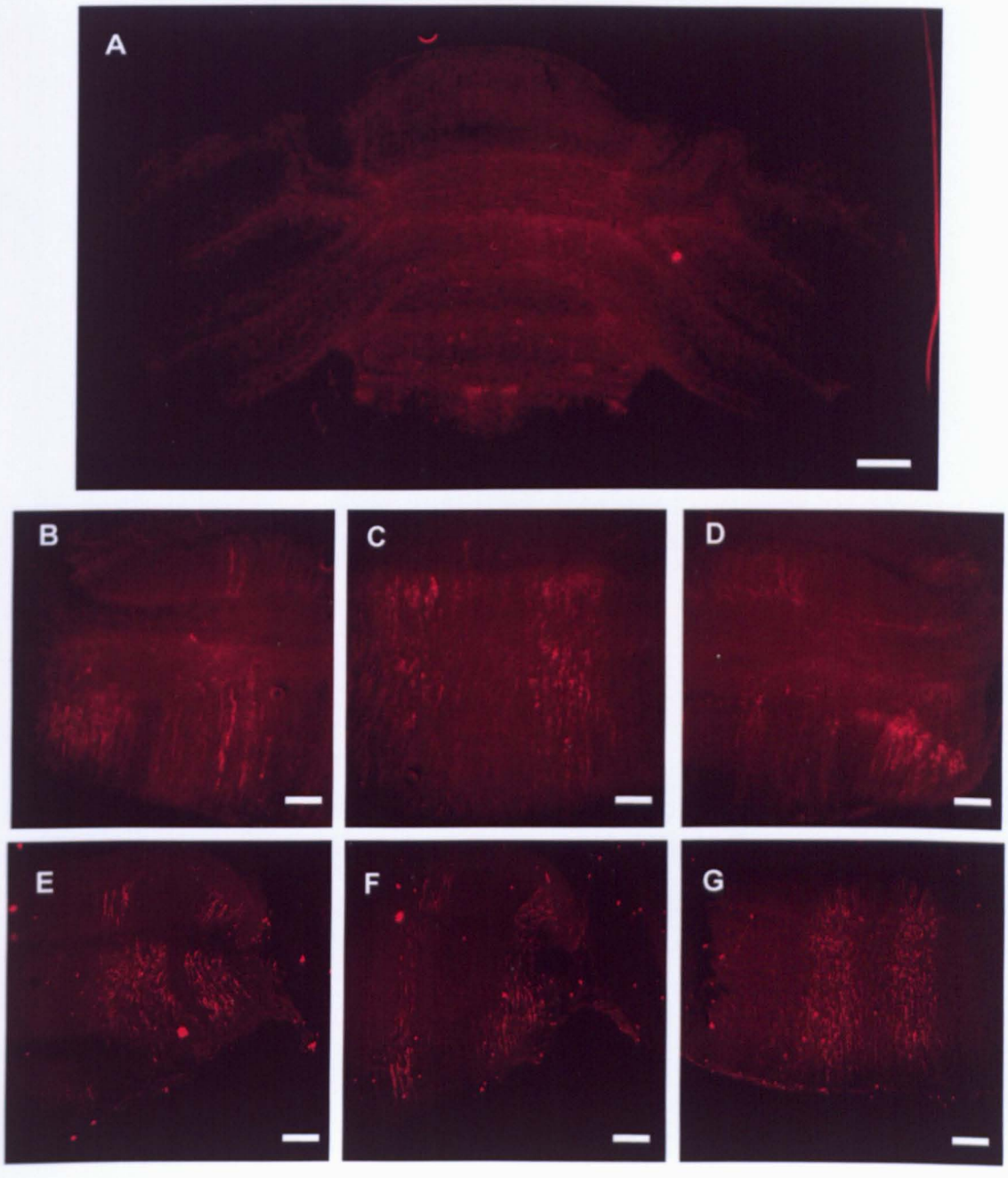

Figure 3.3 CART peptide staining in cerebellar coronal sections.
Coronal sections (125μm) from adult rat cerebella (A-D P52, E-G P48, and F P28) stained for CART peptide (red). A-D images aquired on Ziess upright fluorescence microscope, E-G on Lieca confocal microscope. A – At low magnification CART peptide positive structures were only observed in lobes IX and X. B-D – CART peptide positive fibres are only found in the centre and the lateral edges of the vermis. E-G – Stack of confocal sections (20μm) show similar concentration of CART peptide containing fibers in lobes IX and X, in the center and edges of vermis. Scale bars A 200μm, B-G 40μm

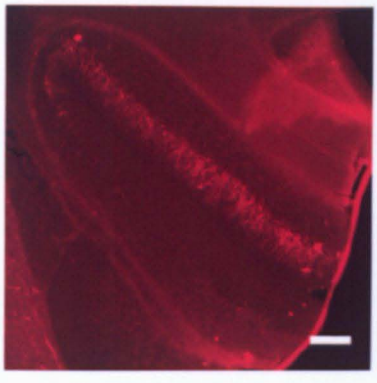

Figure 3.4 CART peptide staining on paraflocculus.
Coronal sections (125µm) from P42 rat paraflocculus stained for CART peptide (red). Paraflocculus showed dense CART peptide positive staining of fibres in the molecular layer. Scale bar 40µm

Purkinje cells, the climbing and parallel fibres, stellate cells and glia. To begin investigating which structures contain CART peptide, I used an antibody against a protein expressed exclusively in Purkinje cells, calbindin D-28K (calbindin). Calbindin is a calcium binding protein, in the cerebellum it is only found in Purkinje cells and is therefore a useful marker of Purkinje cell soma, dendrites and axon. Thus if CART peptide is expressed in Purkinje cell dendrites there should be co-localisation with calbindin.

Parasagittal vermal sections from 7 adult rats (postnatal day 28-42) cerebella were stained for calbindin. Purkinje cells in all the lobes of the cerebellum were stained (fig 3.5). Calbindin stained Purkinje cell dendrites (in the molecular layer), cell bodies and axons (in the granule cell layer). Using confocal microscopy, thin optical sections (2μm) revealed the complex structure of the Purkinje cell dendrites. Small unstained circular spaces in the molecular layer were observed. These are presumably the cell bodies of stellate cells, GABAergic interneurones, which do not express calbindin.

To investigate whether CART peptide and calbindin co-localise, parasagittal vermal sections from 6 adult rats (postnatal day 28-42) cerebella were stained for both CART peptide and calbindin (fig 3.6). Superficial examination suggested that CART peptide positive fibres did co-localise with the calbindin staining in Purkinje cells dendrites in lobes IX and X. However when viewed at a higher magnification (using confocal microscopy), thin optical sections of the molecular layer (2μm) revealed that the CART peptide positive structures were not Purkinje cell dendrites, but instead were structures associated with the surface of Purkinje cell dendrites. These structures could be synaptic boutons making contacts onto Purkinje cell dendrites suggesting a possible signalling role for CART peptide in the cerebellum.

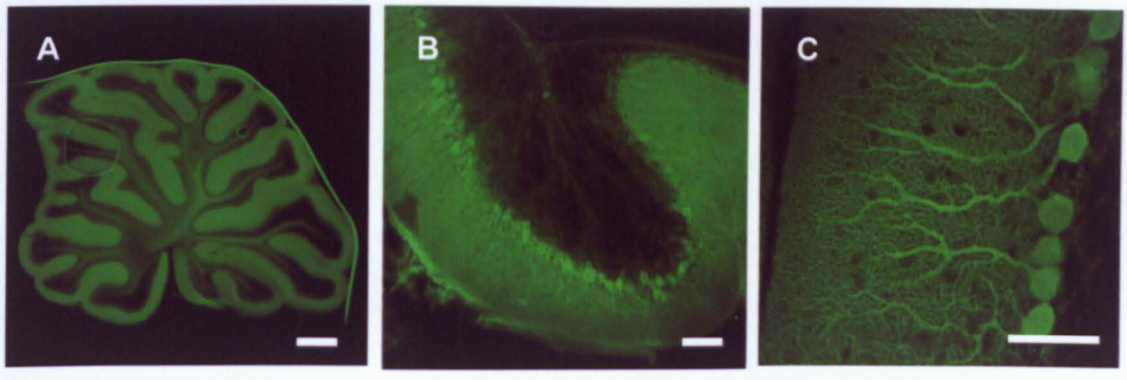

Figure 3.5 Calbindin staining in cerebellar parasaggital sections.
Parasaggital sections (125μm) from adult rat cerebella (A-B P37, C P30) stained for calbindin (green). A-B images aquired on Ziess upright fluorescence microscope C acquired on Lieca confocal microscope. A – At low magnification all of the lobes were stained for calbindin. B – The molecular layer (containing the Purkinje cell dendrites) was densely stained for calbindin and the Purkinje cell bodies were also visible. C – Stack of confocal images (4μm) shows the fine structure of the Purkinje cells and also small holes where presumably the cell bodies of the interneurons are located. Scale bar A 400μm, B-C 40μm

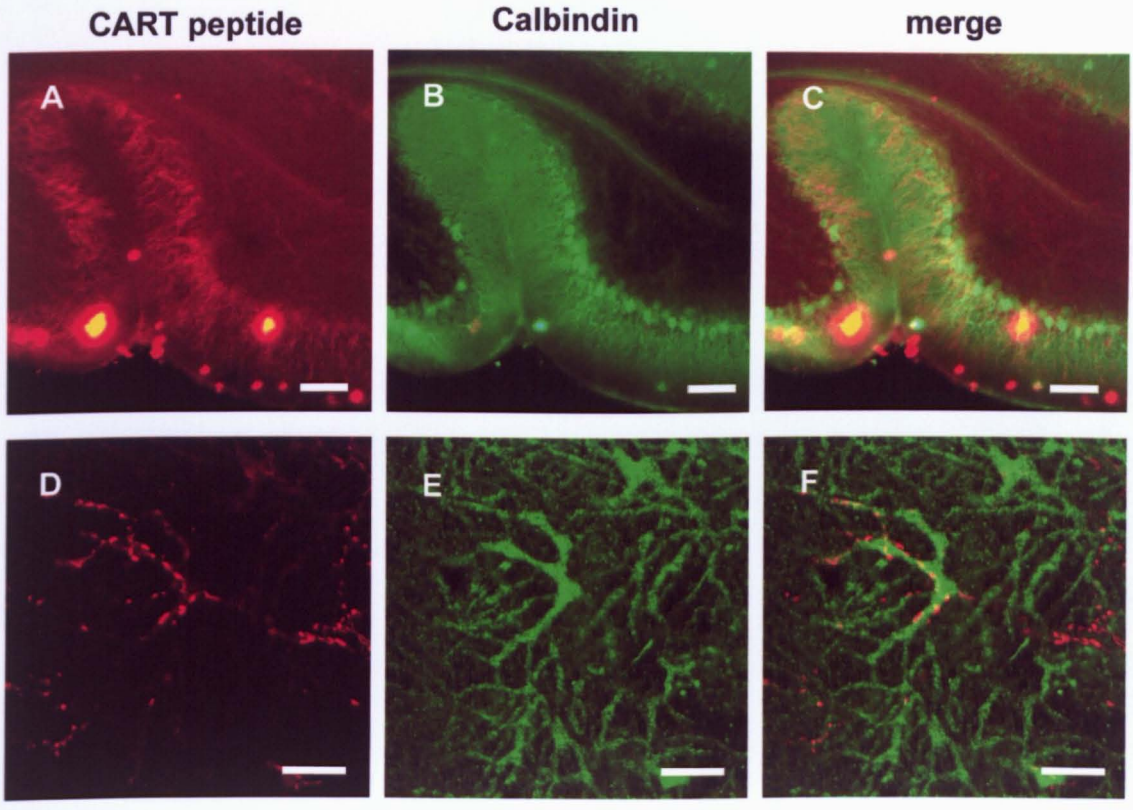

Figure 3.6 Double staining for CART peptide and calbindin.
Parasaggital sections (125μm) from adult rat cerebella (A-C P32, D-E P28) stained for CART peptide (red) and calbindin(green). Where both were present in the same structure they appear as yellow in merged images (C,F). A-C images aquired on Ziess upright fluorescence microscope D-F on Lieca confocal microscope. A-C – The molecular layer containing the Purkinje cell dendrites (green) also contain the CART peptide positive structures (red), and at low magnification these appear to colocalise (C – yellow). D-F – Stack of confocal sections (1μm) shows that CART peptide positive structure are not Purkinje cell dendrites, but are located in what appear to be pre-synaptic structures contacting the Purkinje cell dendrites. The bright structures in images A and C are non-specific binding of the antibody, possibly to dust particles. Scale bar A-C 40μm, D-F 16μm

3.6 – CART peptide in expressed in the inferior olive, source of the climbing fibres.

There are 3 different synapses onto Purkinje cell dendrites in the molecular layer: climbing fibres, parallel fibres and stellate cells. As neuropeptides are manufactured in the soma of neurones and transported down the axons, the soma should also contain CART peptide. However since no staining of either stellate cell or granule cell (parallel fibres are granule cell axons) bodies were observed, these are unlikely to be the sources of the CART peptide positive fibres. Climbing fibres are more likely to be the CART peptide positive fibres as their cell bodies lie outside the cerebellum, in the inferior olive, a nucleus in the medulla. Thus if CART peptide is expressed in climbing fibres, cell bodies in the inferior olive should be positive for CART peptide. To investigate the possibility that the CART peptide containing fibres in the cerebellum were climbing fibres, coronal sections from 3 adult rats (postnatal days 28-42) medullas were stained for CART peptide (fig 3.7). At low magnification the medulla showed dense CART peptide staining on its dorsal side, near the fourth ventricle, and also near the centre line on the ventral side, this is where the inferior olive is located. At higher magnification fibres and cell bodies containing CART peptide were observed. The inferior olive has several subdivisions and the area positive for CART peptide is most likely part of the medial accessory olive (MAO). The MAO projects fibres into the entire vermis and part of the paraflocculus, this includes the areas making up the vestibular cerebellum (Paxinos, 2004).

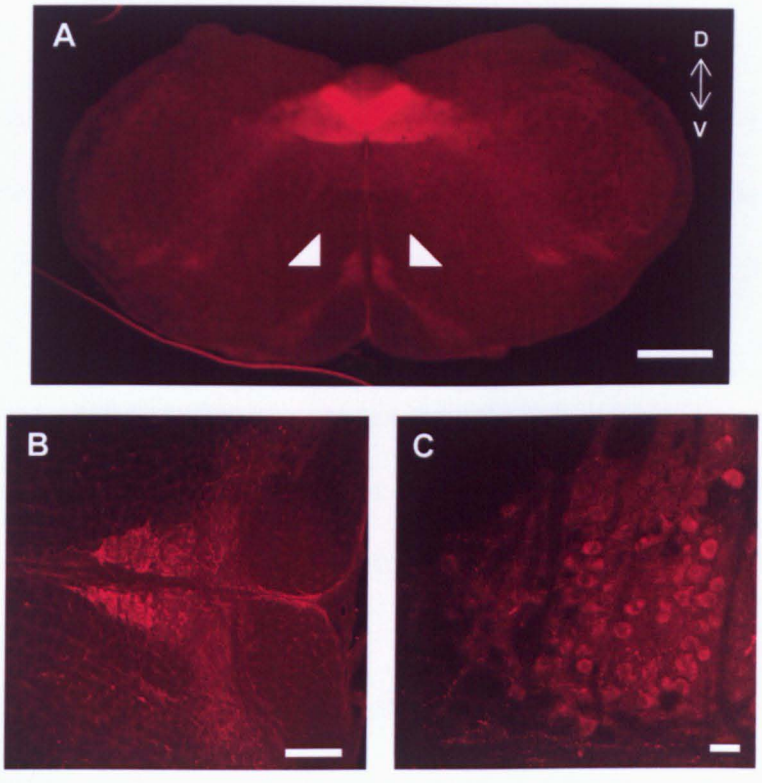

Figure 3.7 CART peptide staining of inferior olive.
Coronal sections (125μm) from P42 rat medulla stained for CART peptide (red). All images aquired on Ziess upright fluorescence microscope. A – Low magnification shows various densities of CART peptide in the medulla, however the area of interest in the inferior olive, a nucleus located medially and ventrally (white triangles). B – Only the medial accessory inferior olive (IOM) is positive for CART peptide. C – Both cell bodies and fibres in the IOM contain CART peptide. Scale bar A 500μm B 200μm C 20μm

3.7 –CART peptide expression mirrors climbing fibre development.

From the previous experiments it is reasonable to suggest that CART peptide is expressed in climbing fibres. Climbing fibres do not arrive in the cerebellum until the first postnatal week (Mariani and Changeux, 1981); therefore if CART peptide is only expressed in climbing fibres then none should be detectable in the cerebella of new born rats.

Parasagittal vermal sections from 2 new born rats (postnatal days 0-1) cerebella and medullas were stained for CART peptide and calbindin (fig 3.8). Because the layer structure of the cerebellum is not well defined at this young age, it is difficult to identify, with certainty, either the molecular layer or lobes IX and X. However no CART peptide was detected in any area of the cerebellum. However CART peptide containing cells were still observed in the inferior olive suggesting that although the climbing fibres have not yet innervated the cerebellum, CART peptide is still being produced.

If CART peptide is present in climbing fibres then CART peptide positive structure should be detected after the first postnatal week when climbing fibres have innervated Purkinje cells. To investigate, this parasagittal vermal sections from a postnatal day 10 rat cerebellum were stained for CART peptide and calbindin (fig 3.9). In these slices CART peptide containing fibres were present, consistent with CART peptide being expressed by climbing fibres.

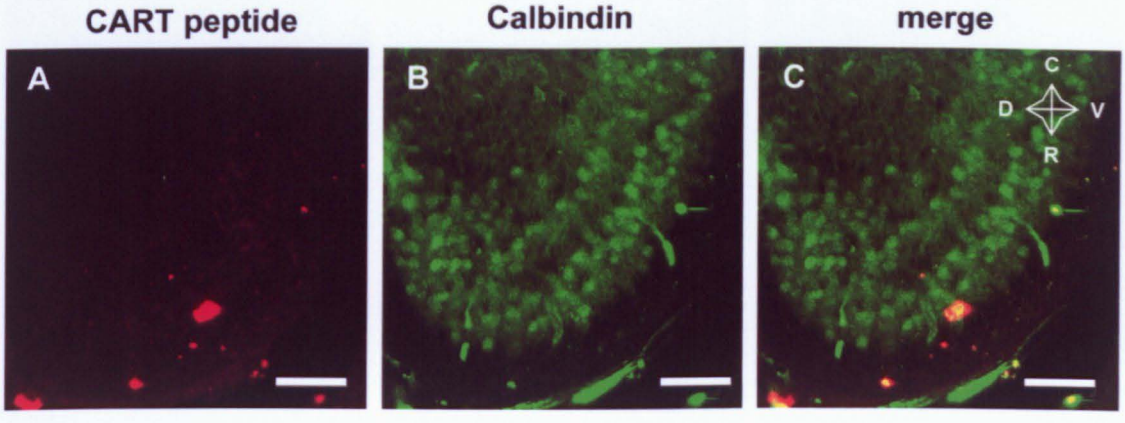

Figure 3.8 Double staining for CART peptide and calbindin in neonatal cerebellum. Parasaggital sections (125μm) from P1 rat cerebella stained for CART (red) and calbindin (green). All images aquired on a Lieca confocal microscope. A-C – Stack of concofocal sections (20μm) contained no CART peptide positive structure. The lobular structure of the cerebellum is not present in the neonatal cerebellum, how the ventral and ventral/rostral area contains the Purkinje cells which will become lobes IX and X. The bright structures in images A and C are non-specific binding of the antibody, possibly to dust particles. Scale bar 40μm

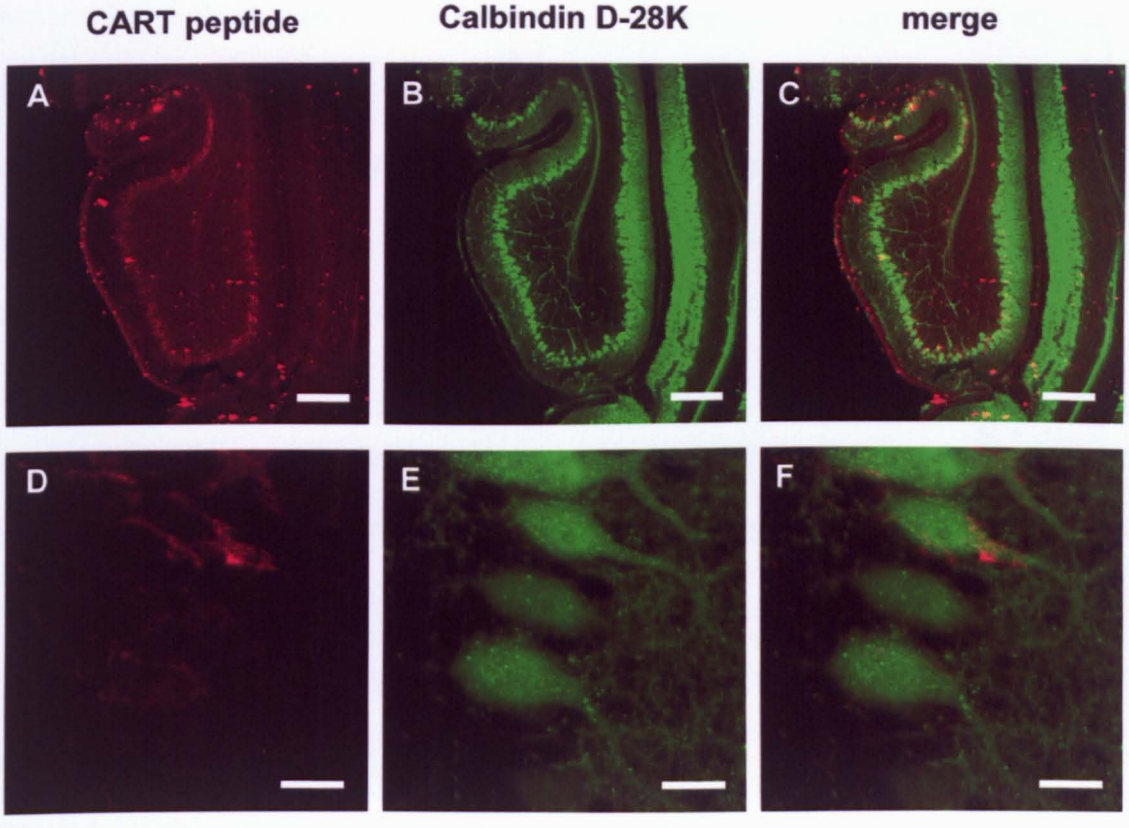

Figure 3.9 Double staining for CART peptide and calbindin in P10 cerebellum. Parasaggital sections (125μm) from P10 rat cerebella stained for CART (red) and calbindin (green). Where both were present in the same structure they appear as yellow in merged images (C,F). All images aquired on a Leica confocal micrcoscope. A-C – Stack of confocal sections (125μm), CART peptide positive structures are observed in the Purkinje cell layer of lobe X. D-F – At higher magnification (2μm thick stack of confocal sections) CART peptide positive structures appear to synapse onto the soma and proximal dendrites of Purkinje cells. Scale bar A-C 200μm, D-F 16μm

3.8 – CRF/CRH could not be used to localise CART peptide expression.

The presence of CART peptide in the inferior olive and the appearance of CART peptide containing fibres at the correct developmental stage is good evidence that CART peptide is present in climbing fibres. To confirm this, I used an antibody as a marker for climbing fibres and looked for co-localisation with CART peptide. Corticotropin-releasing factor (CRF, sometime called corticotropin-releasing hormone) is a widely distributed neuropeptide with roles in energy homeostasis and feeding, but it is also found in the inferior olive and in climbing fibres (van den Dungen et al., 1988). If CART peptide is in climbing fibres, then CRF staining should co-localise with CART peptide staining.

Two commercial antibodies against the neuropeptide CRF were obtained, one raised in rabbit and one in guinea-pig. These antibodies were tested for their effectiveness to detect CRF using the dot blot technique (fig 3.10). Using the rabbit antibody, it was not possible to detect a 10 µl dot of 1 mM CRF peptide (n = 2) thus this antibody is either in-active or has a very low affinity. In contrast, the same dot of CRF was detected by the guinea-pig antibody (n = 2). However a large concentration of antibody together with a long exposure time was required to visualise the CRF dot, suggesting that the antibody was not very effective at detecting CRF.

Parasagittal vermal sections from 2 adult rats (postnatal day 32-40) cerebella were stained for calbindin and CRF, using the guinea pig antibody (fig 3.11). Although clear calbindin staining was observed, no CRF positive structures were detected in any of the slices. This probably reflects the poor effectiveness of the antibody as previous studies have observed CRF staining in the cerebellum (Olschowka et al., 1982). Thus we were unable to use CRF as a marker for climbing fibres

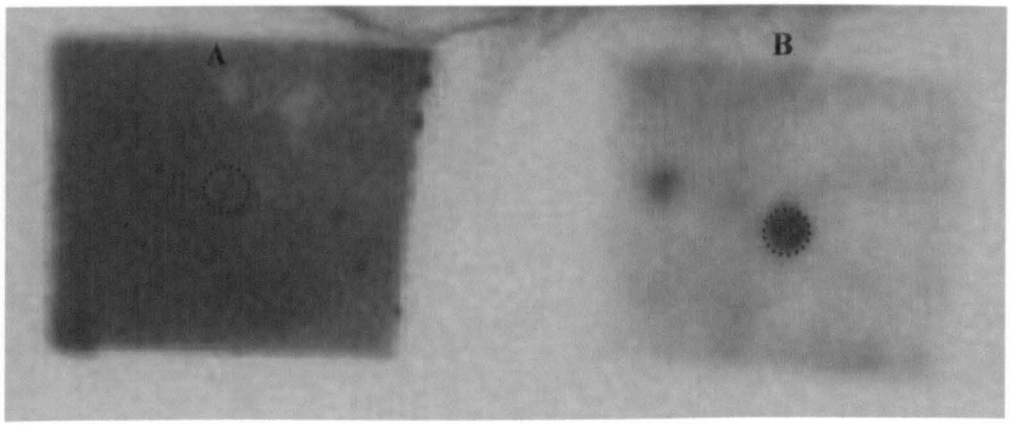

Figure 3.10 Dot blot test sensitivity of CRF antibody.
PVDF membrane dotted with 20µl of 100µM CRF solution (inside red circles). A was treated with 1:500 rabbit anti-CRF and B with 1:500 sheep anti-CRF. Membrane was developed using ECL and exposed on photographic film for 90s. A – High background staining is probably due to none specific binding on antibody to the membrane and not to the dot of CRF. B – Only area dotted with CRF has significant binding of CRF antibody, however long exposure time and high antibody concentration was required, suggests that the antibody has a low affinity for CRF. Figure twice actual size.

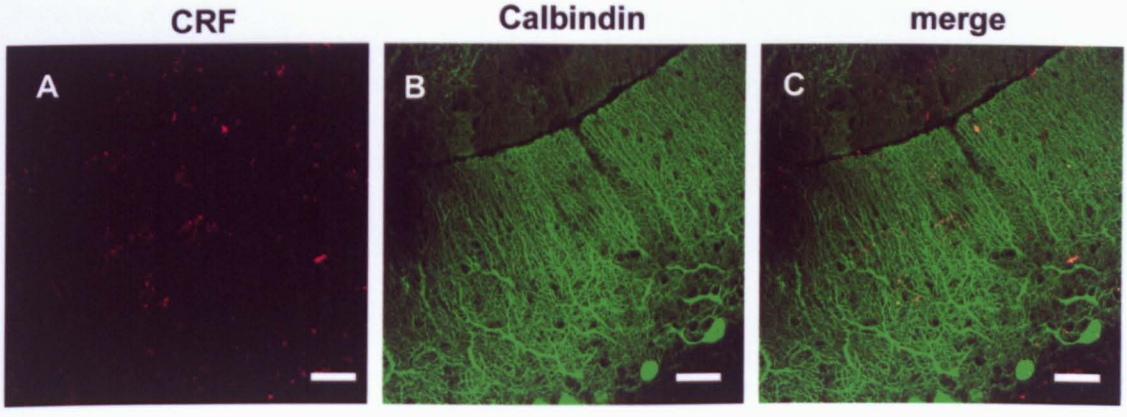

Figure 3.11 Double staining for CRF and calbindin.
Parasaggital sections from P41 rat cerebella stained for CRF (red) and calbindin (green). All images were acquired on a Lieca confocal microscope. A-C –Stack of concofocal sections (5μm) contain no CRF positive fibres. Scale bars 40μm

3.9 – CART peptide is co-localised with VGluT2, a climbing fibre-Purkinje cell synapse marker.

Climbing fibres release the neurotransmitter glutamate, which is packaged into vesicles by the vesicular glutamate transporter 2 (VGluT2). VGluT2 is only expressed in climbing fibres in the cerebellar molecular layer and thus can be used as a marker for climbing fibres (Hioki et al., 2003). Furthermore, because VGluT2 is localised in climbing fibre-Purkinje cell synapses, VGLUT2 is also a pre-synaptic marker for climbing fibre-Purkinje cell synapses. Thus if CART peptide is expressed in climbing fibre-Purkinje cell synapses there should be co-localisation with VGluT2. VGluT2 is also expressed in mossy fibre terminals, but as these are in the granule cell layer they will not obscure climbing fibre observation.

Parasaggital vermal sections from 3 adult rats (postnatal days 28-35) cerebella where stained for VGluT2 and calbindin (fig 3.12). In all of the lobes, VGluT2 positive fibres associated with Purkinje cell dendrites were observed in the molecular layer. In addition, mossy fibres also showed clear VGluT2 staining. The climbing fibres are also reported to make synaptic connections with basket cells (Llinás et al., 2004), however I was unable to observe any structures consistent with climbing fibre-basket cells synapses. There are no reports in literature of VGluT2 being present at the basket cell synapse, however this may be due to the high density of climbing fibre-Purkinje cell synapses masking them, or another glutamate transporter maybe be present at these synapses. When viewed using confocal microscopy, the pre-synaptic climbing fibre terminals were stained for VGluT2.

Parasagittal sections from 2 adult rats (post natal days 31-35) cerebella where stained for VGluT2, CART peptide and calbindin (fig 3.13-14). The fibres in lobes IX and X

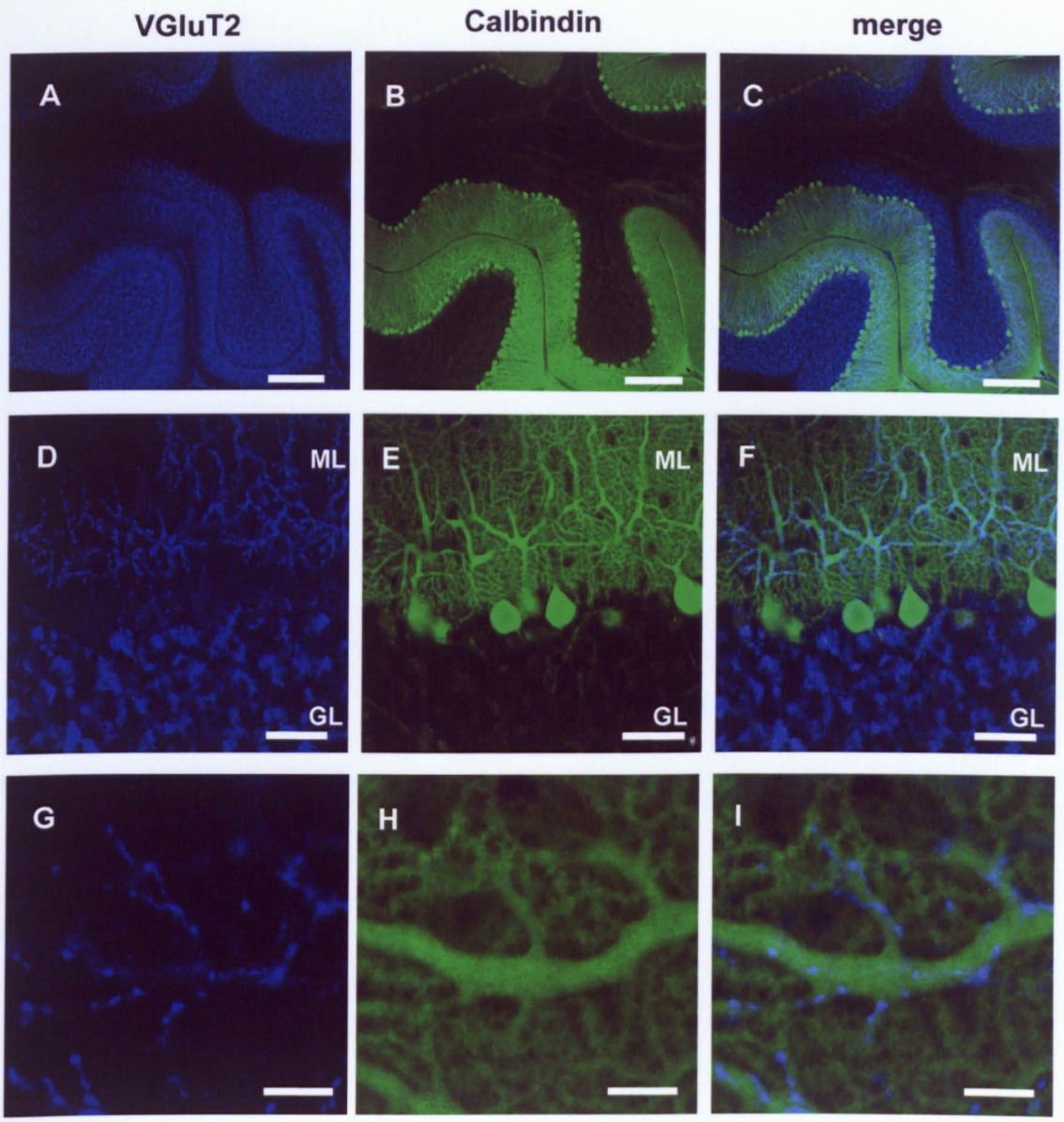

Figure 3.12 Double staining for VGluT2and calbindin.
Parasaggital sections (125µm) from P28 rat cerebella stained for VGluT2 (blue) and calbindin (green). When both were present in the same structure they appear as cyan in merged images (C,F,I). All images acquired on a Lieca confocal microscope.
A-C – As previously reported the VGluT2 antibody stained the climbing fibres in the molecular layer (ML) and the mossy fibre terminals in the granule cell layer (GL).
D-F – There was no staining of the Purkinje cell bodies. G-I – At high magnification the glutamatergic synaptic boutons were positive for VGluT2 which contact Purkinje cell dendrites. Scale bar A-C 200µm, D-F 40µm, G-I 8µm

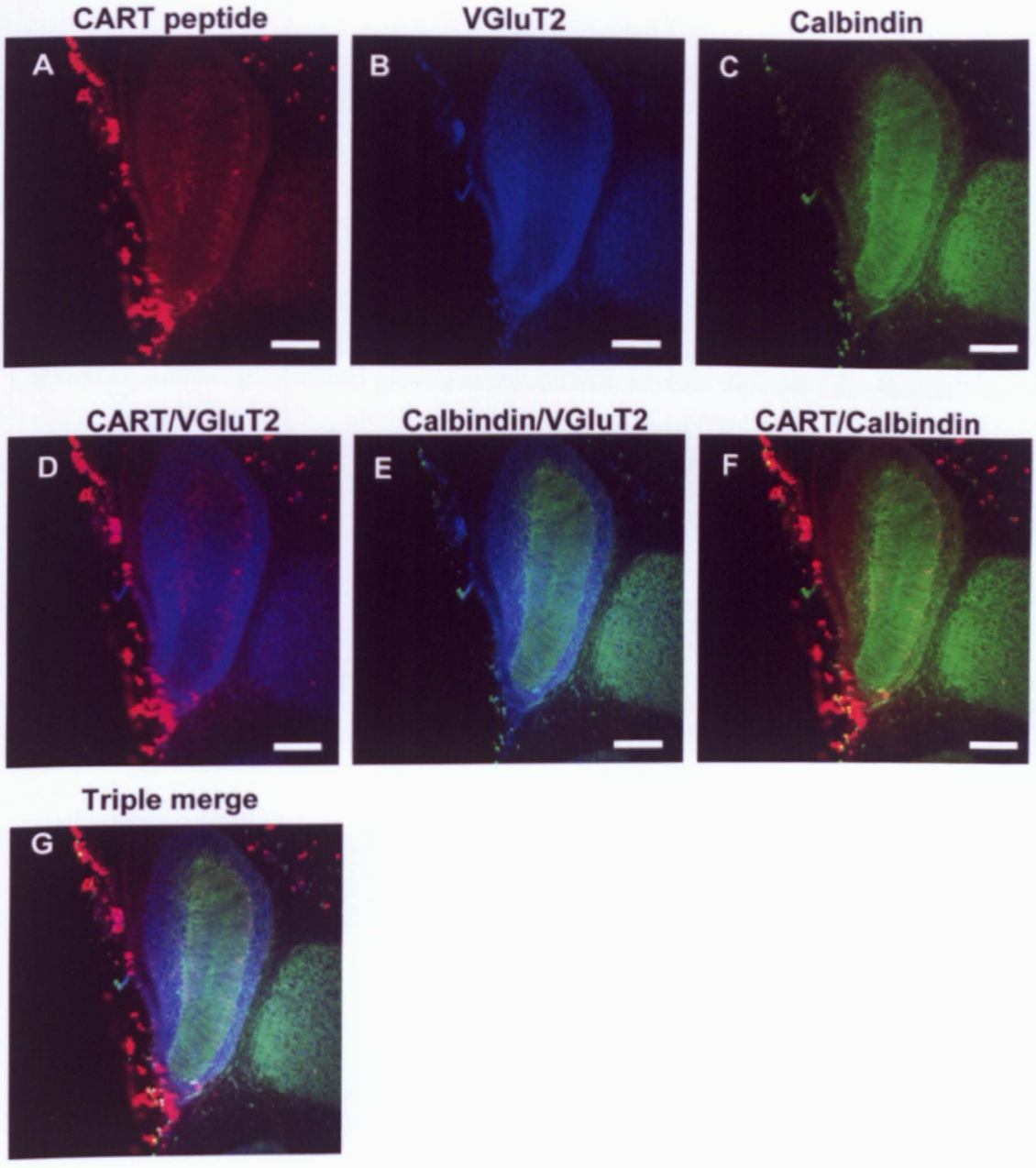

Figure 3.13 Triple staining for CART peptide, calbindin and VGluT2. Parasaggital sections (125μm) from P31 rat cerebella stained for CART (red), VGluT2 (blue) and calbindin (green). For merged images: CART peptide and VGluT2 is magenta (D,G), calbindin and VGluT2 is cyan (E,G), CART peptide and calbindin is yellow (F,G) and CART peptide, calbindin and VGluT2 is white (G). All images acquired on a Lieca confocal microscope. A-G - Stack of confocal sections (20μm) shows CART peptide positive fibres in the molecular layer, however not all climbing fibres in the molecular layer of lobes IX and X are positive for CART peptide (image D). Bright staining on the left hand side of image is probably non-specific binding of antibodies. Scale bars 200μm

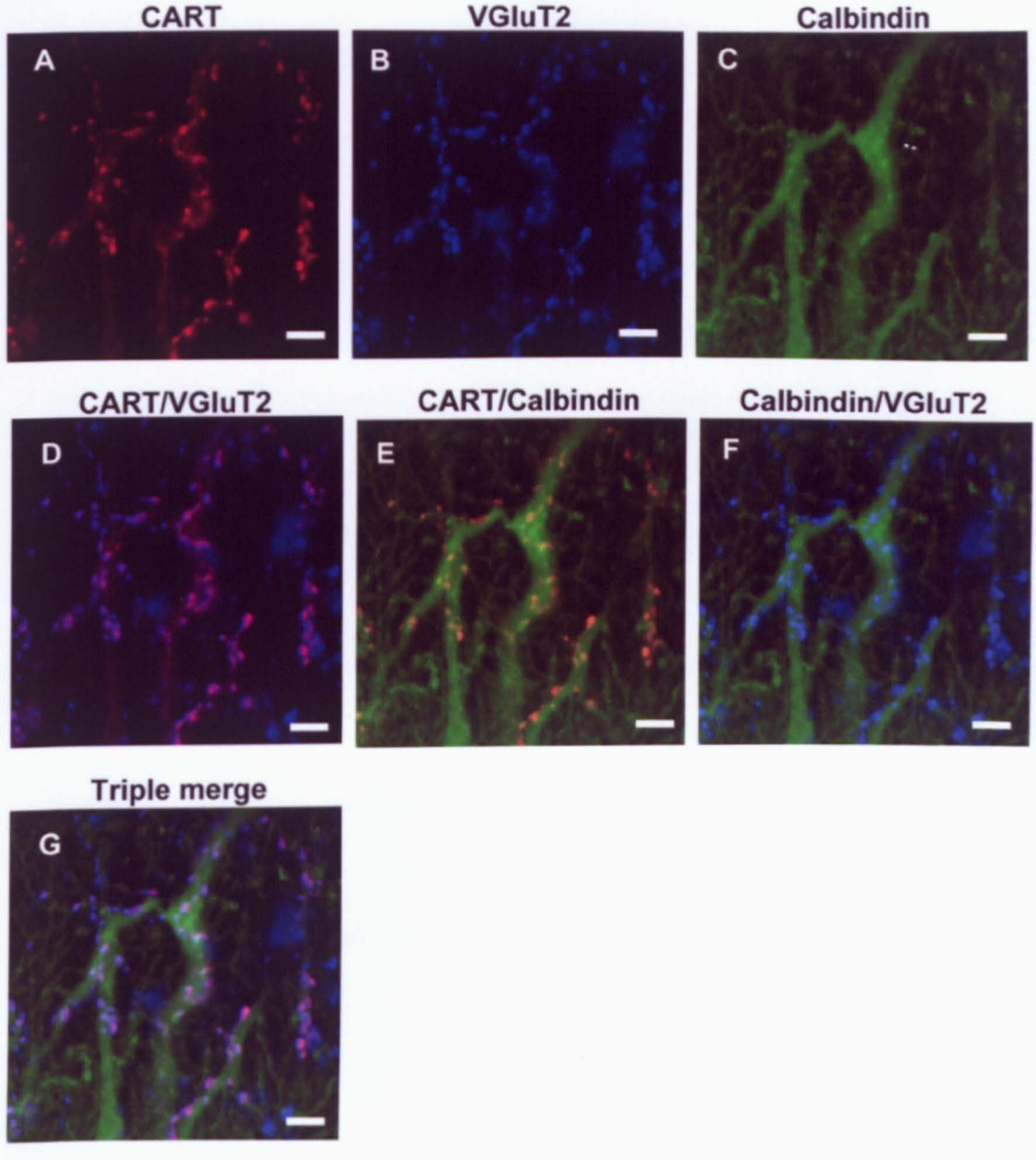

Figure 3.14 Triple staining for CART peptide, calbindin and VGluT2. Parasaggital sections (125μm) from P31 rat cerebella stained for CART (red), VGluT2 (blue) and calbindin (green). For merged images: CART peptide and VGluT2 is magenta (D,G), calbindin and VGluT2 is cyan (E,G), CART peptide and calbindin is yellow (F,G) and CART peptide, calbindin and VGluT2 is white (G). All images acquired on a Lieca confocal microscope. A-G – Stack of confocal sections (2μm) shows synaptic bouton like structures contain glutamate (climbing fibre-Purkinje cell) also contain CART peptide. It appears that if a climbing fibre contains CART peptide then all of it synaptic contacts onto a Purkinje cell contain CART peptide as show by the absence of yellow structures in triple overlay (G)Scale bars 10μm

that expressed CART peptide also expressed VGluT2. Thus VGluT2 is co-localised with CART peptide, confirming that CART peptide is present at climbing fibre-Purkinje cell synapses, and thus may act as a neurotransmitter being co-released with glutamate.

Figure 3.14 shows a section of molecular layer containing one or two large Purkinje cell dendrites. In panel D there are no structures containing only CART peptide (red in figure), but there maybe some structures only containing VGluT2 (blue in figure), this suggests that not all climbing fibre synapses in the vestibular cerebellum contain CART peptide. However looking at panel G (the triple overlay), it is clear that on a single section of dendrite all the pre-synaptic densities which contain VGluT2 also contain CART (magenta or white in figure) and that none of them are only positive for VGluT2 only (blue or green in figure). This was also observed for several other dendrites. As a Purkinje cell is only innervated by a single climbing fibre, this suggests that if a climbing fibre expresses CART peptide then all of its synaptic contacts onto a single Purkinje cell contain CART peptide.

3.10 – The observed patterns of CART peptide expression are not explained by non-specific antibody binding.

To eliminate the possibility that the observed staining is due to non-specific binding of the antibodies, I performed a series of control experiments. Parasagittal vermal sections from a postnatal day 30 rat cerebellum were treated as previously but either the primary antibodies (fig 3.15A-C) or secondary (fig 3.15D-F) antibodies were omitted. When the primary antibody was omitted (n = 3), only a weak background staining was observed for all three secondary antibodies. This demonstrates that the

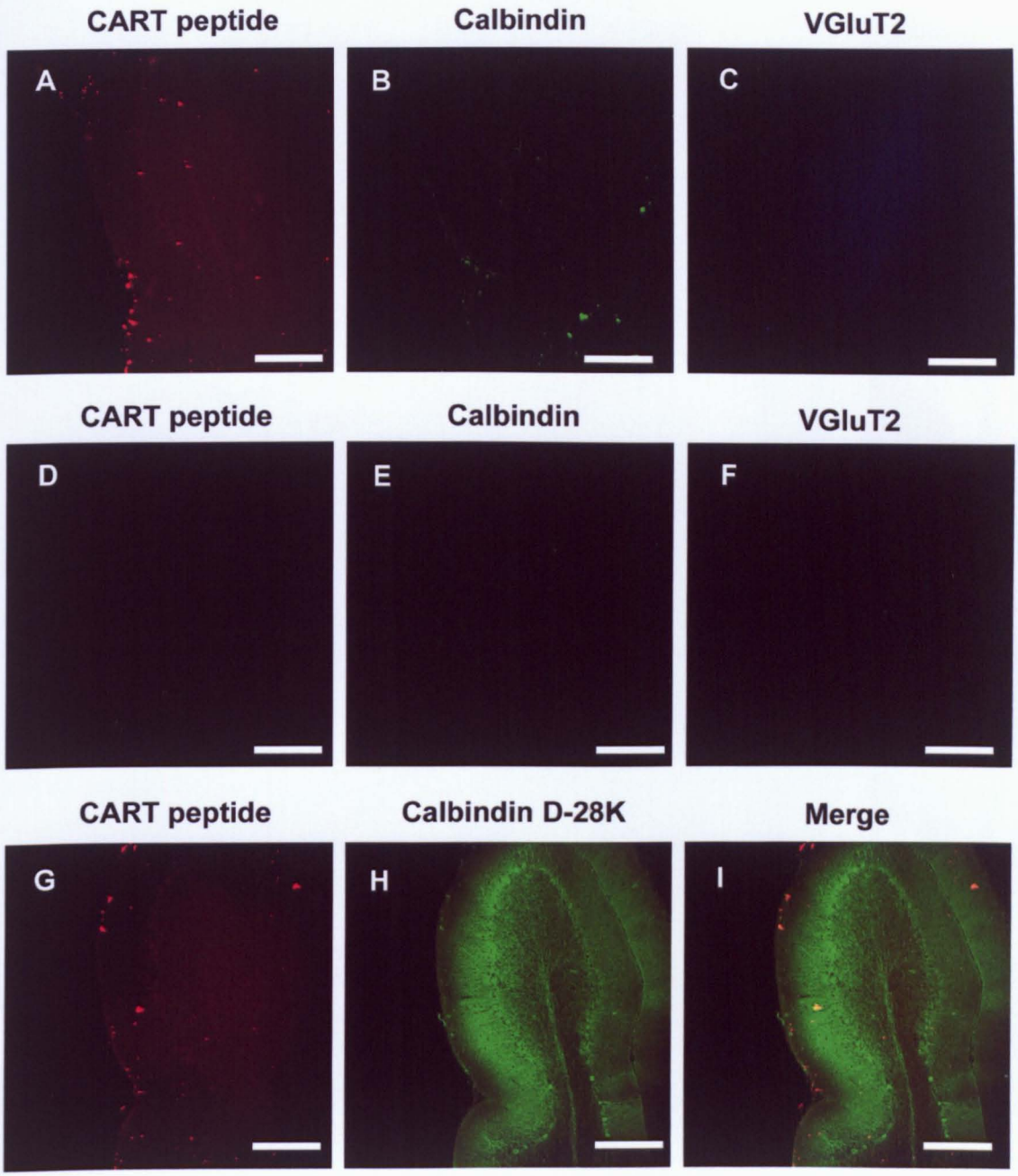

Figure 3.15 Controls.
Parasaggital sections (125μm) from P35 rat cerebella stained for CART (red), VGluT2 (blue) and calbindin (green). Where both CART peptide and calbindin were present in the same structure they appear as yellow in merged images All images acquired on a Lieca confocal microscope. A,B,C – When the primary antibody was omitted, but the secondary antibody was still applied, no specific binding was observed. D,E,F – When the secondary antibody was omitted, but the primary antibody still applied, then no fluorescence was observed. G-I – When the CART antibody was pre-absorbed with 1μm rlCART(55-102) peptide solution, no CART peptide positive structures were observed.
Scale bar 200μm

secondary antibodies do not bind non-specifically to the slices. When the secondary antibodies were omitted (n = 3) no fluorescence was detected from any of the primary antibodies (CART peptide, calbindin or VGluT2), thus the fluorescence detected was not the result of any non-specific background fluorescence. Additional slices (n = 3) were treated with the CART peptide antibody which had been previously incubated with 10 μM CART (55-102) peptide. Only a low level of background staining was observed in these slices (fig 3.15G-I) with no fibre like structures observed. Thus the CART peptide antibody is specific for CART peptide in the slices, as binding can be blocked by prior adsorption of the antibody to freely dissolved CART peptide.

3.11 – Summary

I have confirmed the earlier observation that CART peptide is present in the cerebellum. By using multiple antibodies I have shown that the CART peptide is expressed in a subset climbing fibres in the vestibular cerebellum and that the fibres containing CART peptide make synaptic contact onto Purkinje cells and also contain glutamate. The changing distribution of CART peptide during development provides further confirmation of the presence of CART peptide in climbing fibres. The distribution of CART peptide suggests it may acts as a neurotransmitter or neuromodulator, and this was the next focus of my work.

Chapter 4: Electrophysiological Measurement of CART peptide actions in the vestibular cerebellum.

4.1 – Introduction.

Having established that CART peptide is present at climbing fibre-Purkinje cell synapses, I hypothesise that CART peptide is released (presumably by exocytosis) in response to climbing fibre activity to have actions on the Purkinje cells and/or their synaptic inputs in the vestibular cerebellum. If CART peptide does act as a signalling molecule at this synapse then there are a number of Purkinje cell properties which could be modulated (table 4.1). Because, in most cases, the net effect of these modulations is to change the Purkinje cell firing rate, I initially investigated whether CART peptide changes the firing rate of vestibular Purkinje cells. I then investigated whether CART peptide modulated the various forms of synaptic input to Purkinje cells and also examined whether CART peptide directly affects the membrane properties of Purkinje cells. Finally I investigated whether CART peptide had an affect on synaptic plasticity, by measuring its effects on long term depression (LTD) of the parallel fibre-Purkinje cell synapse.

4.2 – Cell attached recording from Purkinje cells in parasaggital cerebellar slices

To investigate the effects CART peptide has on the spike firing properties of vestibular Purkinje cells, I made cell attached recordings from Purkinje cells in lobes IX and X of parasaggital slices from the vermis of the cerebellum. Purkinje cells *in*

Target	Possible physiological effect on Purkinje cell
Ion channel on Purkinje cell (excitatory).	Increasing simple spike firing rate. Increasing resting membrane potential. Decrease membrane resistance.
Ion channel on Purkinje cell (inhibitory).	Decrease simple spike firing rate. Decrease resting membrane potential. Decrease membrane resistance.
Modulation of response to glutamate.	Modulation of size or kinetics of excitatory post synaptic potentials (EPSP). Change in simple spike firing rate without large change in membrane properties.
Modulation of response to GABA.	Modulation of size or kinetics of inhibitory post synaptic potentials (IPSP). Change in simple spike firing rate without large change in membrane properties.
Pre-synaptic modulation of glutamatergic synaptic transmission.	1)Modulation of size or duration of EPSP. OR 2)Modulation of probability/frequency of release. Both lead to change in simple spike or complex firing rate without large change in membrane properties.
Pre-synaptic modulation of GABAergic synaptic transmission.	1)Modulation of size or duration of IPSP. OR 2)Modulation of probability/frequency of release. Both lead to change in simple spike firing rate without large change in membrane properties.
Secondary messengers in Purkinje cells.	Many possible effects including : change in receptor density/type at synapses, morphological changes in Purkinje cells, changes in mRNA expression, changes to intrinsic membrane properties. Physiological effects could be seen as: slow change in membrane potential, slow and irreversible change in simple spike firing rate and/or membrane properties, change in synaptic plasticity.

Table 4.1 – Overview of different possible effects of CART peptide on Purkinje cells

vivo fire a combination of simple spikes and complex spikes; the simple spikes are high frequency sodium-dependent events driven by a combination of parallel fibre input and the intrinsic electrical properties of Purkinje cells (Llinás et al., 2004). The complex spikes (produced by climbing fibre activity) are a lower frequency event which can be distinguished from simple spikes because they are a compound large sodium event followed by 2-3 smaller calcium events and an extended afterhyperpolarization (AHP). Although in parasaggital slices both the climbing fibres and parallel fibres are cut (and thus the excitatory transmission to Purkinje cells is weak), Purkinje cells still spontaneously fire action potentials (Loewenstein et al., 2005). Furthermore, in parasaggital slices the cell bodies of the Purkinje cells are easily visually identified (by their characteristic morphology and position in the slice) and the Purkinje cell planar dendritic tree of is not damaged during slicing.

Because Purkinje cells are spontaneously active, it is possible to use the cell attached recording method to measure any effects of CART peptide on the firing pattern. Other possible recording methods include extracellular (field) recordings or visually guided whole cell patch clamp recordings. Field recordings were not used as it is difficult to record from single cells. Whole cell patch clamp was not initially used, as cell attached recording is a much less invasive technique (there is no cell cytoplasm dialysis which could potentially change the membrane potential) and thus the firing pattern is more stable over prolonged periods (see later).

4.2.1 – Firing pattern of Purkinje cells at room temperature.

There are many different ways to analyse the firing of Purkinje cells. To determine the best methods, the firing pattern of 10 Purkinje cells was recorded at room temperature. The data was recorded using Clampex 8 (Axon Laboratories) and visually assessed in Clampfit 8 (Axon Laboratories) (Figure 4.1A). Further analysis (detection of each spike for measuring intervals and frequencies) was carried out using Minianalysis (Synaptosoft, see chapter 2 for more detail Figure 4.1B).

In all 10 recordings spike like events were clearly observed and these were confirmed as action potentials by application of TTX (1 μM) to block Na^+ channels. Figure 4.2 shows the analysis of a ten second section of Purkinje cell firing data. Calculating the number of events per second is the simplest way to analyse the firing (Figure 4.2B). For example the mean number of events per second over the 10 second period was 5.5 (because this is the number of spikes in a one second period it is equivalent to the frequency in Hz) which is the same as dividing the total number of spikes (55) by the time (10 s). However this method gives the least information about the firing pattern, if there are periods of high frequency firing interspersed with silent periods this could give the same value of events per second as for a cell that fired tonically at a lower frequency.

Another way of analysing the firing is to calculate the time interval between each event and either plot this against time or construct a cumulative histogram (figure 4.2C,D). This gives more information, however the mean event interval is the same as the inverse of the mean number of events per second. In this case, the mean event interval was 182 ms, the inverse of 5.5 Hz. The advantages of using event interval over events per second are that breaks in firing can be clearly identified and measured,

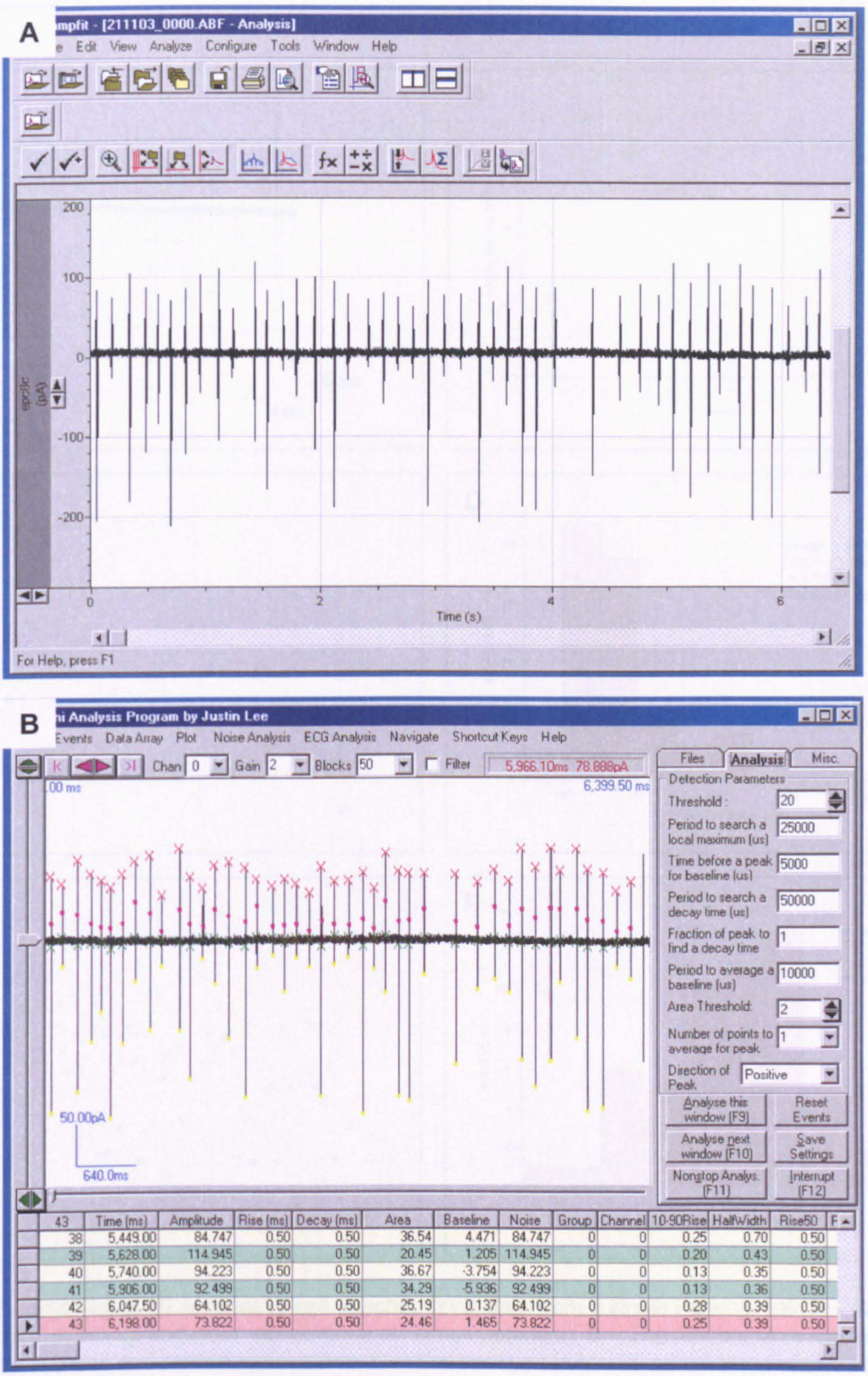

Figure 4.1 – Screen captures of analysis of cell attached raw data. A – Raw data in Clampfit 8 (Axon Laboratories), each simple spike is an up-down deflection. The variability in peak high is due to a low sampling rate (2 kHz) cutting of the top and bottom of some peaks. B – The same raw data displayed in MiniAnalysis. Green crosses mark baseline before peaks, red crosses mark the peak maximums, yellow circles mark the peak minimums and pink circles mark the peak decays

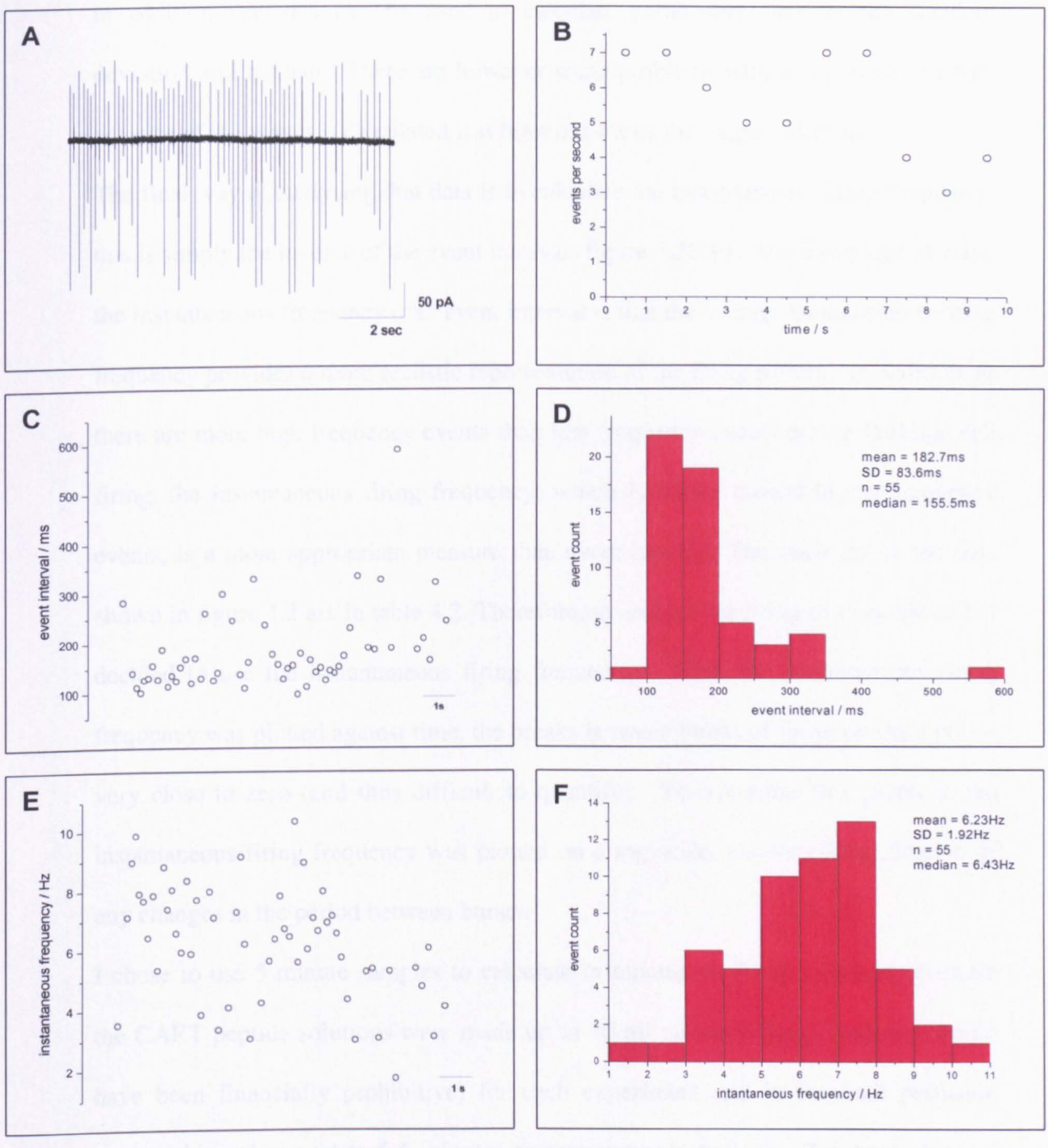

Figure 4.2 – Analysis of 10 seconds of cell attached firing data from a single Purkinje cell. A – Cell attached trace (each up and down deflection is an action potential). B – The number of events per second was counted and plotted against time. C – The event interval was calculated and plotted against time. D – The histogram of event intervals was plotted from data in panel C. E – The instantaneous frequency was calculated by inversing the event interval and plotted against time. F – The histogram of instantaneous frequency plotted from data in panel E.

in addition statistics can be used to calculate parameters such as the standard deviation and median. There are however some problems with using event interval; because of the way it is calculated it is biased towards the longer intervals.

The final way of analysing that data is to calculate the instantaneous firing frequency, this is simply the inverse of the event interval (figure 4.2E,F). The advantage of using the instantaneous frequency over event interval is that the average instantaneous firing frequency provides a more realistic representation of the firing pattern. In addition, as there are more high frequency events than low frequency events during Purkinje cell firing, the instantaneous firing frequency, which is biased toward higher frequency events, is a more appropriate measure than event interval. The statistics on the data shown in figure 4.2 are in table 4.2. Therefore, to analyse the firing of Purkinje cells I decided to use the instantaneous firing frequency. When the instantaneous firing frequency was plotted against time, the breaks between bursts of firing produce points very close to zero (and thus difficult to quantify). To overcome this problem, the instantaneous firing frequency was plotted on a log scale, allowing identification of any changes in the period between bursts.

I chose to use 5 minute samples to calculate instantaneous firing frequency because the CART peptide solutions were made up in 10 ml volumes (larger volumes would have been financially prohibitive) for each experiment and in the bath perfusion system this volume takes 5-6 minutes to pass through the bath. To check that a 5 minute sample of firing is representative of the Purkinje cell firing, I have compared the statistics for 5 minute samples to longer 20 minute samples from 3 recordings (figure 4.3). There was no significant difference between the instantaneous firing frequency measured from the 5 minute samples and 20 minutes sample using a student t-test ($n = 3$).

	10 second sample	5 minute sample	20 minute sample
Mean / Hz	6.23	7.40	7.35
Standard deviation / Hz	1.92	2.30	2.20
Number	55	1038	4038
Standard error of mean / Hz	0.26	0.07	0.04
Coefficient of variance / percentage	31	31	30
5 percentile / Hz	3.04	3.52	3.62
Lower quartile / Hz	5.27	6.02	6.02
Median	6.43	7.44	7.49
Upper quartile / Hz	7.68	8.89	8.70
95 percentile / Hz	9.02	11.00	10.53

Table 4.2 – Statistics on firing frequency from a single Purkinje cell with different sample lengths.

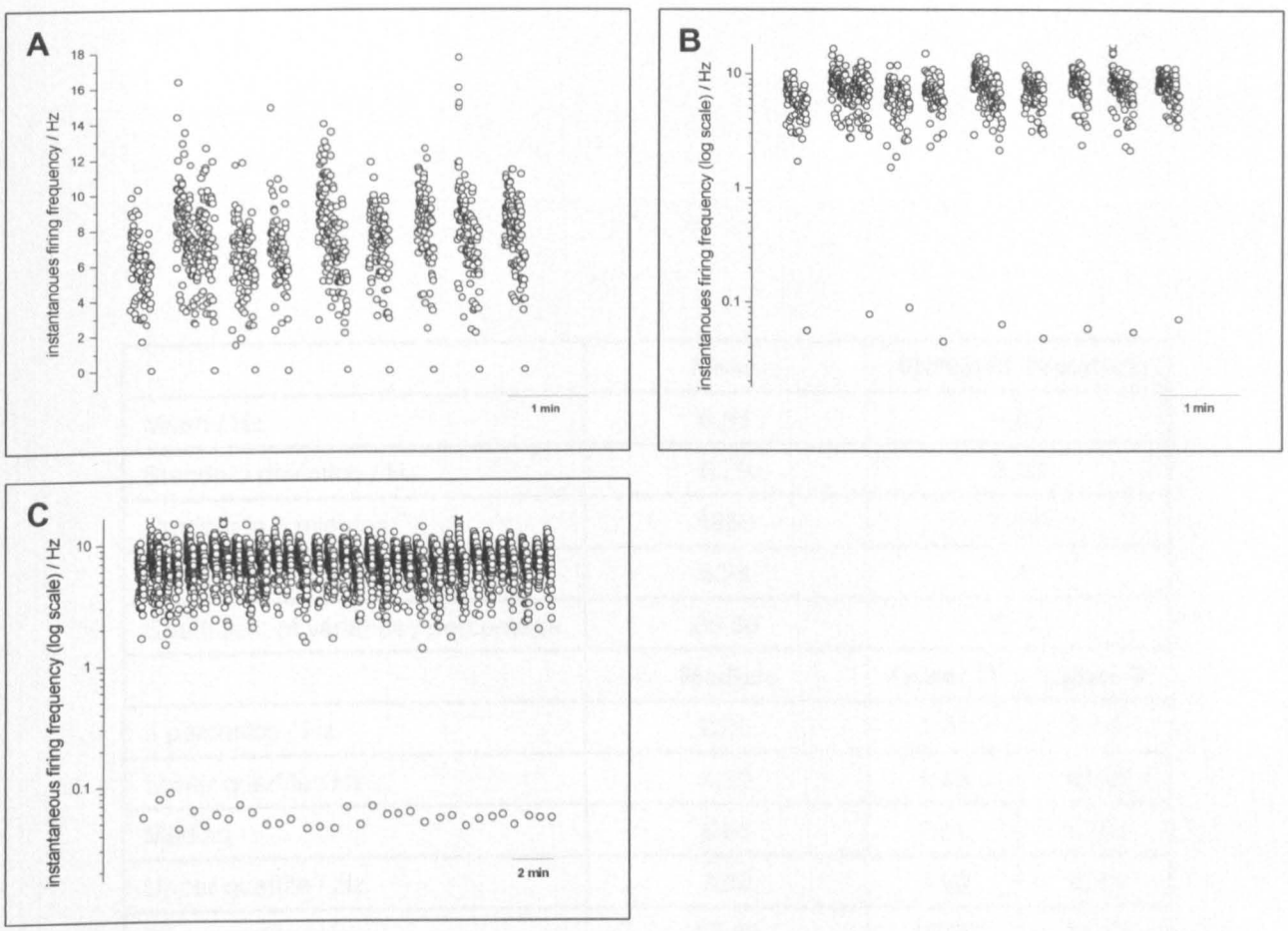

Figure 4.3 – The analysis of 5 and 20 minutes of cell attached firing data from a single Purkinje cell. A – Plot of instantaneous firing frequency against time for a 5 minute sample. B – The same data as panel A but using a log scale. This allows both the high frequency events (inside bursts) and low frequency events (periods between bursts) to be visualised on the same plot. C - Plot of instantaneous firing frequency (log scale) against time for the same Purkinje cell as panel A and B, but for a 20 minute sample.

	Mean	Standard Deviation	
Mean / Hz	9.93	8.86	
Standard deviation / Hz	6.79	5.33	
Number in 5 minutes	1659	1238	
Standard error of mean / Hz	0.28	0.45	
Coefficient of variance / percentage	88.80	72.53	
	Median	**Lower Q**	**Upper Q**
5 percentile / Hz	2.65	1.24	6.16
Lower quartile / Hz	4.59	2.48	10.44
Median	5.85	3.61	12.03
Upper quartile / Hz	7.60	4.98	12.89
95 percentile / Hz	13.69	10.76	16.82

Table 4.3 – Average instantaneous firing frequency statistics from 10 Purkinje cells. Lower Q – Lower quartile (25%) Upper Q – Upper Quartile (75%)

The instantaneous firing frequency of 10 Purkinje cells was measured and then the statistics for 5 minute samples were calculated (table 4.3). The mean instantaneous firing frequency was 9.93 ± 2.80 Hz. and the mean standard deviation was 6.79 ± 1.76 Hz. Thus within each cell there is a large variation in firing frequency. There was also a large variation in firing frequency between cells (standard deviation of 8.86 Hz). I believe that using a mean value is not the best measure of the firing frequency. In order to correctly use the mean, the sample data should come from a normally distributed population, and for a population to be normal each event in that population should be independent of each other. However during spike firing, each event is not independent and therefore the mean is not an appropriate measurement. The median instantaneous firing frequency is a better statistic to compare the firing properties of cells as it does not rely on a normal distribution and is less skewed by extremes than the mean (Campbell, 1989). Although most other investigators use mean events per second to measure Purkinje cell firing rate (Häusser and Clark, 1997; Womack and Khodakhah, 2002; Smith and Otis, 2003), I believe that the median instantaneous firing frequency is a more sensitive measure of changes in firing frequency. The median instantaneous firing frequency of ten cells analysed was 5.85 (3.61, 12.03) Hz, this is more than one SEMs of the mean firing frequency (9.93 ± 2.80 Hz). Also using the Kolmogorov-Smirnov test to compare the data to an ideal shows the data not to be normally distributed.

4.2.2 – Positive controls for the investigating changes in firing frequency.

To check that the cell attached recording method and my analysis method can detect changes in firing frequency, I have used 3 positive controls: raising the extracellular potassium ion concentration; applying bicuculline to block synaptic inhibition; and applying zolpidem to increase synaptic inhibition.

By increasing the extracellular concentration of potassium from 3.1 to 6.2 mM, the Purkinje cells will become depolarized and the firing rate will increase. Application of aCSF containing 6.2 mM potassium resulted in a doubling of the median instantaneous firing frequency from 2.11 Hz to 4.15 Hz ($n = 4$) (figure 4.4A and table 4.4). Thus an increase in the firing rate can be detected.

Bicuculline was also used as a positive control. As expected block of GABAergic synaptic transmission to Purkinje cells, by applying 10μM bicuculline, resulted in an increase in the median instantaneous firing frequency from 3.50 Hz to 6.59 Hz ($n = 13$) (figure 4.4B and table 4.4). Thus the median instantaneous firing frequency can be used to measure changes in the firing rate produced by changes in the synaptic transmission to Purkinje cells. I have also measured changes in the firing rate in response to application of neurotransmitters such as 5-HT and ATP (not illustrated).

Finally it is possible that CART peptide may decrease the firing rate of Purkinje cells, to test whether I could detect this, I applied zolpidem to Purkinje cells. Zoplidem increases the $GABA_A$ receptor affinity for GABA, therefore increasing inhibitory postsynaptic current amplitude and prolonging decay (Wall 2006). This will have the net effect of maintaining the hyperpolarisation and preventing the membrane potential reaching threshold. Bath application of 500 nM zolpidem resulted in a decrease in median instantaneous firing frequency from 7.06 Hz to 4.52 Hz ($n = 7$) (figure 4.4C

	control	6.2 mM K^+	control	10 µM bicuculline	control	500 nM Zolidem
Mean / Hz	1.71	5.15	3.48	6.50	7.06	4.52
Standard deviation / Hz	0.97	4.72	1.18	1.51	2.85	4.95
Number in 5 minutes	310	1010	410	1832	1517	133
Standard error of mean / Hz	0.05	0.15	0.06	0.04	0.07	0.43
Coefficient of variance / percentage	57	92	34	23	40	110
5 percentile / Hz	0.36	1.66	1.60	3.97	3.15	0.11
Lower quartile / Hz	0.97	2.99	2.78	5.41	5.29	0.68
Median	2.11	4.15	3.50	6.59	6.74	2.47
Upper quartile / Hz	2.27	5.36	4.26	7.62	8.43	7.37
95 percentile / Hz	3.47	19.05	5.23	8.86	12.08	13.80

Table 4.4 – Effect on the Purkinje cell-firing frequency of 3 different known modulators.

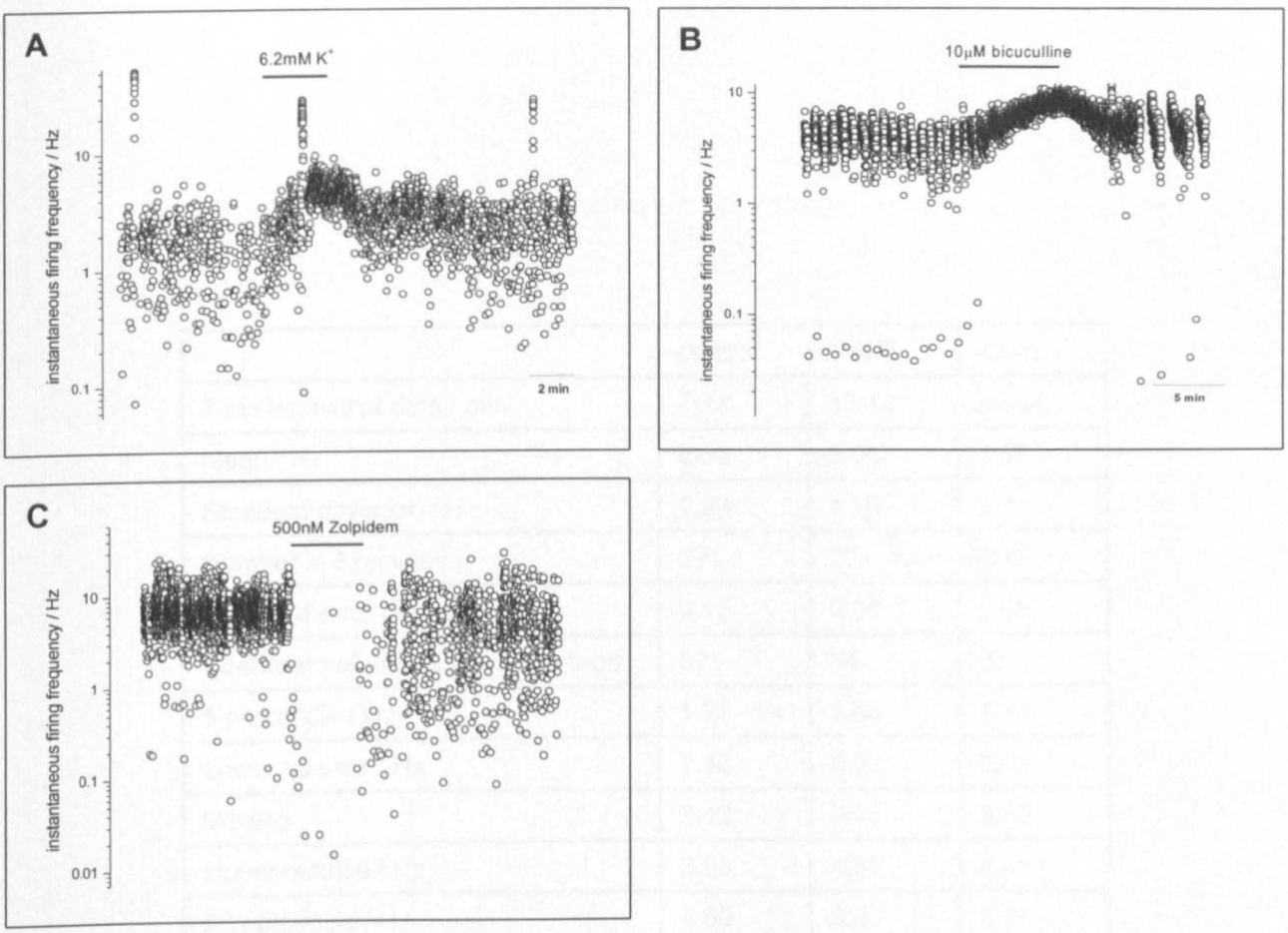

Figure 4.4 – Modulation of firing frequency can be detected using my method of analysis. A – Application of 6.2 mM potassium markedly increased the firing rate. B – Application of 10 μM bicuculline markedly increased the firing rate. C – Application of 500 nM zolpidem markedly decreased the firing rate.

	control	CART	wash
Time interval of data / min	7-12	13-18	29-34
Mean / Hz	3.36	3.55	3.67
Standard deviation / Hz	2.93	1.20	1.21
Number in 5 minutes	374	374	420
Standard error of mean / Hz	0.15	0.06	0.06
Coefficient of variance / percentage	87	34	33
5 percentile / Hz	1.21	1.58	1.71
Lower quartile / Hz	2.46	2.92	2.95
Median	3.43	3.75	3.80
Upper quartile / Hz	3.84	4.30	4.41
95 percentile / Hz	4.89	5.35	5.75

Table 4.5 – Effect of 100 nM CART peptide on a single Purkinje cell at room temperature.

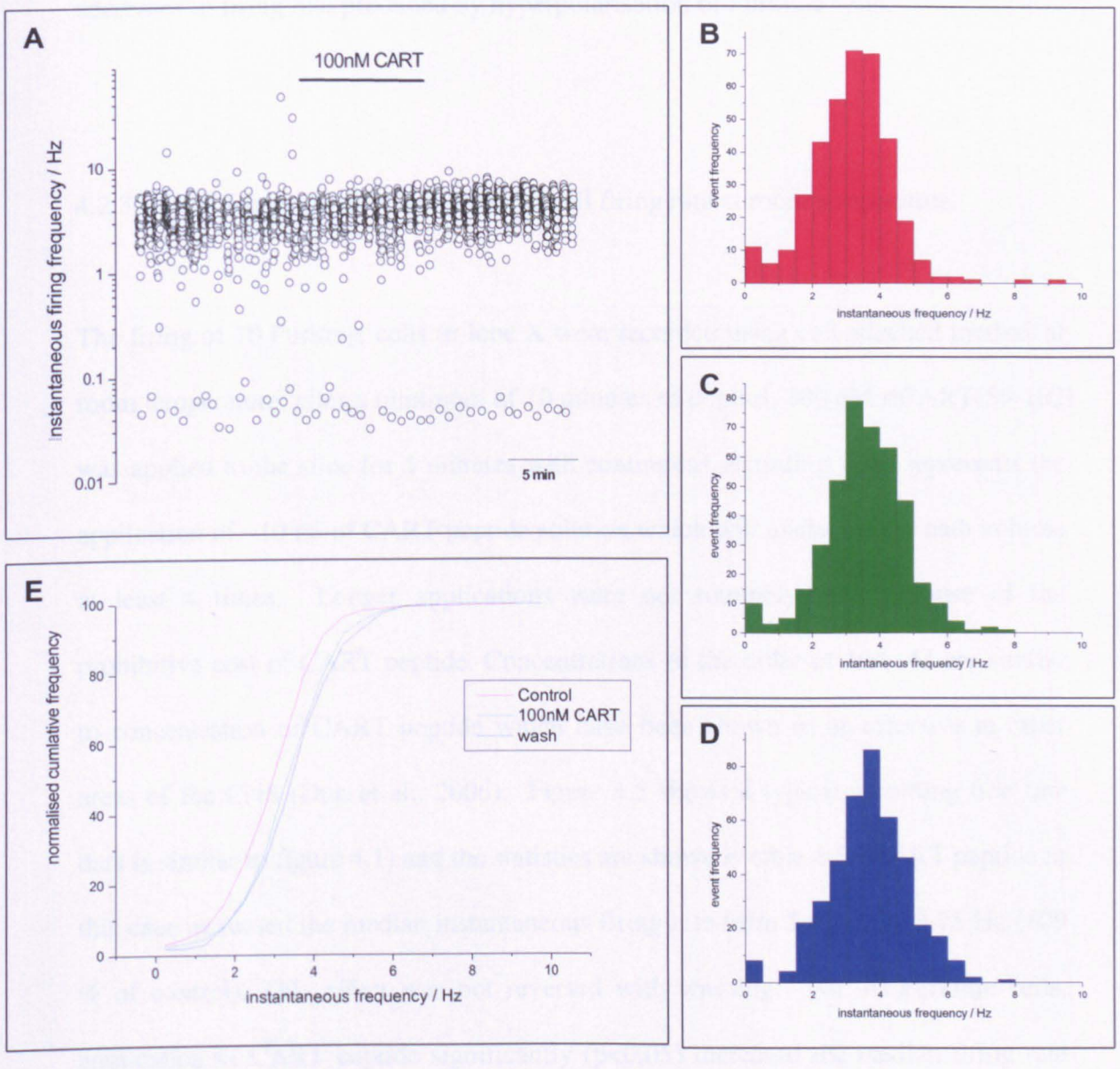

Figure 4.5 – An example of the effects of 100 nM CART peptide on the firing frequency of a single Purkinje cell at room temperature. A – Application of CART peptide increased instantaneous firing frequency. B – Histogram of instantaneous frequency in control, median instantaneous firing frequency was 3.43 Hz. C – Histogram of instantaneous frequency following CART peptide application, the median instantaneous firing was 3.75 Hz. D – Histogram of instantaneous frequency following washout, the median instantaneous firing frequency was 3.80 Hz. E – Normalised cumulative frequency count plotted against instantaneous firing frequency. Although the changes in frequency are not obvious from the histograms, there is a clear increase in frequency in the cumulative frequency plot.

and table 4.4). This implies that median instantaneous firing frequency can detect the decreases in firing rate produced by hyperpolarisation of Purkinje cells.

4.2.3 – CART peptide increases Purkinje cell firing rate at room temperature.

The firing of 10 Purkinje cells in lobe X were recorded using cell attached method at room temperature, after a minimum of 10 minutes of control, 100 nM rlCART(55-102) was applied to the slice for 5 minutes with continuous recording. This represents the application of ~10 ml of CART peptide solution which will exchange the bath volume at least 4 times. Longer applications were not routinely used because of the prohibitive cost of CART peptide. Concentrations of the order of 100 nM are similar to concentration of CART peptide which have been shown to be effective in other areas of the CNS (Dun et al., 2006). Figure 4.5 shows a typical recording (the raw data is similar to figure 4.1) and the statistics are shown is table 4.5. CART peptide in this case increased the median instantaneous firing rate from 3.43 Hz to 3.75 Hz (109 % of control). This effect was not reversed with washing. For 10 Purkinje cells, application of CART peptide significantly ($p<0.05$) increased the median firing rate from 5.85 (3.61, 12.03) Hz to 6.07 (3.99, 13.59) Hz (figure 4.6A). There was little recovery during wash 5.94 (3.99, 12.34) Hz. Because of the large variation in median instantaneous firing frequency between cells it is more convenient to express the change in instantaneous firing frequency as a percentage of control. Thus in CART peptide the firing rate was 110.8 (108.7, 116.7) % of control and 105.5 (95.1, 110.4) % of control after wash (figure 4.6B). The median firing frequency after wash was not significantly different from control.

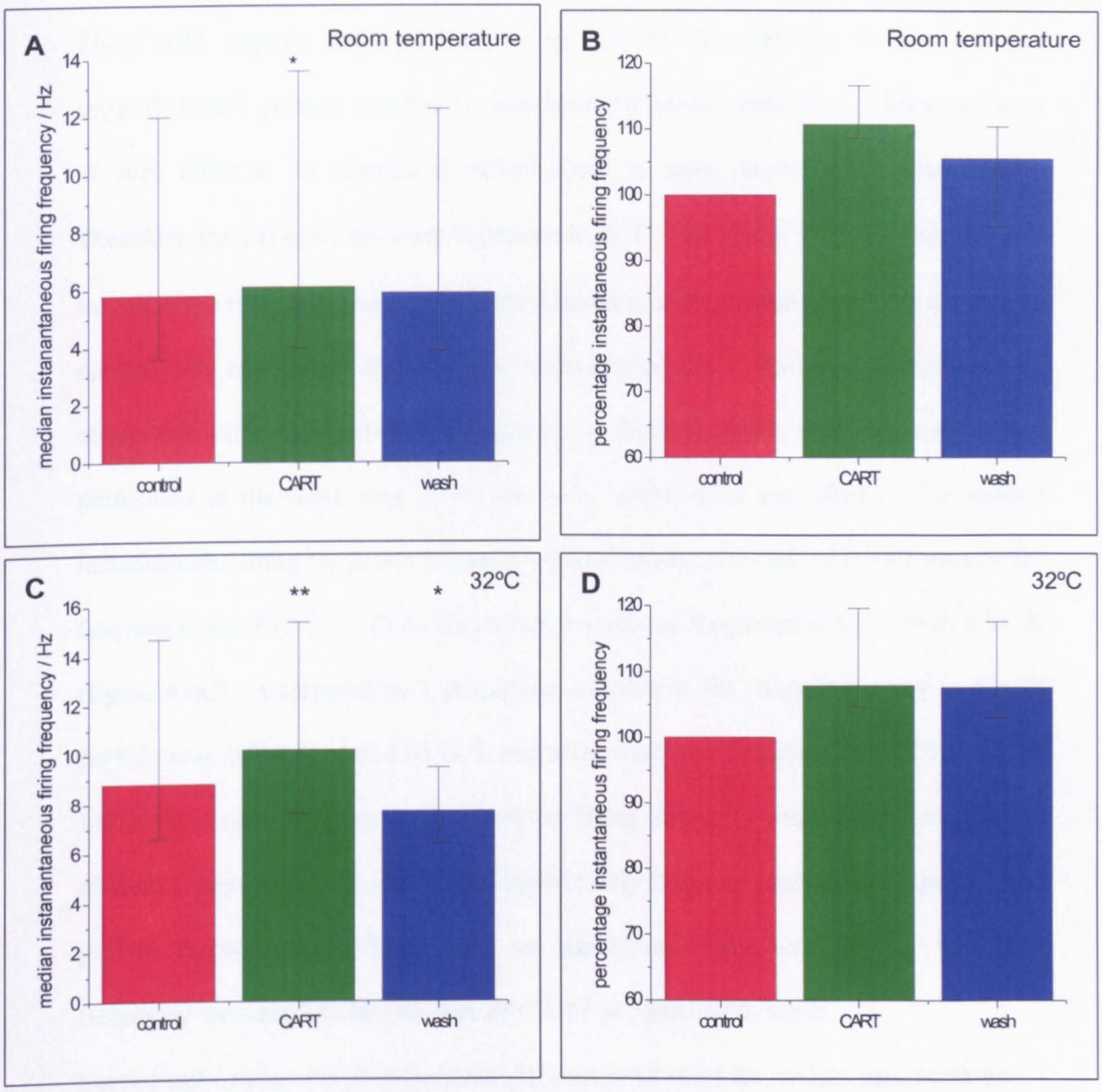

Figure 4.6 – CART peptide (100 nM) significantly increases the median instantaneous firing frequency of Purkinje cells at room temperature (n = 10; panels A and B) and at 32°C (n = 9; panels C and D). Control (red), CART peptide (green) and washout (blue). Error bars are one SEM. * - $p<0.05$, ** - $p<0.01$. Panels A and C show the absolute firing frequencies and panels B and D show frequencies normalised to control.

4.2.4 – CART peptide increases Purkinje cell firing rate at 32°C

The CART peptide-mediated increase in median Purkinje cell firing frequency suggests CART peptide may have a signalling role in the cerebellum. However for an *in vitro* effect to be relevant it should occur at more physiological temperatures. Therefore the experiments were repeated at 32°C. The firing of 9 Purkinje cells in lobe X were recorded using cell attached method, after a minimum of 10 minutes of control 100 nM CART peptide was bath applied for 5 minutes. There was no observable difference between the quality of the raw traces, thus the analysis was performed in the same way as for the room temperature recordings. The median instantaneous firing frequency in control was 8.8 (6.6, 14.7) Hz, in CART peptide the frequency was 10.2 (7.6, 15.4) Hz and after wash the frequency was 7.7 (6.4, 9.5) Hz (figure 4.6C). Expressed as a percentage of control the firing frequency in CART peptide was 107.9 (104.6, 119.6) % and after wash the frequency was 107.7 (103.0, 117.6) % of control (figure 4.6D). Both the firing frequency measured in the presence of CART peptide and in wash were significantly different from control ($p<0.01$ and $p<0.05$ respectively). There was no significant difference between the firing frequency measured in the presence of CART peptide and in wash.

Surprisingly, there was no significant difference between the median instantaneous firing frequencies at room temperature and at 32°C, neither was there a significant difference between the firing frequencies during CART peptide application or a significant difference between the percentage instantaneous firing frequencies during CART peptide application, implying that CART peptide, has an identical effect at both room temperature and 32°C. By plotting the median instantaneous firing frequencies in control against the median instantaneous firing frequency measured in

the presence of CART peptide at both room temperature and 32°C it is clear the data is not split into different groups (figure 4.7A). Combining all the data together, the median control firing rate was 7.5 (4.5, 13.7) Hz, in CART peptide the median firing rate was 7.6 (5.2, 15.3) Hz and in wash the median firing rate was 7.2 (4.4, 10.9) Hz (figure 4.7C). As a percentage of control, the firing rate in CART peptide was 109.4 (105.6, 118.6) % and in wash was 106.4 (101.2, 113.0) % (figure 4.7D). The median instantaneous firing frequency in CART peptide and the median instantaneous firing frequency in wash are both significantly different from control ($p<0.001$ and $p<0.01$ respectively). To investigate whether there is a relationship between the action of CART peptide and the firing frequency in control, the median instantaneous firing frequency in control was plotted against the instantaneous firing frequency in CART peptide (percentage of control, Figure 4.7B). Upon visual investigation there appears to be a negative correlation, suggesting that CART peptide has a larger effect on the firing frequency if the cell is firing at a lower frequency to begin with. However a product-moment correlation was performed and gave an r value of -0.195 with 17 degrees of freedom, which was not significant (Campbell, 1989). Therefore the actions of CART peptide do not depend on the firing frequency in control.

4.2.5 – CART peptide still increases Purkinje cell firing rate in the presence of synaptic blockers.

CART peptide could increase the firing rate directly (by a postsynaptic action on the Purkinje cell) or indirectly (by modulating synaptic inputs to the Purkinje cell). Therefore, to determine the mechanism of CART peptide action, I have recorded the

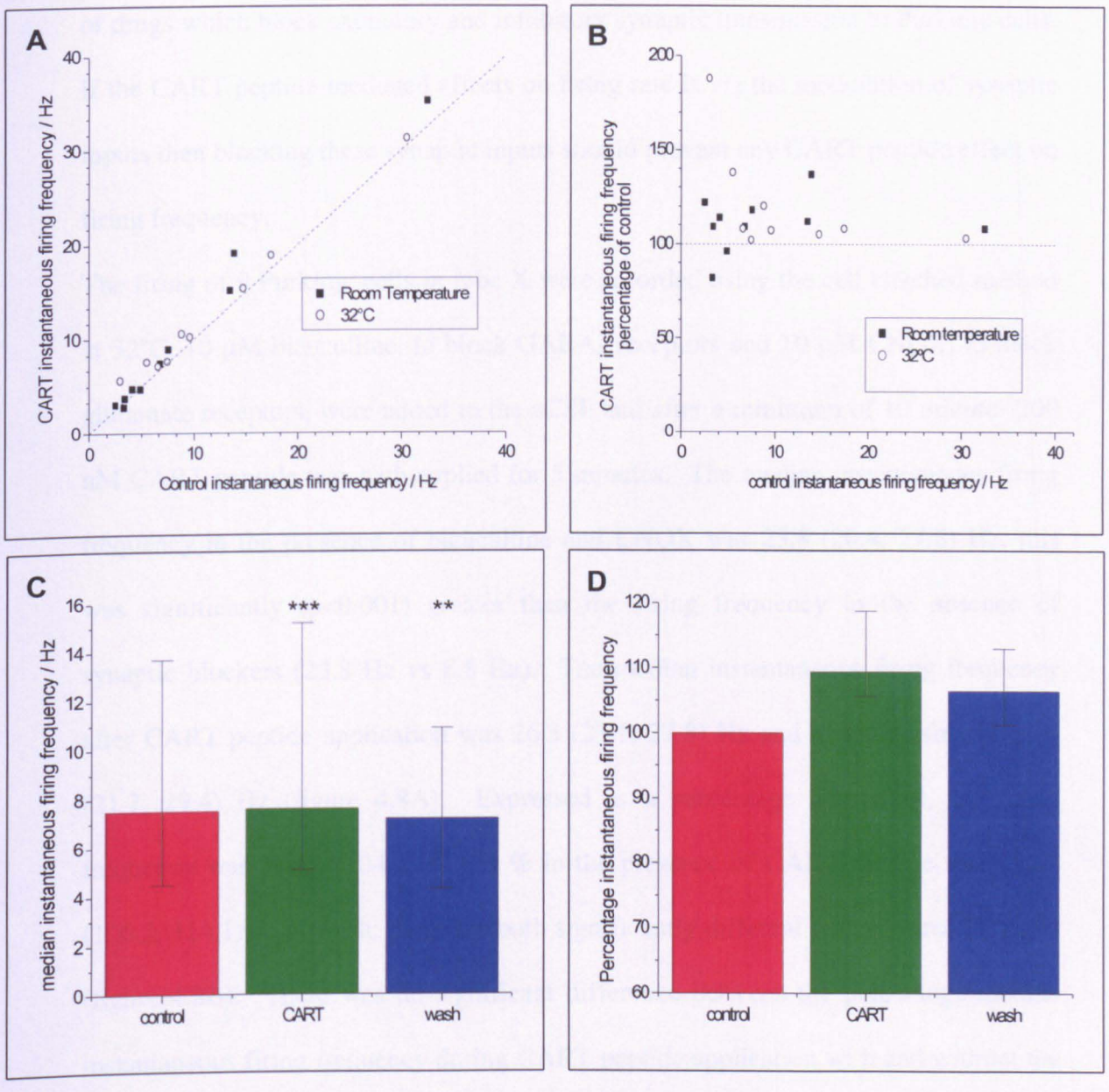

Figure 4.7 – The effects of application of 100 nM CART peptide are not significantly different at room temperature or at 32°C. A – Plot of firing frequency in control against firing frequency in the presence of CART peptide shows that the experiments done at room temperature cannot be visually differentiated from those done at 32°C. Solid squares are room temperature experiments, open circles are 32°C experiments. B – Plot of firing frequency in control against firing frequency in the presence of CART peptide normalised to control. There is no significant correlation. Panel C shows absolute firing frequency for all temperatures and panel D show frequencies normalised to control for all temperatures. Control (red), CART peptide (green) and washout (blue). Error bars are one SEM. ** - $p<0.01$, *** - $p<0.001$.

effect of CART peptide on the median instantaneous firing frequency in the presence of drugs which block excitatory and inhibitory synaptic transmission to Purkinje cells. If the CART peptide-mediated effects on firing rate is via the modulation of synaptic inputs then blocking these synaptic inputs should prevent any CART peptide effect on firing frequency.

The firing of 9 Purkinje cells in lobe X were recorded using the cell attached method at 32°C, 10 μM bicuculline, to block $GABA_A$ receptors and 10 μM CNQX, to block glutamate receptors, were added to the aCSF and after a minimum of 10 minutes 200 nM CART peptide was bath applied for 5 minutes. The median instantaneous firing frequency in the presence of bicuculline and CNQX was 23.8 (20.4, 27.8) Hz, this was significantly ($p<0.001$) greater than the firing frequency in the absence of synaptic blockers (23.8 Hz vs 8.8 Hz). The median instantaneous firing frequency after CART peptide application was 26.3 (23.1, 27.8) Hz and in the wash was 26.3 (21.7, 29.4) Hz (figure 4.8A). Expressed as a percentage of control, the firing frequency was 106.2 (104.2, 117.6) % in the presence of CART peptide and 107.0 (106.2, 114.1) % in wash; these are both significantly different from control ($p<0.05$) (figure 4.8B). There was no significant difference between the percentage median instantaneous firing frequency during CART peptide application with and without the synaptic blockers.

I observed that when CNQX was applied on its own it produced an unexpected increase in the firing frequency of Purkinje cells. This did not reflect a loss of excitatory drive to inhibitory neurones as CNQX still increased the firing rate when applied in the presence of bicuculline (see chapter 5). This paradoxical effect of CNQX could reflect a direct effect on the Purkinje cell, as there is evidence that CNQX directly increases the firing rate of GABAergic neurons

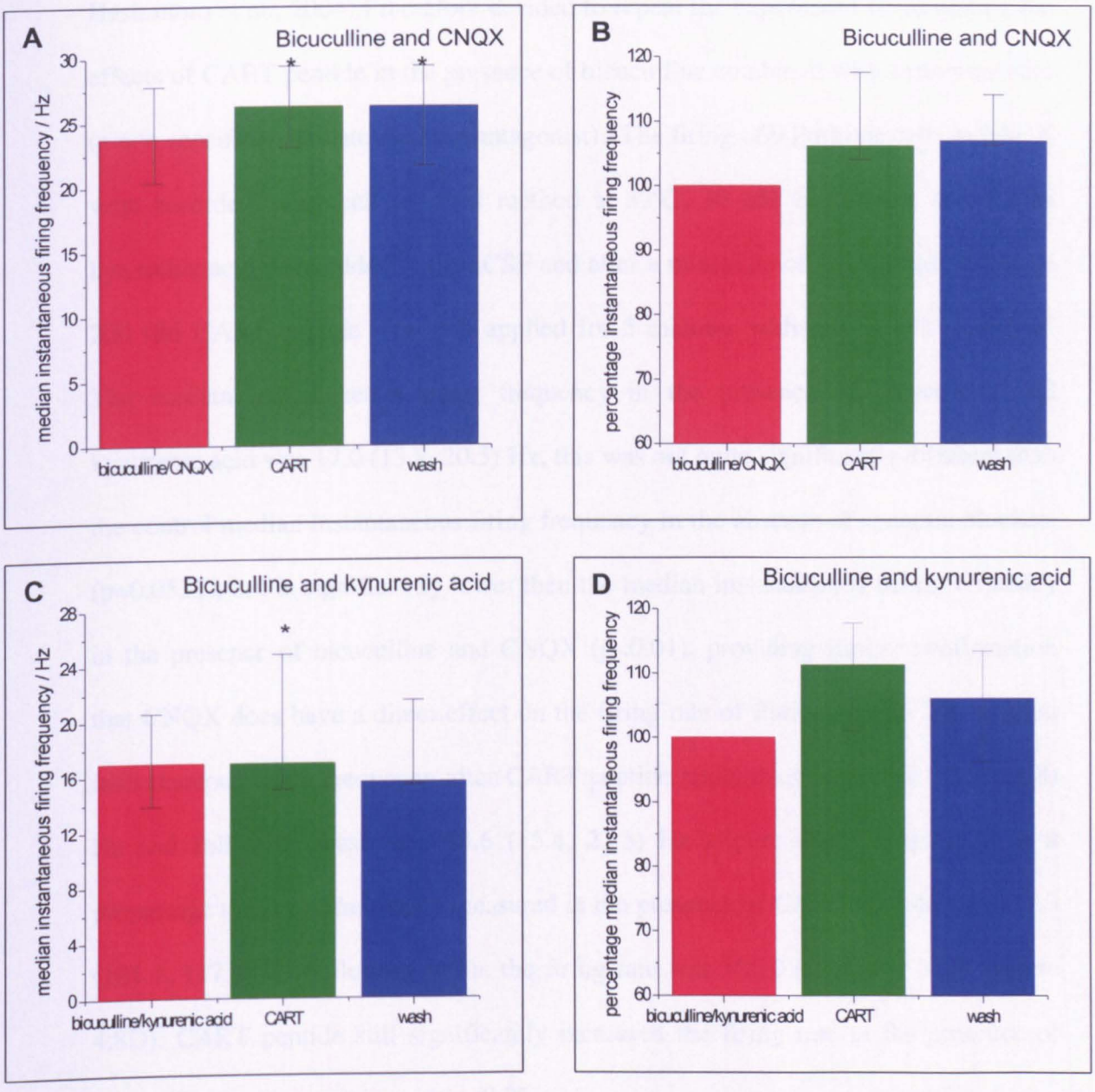

Figure 4.8 – Synaptic blockers did not alter the actions of CART peptide. In the presence of synaptic blockers (panel A and B, 10 μM bicuculline and 10 μM CNQX; panels C and D, 10 μM bicuculline and 5 mM kynurenic acid) 200 nM CART peptide significantly increased the median instantaneous firing frequency of Purkinje cells at 32°C. Control (red), CART peptide (green) and washout (blue). Error bars are one SEM. * - $p<0.05$. Panels A and C show the absolute firing frequencies and panels B and D show frequencies normalised to control.

(McBain et al., 1992; Brickley et al., 2001; Maccaferri and Dingledine, 2002; Hashimoto et al., 2004).I therefore decided to repeat the experiment investigating the effects of CART peptide in the presence of bicuculline combined with kynurenic acid (a non specific glutamate receptor antagonist). The firing of 9 Purkinje cells in lobe X were recorded using cell attached method at 32°C, 10 μM bicuculline and 5 mM kynurenic acid were added to the aCSF and after a minimum of 10 minutes of control 200 nM CART peptide was bath applied for 5 minutes with continuous recording. The median instantaneous firing frequency in the presence of bicuculline and kynurenic acid was 17.0 (13.8, 20.5) Hz, this was not quite significantly different than the control median instantaneous firing frequency in the absence of synaptic blockers ($p=0.0535$), but is significantly lower then the median instantaneous firing frequency in the presence of bicuculline and CNQX ($p<0.01$), providing further confirmation that CNQX does have a direct effect on the firing rate of Purkinje cells. The median instantaneous firing frequency after CART peptide application was 17.0 (15.0, 24.8) Hz and following wash was 15.6 (15.4, 21.5) Hz (figure 4.8C). Expressed as a percentage the firing frequency measured in the presence of CART peptide was 111.3 (101.1, 117,8) %. Following wash, the firing rate was 106.0 (95.9, 113.3) % (figure 4.8D). CART peptide still significantly increased the firing rate in the presence of bicuculline and kynerunic acid ($p<0.05$).

4.2.6 – The CART peptide-mediated increases in firing rate are concentration dependent.

CART peptide was initially used at a concentration of 100-200 nM because CART peptide have been shown to be active at similar concentrations in brain slice physiology experiments (Dun et al., 2006) and the cost of CART peptide would make the routine use of high concentrations difficult. However having shown that CART peptide does have an affect on the firing of Purkinje cells, I was interested in how the effects of CART peptide depended on concentration. I therefore examined the actions of CART peptide at concentrations ranging from 20 to 1000 nM.

The firing pattern of 6 Purkinje cells in lobe X were recorded using the cell attached method, after a minimum of 10 minutes of control, 1000 nM CART peptide was bath applied for 5 minutes with continuous recording. The median instantaneous firing frequency in control was 9.8 (9.1, 10.6) Hz, this increased to 13.9 (12.4, 14.8) Hz in the presence of 1000 nM CART peptide, and was 10.8 (10.1, 17.9) Hz following wash (figure 4.9A). As a percentage of control, in the presence of CART peptide the firing rate was 125.7 (115.5, 141.4) % and in wash the firing rate was 105.5 (104.6, 128.2) % (figure 4.9B). Although the median instantaneous firing frequency was significantly increased in 1000 nM CART peptide compared to control ($p<0.05$), it was not significantly different from the increases observed with 100-200 nM CART peptide.

The firing of 9 Purkinje cells in lobe X were recorded using cell attached method at 32°C, after a minimum of 10 minutes of control 20 nM CART peptide was bath applied for 5 minutes with continuous recording. The median instantaneous firing frequency in control was 16.8 (11.8, 21.1) Hz, in the presence of 20 nM CART

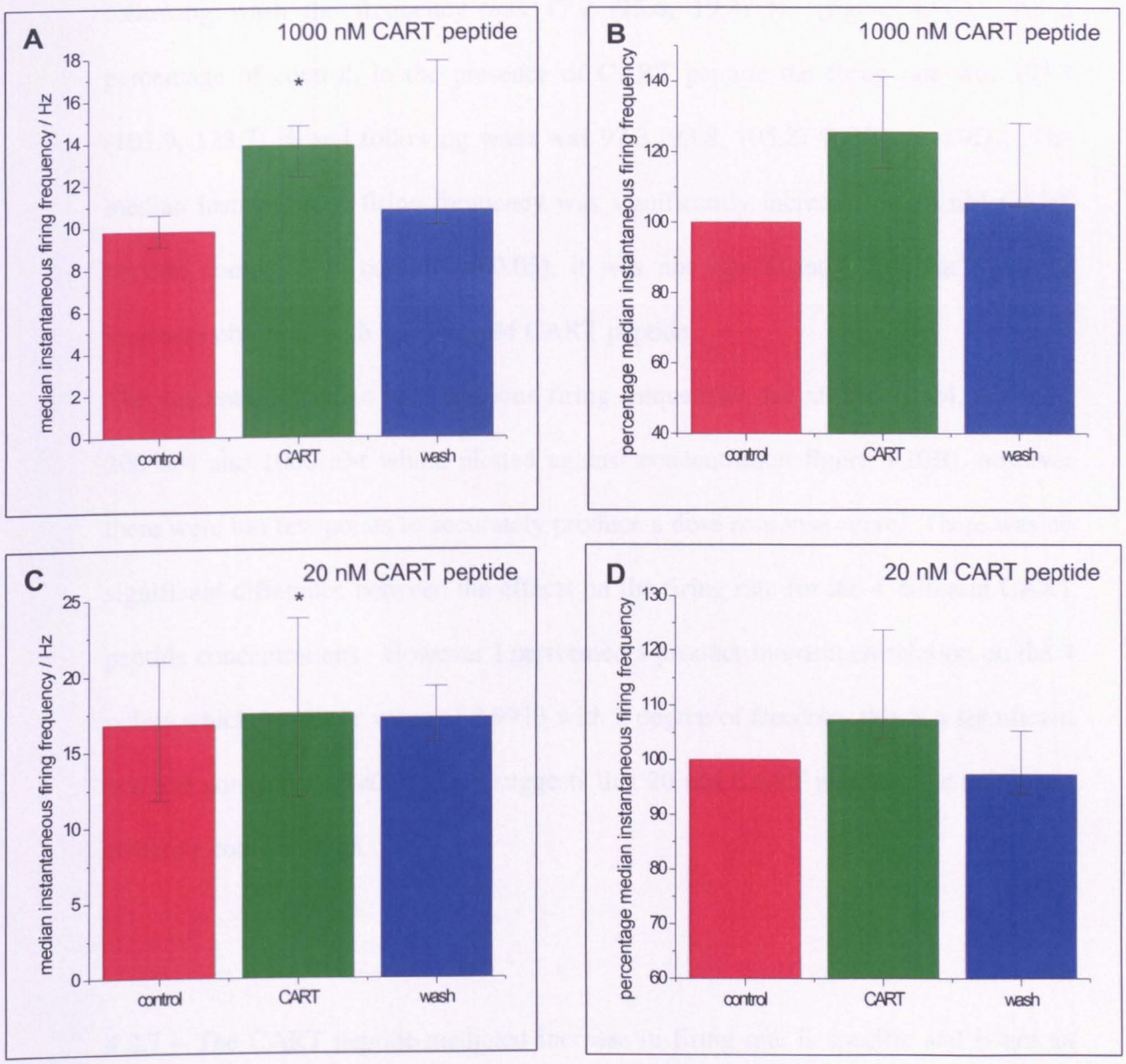

Figure 4.9 – Concentration dependence of CART peptide actions on firing frequency. Application of 1000 nM CART peptide (n = 6, panel A and B), but not 20 nM CART peptide (n = 9, panels C and D) increased the median instantaneous firing frequency of Purkinje cell at 32ºC. Control (red), CART peptide (green) and washout (blue). Error bars are one SEM. * - $p<0.05$. Panels A and C show the absolute firing frequencies and panels B and D show frequencies normalised to control.

peptide the median instantaneous firing frequency was 17.5 (12.0, 23.8) Hz and following wash the frequency was 17.2 (15.6, 19.3) Hz (figure 4.9C). As a percentage of control, in the presence of CART peptide the firing rate was 107.4 (103.9, 123.7) % and following wash was 97.3 (93.8, 105.2) % (figure 4.9D). The median instantaneous firing frequency was significantly increased in 20 nM CART peptide compared to control ($p<0.05$), it was not significantly different from the increases observed with 100-200 nM CART peptide.

The percentage median instantaneous firing frequencies for all the 20nM, 100 nM, 200 nM and 1000 nM where plotted against concentration figure 4.10B), however there were too few points to accurately produce a dose response curve. There was no significant difference between the effects on the firing rate for the 4 different CART peptide concentrations. However I performed a product-moment correlation on the 4 points which gave an r value of 0.9913 with 2 degree of freedom, this is a significant positive correlation ($p<0.01$), and suggests that 20 nM CART is below the maximum effective concentration.

4.2.7 – The CART peptide-mediated increase in firing rate is specific and is not an artefact

Because there is currently no antagonist for CART peptide, the effects of CART peptide are subtle and there is little recovery following wash, it is possible that the observed effects of CART peptide are the result of a drift in the firing rate or flow/temperature artefacts. I have designed my experiments to eliminate any drift in the firing rate during the experiment by using relatively small samples of firing

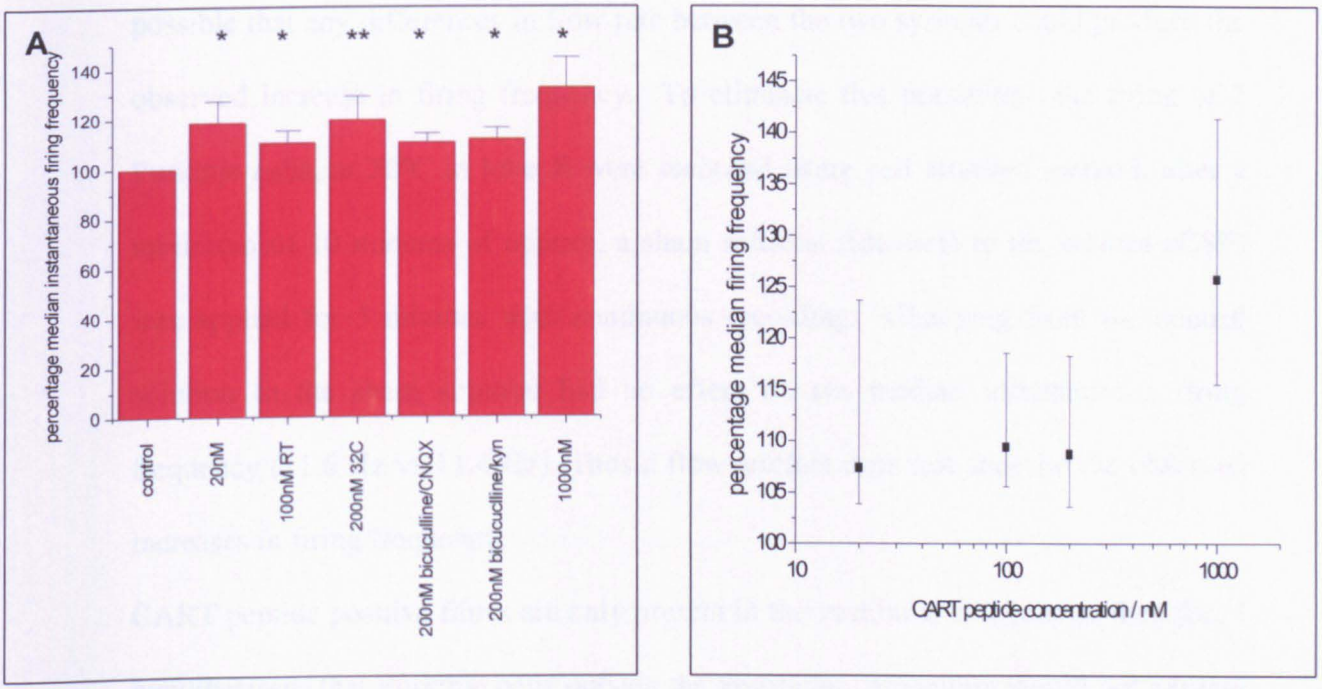

Figure 4.10 – Summary of CART peptide effects on Purkinje cell firing frequency. A – Plot of percentage median instantaneous firing frequency of Purkinje cells in response to CART peptide under different conditions, from left to right: control, 20 nM CART/32ºC, 100 nM CART/RT, 100 nM CART/32ºC, 200 nM/32ºC/10 µM bicuculline/10 µm CNQX, 200 nM CART/32ºC/10 µm bicuculline/5 mM kynurenic acid, 1000 nM CART/32ºC. B – Percentage median instantaneous firing frequency plotted against CART peptide concentration, each point is the average (n = 4-15) of all results for that concentration of CART peptide. Error bars are one SEM. * - $p<0.05$, ** - $p<0.01$.

directly before CART peptide application and in CART peptide. A temperature sensor was present in the bath and the temperature was continually monitored during recordings. There was no correlation between any small temperature changes and the actions of CART peptide. When CART peptide was bath applied, the perfusion was changed from a control syringe to a syringe containing CART peptide solution. It is possible that any differences in flow rate between the two syringes could produce the observed increase in firing frequency. To eliminate this possibility, the firing of 7 Purkinje cells, at 32°C in lobe X were recorded using cell attached method, after a minimum of 10 minutes of control, a sham solution (identical to the control aCSF) was applied for 5 minutes with continuous recording. Changing from the control solution to the sham solution had no effect on the median instantaneous firing frequency (11.6 Hz vs 11.4 Hz). Thus a flow artefact does not underlie the observed increases in firing frequency.

CART peptide positive fibres are only present in the vestibular cerebellum, therefore I hypothesised that Purkinje cells outside the vestibular cerebellum would not express CART peptide receptors and thus would not respond to CART peptide (this is of course unknown as the CART peptide receptor has yet to be identified). If the effects of CART peptide are specific, then I hypothesise that they should not be observed outside the vestibular cerebellum. To test this the firing of 5 Purkinje cells in lobe III to VII were recorded, after a minimum of 10 minutes of control, 100 nM CART peptide solution was bath applied for 5 minutes. The control median instantaneous firing frequency of these cells was 28.7 (20.0, 34.6) Hz; which is significantly ($p<0.05$) higher than the firing frequency of the Purkinje cells in the vestibular cerebellum. Application of CART peptide (100 nM) to these cells had no significant

affect on the firing rate (28.7 vs 31.4 Hz, figure 4.11C). Thus it appears that the actions of CART peptide are specific to the vestibular cerebellum.

4.2.8 – CART peptide increases the firing rate with no significant affect on firing pattern

For the analysis of the effects of CART on firing of Purkinje cells, I have concentrated on the median instantaneous firing frequency because I believe it is the most appropriate measure of changes in firing caused by CART peptide; however there are other parameters which can be measured, such as the mean, coefficient of variance and other parametric statistical measurements. To examine these statistical measurements, I combined room temperature and 32°C 100 nM CART experiments (sections 4.2.2-3) as the control and CART peptide median instantaneous firing frequencies in these two groups were not significantly different.

Table 4.6 shows the results of the other statistical tests, only the mean of the instantaneous firing frequencies are significantly different ($p>0.05$). The other statistical tests which measure the variability of the data (standard deviation, coefficient of variance, 90% interval and 50% interval) were not statistically different. Therefore I conclude that CART peptide increases the firing frequency without affecting variability and thus not changing the firing pattern (also see chapter 5)

	Control	CART	Percentage change	Significances
Mean / Hz	11.14 ± 1.92	12.36 ± 2.06	110.9 ± 6.82	0.05
Standard Deviation / Hz	7.44 ± 1.64	7.55 ± 1.80	110.8 ± 18.28	Not significant
Coefficient of Variance / %	90.2 ± 21.7	67.6 ± 16.0	92.4 ± 11.8	Not significant
90% interval / Hz	9.80	8.46	83.1	Not significant
50% interval / Hz	2.78	3.23	97.6	Not significant

Table 4.6 – Other statistic on the effects of 100 nM CART on Purkinje cell firing at room temperature and 32°C (data pooled). For mean, standard deviation and coefficient of variance, means and student t-tests were used. For 90% and 50% intervals, medians and wilcoxen t-tests were used.

4.3 – CART peptide does not modulate basal climbing fibre-Purkinje cell synaptic transmission.

My results demonstrate that CART peptide has a direct affect on the firing pattern of Purkinje cells and this effect is not via modulation of glutamatergic or GABAergic synaptic inputs. However in parasaggital slices both the climbing fibres and parallel fibres are cut, therefore the excitatory transmission to Purkinje cells is weak (kynurenic acid has no direct on the firing rate; chapter 5). Furthermore the climbing fibres are inactive in parasaggital slices and thus if CART peptide did modulate climbing fibre synaptic transmission this effect would probably not be detectable via a change in Purkinje cell firing rate. Thus I have directly stimulated climbing fibres and investigated whether CART peptide modulates the resultant excitatory postsynaptic currents (EPSCs) measured in Purkinje cells using whole cell voltage clamp.

EPSCs were evoked using a stimulating electrode placed on the granule cell layer, adjacent to the Purkinje cell body that was being recorded from. To prevent any interference from inhibitory synapses, 10 μM bicuculine was added to the aCSF to block $GABA_A$ receptors. In order to increase the signal to noise ratio, an internal pipette solution based on caesium chloride was used. The cells where held at -20 mV, in order to reduce EPSC amplitude and increase the quality of the voltage clamp. The climbing fibre EPSCs were identified by four criteria: 1) the EPSCs had a large amplitude (>-200 pA); 2) by using a pair pulse protocol (interval 100 ms), the amplitude of the second EPSC was smaller than that of the first EPSC (paired pulse depression; figure 4.12B), which is characteristic of climbing fibre synapses (Hashimoto and Kano, 1998); 3) as there is only one climbing fibre innervating each

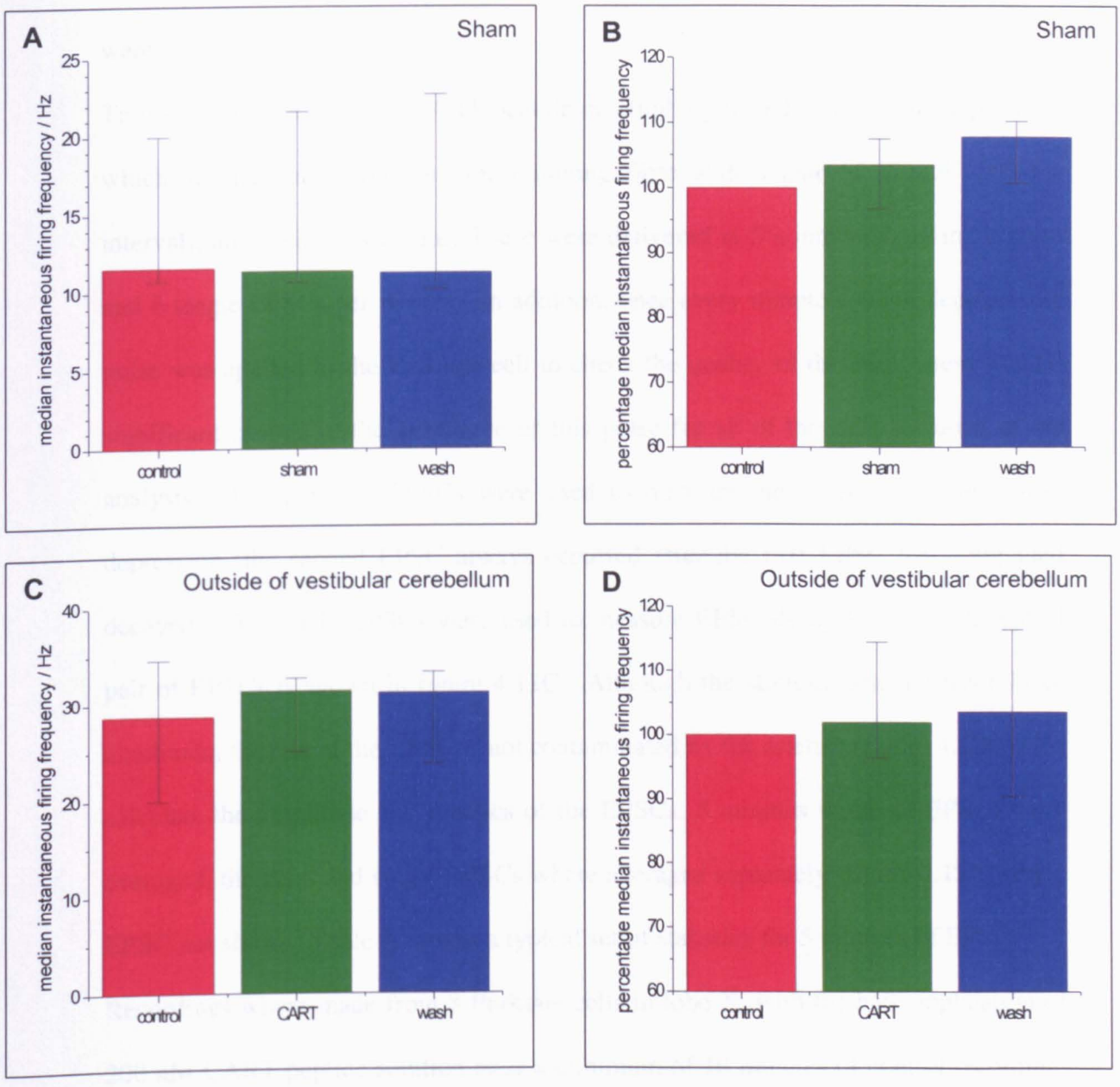

Figure 4.11 – The actions of CART peptide are not non-specific. Purkinje cell firing frequency is not significantly different following sham applications (n = 7; panels A and B). The firing frequency of Purkinje cells outside the vestibular cerebellum are not increased by CART peptide (n = 5; panels C and D). Red – control, Green (A,B) – sham, Green (C,D) – 100nM CART peptide, blue - washout. Error bars are one SEM. Panels A and C show the absolute firing frequencies and panels B and D show frequencies normalised to control.

Purkinje cell, the stimulus response curve was all or none (n = 2) (figure 4.12A); 4) the EPSCs were blocked by 10 μM CNQX (n = 3) (figure 4.12B) confirming that they were glutamatergic.

To investigate the effect of CART peptide on climbing fibre EPSCs, I used a protocol which alternatively stimulated the climbing fibre with a pair of stimuli (100 ms interval), and a single stimulus. These were delivered at 5 s intervals, giving 6 pairs and 6 single EPSCs per minute. In addition, once every minute a small depolarising pulse was applied to the Purkinje cell to check the quality of the seal. There was no significant change in the amplitude of this pulse for all of the cells included in the analysis. The pairs of EPSCs were used to measure the degree of paired pulse depression (the second EPSC always occurred after the first EPSC had completed decayed). The single EPSCs were used to measure EPSC decay kinetics. A typical pair of EPSCs is shown in figure 4.12C. Although the stimulus artefact has a large amplitude, the rise of the EPSC is not contaminated by the artefact (figure 4.12D). To calculate the amplitude and kinetics of the EPSCs, 5 minutes worth of EPSCs were averaged, the pairs and single EPSCs where averaged separately (figure 4.12E, single EPSC not show). Table 4.7 gives a typical set of statistics for 5 minutes of EPSCs.

Recordings where made from 8 Purkinje cells in lobe X, with the bath application of 200 nM CART peptide solution after a minimum of 10 minutes of control recording. Figure 4.13A-C shows a typical recording, in this example there was a slight decrease in EPSC amplitude following the application of CART peptide however the reverse was observed in other recordings (figure 4.13D). If the compensation in voltage clamp was not perfect, or changes in seal resistance occurred during the recording then a slight hump was observed in the EPSC decay (figure 4.13D). If the humps were

	1st EPSC	2nd EPSC	PPR
Peak amplitude / pA	765	644	84%
10%-90% rise time / ms	0.45	0.51	n/a
Tau1 / ms	5.64	3.38	n/a
A1 / pA	-275	-249	n/a
Tau2 / ms	12.87	12.32	n/a
A2 / pA	-414.33	-341.59	n/a
Tau(weighted) / ms	9.99	8.55	n/a

Table 4.7 – Statistic for a typical climbing fibre EPSC experiment

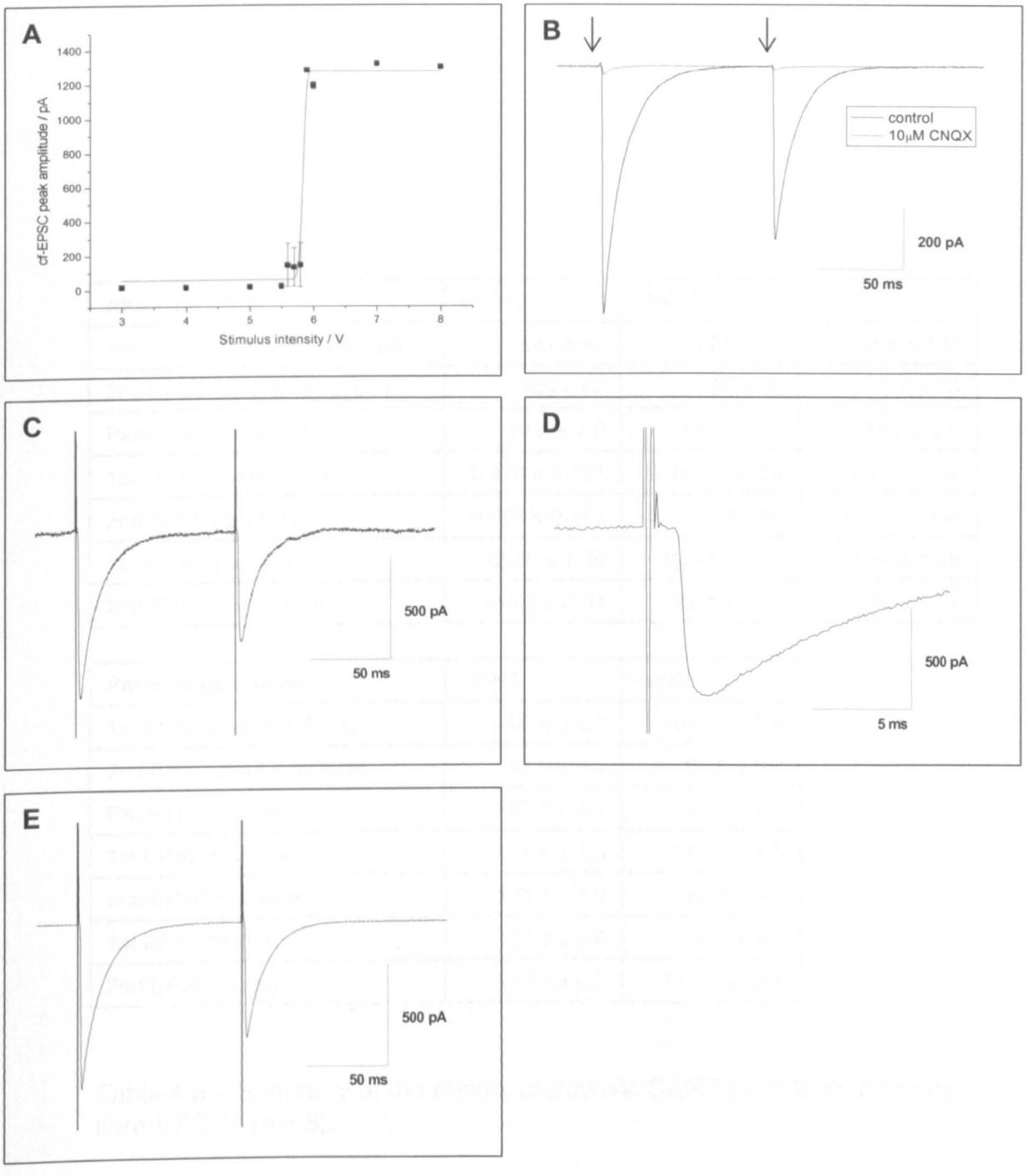

Figure 4.12 – Properties of evoked climbing fibre-excitatory post synaptic currents (EPSCs). A – Climbing fibre-EPSCs show an all or nothing response to increasing stimulus strength. B – Climbing fibre-EPSCs were blocked by 10 μM CNQX.C – A single pair of climbing fibre-EPSCs illustrating paired pulse depression. D – EPSCs occur after the stimulus artefact. E – Average of 30 pairs of EPSCs, showing that the second EPSC occurs after the first EPSC has completely decayed (grey dotted line).

Absolute value	Control	CART	wash
1st EPSC peak amplitude / pA	581 ± 89	555 ± 99	565 ± 100
2nd EPSC peak amplitude / pA	445 ± 62	421 ± 69	424 ± 73
Paired pulse ratio / %	78.2 ± 2.9	83.0 ± 5.3	75.6 ± 3.6
1st EPSC rise time / ms	0.479 ± 0.027	0.485 ± 0.028	0.514 ± 0.032
2nd EPSC rise time / ms	0.768 ± 0.163	0.788 ± 0.166	0.672 ± 0.056
1st EPSC tau(w) / ms	12.85 ± 1.36	13.63 ± 1.32	12.08 ± 1.26
2nd EPSC tau(w) / ms	11.01 ± 2.04	12.64 ± 2.16	11.31 ± 1.67

Percentage change	CART	wash
1st EPSC peak amplitude	92.4 ± 4.0	102.5 ± 11.2
2nd EPSC peak amplitude	98.0 ± 6.1	97.8 ± 8.6
Paired pulse ratio	105.9 ± 4.1	96.7 ± 2.6
1st EPSC rise time	101.4 ± 1.6	107.1 ± 1.3
2nd EPSC rise time	103.1 ± 1.6	98.7 ± 8.2
1st EPSC tau(w)	107.3 ± 2.8	98.4 ± 9.1
2nd EPSC tau(w)	117.2 ± 8.9	111.3 ± 12.8

Table 4.8 – Summary of the effects of 200 nM CART peptide on climbing fibre-EPSCs (n = 8).

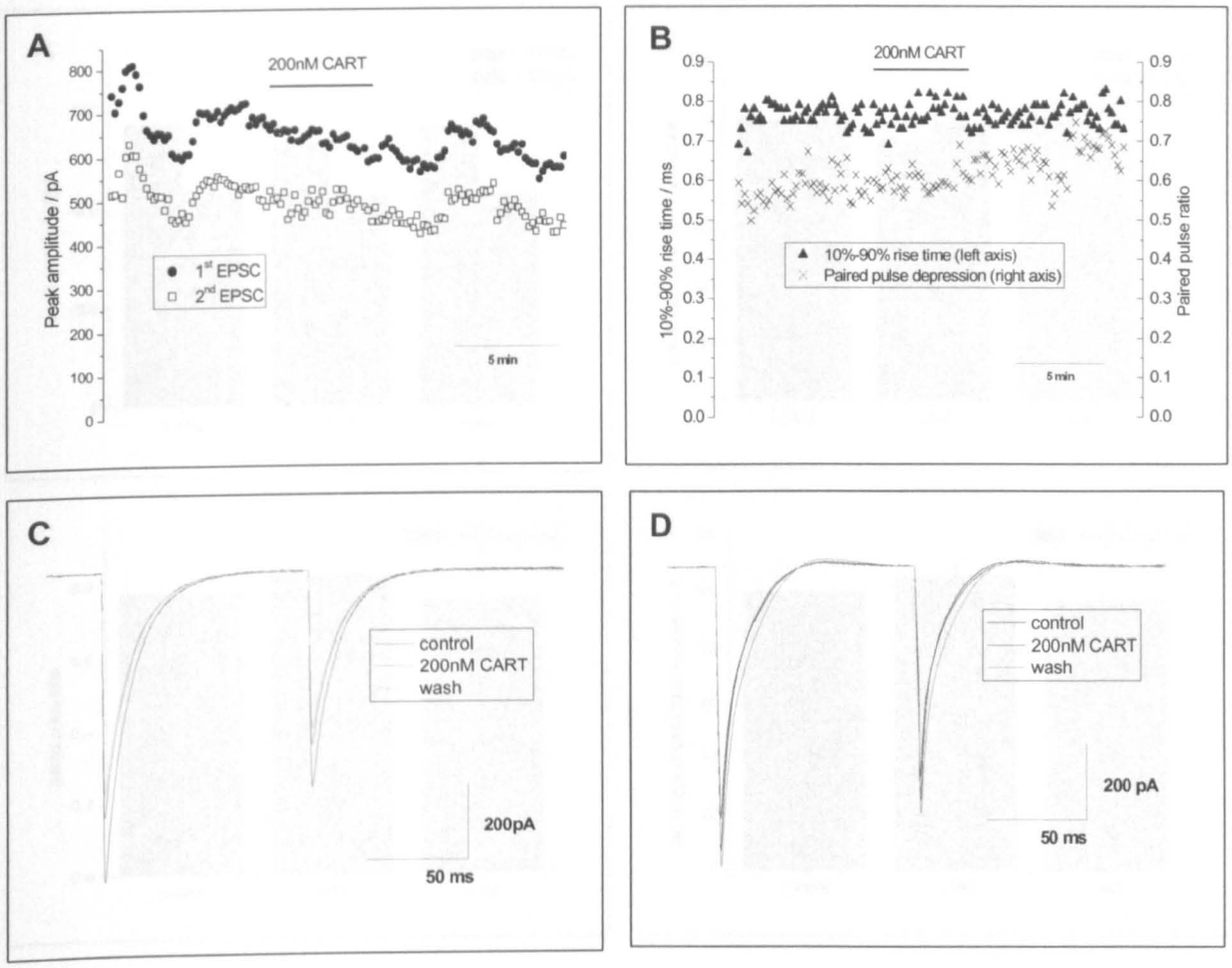

Figure 4.13 – An example of the affects of 200 nM CART peptide on climbing fibre-EPSCs from a single Purkinje cell (panel A-C). A – Plot of EPSC amplitudes against time for pairs of EPSCs. CART peptide did not effect the amplitude of the 1st or 2nd EPSC. B – Plot of EPSC 10-90 % rise time and paired pulse ratio against time. CART peptide did not significantly effect the paired pulse ratio or 10-90 % rise time. C – The average EPSCs in control, during CART peptide application and following wash, superimposed. D –The average EPSCs in control, during CART peptide application and following wash, superimposed. There is a outward deflection above the baseline (grey dotted line) in the decay the EPSCs which may be due to a loss of clamp.

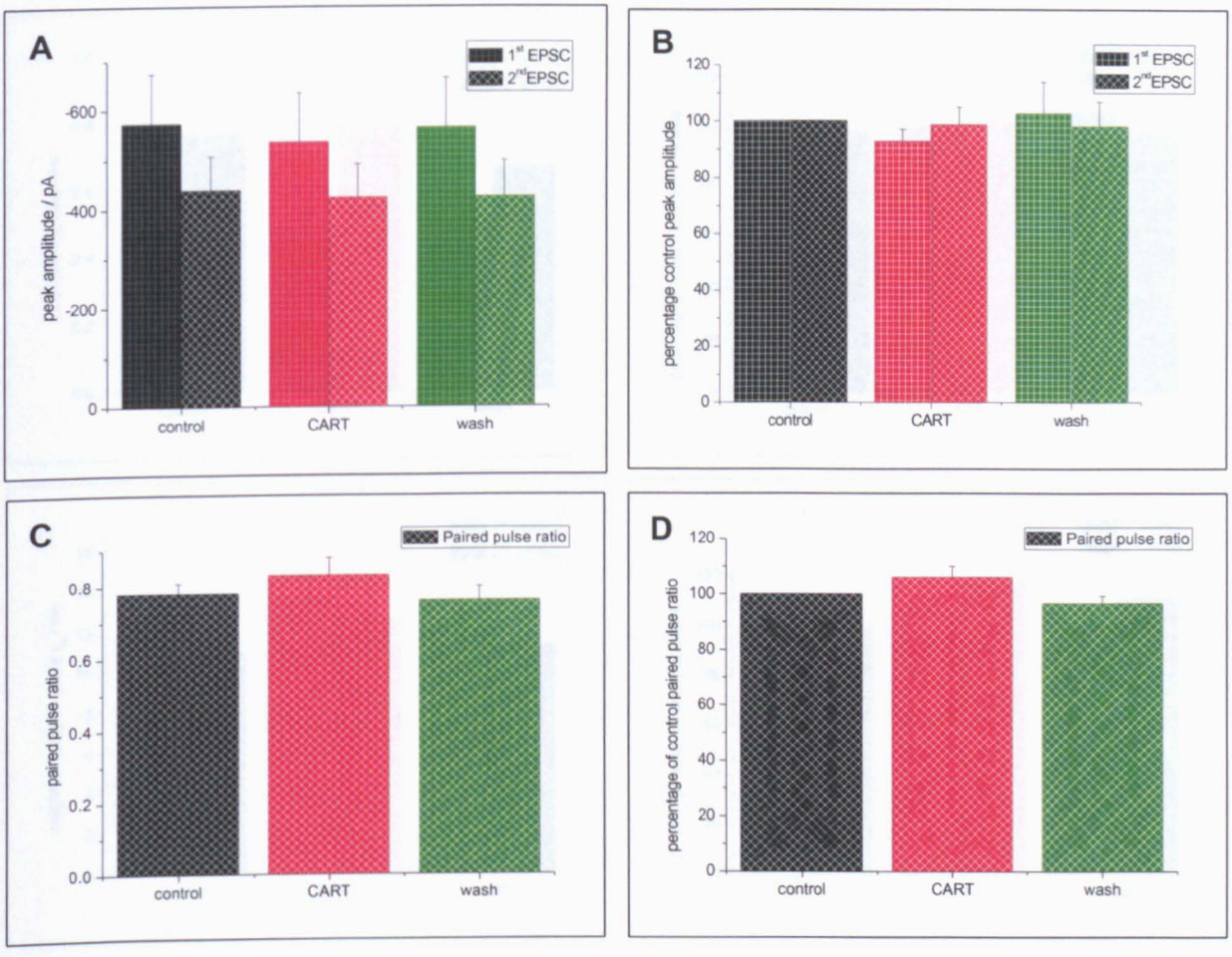

Figure 4.14 – CART peptide (200 nM) does not significantly change the amplitude (panels A and B) or paired pulse ratio (panels C and D) of climbing fibre-EPSCs. Error bars are one SEM. Panels A and C show the absolute values and panels B and D show values normalised to control.

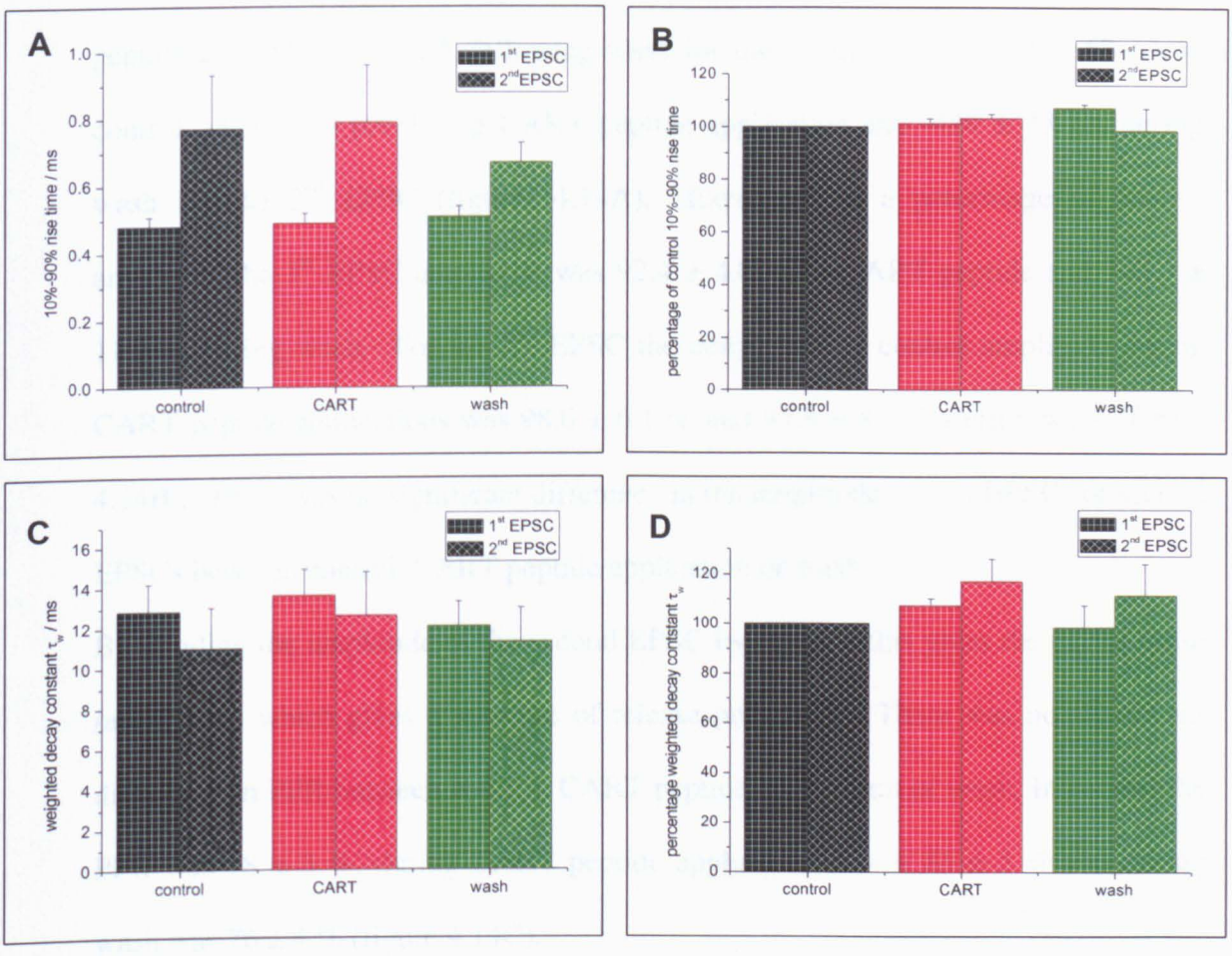

Figure 4.15 – CART peptide (200 nM) does not significantly change the 10-90 % rise time (panels A and B) or weighted decay constant, tau(w) (panels C and D) of climbing fibre-EPSCs. Error bars are one SEM. Panels A and C show the absolute values and panels B and D show values normalised to control.

consistent throughout the recording, then these recordings were used to calculate EPSC statistics and they were included in the final data set.

The mean EPSC amplitude was -580 ± 89 pA in control, -535 ± 99 pA in CART peptide and -565 ± 100 pA following wash for the 1st EPSC, and -445 ± 62 pA in control, -421 ± 69 pA during CART peptide application and -424 ± 73 pA during wash for the 2nd EPSC (figures 4.14A). Expressed as a percentage of control amplitude the 1st EPSC amplitude was 92.4 ± 4.0 % in CART peptide and 102.5 ± 11.2 % during wash. For the 2nd EPSC the percentage of control amplitude during CART peptide applications was 98.0 ± 6.1 % and 97.8 ± 8.6 % during wash (figure 4.14B). There was no significant difference in the amplitude of first EPSCs or second EPSCs between control, CART peptide application or wash.

By dividing the amplitude of the second EPSC by the first this gives the paired pulse ratio (PPR) which gives a measure of release probability. There was no significant difference in PPR between control, CART peptide application or wash. In control the PPR was 78 ± 3 %, during CART peptide application it was 83 ± 5 % and during wash was 76 ± 4 % (figure 4.14C).

There was also no significant difference in the 10-90 % rise time for first EPSC or second EPSC between control, CART peptide application or wash. The mean 10-90 % rise time for the first EPSC was 0.48 ± 0.03 ms during control, 0.49 ± 0.03 ms during CART peptide application and 0.51 ± 0.03 ms during wash. The mean 10-90 % rise time for the second EPSC was 0.77 ± 0.16 ms during control, 0.79 ± 0.17 ms during CART peptide application and 0.77 ± 0.06 ms during wash (figure 4.15A).

The decay of the averaged EPSCs was fitted with a double exponentials and the weighted decay constant (τ_w) was calculated to compare the kinetics of decay. There was no significant difference in the weighted decay constant for the first EPSC or

second EPSC between control, CART peptide application or wash. The average weighted decay constant for the first EPSC was 12.9 ± 1.4 ms in control, 13.6 ± 1.3 ms in CART peptide and 12.1 ± 1.3 ms following wash. The average weighted decay constant for the second EPSC was 11.0 ± 2.0 ms in control, 12.6 ± 2.2 ms in CART peptide and 11.3 ± 1.7 ms following wash (figure 4.15C).

These results suggest that CART peptide does not modulate basal synaptic transmission at the climbing fibre to Purkinje cell synapse, either post-synaptically or pre-synaptically. It is possible that CART peptide changes the threshold potential for transmitter release from climbing fibres, has effects during trains of EPSCs or has a very slow modulatory effect on the climbing fibre-Purkinje cell synapse, but using this method I was unable to investigate these possibilities.

4.4 – CART peptide does not modulate basal parallel fibre-Purkinje cell transmission

The expression of CART peptide at the climbing fibre-Purkinje cell synapse suggests that the climbing fibre synapse would be the most likely target of CART peptide modulation. However it is possible that CART peptide spills out from the climbing fibre synapse to act at other Purkinje cell synapses, for example parallel fibre synapses. To investigate the effects of CART peptide on parallel fibre-Purkinje cell synapses, I stimulated parallel fibres and investigated whether CART peptide modulates the excitatory postsynaptic currents measured using whole cell voltage clamp of Purkinje cells.

EPSCs were evoked using a stimulating electrode placed on the molecular layer, close to the recorded Purkinje cell. To prevent any interference from inhibitory synapses,

10μM bicuculine was added to the aCSF to block $GABA_A$ receptors. Parallel fibre EPSCs are smaller than climbing fibre EPSCs and therefore the cells where held at -70 mV, in order to increase EPSC amplitude. The parallel fibre EPSCs were identified by four criteria: 1) the EPSCs had a small amplitude (<-1000 pA, a climbing fibre EPSC recorded at -70 mV would be >3 nA); 2) by using a paired pulse protocol (interval 50 ms), the amplitude of the second EPSC was larger than that of the first EPSC (paired pulse facilitation), which is a characteristic of parallel fibre synapses (Perkel et al., 1990); 3) as multiple parallel fibres innervate Purkinje cells, increasing the stimulus strength recruited more fibres and thus the stimulus-response curve was linear (n = 4) (figure 4.16A); 4) EPSCs were blocked by 10μM CNQX (n = 3) (figure 4.16B) confirming they were glutamatergic.

To investigate the effect of CART peptide on parallel fibre EPSCs, I used a similar protocol as for climbing fibre EPSCs (section 4.3) only a shorter (50 ms) interval was used to measure paired pulse facilitation. The parallel fibre stimulation strength was chosen to give as large an EPSC as possible (for ease of measurement) without loss of clamp and these were delivered at 5 s intervals, giving 6 pairs and 6 single EPSCs per minute. As before, a small depolarising pulse was applied once per minute to check the quality of the seal and the same analysis methods were used as climbing fibre EPSCs (see above).

Recordings where made from 9 Purkinje cells in lobe X, with the bath application of 200 nM CART peptide solution after a minimum of 10 minutes of control recording. Figure 4.17A-D shows a typical application of CART peptide. The mean EPSC amplitude (n = 9) was -200 ± 48 pA in control, -180 ± 37 pA during CART peptide application and -169 ± 38 pA following wash for the 1st EPSC, and -372 ± 85 pA in control, -394 ± 73 pA during CART peptide application and -360 ± 74 pA during

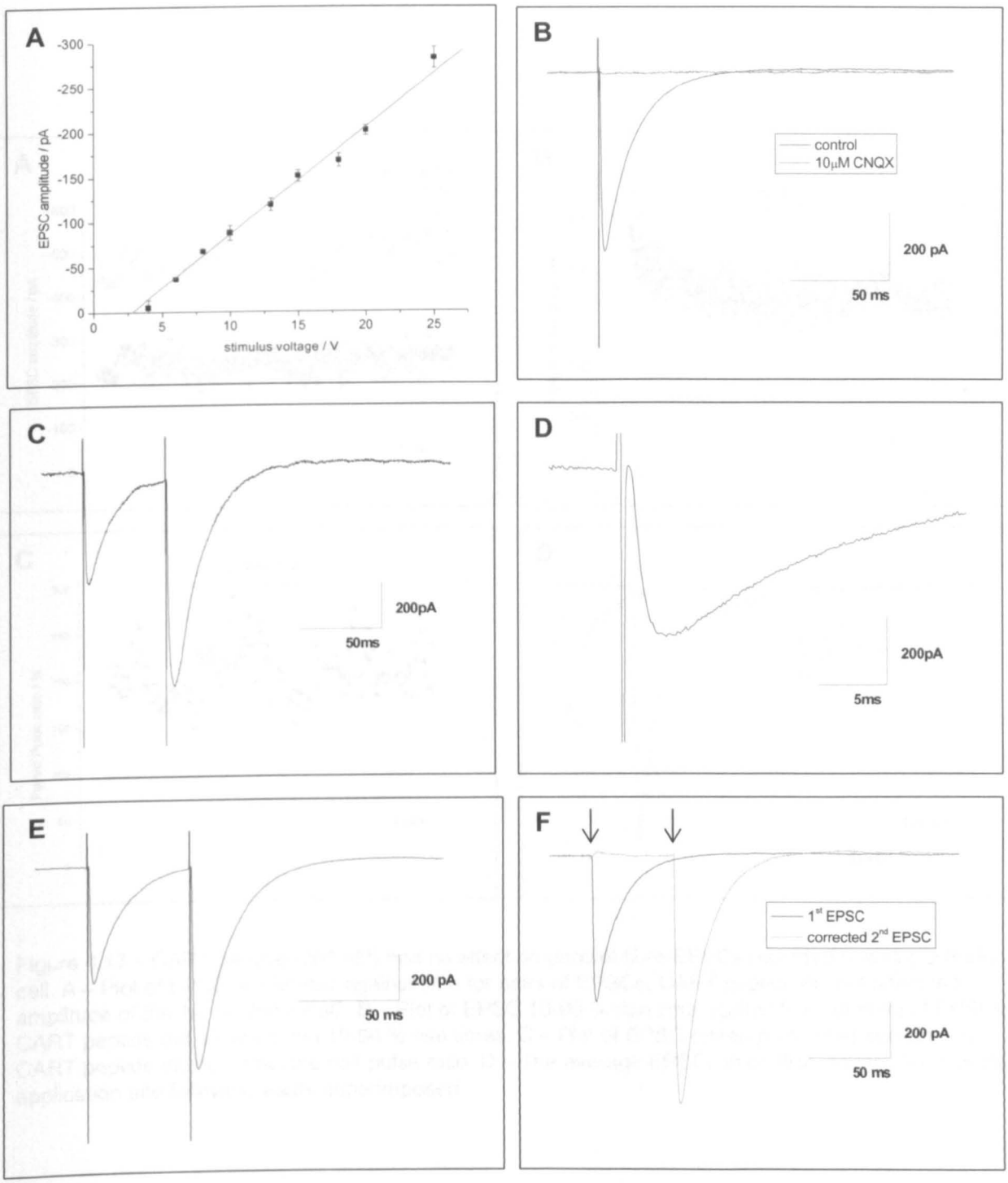

Figure 4.16 – Properties of evoked parallel fibre-excitatory post synaptic currents (EPSCs) from a single Purkinje cell. A –EPSCs show a linear relationship to increasing stimulus strength. B – EPSCs are blocked by 10 μM CNQX. C – Example of a single pair of parallel fibre-EPSCs illustrating paired pulse facilitation. D – EPSCs occur after the stimulus artefact. E – Average of 30 pairs of EPSCs, showing that the second EPSC occurs in the decay of the first EPSC. F – The average of the scaled single EPSC was substracted from the averaged paired EPSCs. Finally the stimulus artefacts were removed (arrows).

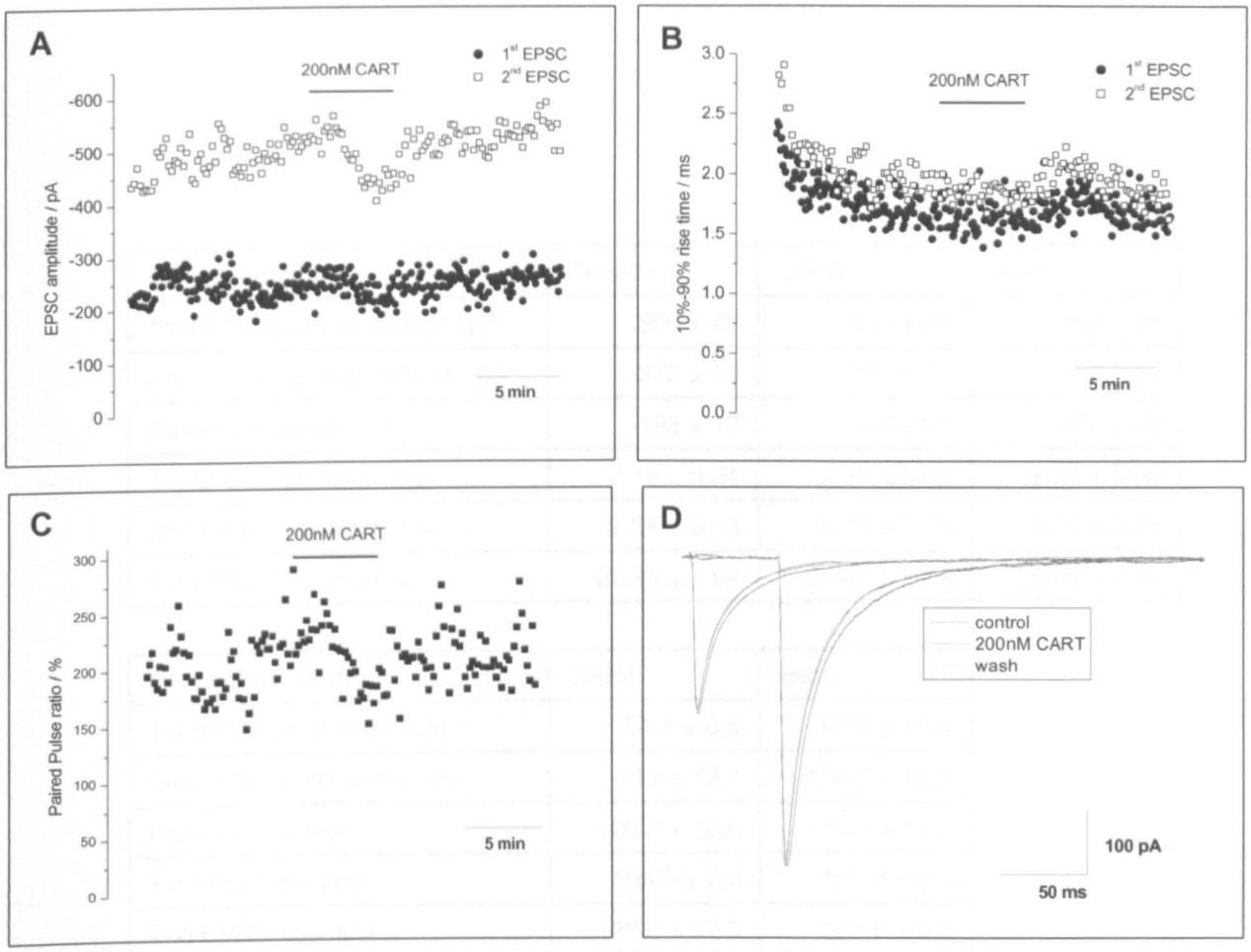

Figure 4.17 – CART peptide (200 nM) had no effect on parallel fibre-EPSCs recorded in a single Purkinje cell. A – Plot of EPSC amplitudes against time for pairs of EPSCs. CART peptide did not affect the amplitude of the 1st or 2nd EPSC. B – Plot of EPSC 10-90 % rise time against time for pairs of EPSCs. CART peptide did not affect the 10-90 % rise times. C – Plot of EPSC paired pulse ratio against time. CART peptide did not affect the pair pulse ratio. D – The average EPSCs in control, during CART peptide application and following wash, superimposed

Absolute value	Control	CART	wash
1st EPSC peak amplitude / pA	200 ± 48	180 ± 37	169 ± 38
2nd EPSC peak amplitude / pA	372 ± 85	393 ± 73	360 ± 74
Paired pulse ratio / %	193 ± 12	229 ± 20	224 ± 23
1st EPSC rise time / ms	2.16 ± 0.31	2.21 ± 0.26	2.20 ± 0.30
2nd EPSC rise time / ms	2.34 ± 0.28	2.75 ± 0.28	2.56 ± 0.38
1st EPSC Tau(w) / ms	21.95 ± 1.89	24.40 ± 2.76	25.63 ± 2.48

Percentage change	CART	wash
1st EPSC peak amplitude	94.4 ± 6.5	92.8 ± 15.4
2nd EPSC peak amplitude	113 ± 12.7	106.2 ± 18.1
Paired pulse ratio	120.2 ± 10.8	118.3 ± 13.7
1st EPSC rise time	105.9 ± 7.0	103.2 ± 5.5
2nd EPSC rise time	122.6 ± 12.0	109.0 ± 5.3
1st EPSC Tau(w)	110.4 ± 5.6	118.7 ± 10.4

Table 4.9 – Summary of the effects of 200 nM CART peptide on parallel fibre-EPSCs ($n = 9$).

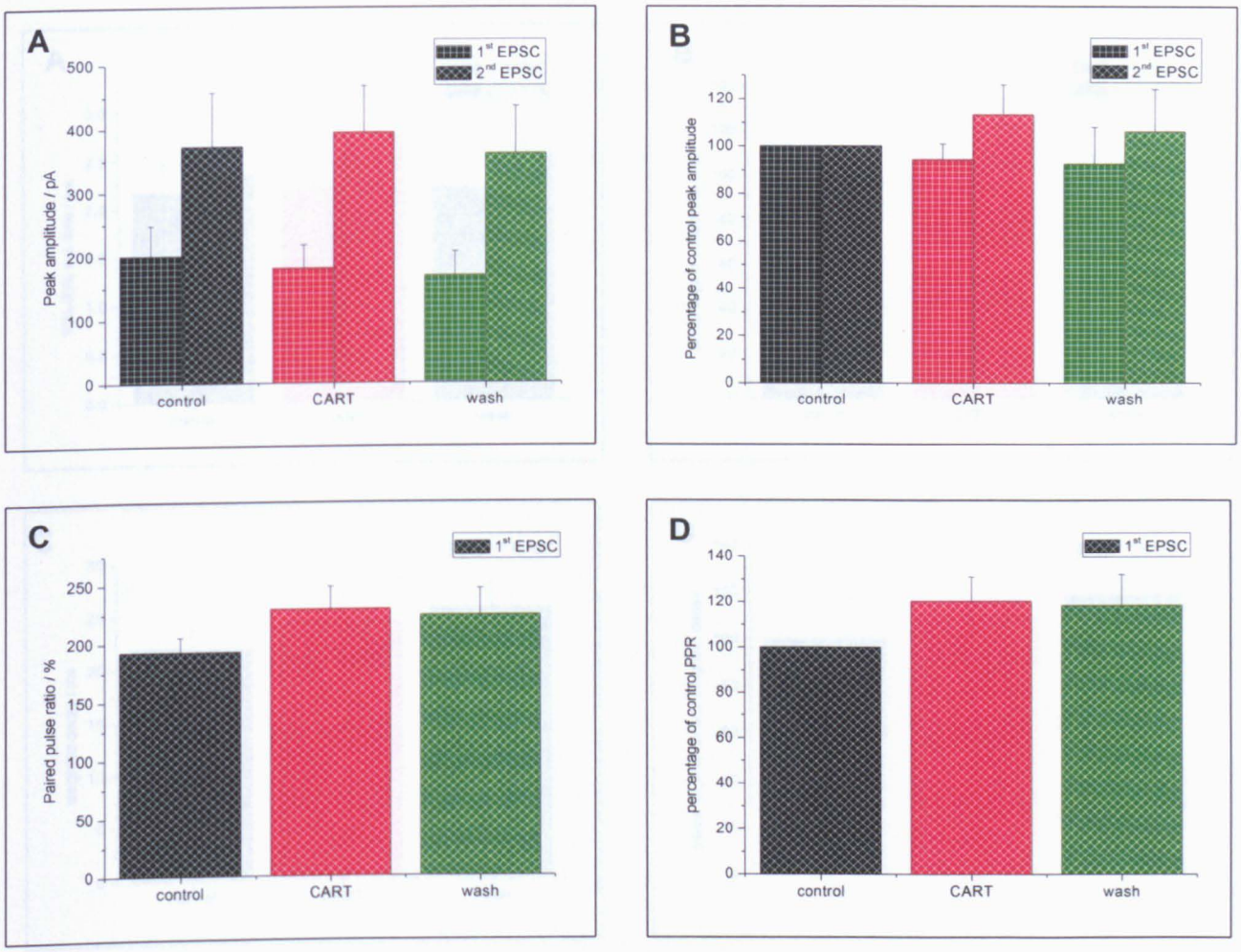

Figure 4.18 – CART peptide (200 nM) did not significantly change the amplitude (panels A and B) or paired pulse ratio (panels C and D) of parallel fibre-EPSCs. Error bars are one SEM. Panels A and C show the absolute values and panels B and D show values normalised to control.

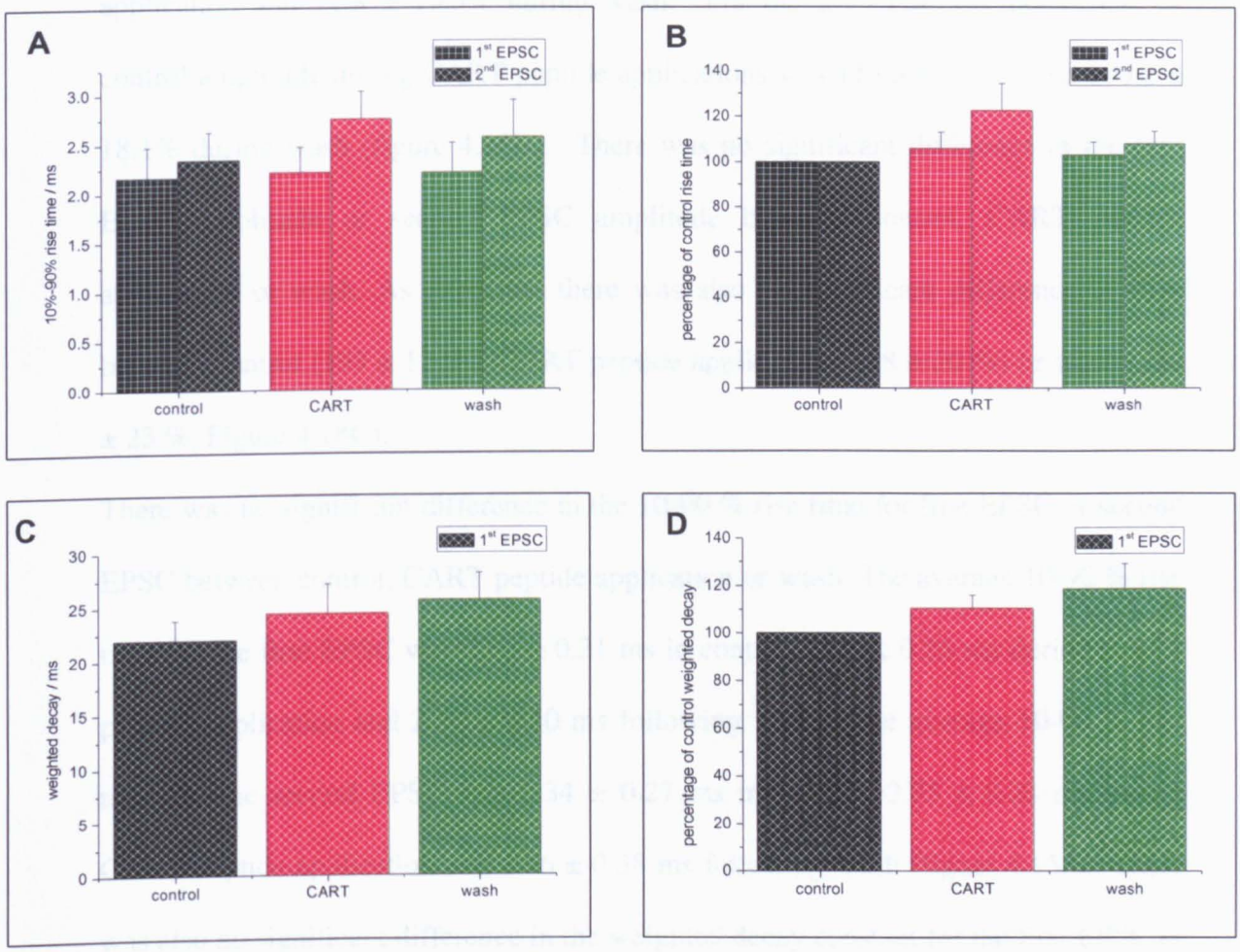

Figure 4.19 – CART peptide (200 nM) does not significantly change the 10-90 % rise time (panels A and B) or weighted decay constant, tau(w) (panels C and D) of parallel fibre-EPSCs. Error bars are one SEM. Panels A and C show the absolute values and panels B and D show values normalised to control.

wash for the 2nd EPSC (figures 4.18A). Expressed as a percentage of the control amplitude, the 1st EPSC amplitude was 94.4 ± 6.5 % during CART peptide application and 92.8 ± 15.3% during wash. For the 2nd EPSC the percentage of control amplitude during CART peptide applications was 113.3 ± 12.7% and 106.2 ± 18.1% during wash (figure 4.18B). There was no significant difference in the first EPSC amplitude or second EPSC amplitude between control, CART peptide application or wash. As expected, there was also no significant difference in PPR between control (193 ± 12 %), CART peptide application (228 ± 20 %) or wash (224 ± 23 %, Figure 4.18C).

There was no significant difference in the 10-90 % rise time for first EPSC or second EPSC between control, CART peptide application or wash. The average 10-90 % rise time for the first EPSC was 2.16 ± 0.31 ms in control, 2.21 ± 0.26 ms during CART peptide application and 2.20 ± 0.30 ms following wash. The average 10-90 % rise time for the second EPSC was 2.34 ± 0.27 ms in control, 2.75 ± 0.28 ms during CART peptide application and 2.56 ± 0.38 ms following wash (figure 4.15A). There was also no significant difference in the weighted decay constant for the first EPSC or second EPSC between control, CART peptide application or wash.

The average weighted decay constant for the first EPSC was 22.0 ± 1.9 ms in control, 24.4 ± 2.8 ms during CART peptide application and 25.6 ± 2.5 ms following wash.

These results suggest that CART peptide does not act to modulate basal synaptic transmission at the parallel fibre to Purkinje cell synapse, either post-synaptically or pre-synaptically. Because the parallel fibre EPSC measures the effect of transmitter released from multiple fibres it is unlikely that CART peptide changes the threshold potential for transmitter release as this would have changed the EPSC amplitude. However it is possible the CART peptide may have an effect during trains of EPSCs

or have a very slow modulatory affect on the parallel fibre-Purkinje cell synapse, but using my method I was unable to investigate these possibilities.

4.5 – CART peptide does not modulate GABAergic miniature inhibitory postsynaptic currents (mIPSCs)

CART peptide does not appear to modulate basal synaptic transmission at either climbing fibre or parallel fibre-Purkinje cell synapses. However Purkinje cells also receive synaptic connects from two other cells types in the cerebellum: the basket and stellate cells. These cells are both GABAergic and are often considered together as local interneurones. They have different morphology and make synaptic connections onto different areas of the Purkinje cell; the stellate cells make synapses onto the dendrites whereas the basket cells make their synaptic connections onto the cell body. As they both receive excitatory inputs from parallel and climbing fibres and inhibit Purkinje cells they may be considered as feed-forward inhibitory neurons.

In parasaggital slices, these interneurones play a role in determining Purkinje cell firing rate, (unlike the parallel or climbing fibres), as demonstrated by the increase in Purkinje cell firing rate after the block of $GABA_A$ receptors (see above and chapter 5). Given that the effects of CART peptide were similar with or without GABAergic synaptic transmission, it seems unlikely that CART peptide modulates the synaptic transmission between interneurones and Purkinje cells. However the effects of CART peptide on GABAergic may be subtle and not produce a marked change in Purkinje cell firing rate. Thus I investigated the actions of CART peptide on miniature

inhibitory post synaptic currents (mIPSCs) recorded from Purkinje cells using whole cell voltage clamp.

Miniature inhibitory post synaptic currents were recorded in the presence of the sodium channel blocker TTX (1 μM), and kynurenic acid (5 mM) to block glutamate receptors. Miniature IPSCs occured at a low frequency, had a small amplitude and resulted from the spontaneous exocytosis of GABA. They are useful because a change in mIPSC amplitude indicates post-synaptic modulation, whereas changes in mIPSC frequency indicates pre-synaptic modulation

Miniature IPSCs where recorded from 6 Purkinje cells in lobe X using an internal patch clamp solution based on caesium chloride. Purkinje cells where held at -70 mV and under these conditions the mIPSCs were inward. A small depolarising pulse was applied once a minute to check the quality of the seal and there was no significant change in the amplitude of this pulse during the recordings. CART peptide was bath applied after a minimum of 10 minutes of control and statistics were calculated for 5 minutes intervals: before CART peptide application (control), during CART peptide application (CART) and 5 minutes after washout of CART peptide. At the end of the recording, bicuculline was applied and all currents were abolished confirming they were GABAergic. Figure 4.20 shows a typical recording.

For the 6 recordings, the mean mIPSC amplitude in control was -51.5 ± 11.5 pA with an average SD of 45.8 ± 9.1 pA, the mean mIPSC amplitude during CART peptide application was -43.6 ± 7.0 pA with an average SD of 32.8 ± 4.8 pA and the mean mIPSC amplitude after wash was -47.0 ± 7.4 pA with an average SD of 36.8 ± 4.8 pA (figure 4.21A). The average mIPSC frequency in control was 6.2 ± 2.8Hz with an average SD of 7.2 ± 1.5 Hz, the average mIPSC frequency during CART peptide application was 5.7 ± 2.8 Hz with an average SD of 6.3 ± 1.8 Hz and the average

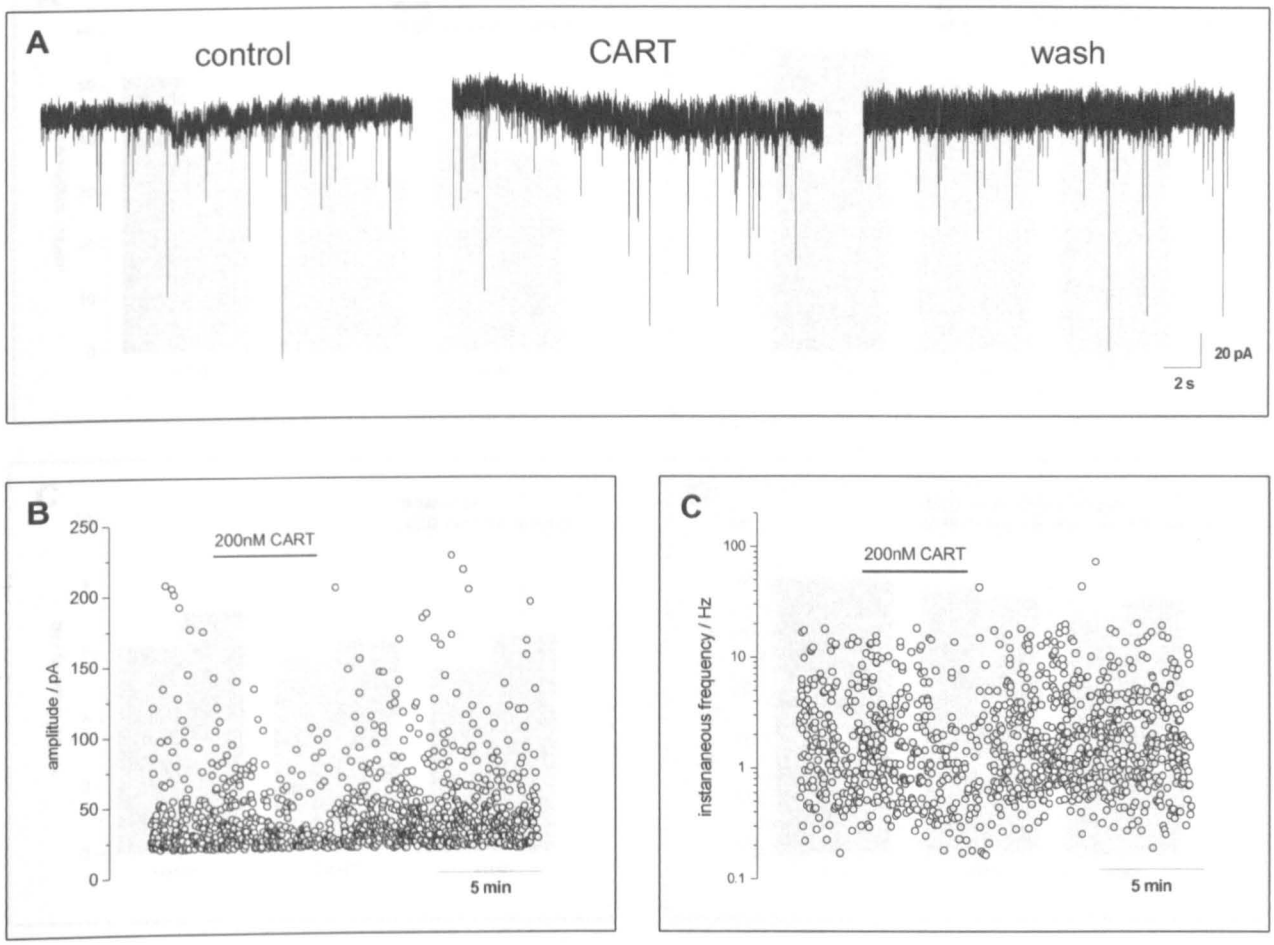

Figure 4.20 - CART peptide (200 nM) has no effect on GABAergic mini IPSCs (mIPSCs) recorded in a single Purkinje cell. A – Raw voltage clamp traces in control, during CART peptide application and after wash. B – Plot of mIPSC amplitude against time. Application of CART peptide did not significantly change mIPSC amplitude. C – Plot of mIPSC instantaneous frequency against time. Application of CART peptide had no significant effect on frequency.

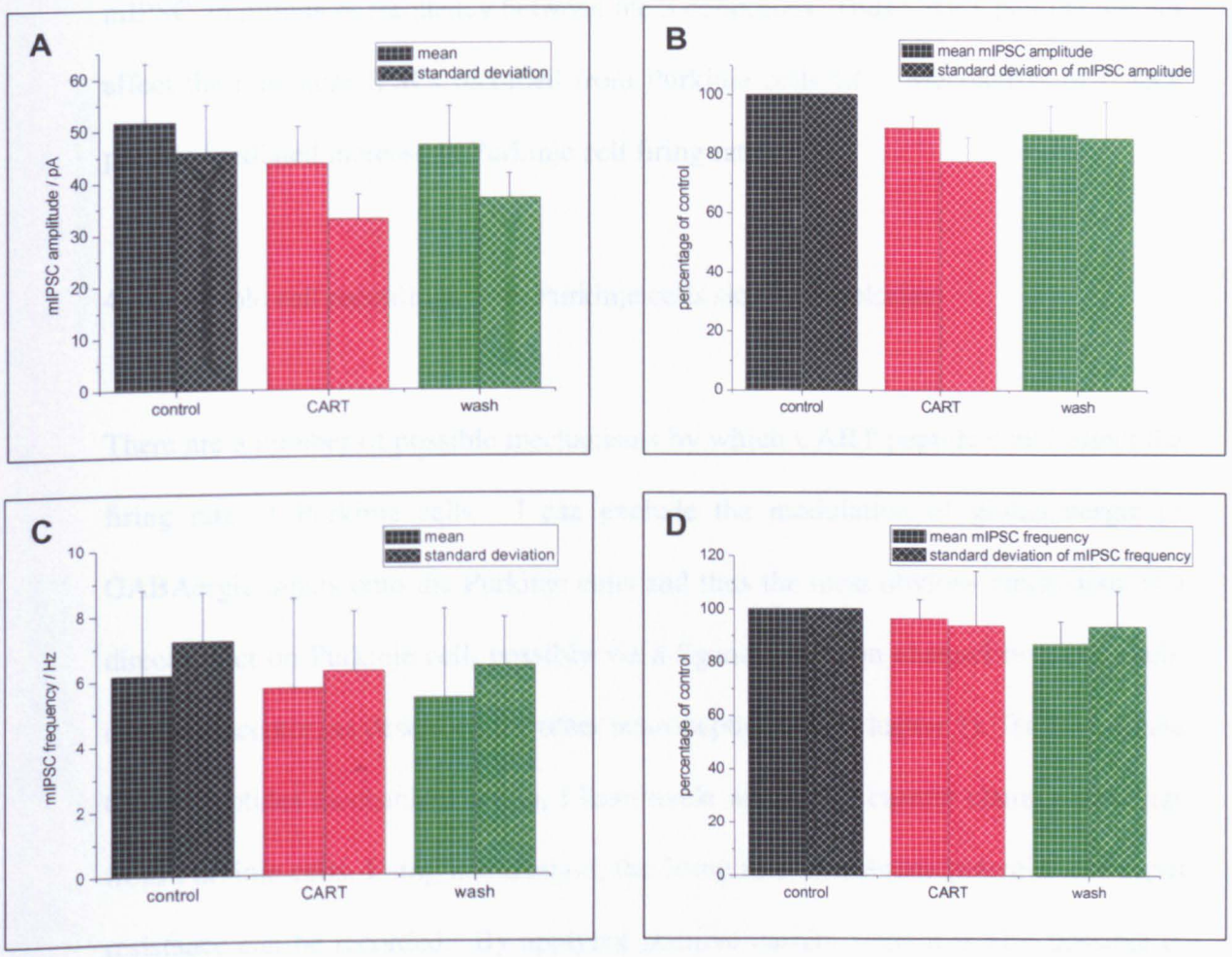

Figure 4.21 – CART peptide (200 nM) does not significantly change the amplitude (panels A and B) or instantaneous frequency (panels C and D) of mIPSCs. Error bars are one SEM. Panels A and C show the absolute values and panels B and D show values normalised to control.

mIPSC frequency after wash was 5.4 ± 2.7 Hz with an average SD of 6.4 ± 1.5 Hz (figure 4.21C). There was no significant difference in the mean or SD of either mIPSC amplitude or frequency between the 3 conditions. Thus CART peptide did not affect the miniature IPSCs recorded from Purkinje cells.4.6 – Mechanism of CART peptide-mediated increase in Purkinje cell firing rate.

4.6.1- Whole cell recordings from Purkinje cells slowly depolarise.

There are a number of possible mechanisms by which CART peptide could affect the firing rate of Purkinje cells. I can exclude the modulation of glutamatergic or GABAergic inputs onto the Purkinje cells and thus the most obvious mechanism is a direct effect on Purkinje cell, possibly via a ligand-gated ion channel or a G-protein coupled receptor, as described for other neuropeptides (see chapter 1). To investigate CART peptides mechanism action, I have made whole cell current clamp recordings from Purkinje cells. Using this method, the firing rate, membrane potential and input resistance can be recorded. By applying positive current steps it is also possible to measure the excitability of Purkinje cells.

Using an intracellular patch solution based on potassium gluconate and containing ATP and GTP, I made whole cell current clamp recordings from 6 Purkinje cells in the vestibular cerebellum at 32°C. Of these 6 cells, 4 of them were spontaneously active at rest (figure 4.22A-B) but all fired action potentials in response to current injection. From current steps, I calculated the resting membrane potential and membrane resistance (figure 4.22C-D). The resting membrane potential and resistance were measured 5 minutes after establishing the whole cell recording, to allow equilibration. For all 6 cells, the mean membrane potential was -56.9 ± 3.1 mV,

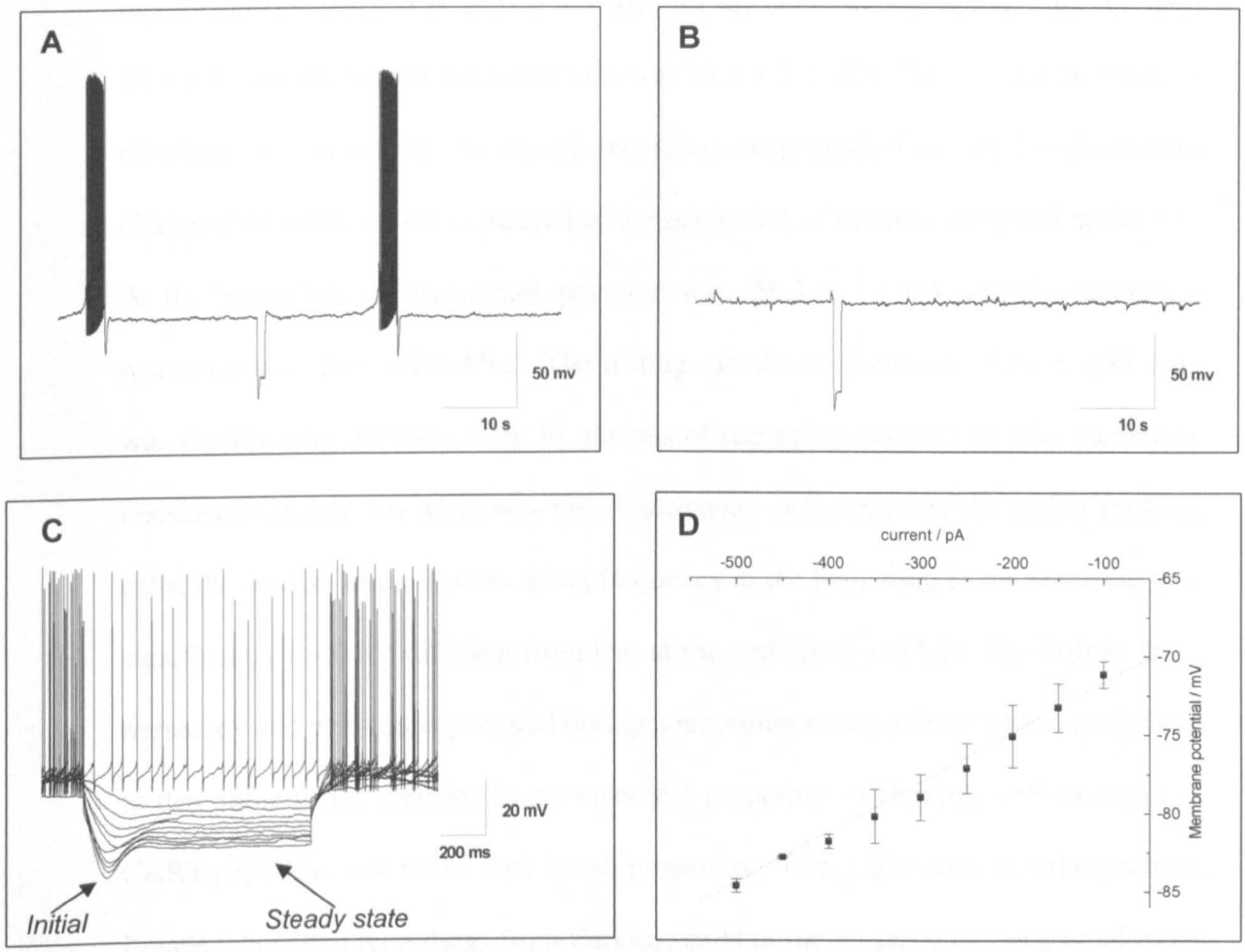

Figure 4.22 – Examples of typical whole cell recordings from Purkinje cells. A – Recording from a constituently active cell. B – Recording from a silent cells. The square downward deflections in A and B are injection of negative current to measure membrane resistance. C - A typical Purkinje cell current voltage relationship (IV) (-450 pA-0 pA in 50 pA steps). D – Plot of current against voltage (*initial*) for cell in C (average of 3 IV protocols). The calculated resting membrane potential was -68.1 mV and the membrane resistance was 34.0 MΩ.

the active Purkinje cells had a membrane potential of -53.0 ± 2.6 mV and the quiescent Purkinje cells had a membrane potential of -64.5 ± 4.1 mV. The mean membrane resistance was 26.0 ± 2.3 MΩ for all cells, for the active Purkinje cells 26.3 ± 3 MΩ and for the quiescent cells was 27.1 ± 3.2 MΩ. To measure the stability of whole cell recordings, 30 minute recordings were made from all 6 cells and the electrical properties were compared at the beginning of the recording and at the end. At the beginning, the membrane potential was -56.7 ± 3.1 mV and the membrane resistance was 26.6 ± 2.3 MΩ. The resting membrane potential (-50.8 ± 2.81 mV) was significantly different after 30 minutes of recording ($p>0.01$) but the membrane resistance (26.2 ± 3.0 MΩ) was not significantly different. For the active Purkinje cells, the median instantaneous firing frequency at the beginning of the recording was significantly ($p<0.05$) different from that at the end (10.8 vs 15.1). The drift in firing frequency and membrane potential during a recording means it would be very difficult to determine if any changes in the electrical properties of Purkinje cell were due to CART peptide or due to the drift in cell properties. To try and overcome this problem, I made whole cell recordings from Purkinje cells in the presence of synaptic blockers (kynurenic acid to block glutamate receptors and bicuculline to block $GABA_A$ receptors) and the sodium channel blocker TTX. I suspected that the drift maybe due to an accumulation/or loss of cellular factors that under normal conditions would be controlled by intracellular processes, but are disrupted by cell dialysis. By reducing the activity of Purkinje cells and the number of active conductances, this may stop cell dialysis having such a large effect on the electrical properties.

4.6.2 – CART peptide may change electrical properties of Purkinje cells with synaptic activity and action potentials blocked

I used a protocol of negative currents steps to acquire current voltage relationships from Purkinje cells and from this calculated the resting membrane potential and membrane resistance of Purkinje cells and then investigated the effect of CART peptide

I recorded current voltage relationships in whole cell current clamp from 6 Purkinje cells in lobe X at 32°C every 10 minutes for 30 minutes in the presence of 1 μM TTX, 10 μM bicuculline and 5 mM kynurenic acid. The current voltage relationships were similar to those acquired in control but clearly no action potentials were observed and the membrane resistance was consistently higher (as a number of conductances were blocked). The mean resting membrane potential was initially -54.7 ± 1.4 mV, after 10 minutes was -54.3 ± 1.4 mV, after 20 minutes was -55.2 ± 1.4 mV and after 30 minutes was -55.2 ± 1.7 mV (figure 4.23A). The mean membrane resistance was initially 69.2 ± 3.4 MΩ, after 10 minutes was 70.0 ± 2.5 MΩ, after 20 minutes was 70.7 ± 2.5 MΩ and after 30 minutes was 72.4 ± 2.7 MΩ (figure 4.23B). There was no significant difference in resting membrane potential or membrane resistance between any of the time intervals.

Having established that the recording was stable over 30 minutes, I repeated the same protocol as above for 9 Purkinje cells to which 100 nM CART peptide was applied for 5 minutes, 7 minutes into the recording. The current voltage relationships were similar to those acquired without CART peptide. The average resting membrane potential was initially -50.6 ± 1.9mV, during CART peptide application (10 minutes) was -50.1 ± 2.7 mV, after initial CART peptide wash (20 minutes) was -50.0 ± 3.1

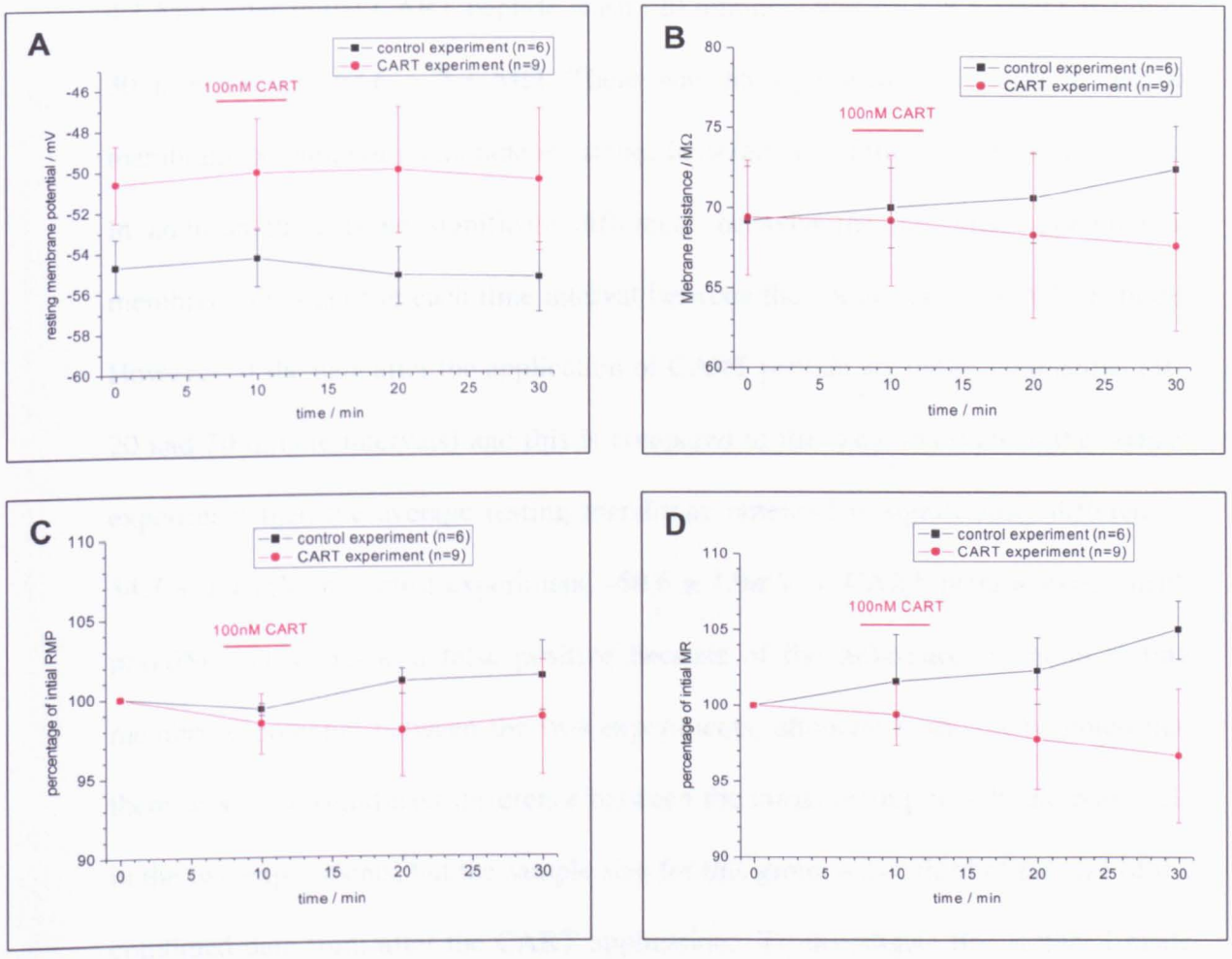

Figure 4.23 – There is no obvious effect of CART peptide on Purkinje cell membrane properties. Recordings of current voltage relationships from Purkinje cells in the presence 1 μM TTX, 10 μM bicuculline and 5 mM kynurenic acid, with (in red; n = 9) and without (in black; n = 6) the application of 100 nM CART peptide. The mean resting membrane potential (panels A and C) and the mean membrane resistance (panels B and D) was not significantly different at any of the time points. Panels A and B show absolute values and panels C and D show values normalised to control.

mV and after 30 minutes was -50.5 ± 3.5 mV. The average membrane resistance was initially 69.4 ± 3.6 MΩ, during CART peptide application (10 minutes) was 69.2 ± 4.1 MΩ, after initial CART peptide wash (20 minutes) was 68.3 ± 5.2 MΩ and after 30 minutes was 67.6 ± 5.3 MΩ. There was no significant difference in resting membrane potential or membrane resistance between any of the time intervals.

In addition there is no significant difference between the membrane potential or membrane resistance at each time interval between the control and in CART peptide. However, if the data after the application of CART peptide are collected together (10, 20 and 30 minute intervals) and this is compared to the same intervals in the control experiment then the average resting membrane potential is significantly different (-54.7 ± 1.4 mV in control experiment, -50.6 ± 1.9mV in CART peptide experiment, $p>0.05$). This maybe a false positive because of the difference in initial resting membrane potential between the two experiments, although it should be noted that there was not a significant difference between the initial resting membrane potentials in the two experiments, but the sample size for this group was a third of the size of the combined data from after the CART application. To investigate this further I made graphs of the percentage of initial resting membrane potential (figure 4.23C) and percentage of initial membrane resistance (figure 4.23D). Although these graphs cannot be used to make a statistical analysis, I believe they indicate that there is a difference in both resting membrane potential and the membrane resistance of the Purkinje cell, after the application of CART peptide as compared to the control.

4.6.3 – CART peptide reduces the membrane resistance of Purkinje cells with clamped membrane potential

Purkinje cells have many ion channels in their membrane, and many of these channels are active at the resting potential of the Purkinje cell membrane, in addition some of these ion channels have the specific function of rectifying the membrane resistance (for example I_h current depolarises the membrane during hyperpolarisation and I_A current hyperpolarises the membrane during depolarisation). A change in resting membrane potential, for example depolarisation, may active these channels which then act to oppose the change in membrane potential. If there is a large change in membrane resistance then the different effects of various rectifying currents may be small, but if there is a small change in membrane resistance then the rectification by the currents may mask the initial change. In the previous experiments there was significant variation in the resting membrane potential, if the CART peptide was having a small effect on membrane resistance then the variation in resting membrane potential may mask any CART peptide effect. One way of overcoming this problem is to fix the resting membrane potential by injecting current into the Purkinje cell via the patch electrode. By holding the Purkinje cell at a fixed membrane potential it is possible to investigate if CART peptide is altering the membrane resistance because the channels which oppose changes in the membrane potential will not be activated.
I was also concerned that the electrical properties of Purkinje cell may be changing over time. To overcome this possible problem I made recording from Purkinje cells in lobe X and after 10 minutes of control applied either a 100 nM CART peptide solution (n = 16) or a control solution (n = 24). Purkinje cells were held at -75 mV and current voltage relationships where recorded using negative current steps (figure

4.24A), and also firing rate and excitability data was recorded using positive current steps. To reduce systematic error the solution (CART peptide or control) was chosen at random before the Purkinje cell had been patched. Two of the control recordings were rejected during analysis as there was evidence that the patch had sealed up.

The mean control resting membrane potential (n = 22) was -75.8 ± 0.9 mV and the mean resting membrane potential (n = 16) in CART peptide was -75.4 ± 0.8 mV (figure 4.24B); as expected these where not significantly different as the cells were held at -75 mV. The mean current required to keep the cell at -75 mV in control was 302 ± 35 pA and in CART peptide the mean current was 295 ± 34 pA (figure 4.24C); these currents are not significantly different. However, the mean membrane resistance in control (38.9 ± 9.0 MΩ) was significantly ($p>0.01$) higher than that measured in CART peptide (32.6 ± 4.7 MΩ, figure 4.24D). This reduction in input resistance suggests that CART may act by opening a conductance.

One of the major rectifying currents in the Purkinje cell is the hyperpolarisation activated current, I_h, it is possible to calculate the size of I_h conductance and also the baseline I_h current from the current voltage relationship. The mean I_h conductance in control was 66.1 ± 15.1 nS and in CART peptide was 75.2 ± 19.7 nS (figure 4.25A); these were not significantly different. The average baseline I_h current in the control experiment was 21.7 ± 22.9 pA and in the CART experiment was 31.0 ± 50.2 pA (figure 4.25B); these are not significantly different.

In addition to negative current steps in determine the current voltage relationship of the Purkinje cell; I also recorded the firing of the Purkinje cell at different positive current steps. Only one of the cells recorded from didn't firing action potentials (in the control group). The average threshold voltage for firing action potentials in the control experiment (n = 21) was -70.3 ± 1.6 mV and in the CART peptide experiment

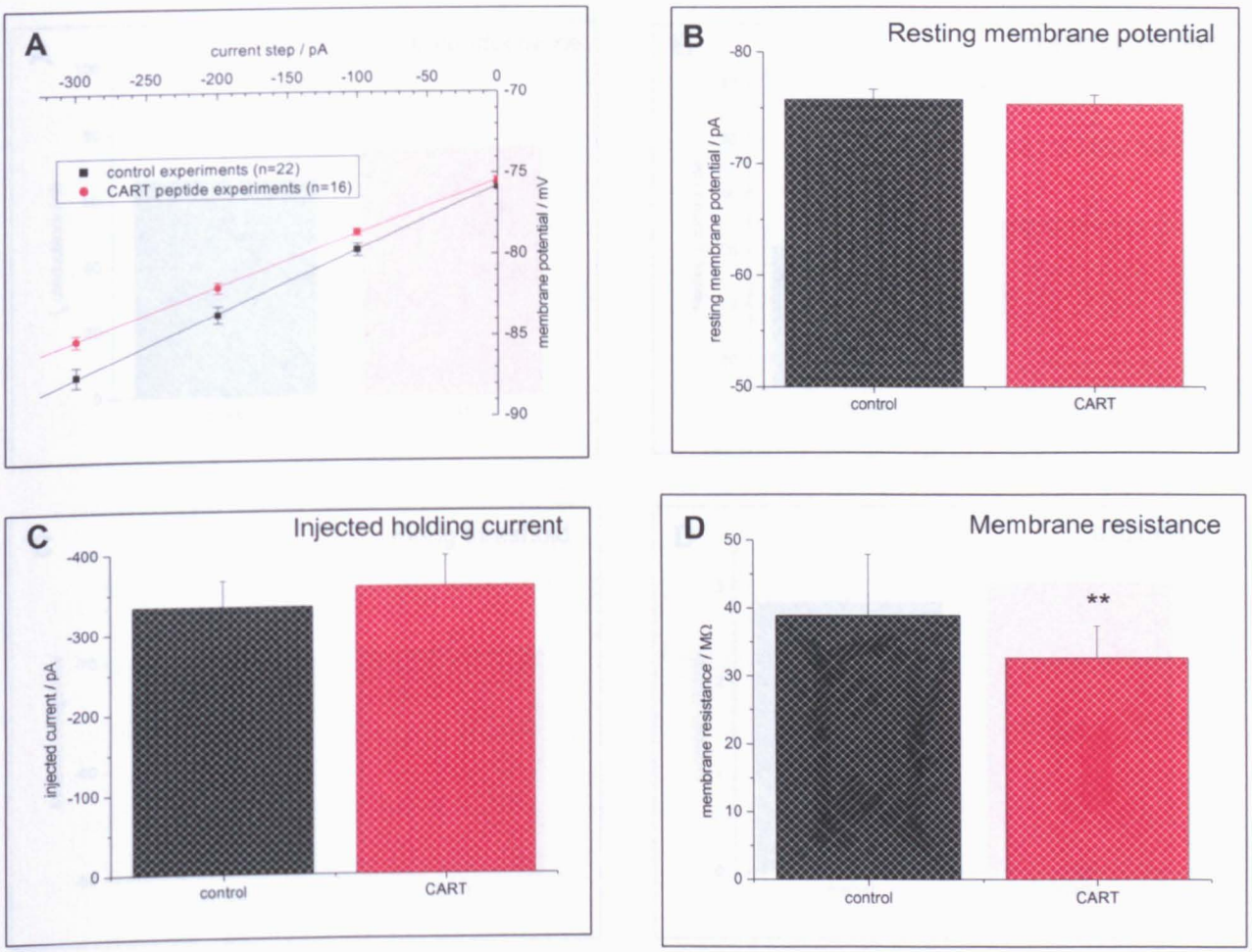

Figure 4.24 – Recordings of current voltage relationships with (in red; *n*=16) and without (in black; *n*=22) 100 nM CART peptide with the resting membrane potential fixed at -75 mV (panel A). The membrane resistance (panel D) with significantly lower in the presence of CART peptide. The resting membrane potential (panel B) and injected holding current (panel C) where not significantly different. (**-p<0.01).

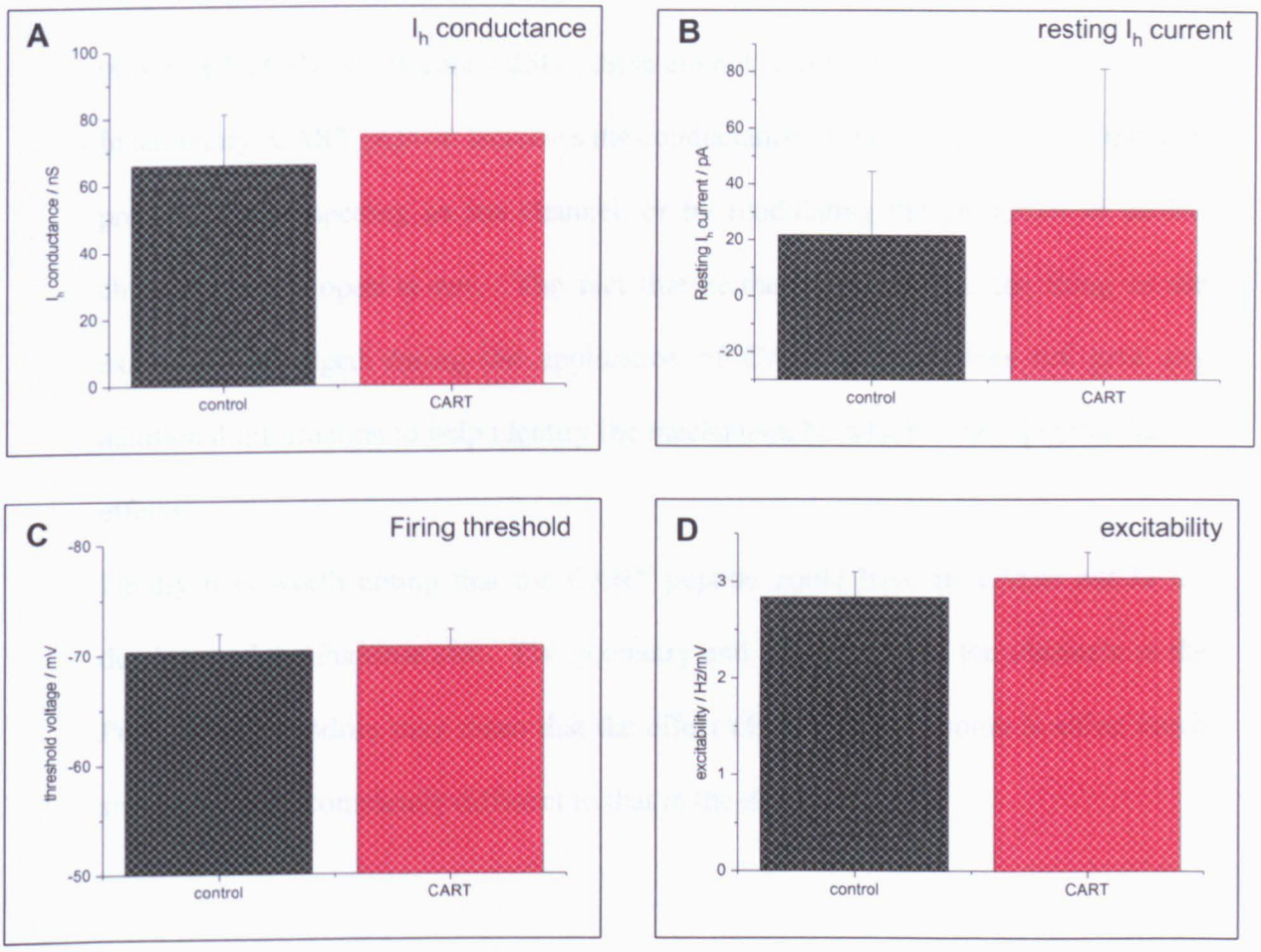

Figure 4.25 – Recordings of current voltage relationship with (in red; *n*=16) and without (in black; *n*=22) 100 nM CART peptide with the resting membrane potential fixed at -75 mV. The I_h conductance (panel A), resting I_h current (panel B), threshold for firing (panel C) and excitability (panel D) were not significantly different.

(n = 16) was -70.8 ± 1.5 mV (figure 4.25C); these are not significantly different. The average excitability of the Purkinje cell in the control experiment was 0.104 ± 0.008 Hz/pA or 2.84 ± 0.27 Hz /mV and in the CART experiment was 0.097 ± 0.007 Hz/pA or 3.04 ± 0.26 Hz/mV (figure 4.25D); these are not significantly different.

In summary, CART peptide increases the conductance of the Purkinje cell membrane, presumably by opening an ion channel, or by modulating the properties of an ion channel already open at rest. The fact that neither the threshold for firing or the excitability changed during the application of CART peptide does not give any additional information to help identify the mechanism by which CART peptide has its effects.

Finally it is worth noting that the CART peptide could have its effects out in the dendrites of the Purkinje cell. The geometry and distribution of ion channels in the Purkinje cell dendrite may mean that the effect observed at the soma is either much smaller or even completely different to that in the dendrites.

4.7 –CART peptide does not modulate parallel fibre long term depression.

Purkinje cells show various forms of synaptic plasticity, one of the most important is long term depression (LTD). With low frequency simultaneous stimulation of climbing fibres and parallel fibres, a prolonged reduction in the amplitude of events evoked by parallel fibre stimulation is observed. This form of plasticity may underlie motor learning in the cerebellum in a similar way that long term potentiation (LTP) is thought to underlie learning and memory in the hippocampus (for review see Ito 2000). More recent evidence suggests that LTD may not be involved in learning and

memory but may be a neuro-protective mechanism when there is excess activity (Llinás et al., 1997). Neuropeptides such as corticotropin-releasing factor (CRF) have been implicated in modulation of LTD in the cerebellum (Miyata et al., 1999; Schmolesky et al., 2007). Therefore it is possible that CART peptide may also have a role in modulating LTD in the vestibular cerebellum. To investigate this, I recorded parallel fibre EPSCs, then induced LTD (Kimura et al., 2005) either in control aCSF or in the presence of 100 nM CART peptide. To reduce systematic error, which solution to apply was chosen at random before the cell was patched.

Whole cell voltage clamp recordings were made from 27 Purkinje cells in lobe X at room temperature (25°C). LTD was induced in 12 slices in control and in 15 slices in the presence of CART peptide. The parallel EPSCs were recorded by stimulation in the molecular layer (section 4.4) every 5 seconds. The LTD protocol consisted of 5 minutes of stimulation of the parallel fibre at 1 Hz while the Purkinje cell was simultaneously depolarised to a membrane potential of 0 mV (Kimura et al., 2005). A small depolarising pulse was applied once a minute to check the membrane resistance. Out of 12 control experiments, 3 recordings were lost during the induction of LTD. Of the 15 recordings in CART peptide, 6 recordings were lost during LTD induction. The amplitude of the parallel fibre EPSCs before the LTD protocol was not significantly different between control and in the presence of CART peptide (table 4.10), suggesting the quality of the recordings was similar and the average number of parallel fibres activated was equivalent. In addition there was no significant difference between the amplitude of EPSCs in experiments in which the recording was lost during LTD induction and in those which survived the protocol (figure 4.26A). Thus it is not possible to identify cells which will survive or not survive the LTD protocol at the beginning of the experiment. Parallel fibre EPSCs were recorded

	Amplitude / pA
Control, cells lost during LTD protocol (n=3)	334 ± 96
Control, survive LTD protocol (n=9)	408 ± 38
CART peptide, cells lost during LTD protocol (n=6)	591 ± 73
CART peptide, survive LTD protocol (n=9)	525 ± 42
All control experiments (n=12)	527 ± 66
All CART peptide experiments (n=15)	478 ± 32
All cells lost during LTD protocol (n=9)	384 ± 39
All survive LTD protocol (n=18)	558 ± 41
All experiments (n=21)	500 ± 34

Table 4.10 – Summary of parallel fibre-EPSC amplitudes before LTD.

	Control (n = 9)	CART peptide (n = 9)
Rise time before LTD / ms	2.41 ± 0.19	2.43 ± 0.22
Rise time, 5 min after LTD / ms	2.53 ± 0.28	2.39 ± 0.24
Rise time, 20 min after LTD / ms	2.77 ± 0.36	2.58 ± 0.28
Decay constant before LTD / ms	21.6 ± 1.3	21.8 ± 1.6
Decay constant, 5 min after LTD / ms	22.0 ± 1.0	24.5 ± 2.2
Decay constant, 20 min after LTD / ms	22.7 ± 1.5	26.5 ± 2.4
Holding current before LTD / pA	380 ± 55	391 ± 31
Holding current, 5 min after LTD / pA	305 ± 52	322 ± 29
Holding current, 20 min after LTD / pA	331 ± 54	304 ± 28
Membrane resistance before LTD / MΩ	52.9 ± 6.7	53.9 ± 5.0
Membrane resistance, 5 min / MΩ	61.9 ± 9.3	63.6 ± 5.2
Membrane resistance, 20 min / MΩ	65.1 ± 7.2	74.2 ± 5.4

Table 4.11 – Summary of parallel fibre LTD experiments

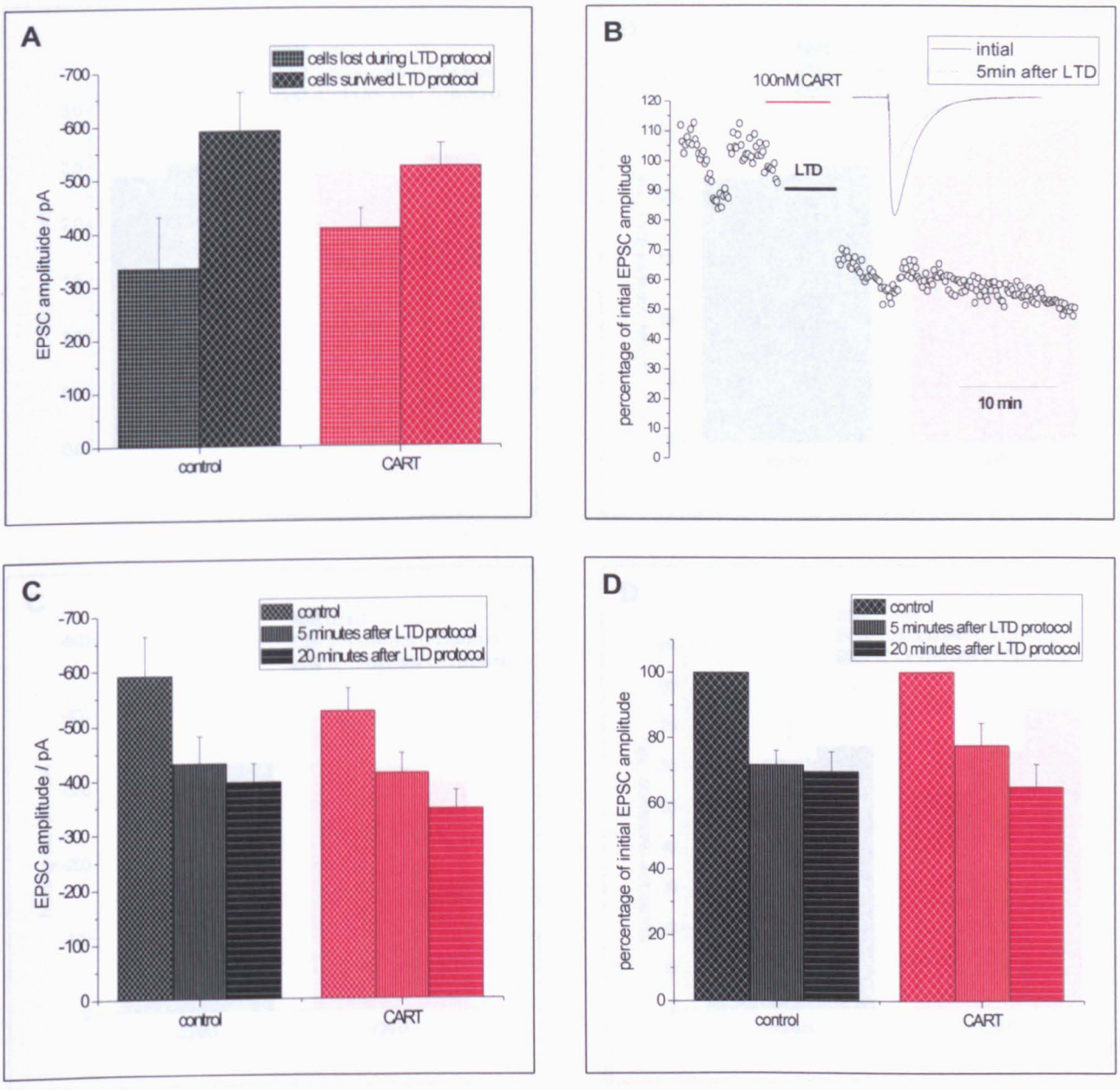

Figure 4.26 – CART peptide (100 nM) did not effect long term depression (LTD) at the parallel fibre-Purkinje synapse. A – There was no significant difference between the amplitudes of parallel fibre-EPSCs before the LTD protocol .B – A typical recording from a single Purkinje cell with induction of LTD, the insert shows superimposed averages of 30 EPSCs before and after the LTD protocol. C-D – As expected the LTD protocol significantly reduced EPSC amplitudes, but the application of CART peptide during the LTD protocol did not significantly change EPSC amplitude. Panel C shows absolute values and panel D shows values normalised to pre-LTD amplitude.

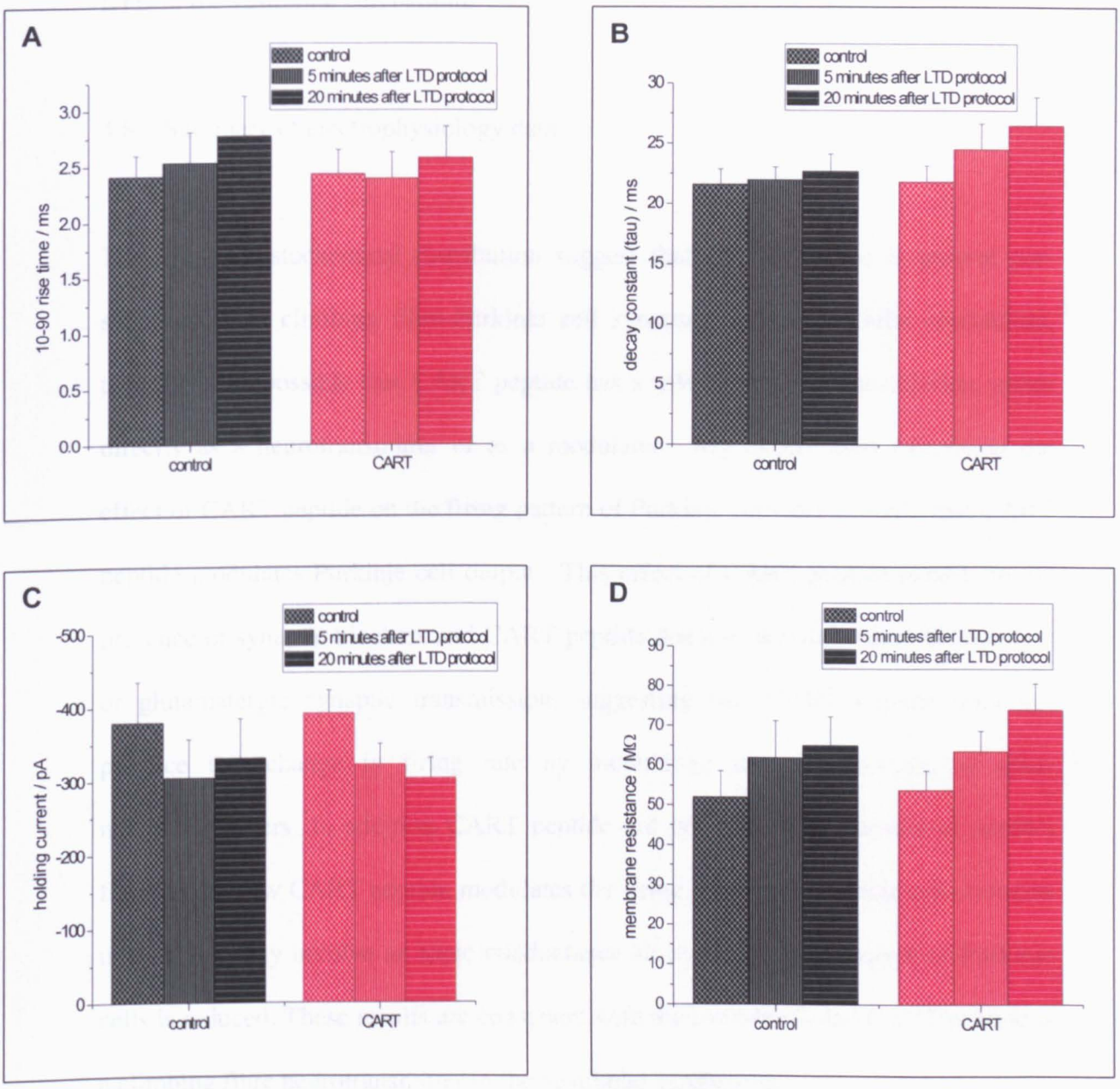

Figure 4.27 – CART peptide has no effect of parallel fibre LTD. CART peptide did not significantly alter the effect of LTD on EPSC 10-90 % rise time (panel A), EPSC decay constants (panel B), the holding current required to keep the cell at -70 mV (panel C) or the Purkinje cell membrane resistance (panel D).

same time interval. Thus CART peptide appears to have no effect on parallel fibre LTD in the vestibular cerebellum.

4.8 – Summary of electrophysiology data

The immunohistochemical distribution suggest that CART peptide is present pre-synaptically in climbing fibre-Purkinje cell synapses in the vestibular cerebellum, therefore it is possible that CART peptide has a role in synaptic transmission, either directly as a neurotransmitter or as a modulator. My experiments examining the effect of CART peptide on the firing pattern of Purkinje cells demonstrate that CART peptide modulates Purkinje cell output. This effect of CART peptide persists in the presence of synaptic blockers and CART peptide doe not modulate basal GABAergic or glutamatergic synaptic transmission, suggesting that CART peptide does not produce this change in firing rate by modulating the release/action of other neurotransmitters. In addition CART peptide did not alter the induction of parallel fibre LTD. How CART peptide modulates the firing pattern of Purkinje cells remains unclear but may involve an ionic conductance since the input resistance of Purkinje cells is reduced. These results are consistent with the hypothesis that CART peptide is a climbing fibre neurotransmitter in the vestibular cerebellum.

However, my experiments were not exhaustive, it is possible that CART peptide may modulate the response of other neurotransmitters present in the cerebellum, for example serotonin, norepinephrine, dopamine or acetylcholine. It is also possible that CART peptide be involved in synaptic or non-synaptic plasticity other than long term depression (see discussion).

Chapter 5: Determination of Purkinje cell firing patterns

5.1 – Introduction.

Purkinje cells are the sole output of the cerebellar cortex and both *in vivo* and *in vitro* are constituently active (firing action potentials without stimulation). I have already shown that CART peptide increases the firing frequency of Purkinje cells, but I was interested in what determines the different firing patterns of Purkinje cells (chapter 1). In particular how Purkinje cell synaptic inputs affect the firing frequency and pattern. I have also observed that CNQX (a commonly used AMPA receptor antagonist) increases the firing frequency of Purkinje cells (chapter 4), which was unexpected as blocking glutamate receptors would be expected to decrease the firing frequency. Therefore I investigated whether this was a direct effect on the Purkinje cell or whether if could be explained by an indirect mechanism (for example a reduction in the excitation of inhibitory interneurones).

5.2 – Classification of Purkinje cell firing patterns.

It is clear, from examining the cell attached data, that Purkinje cells can produce distinct firing patterns. Superficially, there appears to be 4 firing patterns. The first of these patterns is characterised by large and irregular intervals between spikes (figure 5.1A); this type of firing was often observed in control and also following increases in synaptic inhibition (e.g. with zolpidem). The second pattern is characterised by a high frequency of firing, either continuously or in bursts (figure 5.1B); this type of firing

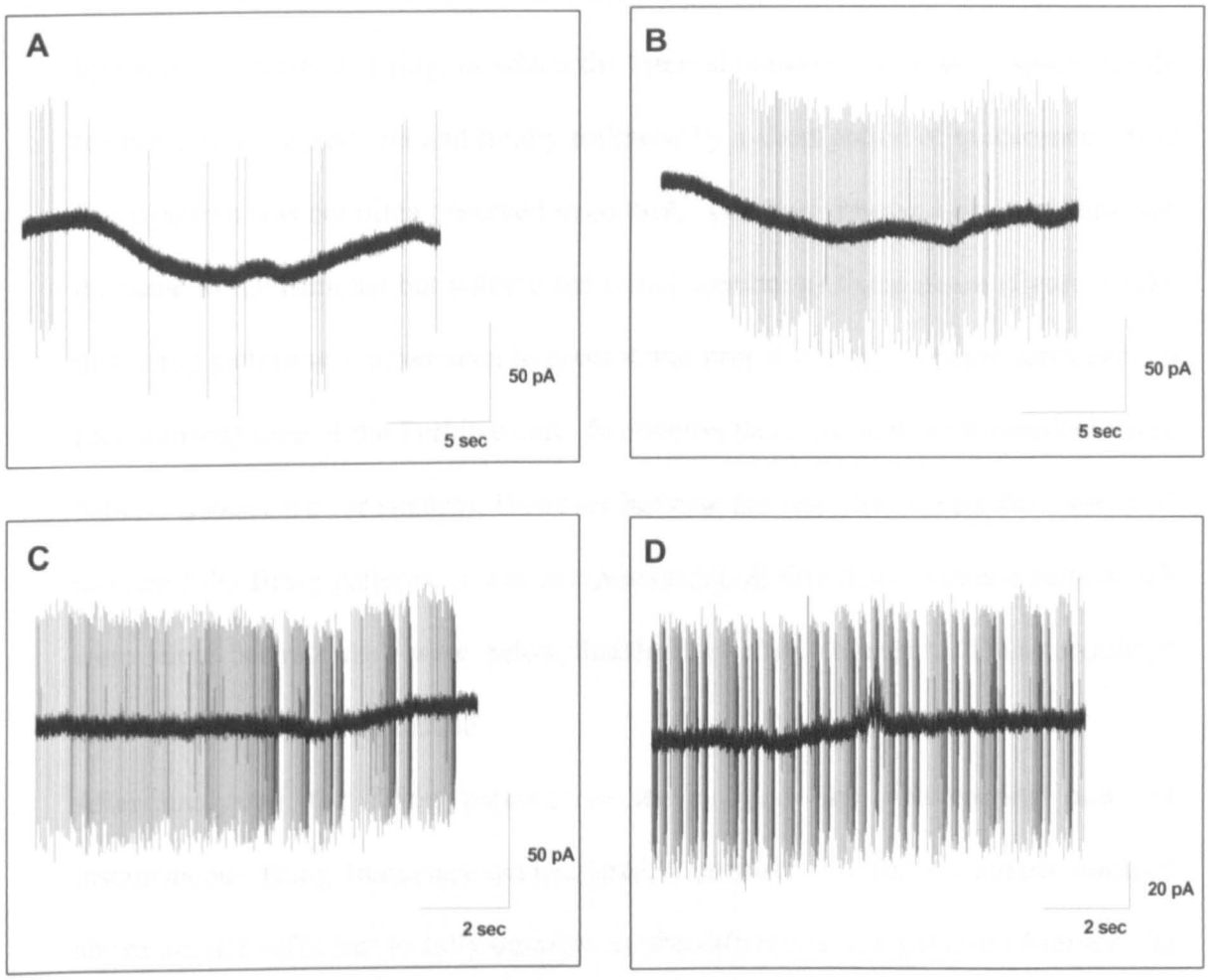

Figure 5.1 – From all Purkinje cells 4 different firing patters were observed. A – Slow irregular firing. B – High frequency tonic firing, sometimes in bursts. C – Trimodal firing. D – Short bursts of very high frequency firing, similar to the 2nd phase of trimodal firing.

was by far the most commonly observed in control conditions, and is the most similar to that reported *in vivo.* and *in vitro* (see chapter 1). The third firing pattern is similar to the reported trimodal pattern (Womack and Khodakhah, 2002) (figure 5.1C); this type of firing is characterised by 3 distinct phases, initial continuous firing, followed by short fast bursts of firing, in which the interval between progressive spikes inside the burst gets less and less and finally followed by a short period of quiescence. This firing pattern was not often observed in control. The final observed firing pattern was the same as the trimodal but without the initial continuous firing phase (figure 5.1D); this firing pattern was never seen in control and probably represents the most excited (depolarised) state of the Purkinje cell. In addition there is one more theoretical firing pattern: quiescence (or silence). However because the cell attached method was used to record the firing patterns, it was not possible to differentiate between cells which were silent because they were below threshold or were damaged. Thus recordings from silent cells were discarded.

After analysing the firing patterns in more detail and constructing plots of instantaneous firing frequency against time, I propose that the 4 patterns outlined above are not sufficient to fully describe all the different firing patterns observed. In particular, the second firing pattern (high frequency continuous or bursts of firing) appears to consist of 4 distinct patterns. Thus I propose that there are 7 different firing patterns (lettered A-E Figure 5.2 A-G):

A – Infrequent spikes, with a seemingly random distribution, low median firing frequency (figure 5.2 A,H).

B1 - Continuous firing with a narrow range of firing frequencies (figure 5.2 B,I).

B2 – The same as B1 but firing in bursts (figure 5.2 C).

C1 – Continuous firing but with a larger range of firing frequencies (figure 5.2 D,J).

C2 – The same as C1 but firing in bursts (figure 5.2 E).

D – The trimodal firing pattern (figure 5.2F).

E – The high frequency bursts, in which the interval between successive spikes in each burst gets shorter during the burst (figure 5.2G).

In the majority of recordings, the firing pattern could easily be classified into one of the firing patterns detailed above simply by visual inspection of plots of log frequency against time combined with a number of rules. Firstly, the firing patterns were separated into bursting and tonic types, if there were any breaks in the firing of more than a second then the cell was classified as bursting (types A, B2, C2, D and E). The non-bursting types (B1 and C1) were separated on the variance of the firing rate (assessed from the log plots), if the plot did not have a very narrow range of instantaneous firing frequencies then it was assigned as C1, all the other continues firing types were assigned as B1. The firing pattern A was grouped with the bursting patterns, but was easily differentiated from the other bursting patterns because there was always a smooth gradient of instantaneous firing frequency from the high to low frequency. Firing patterns B2 and C2 were separated using the same procedure as B1 and C1, leaving just patterns D and E. The distinguishing feature of both these firing patterns is short fast bursts. If only these short fast bursts were present and no longer slower bursts were present then the firing pattern was assigned as E, otherwise it was assigned as D.

Because I plotted the instantaneous firing frequency of the different firing patterns on a log scale it maybe that the continuous patterns (A, B1 and C1) are all the same only shifted to different firing frequencies. To investigate this, I plotted out typical A, B1 and C1 firing patterns on identical linear scales (figure 5.2H-J). Visually they look different on both linear and log scales, suggesting that they probably are different

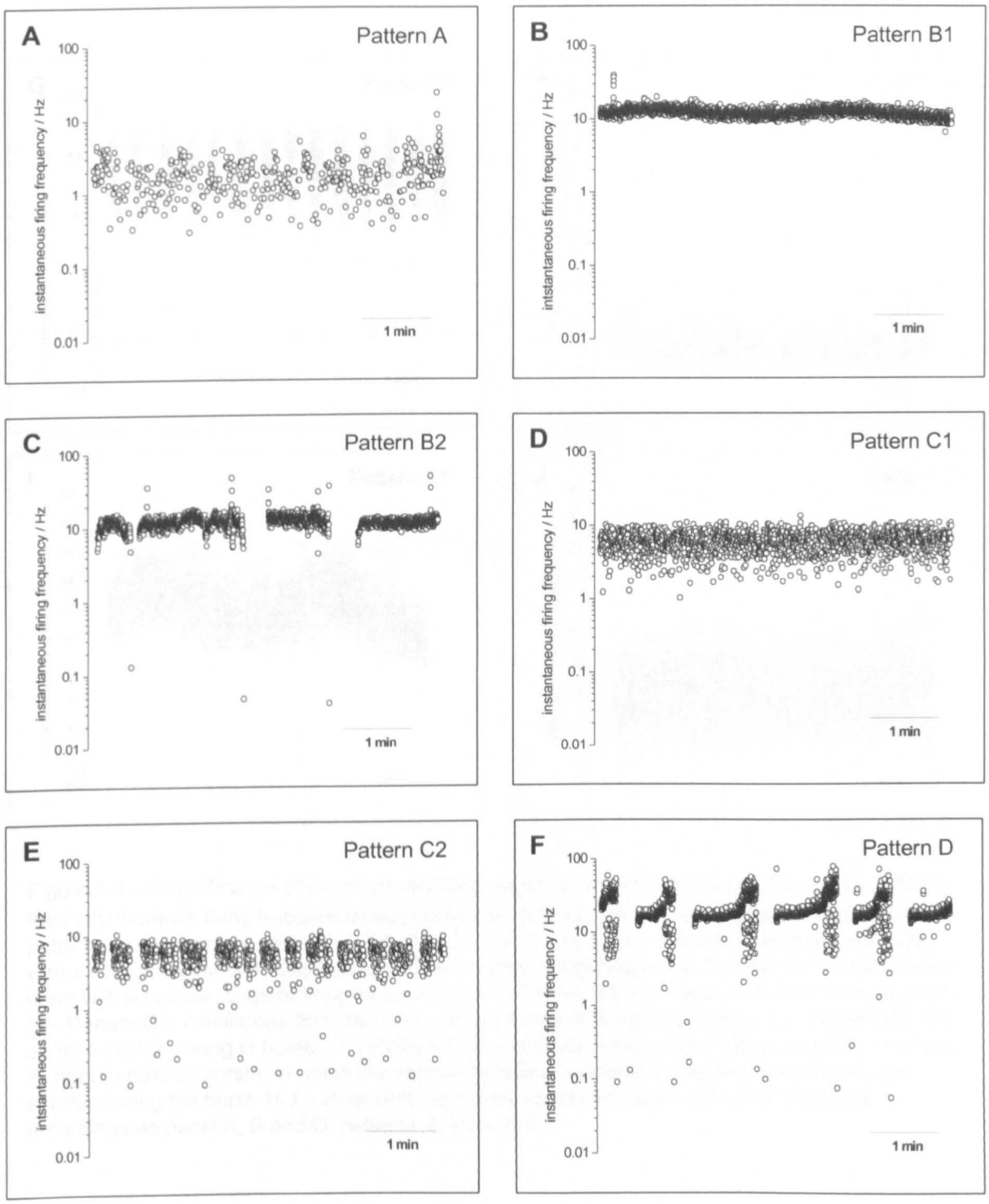

Figure 5.2 – Classification of the observed firing patterns (*continued over page*)

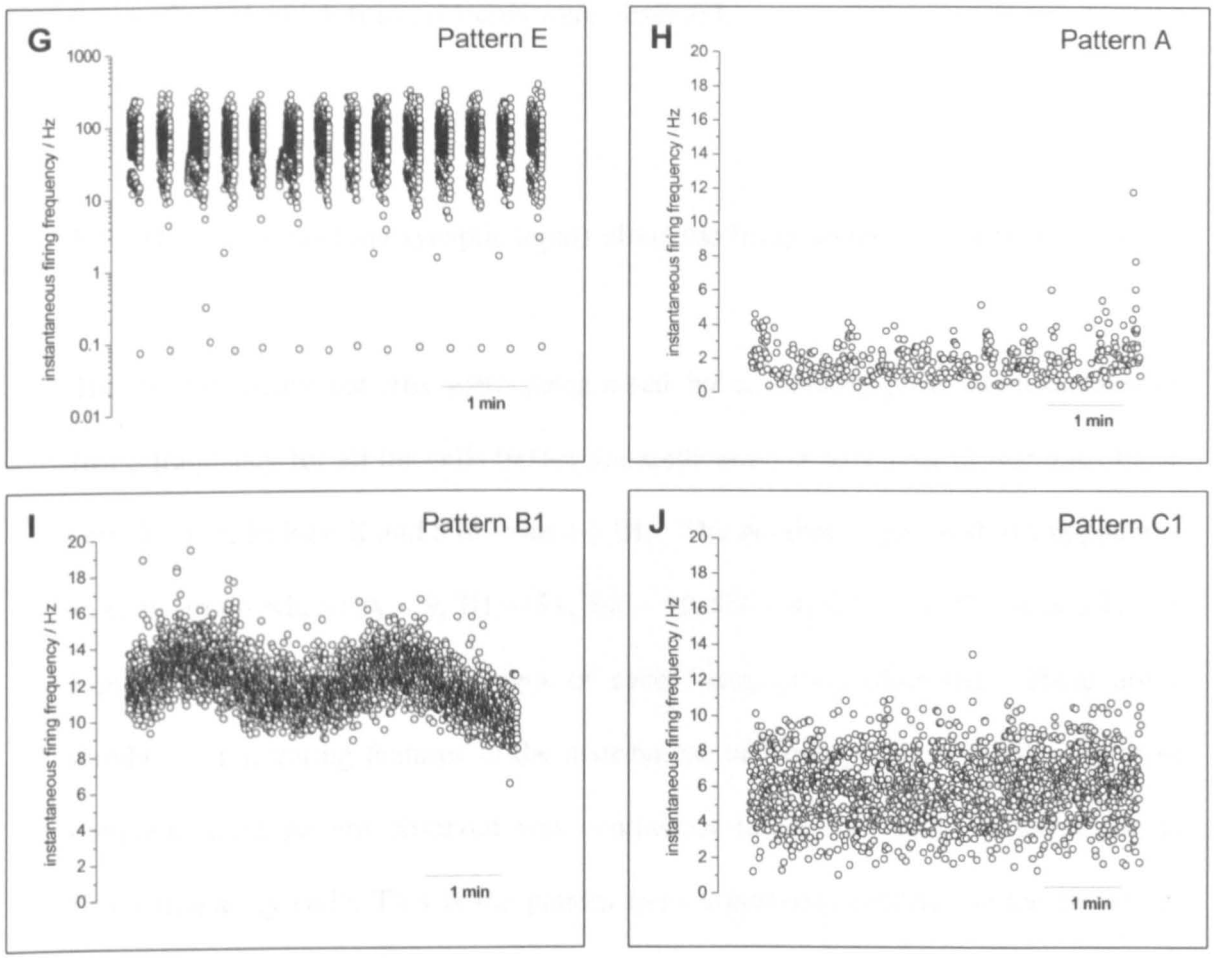

Figure 5.2 – Classification of the observed firing patterns (*continued from previous page*). When the instantaneous firing frequencies (log scale) are plotted against time 7 different distinct firing patterns were observed (termed A, B1, B2, C1, C2, D and E). A – Pattern A, infrequent events, with a seemingly random distribution and low median firing frequency. B – Pattern B1,continuous firing with a narrow range of firing frequencies. C – Pattern B2, the same as B1 but firing in bursts. D – Pattern C1, continuous firing but with a larger range of firing frequencies. E – Pattern C2, the same as C1 but firing in bursts. F – Pattern D, the trimodal firing pattern (figure 5.2F).G – Pattern E, high frequency bursts, in which the interval between successive events in each burst gets shorter during the burst. H-J – Plots of firing frequency (linear) against time for the same recordings as panel A, B and D, patterns A, B1 and C1.

firing patterns. Having characterised the different firing patterns of Purkinje cells, I was interested in their frequency of occurrence, and how the application of different drugs affected which firing patterns were observed.

5.3 – How does blocking synaptic inputs affect the firing pattern of Purkinje Cells?

The control firing patterns were categorised by examining plots of instantaneous firing frequency for all the cells before the application of any drug (n = 90) (of these cells 85 were in lobe X and 5 in lobes I-VIII). The number of cell with firing patterns in each group where: A – 9, B1 – 31, B2 – 19, C1 – 4, C2 – 23, D – 4 and E – 0. Figure 5.3A shows the percentages of each firing group observed. There are a number of interesting features in the distribution of firing patterns. Firstly, the most common firing pattern observed was continuous firing with small variation in the firing frequency (B1). This is the pattern most commonly reported in the literature. Secondly, there were very few cells (4) which fired the trimodal pattern (D), suggesting that it is not a common firing pattern for the Purkinje cell at rest. Finally, although many cells fired in bursts both with high and variation in the firing frequency (B2 and C2), very few cells (4) fired continuously with a large variation in the firing frequency.

To investigate whether these firing patterns were produced by synaptic inputs, I examined the firing patterns from cells to which I applied bicuculline (10 μM), blocking inhibitory (GABAergic) synapses, and then added kynurenic acid (5 mM), blocking excitatory (glutamatergic) and GABAergic synapses, (n = 13, figure 5.3B). In control the number of cells in each group was: A – 1, B1 – 6, B2 – 2, C1 – 1, C2 –

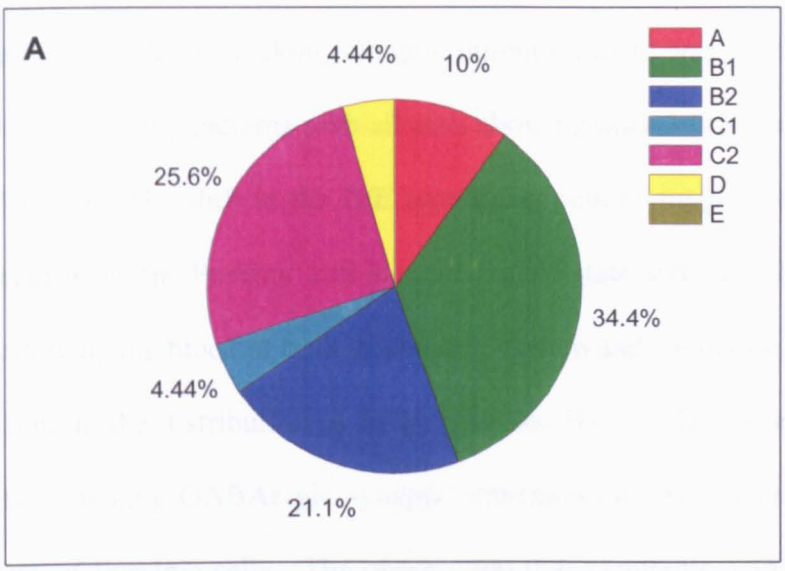

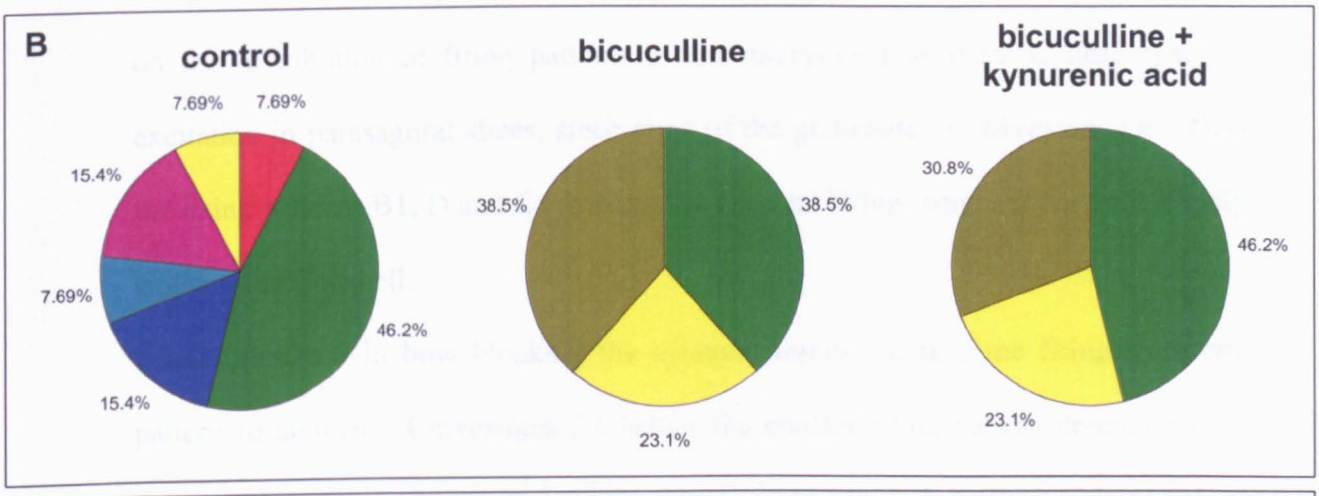

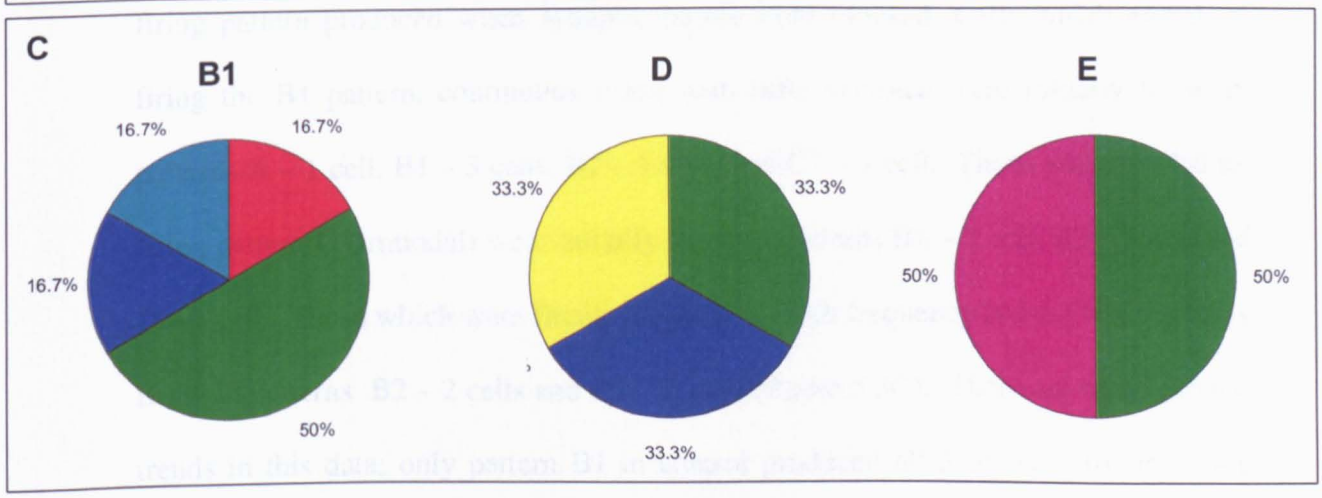

Figure 5.3 – Pie charts summarising the occurrence of different firing patterns. A – Plot of all the firing patterns observed in control (n = 90). B – The effect on firing pattern of the sequential application of 10 μM bicuculline and 5 mM kynurenic acid (n = 13). Blocking GABAergic transmission has a large effect on firing patterns, but blocking glutamateric transmission does not. C – The distribution of different firing rates in control which gave firing rate B1, D and E after synaptic currents were blocked.

2, D – 1 and E - 0. After blocking synaptic inhibition there was a striking change in the distribution of firing patterns with all cells showing only 3 firing patterns: B1 – 5, D – 3 and E – 5. The shift to the D/E type firing pattern suggests that these firing patterns occur when the Purkinje cell is in an excited state and thus are rarely seen in control. Following the block of both synaptic inhibition and excitation, there was little further change in the distribution of firing patterns: B1 – 6, D – 3 and E – 4. This suggests that blocking GABAergic synaptic transmission has a strong affect on the firing pattern of Purkinje cells. The observation that kynurenic acid has little effect on the distribution of firing patterns is not unexpected as there is little synaptic excitation in parasagittal slices, since most of the glutamatergic fibres are cut. Thus the firing patterns B1, D and E represent the inherent firing pattern of the synaptically isolated Purkinje cell.

I was interested in how blocking the synaptic inputs changes the firing from one pattern to another. I investigated whether the control firing pattern determines the firing pattern produced when synaptic inputs were blocked. Cells which ended up firing the B1 pattern, continuous firing with little variance were initially firing in patterns A – 1 cell, B1 – 3 cells, B2 – 1 cells and C1 – 1 cell. Those which ended up firing pattern D (trimodal) were initially firing in patterns B1 – 1 cell, B2 – 1 cell and D – 1 cell. Those which were finally in group E (high frequency bursts) were initially firing in patterns B2 – 2 cells and C2 – 2 cells (figure 5.3C). There are some general trends in this data; only pattern B1 in control produced all 3 of the different firing patterns observed after the synaptic inputs were blocked, suggesting that the synaptic inputs are able to covert all the different firing patterns back to the most commonly observed pattern. Also it is worth noting that the only cell firing the trimodal pattern remained firing in this pattern, and was not converted to pattern E, and that all of the

cells firing in mode C2 were converted to E. This suggests that E is not necessarily a progression from D (which it appears to be by visual investigation), but in fact the firing pattern resulting from removing inhibition from those cells firing in mode C2 (bursting with large variance).

5.4 – CART peptide does not affect the firing patterns of Purkinje cells.

In chapter 4, I demonstrated that CART peptide had a small but significant effect on the median instantaneous firing frequency of Purkinje cells in the vestibular cerebellum; I was interested to see if this change in firing rate was accompanied by a change in the firing pattern. I collected together all the CART peptide experiments which gave significant increases in median firing frequency (room temperature and 32°C, 100 nM and 1000 nM CART peptide experiments) and quantified the firing patterns before and during CART peptide applications (n = 31) (figure 5.4). In control the firing patterns were: A – 3 cells, B1 – 10 cells, B2 – 5 cells, C1 – 1 cell, C2 – 11 cell, D – 1 cell and E – 0 cells. After the application of CART peptide the firing pattern distribution was almost exactly the same (A – 3, B1 – 10, B2 – 5, C1 – 1, C2 – 11, D – 1 and E – 0). This is expected as the small change in firing rate produced by CART peptide is unlikely to change the firing pattern.

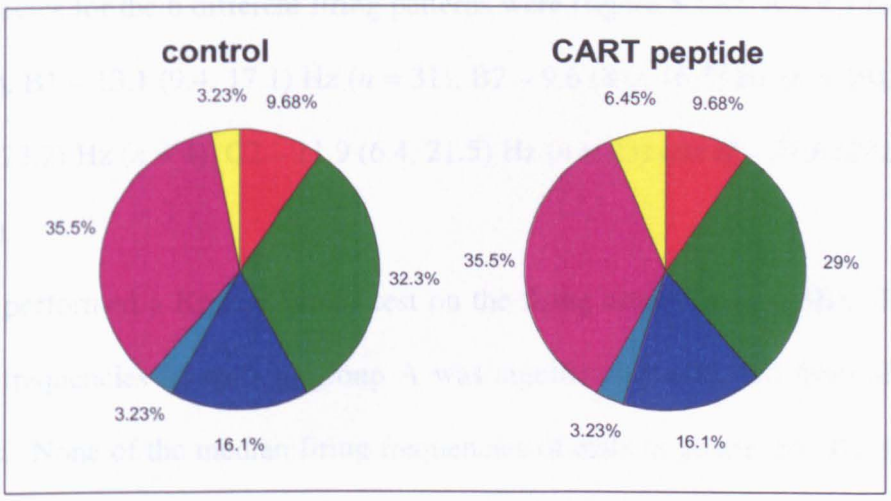

Figure 5.4 – CART peptide (100-1000 nM) did not change the overall distribution of firing patterns (n = 31).

5.5 – The relationship between firing pattern and median firing frequency

In control conditions, Purkinje cells fire in one of 6 different firing patterns (pattern E was never seen in control). I was interested in whether the median instantaneous firing frequency was different for each of these firing patterns and could therefore be used to distinguish between the patterns. Taking the 90 control firing cells (85 of these cells were in lobe X and 5 outside of lobe X); I averaged together the median firing frequencies for cells with the same firing pattern. The median firing frequencies for the 6 different firing patterns were (figure 5.5A): A – 4.7 (3.3, 5.7) Hz (n = 9), B1 – 13.1 (9.4, 17.1) Hz (n = 31), B2 – 9.6 (8.0, 16.5) Hz (n = 19), C1 – 21.4 (17.9, 23.2) Hz (n = 4), C2 – 11.9 (6.4, 21.5) Hz (n = 23) and D – 27.8 (23.8, 31.5) Hz (n = 4).

I then performed a Krustal-Wallis test on the firing rates (figure 5.5B). The median firing frequencies of cells in group A was significantly different from all the other groups. None of the median firing frequencies of cells in groups B1, B2, C1, C2 and D were significantly different from each other. I believe that group D must be considered different from the other patterns. Therefore I combined groups B1, B2, C1 and C2, thus giving 3 different groups of firing patterns based on firing frequency (figure 5.5C). The median firing frequencies of cells in each group were: A –4.7 (3.3, 4.7) Hz (n = 9), B/C –11.9 (8.2, 20.3) Hz (n = 77) and D – 27.8 (23.8, 31.5) Hz (n = 4). These groups were all significantly different from each other (A vs B/C – $p>0.0001$, A vs D – $p>0.01$ and B/C vs D – $p>0.05$).

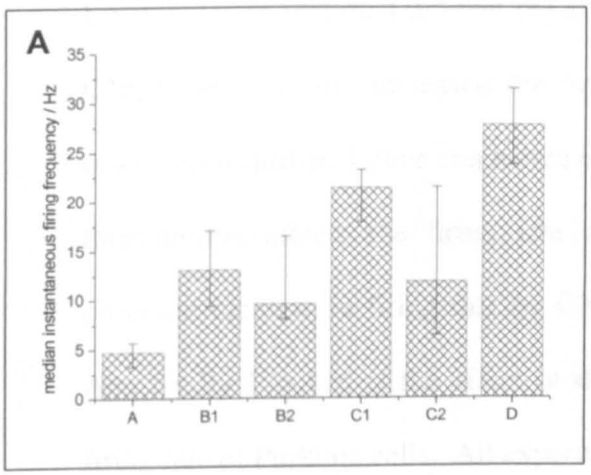

B

	A	B1	B2	C1	C2
B1	***				
B2	*	ns			
C1	**	ns	ns		
C2	**	ns	ns	ns	
D	***	ns	ns	ns	ns

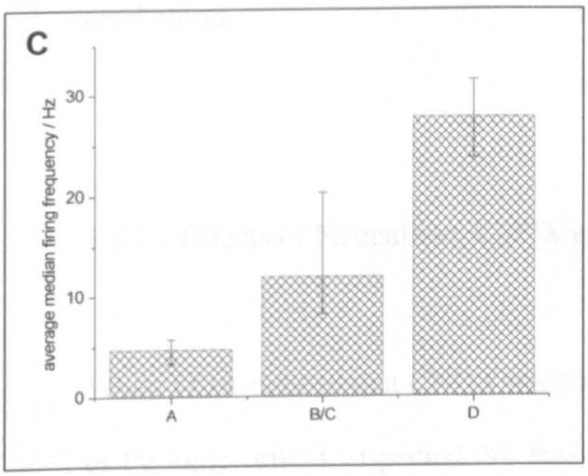

Figure 5.5 – The median instantaneous firing frequencies for Purkinje cells with different firing patterns (n = 90). A – Plot of average median instantaneous firing frequency for all the different firing patterns. B – Table summarising the results of t-tests between median firing frequencies of different firing patterns. * - $p<0.05$, ** - $p<0.01$ and *** - $p<0.001$.There was no significant differences between the firing frequencies in groups B1, B2, C1 and C2, therefore they were combined into one group, B/C. C- Plot of average median instantaneous firing frequency for the 3 different firing pattern groups, A, B/C and D.

5.6 – Effect of synaptic blockers on instantaneous firing rate

I mentioned in section 4.2.5 that the application of the glutamate receptor antagonist, CNQX unexpectedly increased the firing rate of Purkinje cells. To investigate this observation further, I have conducted experiments to examine how blocking synaptic transmission affects the firing rate of Purkinje cells and demonstrated that the observed increase in firing rate by CNQX was a direct effect on the Purkinje cell. And finally I looked at the effect of the benzodiazepine-like drug, zolpidem, on the firing rate of Purkinje cells. All experiments were carried out on cells in lobe X of the cerebellum.

5.6.1 – Effects of bicuculline, CNQX and kynurenic acid on firing rate.

When I first noticed that CNQX had the unexpected effect of increasing the firing rate of Purkinje cells, I suspected this was due to the block of glutamatergic transmission onto the inhibitory interneurons, reducing the level of inhibition experienced by the Purkinje cell. This hypothesis has some circumstantial evidence to support it; there are approximately 10 inhibitory interneurones to every Purkinje cell and unlike granule cells, they only synapse onto Purkinje cells near to their cell bodies. This means a larger proportion of the inhibitory synapses will be present in the parasaggital slices compared to excitatory synapses. In addition there is evidence that it is the interneurons that are responsible for setting the firing rate of Purkinje cells (Häusser and Clark, 1997) and decreases in the strength of the parallel fibre inputs results in an

increase in Purkinje cell firing rate as decreased inhibition has a greater effect than a reduction in direct excitation (Mittmann and Häusser, 2007).

My first experiment was to sequentially bath apply CNQX and bicuculline. The firing of 9 Purkinje cells, at 32 °C, in lobe X, were recorded with a minimum of 5 minutes in control, then a solution containing 10 μM CNQX was bath applied for 10 minutes and then a solution containing both 10 μM CNQX and 10 μM bicuculline was bath applied for a further 10 minutes. The median instantaneous firing frequency in control was 13.6 (5.9, 24.4) Hz, in CNQX was 18.1 (11.4, 30.4) Hz and in both CNQX and bicuculline was 35.0 (28.4, 48.2) Hz (figure 5.6A). Expressed as a percentage of control median instantaneous firing frequency the firing rate in CNQX was 123.5 (117.1, 137.6) % and in CNQX and bicuculline was 215.8 (189.4, 430.1) % (figure 5.6B). The firing rate in the presence of CNQX was significantly higher than in control ($p<0.01$), the firing rate in CNQX and bicuculline was significantly greater than control ($p<0.01$) and significantly higher than in the presence of CNQX alone ($p<0.01$). One might expect this result if CNQX is acting to reduce inhibition: a reduction in inhibition (via loss of interneurone excitation) would be expected to produce a smaller increase in Purkinje cell firing rate compared to a complete abolition of inhibition.

If the increase in Purkinje cell firing rate only resulted from a decrease in the excitation of interneurones, then blocking synaptic inhibition (with bicuculline) followed by blocking synaptic excitation (with bicuculline and CNQX) should initially give a large increase in the firing rate followed by either no change or a small decrease in firing rate. The firing of 6 Purkinje cells, at 32°C, in lobe X, were recorded with a minimum of 5 minutes in control, then 10 μM bicuculline was bath applied for 10 minutes and then 10 μM bicuculline and 10 μM CNQX were bath

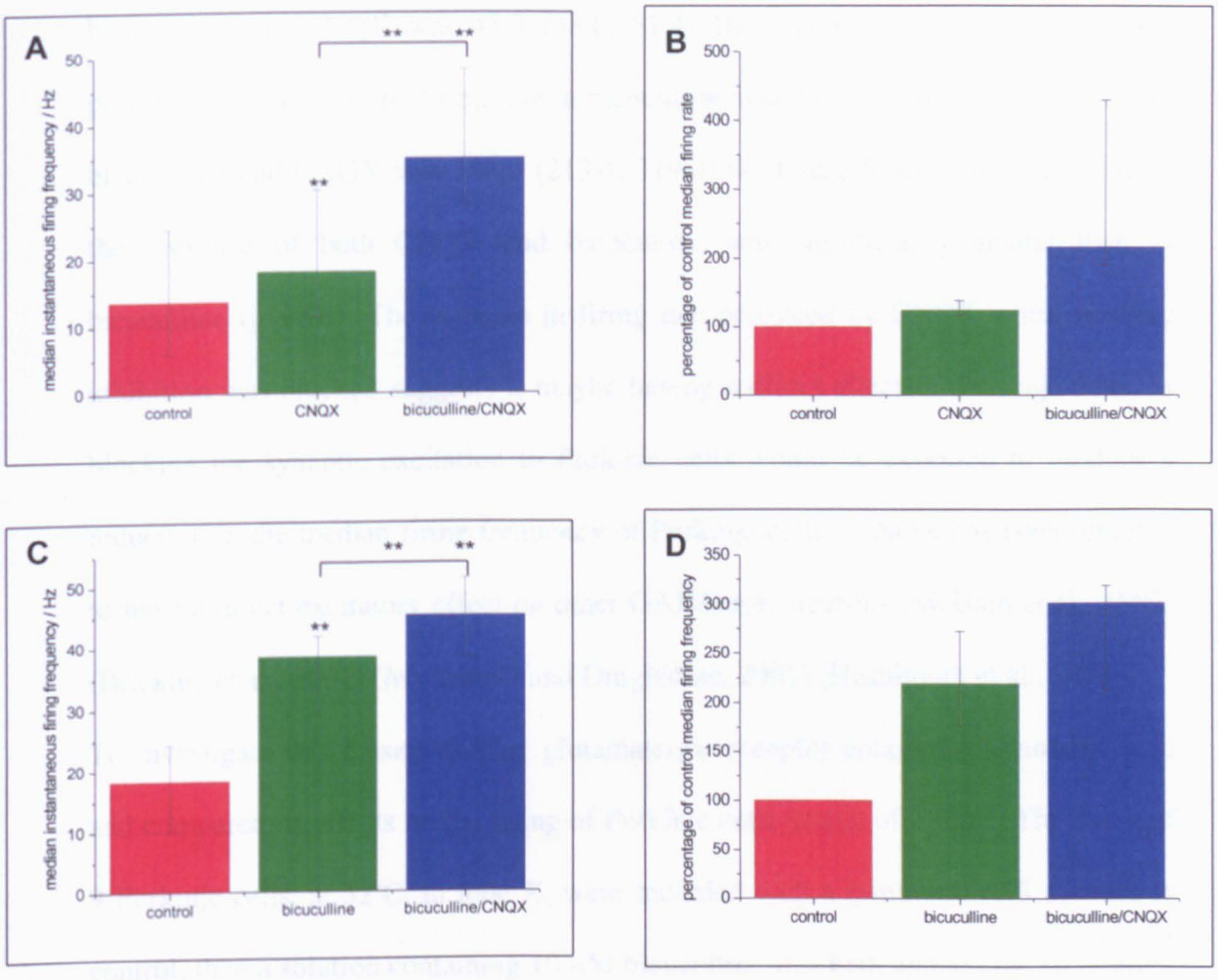

Figure 5.6 – Blocking synaptic inputs to Purkinje cells increases their median instantaneous firing frequency. A-B – Application of 10 μM CNQX significantly increased the firing frequency, addition of 10 μM bicuculline further increased the firing frequency (n = 9). C-D – Application of 10 μM bicuculline significantly increased the firing frequency, addition of 10 μM CNQX further increased the firing frequency (n = 6). ** - $p<0.01$,*** - $p<0.001$. Panels A and C show absolute values and panels B and D show values normalised to control values.

applied for a further 10 minutes. The median instantaneous firing frequency in control was 18.2 (10.2, 24.2) Hz, in bicuculline was 38.4 (28.8, 41.8) Hz and in bicuculline and CNQX was 45.3 (38.6, 51.4) Hz (figure 5.6C). Expressed as a percentage of control, the firing rate in bicuculline was 219.4 (176.9, 272.1) % and in bicuculline and CNQX was 301.0 (213.4, 319.0) % (figure 5.6D). The firing rate in the presence of both CNQX and bicuculline was significantly greater than in bicuculline ($p>0.01$). The increase in firing rate produced by CNQX when synaptic inhibition was blocked suggests it maybe having a direct effect on Purkinje cells, as blocking the synaptic excitation to Purkinje cells would be expected to produce a reduction in the median firing frequency of Purkinje cells. CNQX has been reported to have a direct excitatory effect on other GABAergic neurons (McBain et al., 1992) (Brickley et al., 2001) (Maccaferri and Dingledine, 2002) (Hashimoto et al., 2004).

To investigate this I used another glutamatergic receptor antagonist kynurenic acid and compared its effects on the firing of Purkinje cells to that of CNQX. The firing of 9 Purkinje cells, at 32°C, in lobe X, were recorded with a minimum of 5 minutes in control, then a solution containing 10 μM bicuculline was bath applied for 10 minutes and then a solution containing both 10 μM bicuculline and 5 mM kynurenic acid was bath applied for a further 10 minutes. The median instantaneous firing frequency in control was 17.9 (14.0, 26.7) Hz, in bicuculline was 23.3 (21.3, 32.3) Hz and in both bicuculline and kynurenic acid was 26.8 (20.1, 36.1) Hz (figure 5.7A). Expressed as a percentage of control median instantaneous firing frequency the firing rate in bicuculline was 151.1 (129.2, 209.7) % and in bicuculline and kynurenic acid was 154.2 (121.0, 207.7) % (figure 5.7B). As expected the firing rate in the presence of bicuculline was significantly higher than in control ($p<0.001$) and the firing rate in both bicuculline and kynurenic acid was significantly higher than control ($p<0.01$).

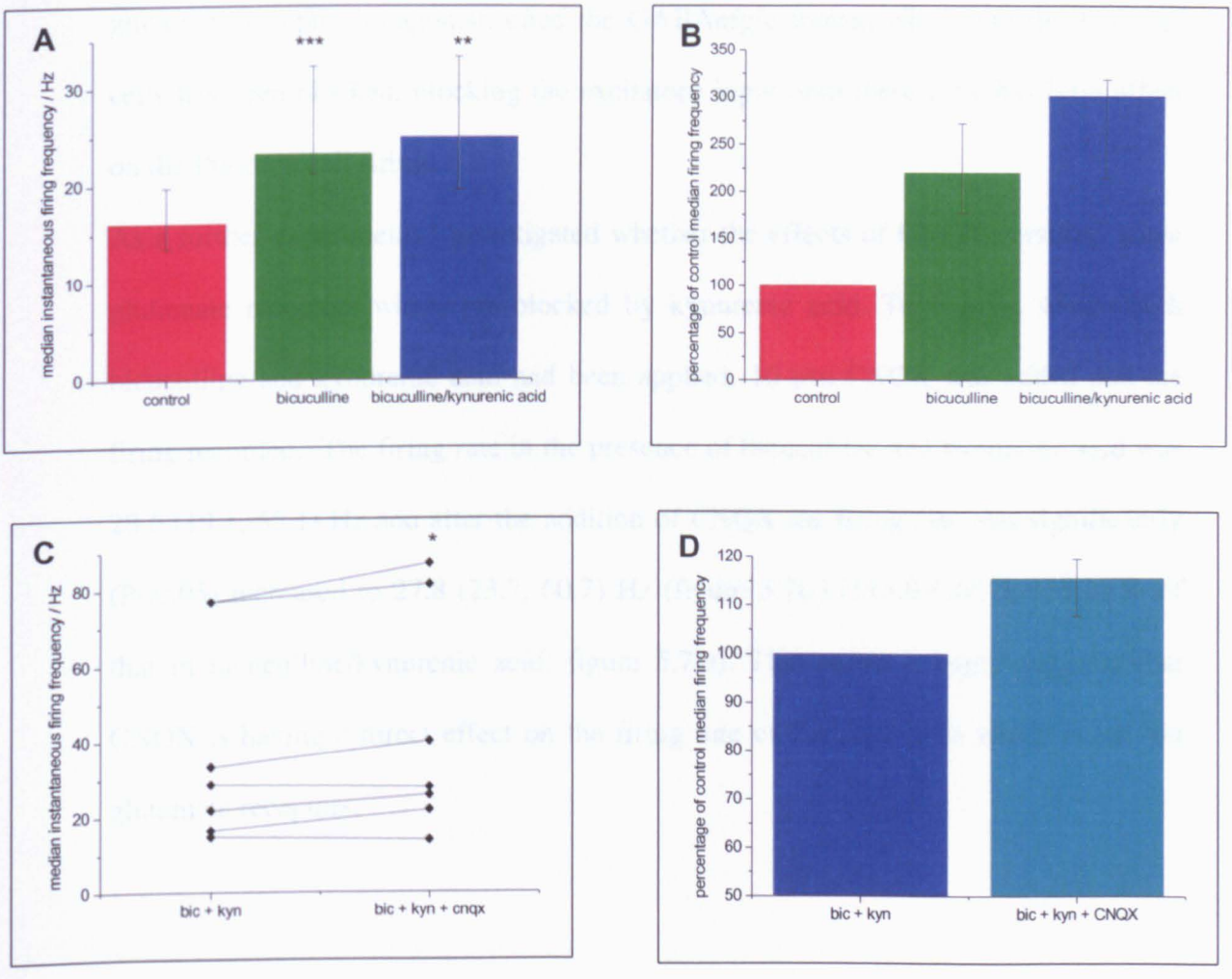

Figure 5.7 – CNQX has a direct effect on the firing rate of Purkinje cells, not mediated via reduction of interneurone inhibition. A-B – Application of 10 μM bicuculline significantly increased the firing frequency, addition of 5 mM kyurenic acid did not further increased the firing frequency (n = 9). C-D – Application of 10 μM CNQX in the presence of bicuculline and kynurenic acid significantly increased the firing frequency by 113 % (n = 6). * - $p<0.05$. Panels A and C show absolute values and panels B and D show values normalised to control values.

However the firing rate in both bicuculline and kynurenic acid was not significantly different from that just in bicuculline. Thus kynurenic acid is acting as expected for a glutamate receptor antagonist, once the GABAergic transmission onto the Purkinje cells has been blocked, blocking the excitatory input onto these cells has little affect on the Purkinje cell firing.

As a further experiment, I investigated whether the effects of CNQX persisted when glutamate receptors where pre-blocked by kynurenic acid. To 6 cells, which both bicuculline and kynurenic acid had been applied, 10 μm CNQX was added and the firing recorded. The firing rate in the presence of bicuculline and kynurenic acid was 28.6 (19.1, 55.1) Hz and after the addition of CNQX the firing rate was significantly ($P<0.05$) increased to 27.8 (23.7, 60.7) Hz (figure 5.7C) (113.0 (101.5, 119.0) % of that in bicuculline/kynurenic acid; figure 5.7D). This result strongly suggests that CNQX is having a direct effect on the firing rate of Purkinje cells which is not via glutamate receptors.

5.6.2 – Effect of zolpidem of Purkinje cell firing.

The $GABA_A$ receptor has a binding site which increases the receptors affinity of GABA, the so called benzodiazepine (BDZ) binding site (Barker and Barasi, 2003). It has been demonstrated that zolpidem both increases the amplitude and decay time of inhibitory post synaptic currents recorded in Purkinje cells (Wall, 2005). I was interested in how this modulation of synaptic inhibition onto Purkinje cells would affect the firing pattern.

To investigate this I recorded the firing of 7 Purkinje cells, in lobe X, at 32°C. After a minimum of 5 minutes control, 500 nM zolpidem was applied for 5 minutes then following a 10 minute wash, 10 μM bicuculline was applied. The median instantaneous firing frequencies were: in control 9.9 (7.8, 12.3) Hz, in zolpidem 4.5 (3.3, 5.9) Hz, following wash 6.4 (5.0, 10.7) Hz and in bicuculline 21.3 (16.3, 29.9) (figure 5.8A). Expressed as percentages of control the firing rates were: in zolpidem 36.3 (31.9, 58.1) %, following wash 69.5 (54.5, 89.7) % and in bicuculline 203.2 (157.8, 230.3) % (figure 5.8B). The firing rate was significantly lower in the presence of zoplidem ($p>0.05$) and significantly higher in the presence of bicuculline ($p>0.05$), compared to control. There was no significant difference between the firing rate in control and following wash.

It is clear that zolpidem has a significant effect on the firing properties of Purkinje cells, but what is more interesting is the relationship between the firing rate in the presence of bicuculline and in the presence of zolpidem (figure 5.8C). You might expect that if the GABAergic inhibition was setting the firing rate of Purkinje cells, then variations in inhibitory transmission would underlie variations in the Purkinje cell firing pattern. Thus in the presence of bicuculline the firing rates would all be similar, however this is not what I observed. The amount of variation was higher in the presences of bicuculline (inter quartile range of 13.7 Hz, 64.3 % of the median) than in control (inter quartile range of 4.4 Hz, 44.3 % of the median), suggesting that rather than GABAergic inhibition setting the frequency of the Purkinje cell, it is in fact modulating the intrinsic firing frequency to give a narrower range of frequencies. The effect on variance of zolpidem was to decrease the inter quartile range (from 4.4 to 2.6 Hz), but because the median frequency also decreased there was an overall increase in the variance (44.3 % to 58.1 %). This increase in variance seems to add

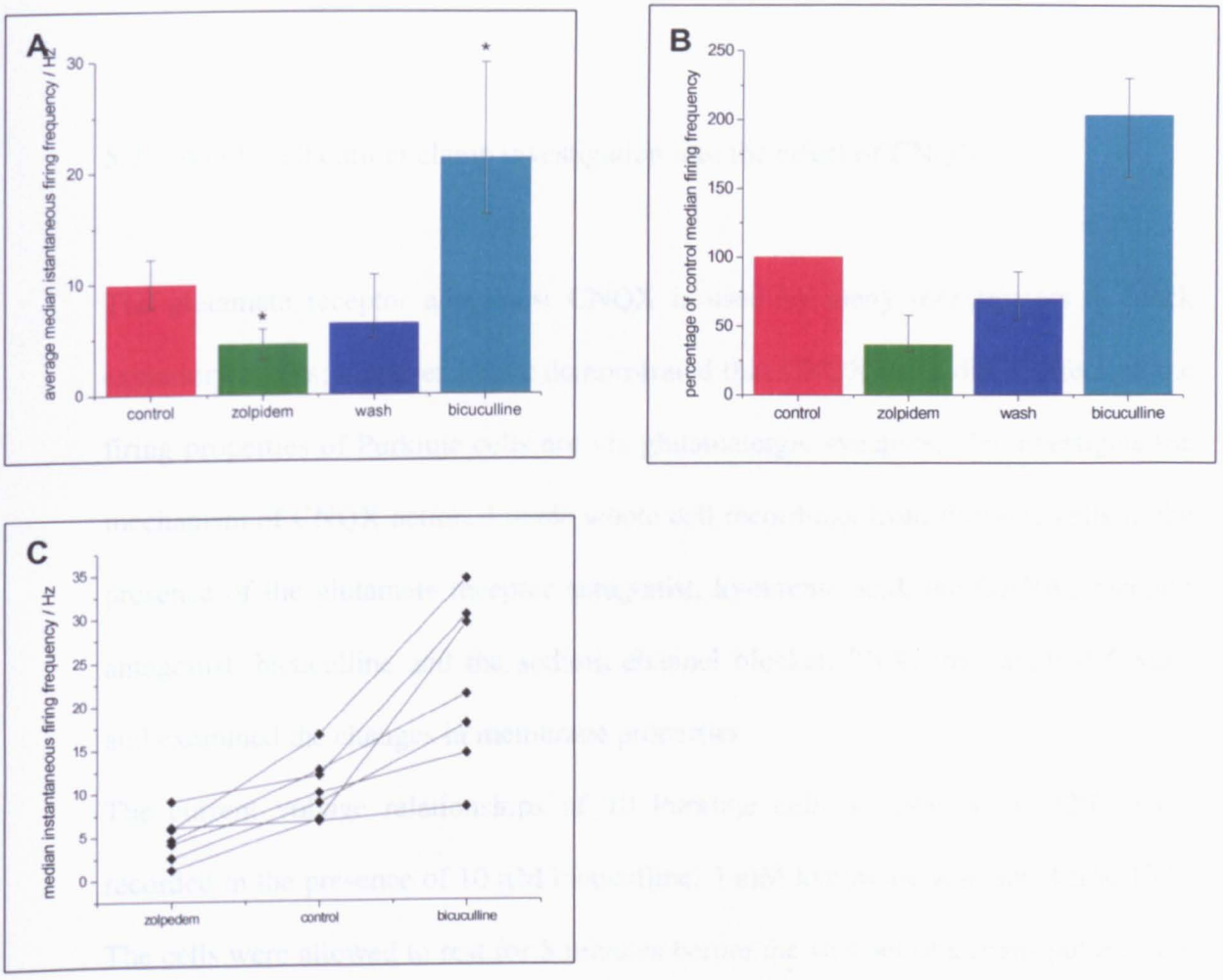

Figure 5.8 – Increasing the $GABA_A$ receptor affinity for GABA with zolpidem decreases Purkinje cell firing frequency. A-C – Application of 500 nM zolpidem significantly decreases Purkinje cell firing and this affect is reversed with washing and application of 10 μM bicuculine significantly increase Purkinje cell firing frequency (n = 9). * - $p<0.05$. Panels A and B shows absolute values, panels B shows values normalised to control values

weight to the hypothesis that the interneurones are acting to reduce the variability of Purkinje cell firing.

5.7 – Whole cell current clamp investigation into the effect of CNQX.

The glutamate receptor antagonist CNQX is used by many investigators to block excitatory events; however I have demonstrated that CNQX has a direct effect on the firing properties of Purkinje cells not via glutamatergic synapses. To investigate the mechanism of CNQX action, I made whole cell recordings from Purkinje cells in the presence of the glutamate receptor antagonist, kynurenic acid, the $GABA_A$ receptor antagonist, bicuculline and the sodium channel blocker, TTX, then applied CNQX and examined the changes in membrane properties.

The current voltage relationships of 10 Purkinje cells in lobe X, at 32°C, were recorded in the presence of 10 μM bicuculline, 5 mM kynurenic acid and 1 μM TTX. The cells were allowed to rest for 5 minutes before the first set of current pulses were applied, then after the application of 10 μM CNQX, another set of current steps was applied. CNQX significantly ($P<0.05$) depolarised the membrane potential (from -68.4 ± 1.8 to -66.9 ± 1.9 mV, figure 5.9A) but had little affect on the membrane resistance (63.2 ± 4.4 Vs 66.9 ± 1.9 MΩ; figure 5.9B). By plotting out the average membrane potential against injected current for both the control and the CNQX data a visual representation of the current voltage relationship can be obtained (figure 5.8C). The point where these two lines cross gives an estimate of the reversal potential for the ionic current which is affected by CNQX. Extrapolating the lines back gives an approximate reversal potential of ~ -135 mV, the closest calculated reversal potential

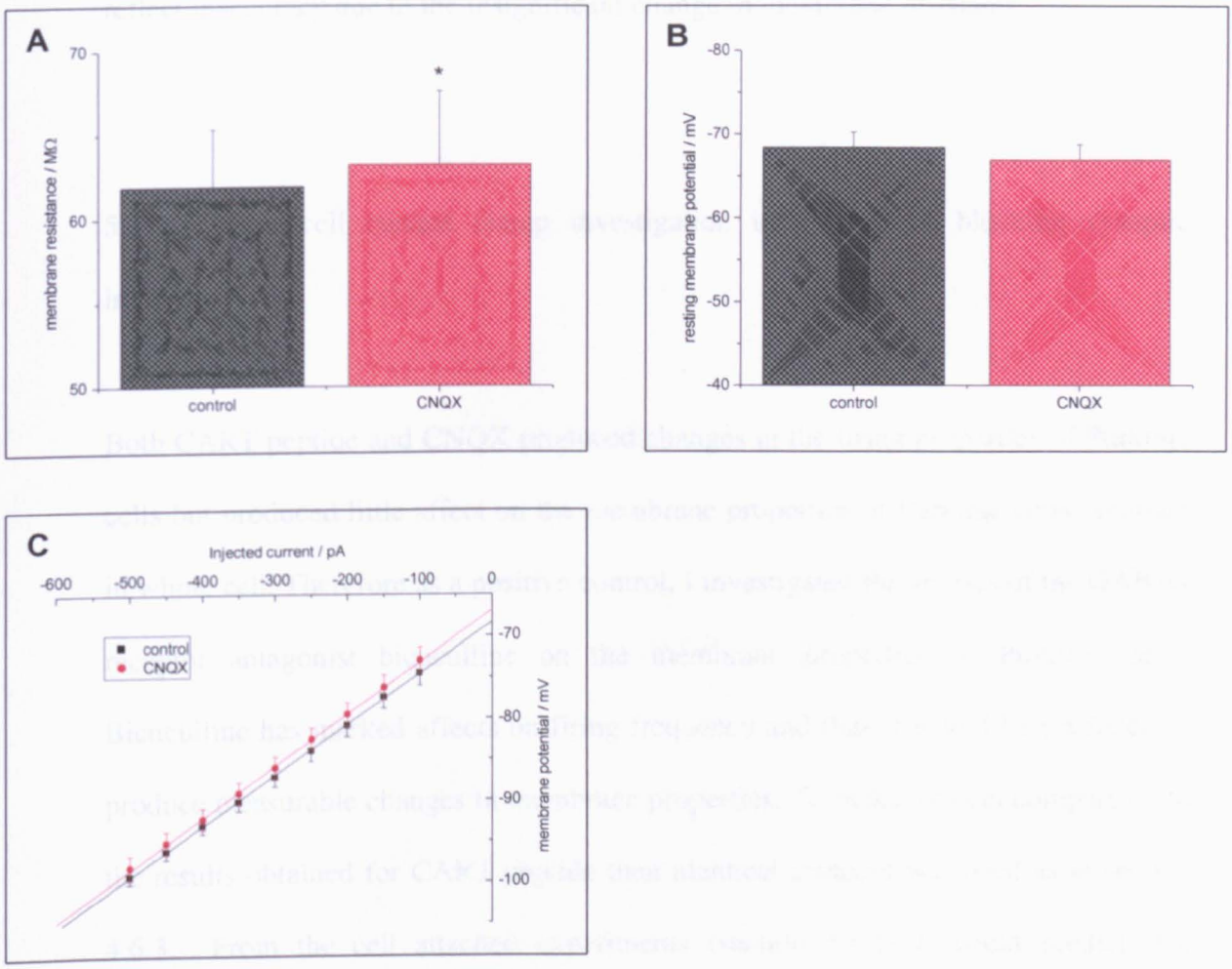

Figure 5.9 – CNQX (10 μM) has a direct effect on the membrane properties of Purkinje cells (n = 10. All recordings where made in the presence of 1 μM TTX, 10 μM bicuculline and 5 mM kynurenuc acid. A - Application of CNQX does not significantly alter the membrane resistance. B – Application of CNQX significantly increases the resting membrane potential. C – Plotting out the average current voltage relationships before and CNQX application. * - $p<0.05$.

to this is that for K^+ ions (-100 mV), so the CNQX effect may be mediated by closing or blocking a potassium channel. The differences between the reversal potentials may reflect inaccuracy due to the insignificant change in membrane resistance.

5.8 – Whole cell current clamp investigation into effect of blocking synaptic inhibition

Both CART peptide and CNQX produced changes in the firing properties of Purkinje cells but produced little affect on the membrane properties of Purkinje cells recorded in whole cell. Therefore as a positive control, I investigated the actions of the $GABA_A$ receptor antagonist bicuculline on the membrane properties of Purkinje cells. Bicuculline has marked affects on firing frequency and thus it would be predicted to produce measurable changes in membrane properties. To make a direct comparison to the results obtained for CART peptide then identical protocol was used as in section 4.6.3. From the cell attached experiments (section 5.4.1) I would predict that bicuculline would depolarise the Purkinje cell membrane, but in the protocol used the membrane potential is held at -75 mV. Simplistically, if the bicuculline was to depolarise the Purkinje cell membrane then you might expect that a larger holding current would be required to keep the cell at -75 mV, however if the depolarisation is limited to the dendrites then the amount of current required to hold the soma down at -75 mV may not change significantly. A similar case maybe be true of the membrane resistance, blocking the $GABA_A$ receptor may increase the membrane resistance if enough channels on the soma are open under control conditions, but if only a few

channels are open on the soma, or the channels that are open are in the distal dendrites then there may not be a significant change in the measured membrane resistance.

It is equally hard to predict what effect bicuculline will have on the excitability and firing threshold of the Purkinje cell.

The current voltage relationships of 9 Purkinje cells in lobe X at 32°C were recorded using a protocol identical to that used in section 4.6.3 with the application of 10 μM bicuculline and the results were compared to the control data acquired in section 4.6.3 (n = 24). The resting membrane potential was -76.1 ± 0.3 mV in bicuculline compared to -75.8 ± 0.2 mV in control (figure 5.10B), the holding current was -247.5 ± 33.5 pA in bicuculline compared to -333.8 ± 33.2 pA in control (figure 5.10C) and the membrane resistance was 35.8 ± 1.2 MΩ in bicuculline compared to 38.8 ± 1.8 MΩ in control (figure 5.9D); none of these values were significantly different.

There was a clear difference in the firing rate of the Purkinje cells in bicuculline compared to control (figure 5.11A). The excitability in bicuculline was 3.9 ± 0.6 Hz/mV compared to 2.8 ± 0.3 Hz/mV in control (figure 5.11B) and the firing threshold in bicuculline was -76.5 ± 1.9 mV as compared to -70.3 ± 1.6 mV in control (figure 5.11C). It is possible to extrapolate back the plots of firing rate against injected current, and the point at which they cross should be the reversal potential of the ion producing the bicuculline effect. The reversal potential estimated from the plots of firing against injected current was ~ 90 mV, which given the large variation in firing rate is in good agreement to the calculated Cl^- reversal potential.

It appears from these results that bicuculline is having it affect on firing by changing the properties of the dendrites, the decrease in inhibition is causing an increase, presumably, in the calcium type action potentials and/or an increase depolarisation, this translates into an increase in firing at the soma, without significant changes in the

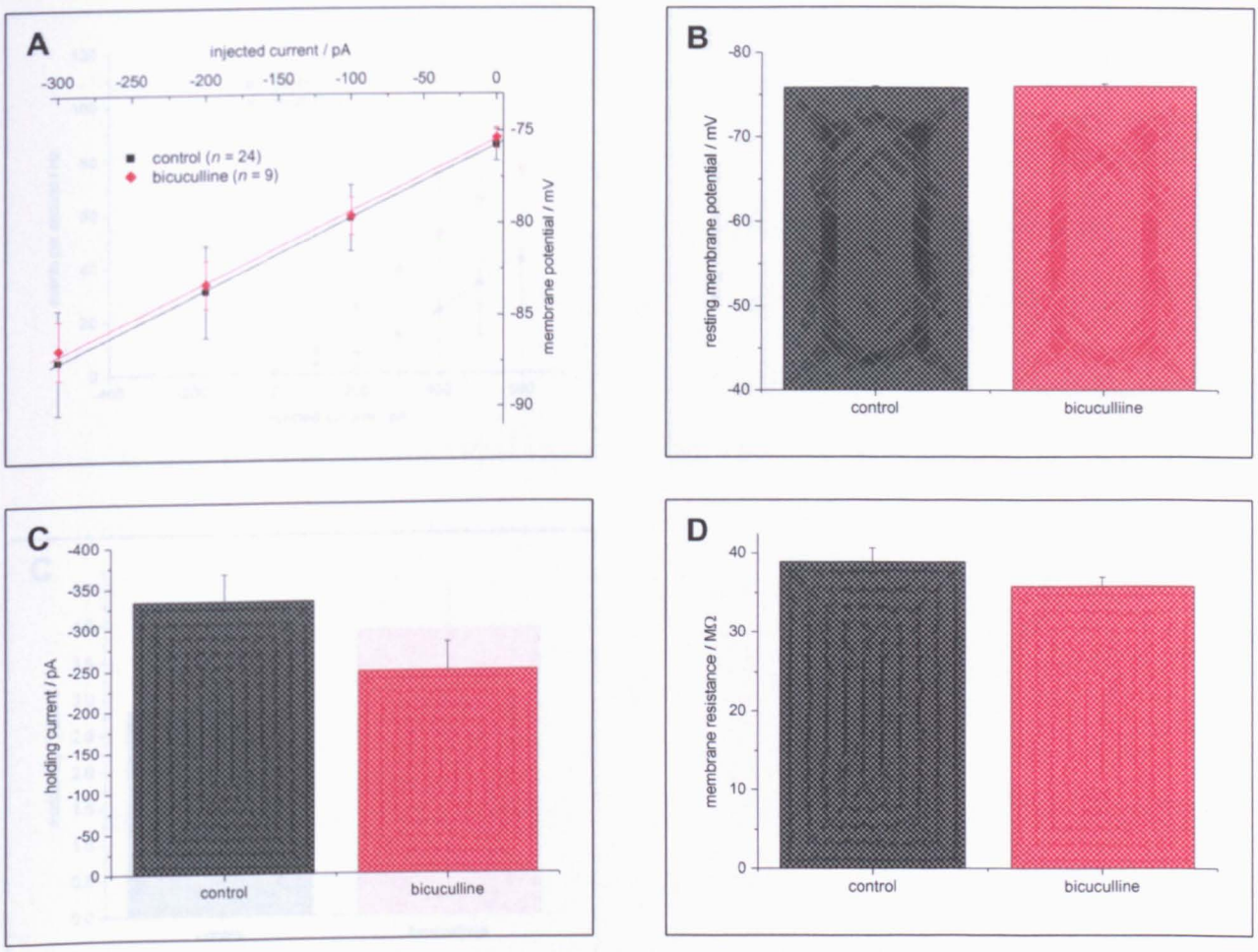

Figure 5.10 – Blocking the GABAergic transmission (with 10 μM bicuculline) does not significantly change the intrinsic electrical properties of the Purkinje cell membrane. Recording were made with membrane potential held at -75 mV. A – Plot of average current voltage relationship in control cells (n = 24) and in bicuculline (n = 9). There was no significant different in resting membrane potential (panel B), injected holidng current (panel C) or membrane resistance (panel C) between control and bicuculline cells.

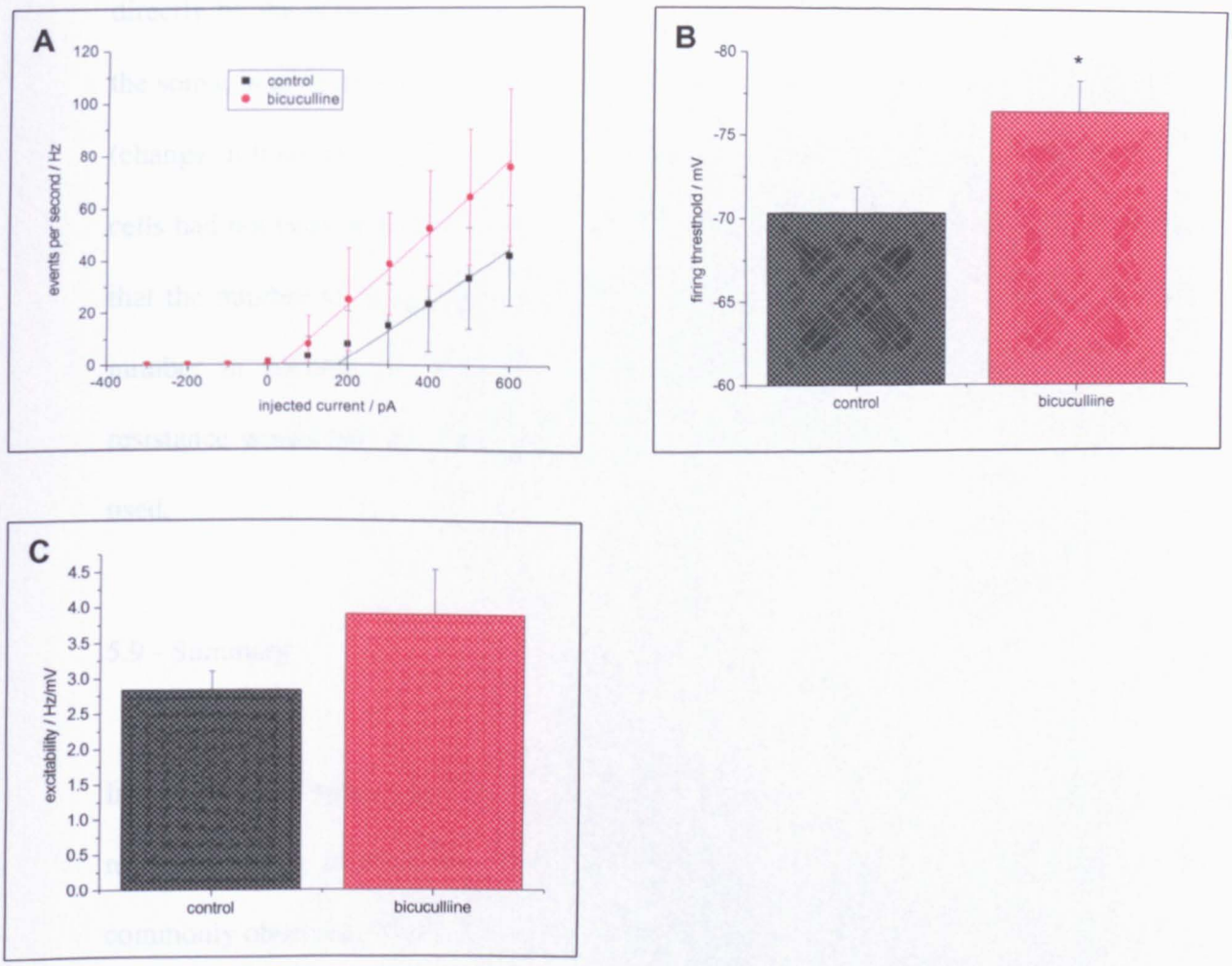

Figure 5.11 – Blocking the GABAergic transmission (with 10 μM bicuculline) does significantly change the intrinsic firing properties of Purkinje cells. Recording were made with membrane potential held at -75 mV. A – Plot of average current firing rate relationship in control cells (n = 24) and in bicuculline (n = 9). B – The threshold for firing is significantly lower in the presence of bicuculline. C – The excitability of the Purkinje cell is not significantly different in the presence of bicuculline. * - $p<0.05$.

membrane resistance. It is likely that this increase in firing at the soma will also be accompanied by a depolarisation, however because this depolarisation is being cause directly by the effect on bicuculline on ion channel present in the cell membrane of the soma, in my experiment on significant change in the holding current was observed (change in holding current would imply change in resting membrane potential if the cells had not been held at a constant membrane potential). Finally it is worth nothing that the number of cells which bicuculline was applied to was much fewer than the number in control, if could be possible that the excitability and/or membrane resistance would become significantly different if a larger sample of cells had been used.

5.9 - Summary

In this chapter I have tried to address a number of different questions. My method of recording firing of Purkinje cells gives agreement with the types of firing most commonly observed. In control conditions the majority of cells (86 %) fired tonically either continuously or with interspersed periods of quiescence. In the presence of synaptic blockers the majority of cells fired continuously without quiescence (46 %), but also showed trimodal behaviour (23 %) and sometimes fired high frequency bursts (type E, 31 %). These results are a little different from other investigators who report either all cells firing in the tonic or the trimodal firing modes. It is possible that other investigators do not report the type E pattern as they only distinguish patterns by measuring events per second. Using this measure, pattern E and patterns B/C cannot be distinguished. I have also shown that CART peptide does not change the type of firing pattern only the median firing frequency.

The observation that CNQX has a direct affect on, not only the firing, but the resting membrane potential is not a new observation for CNQX, but it is the first time it has been reported for Purkinje cells. Given that CNQX is commonly used to block AMPA/kainate receptors in the cerebellum, the additional direct effect of CNQX on Purkinje cells may complicate the interpretation of results. This is especially true in experiments where the firing rate is being measured, and under these conditions CNQX may not be an appropriate antagonist to use. It is still unclear how CNQX is having its effect, although my results are consistent with the closure of a potassium channel, thereby depolarising the cell and increasing the firing rate. The only way to confirm how the CNQX is affecting the firing of Purkinje cells is to block possible targets until the effect of CNQX is abolished.

Chapter 6 – Discussion

6.1 – Implications of location of CART peptide in cerebellum.

I have shown that CART peptide is expressed in a subset of climbing fibres innervating Purkinje cells in the vestibular cerebellum (lobes IX and X of the vermis and the paraflocculus). This observation leads to some obvious questions: What is the function of CART peptide in the vestibular cerebellum? And why is it only expressed in a subset of fibres? It is possible that CART peptide is associated with all areas of the vestibular system; in the same way that CART peptide is found at all levels of the HPA axis (Dun et al., 2006). However, to my knowledge, no-one has specifically examined the vestibular nuclei (in the brainstem) or the organs of the ear, for the presence of CART mRNA or CART peptide expression. If CART peptide is associated with all regions of the vestibular system, then why is the distribution not uniform across the vestibular cerebellum? Thus it seems unlikely that CART peptide is generally associated with the vestibular system, but instead serves a specific role in the vestibular cerebellum.

The banding of gene activity and peptide expression in zones across the cerebellum has been shown for many different genes and peptides (Oberdick et al., 1998), some of these have been implicated in cerebellar development for example: wingless-type MMTV integration site family genes (wnt) and engrailed (en) ((Millen et al., 1995). It may be that CART peptide is also involved in development, for example CART peptide may have a role in guiding climbing fibres to specific targets (Purkinje cells) and its presence in the adult cerebellum may serve to consolidate these connections. If this was the case then the direct electrophysiological effects I observed, may

represent only a minor action of CART peptide, the primary effect being synaptogenesis.

It is possible that the major role of CART peptide in the vestibular cerebellum is electrophysiological. If this was the case, why is there a banded distribution of CART peptide expression across the nodulus? It may be that the climbing fibres not expressing CART peptide express another, as of yet, unidentified neuropeptide, which serves a similar role to CART peptide. It is also possible that CART peptide plays a signalling role in climbing fibres that are part of specific pathways within the vestibular cerebellum.

There is another neuropeptide that is expressed in climbing fibres; corticotrophin releasing factor (CRF) (van den Dungen et al., 1988). CRF is expressed in the vestibular cerebellum and also has a banded distribution (Cummings, 1989). Thus it is possible that CRF and CART have similar roles in the vestibular cerebellum. However, CRF is also found in climbing fibres all over the cerebellum as well as in mossy fibres (Primus et al., 1997; Chen et al., 2000). I have been interested in whether CART and CRF are co-localised in the same climbing fibres or whether they represent different and distinct groups of climbing fibres. However the CRF antibodies were not very effective and did not label cerebellar slices.

The CART peptide knockout mouse does not show a phenotype typical of cerebella dysfunction and thus CART peptide signalling may play only a minor role in cerebellar function (Moffett et al., 2006). However there are no reports of locomotor tests such as the rotarod being carried out with the knockout mice and thus subtle defects in motor control may have been missed. It would be interesting to make electrophysiological recordings from the Purkinje cells in the vestibular cerebellum of

the CART knockout mice to see if there were any significant differences in their properties.

Future work

There are a number of experiments which could be carried out to further investigate the expression of CART peptide. For example single vestibular Purkinje cells could be filled (using a patch pipette) with either a fluorescent dye or with biocytin, and then examined for CART peptide and VGluT2 expression. This would provide elegant confirmation of my observation, that all the connections from a single climbing fibre contain CART peptide. It would also be interesting to fill the Purkinje cells from which the whole-cell recordings were made and then identify whether or not the cells were all innervated by CART peptide containing climbing fibres. My experiments suggest that not all Purkinje cells are innervated within the vestibular cerebellum and yet all respond to CART peptide. It maybe that some of the cells I included into my results did not respond to CART peptide, but it is not possible to separate responding cell and none responding cells. If I had been able to remove the cell which did not respond to CART peptide my observed effects may have been larger. I did add biocytin to my internal pipette solution, and then fixed and labelled the slices, but the biocytin filled Purkinje cells were not visible, presumably because the cells had died when the patch pipette was removed. Although filling Purkinje cells is usually a straight forward procedure, the long recording time (> 30 minutes) may have contributed to the loss of filled cells.

It would also be interesting to investigate how CART peptide containing fibres are localised with other structures in the cerebellum, for example with interneurones

(using antibody against GAD). Climbing fibres make contacts onto basket cells, so it may be that CART peptide is associated with these synapses. It is possible that CART peptide may modulates cholinergic or catecholaminergic synaptic transmission, in my experiments looking at firing rate I did not block either of these inputs. To investigate this one could look for association between acetylcholine containing fibres (using antibody against ChAT) or noreadrenaline/dopamine containing fibres (using antibody against tyrosine hydroxylase) and CART peptide containing climbing fibres. Further work, which would have been difficult for me to perform, but would be of considerable interest, is to examine CART peptide localisation using electron microscopy (gold particle immunolabelling). In particular, to confirm that CART peptide is present in LDCVs in climbing fibre terminals together with SSVs containing glutamate.

6.2 – A possible signalling role of CART peptide?

My experiments have shown that CART peptide has a small but significant effect on the firing rate of Purkinje cells in the vestibular cerebellum, probably by increasing a membrane conductance. CART peptide does not appear to modulate either the excitatory (glutamatergic) or inhibitory (GABAergic) inputs to Purkinje cells or modulate the induction of LTD. If CART peptide is released from climbing fibres it could modulate the output of the cerebellum (DCN cell firing) in two ways: Firstly, the increase in Purkinje cell simple spike firing leads to the increased inhibition of DCN neurones (as Purkinje cells release GABA). This would be interesting, as the general effect of climbing fibre discharge is to reduce the Purkinje cell-mediated

inhibition of neurones in the DCN because the AHP following a complex spike prevents simple spiking (McKay et al., 2007). If CART peptide release is produced by the high frequency stimulation of climbing fibres (as some other neuropeptides are (Stjärne, 1989)) then CART peptide could maintain simple spike firing which would counter the disinhibition of DCN neurones.

Sercondly, the extended AHP of the complex spikes is caused by the large depolarisation of the Purkinje cell dendrite; if CART peptide increased this depolarisation then it could increase the length of the complex spike AHP and therefore decrease the inhibition of DCN neurones. Functionally this could be important because both simple spikes and complex spikes are indistinguishable by the time they reach the Purkinje cell synapses in the DCN (Khaliq and Raman, 2005). If CART peptide is released under high frequency stimulation then it might act to further reduce the firing of simple spikes, compensating for the increase in complex spike frequency. Of course these hypothesises both rely on the assumption that CART peptide is released during high frequency activation of climbing fibres, and although this may be a reasonable assumption there is no direct evidence for it from the data. Work in our lab has been done to try and detect CART peptide release (using western blots from slice supernatant), but following trains of stimuli to vestibular climbing fibres no CART peptide could be detected (Wall, personal communication.

If CART peptide modulates cerebellar output what effect could this have on behaviour? How the Purkinje cells regulate balance is not fully understood, but I hypothesise that to correct posture, in order to maintain balance, would require the neurones of the DCN to fire action potentials to inform the motor centres to contract or relax particular muscles, and to inform higher brain areas of the expected change in

body position (Bear et al., 2007). To induce activity in the neurones of the DCN would require a reduction in the activity of Purkinje cells innervating them. Because CART peptide could either increase or decrease the simple spike firing rate of Purkinje cells, it is unclear that effect it has on balance. It would seem likely that its role is to somehow to compensate the output of the vestibular system in such a way to improve balance.

Future work

In my experiments, I examined the most obvious targets for CART peptide, but of course there are many things I did not investigate; these include the effect of CART peptide on LTP at the parallel fibre-Purkinje cell synapse (Hartell, 2002), the effect on DSI/DSE (Llano et al., 1991a; Kreitzer and Regehr, 2001), effects of CART peptide on intracellular signalling molecules, for example; calcium (Bird and Putney Jr., 2006), ERK/MAPK (Lakatos et al., 2005) or cAMP (Jones and Kuhar, 2005).

6.3 – Mechanism of CART peptides action.

The increase in firing rate observed after the application of CART peptide seems to be explained by the opening of a conductance, which depolarises the Purkinje cell. CART peptide has been shown to modulate ion channels, for example it inhibits L-type calcium channels in hippocampal neurones (Yermolaieva et al., 2001). However because Purkinje cells possess many different conductances active around the resting

membrane potential, it is not possible to say for definite which type of ion channel is modulated by CART peptide.

The work done by Wall and Spanswick (2004) suggests that CART peptide can directly depolarise or hyperpolarise sympathetic preganglionic neurones without affecting their membrane resistance. I propose that this effect is not a direct effect, but rather that CART peptide is modulating inhibitory interneruones and this is explained by the fact the effect of CART which they observe is blocked by the $GABA_A$ receptor antagonist bicuculline.

Future work

To further investigate which channels CART peptide modulates, I would like to repeat the whole-cell voltage clamp experiments looking at the current voltage relationships with the membrane potential fixed at -75 mV. In particular, I would investigate whether the effect of CART peptide persists in the presence of TTX, bicuculline and kynurenic acid (to block synaptic transmission). Although using this method, I would be unable to measure the reversal potential (because the two current voltage relationship plots would cross at -75 mV), there would be no run up during the recording. I would also repeat the experiment in the presence of cadmium to block calcium channels; this would tell us whether CART peptide modulates calcium channels (Lansman et al., 1986). Furthermore, it would be interesting to see if the effect of CART peptide was blocked by the $G_{i/o}$ inhibitor pertussis toxin, since CART peptide has been shown to signal via $G_{i/o}$ activation (Lakatos et al., 2005). The effects of CART peptide on Purkinje cells are small and thus finding the mechanism of action

is difficult. Therefore a better approach may be to identify the element on Purkinje cells that CART peptide binds to.

Identifying the CART peptide receptor

So far only one protein has been show to have a high affinity interaction with CART peptide, the SDHB mitochondrial protein (Mao et al., 2007), and further studies with this protein may identify the CART peptide binding domain and help identify possible binding motifs in GPCRs or other membrane bound proteins which may interact with CART peptide.

To investigate whether CART peptide binds to an extracellular receptor, a number of approaches could be taken. It may be possible to tag CART peptide (iodination or fluorescence), and then apply the fluorescent CART peptide construct to the cerebellum. Stimulation of neuropeptide receptors causes their internalisation, and thus if CART peptide binds to specific receptors, then the CART peptide will be taken up into cells together with the receptors and the cells will fluoresce. A similar mechanism has been described for substance P (Larsen et al., 1989). Because we know that CART peptide is only expressed in climbing fibres innervating Purkinje cells in the vestibular cerebellum, the other areas of the cerebellum could be used as a perfect negative control.

If CART peptide is not be internalised then another approach would be to use a ligand binding assay, competing radiolabelled CART with increasing concentrations of unlabelled CART peptide. Such an experiment would demonstrate that CART peptide specifically binds to a receptor-like element in the vestibular cerebellum and give

values for parameters such as B_{max} and K_d and this has been shows for CART peptide in dissociated hypothalamic neurons (Vicentic et al., 2005).

Whether CART peptide is internalised or not if might be useful to use the membrane-extract from the vestibular cerebellum and look for binding using immunoprecipitation (Playfair and Chain, 2005) with CART peptide and CART antibody (either in solution or fixed to a column), followed by some form of protein sequencing (Steen and Mann, 2004). This might succeed in identifying a receptor where other techniques have failed because of the smaller area of the brain reducing non-specific interactions. It could be that CART peptide binds to a membrane protein which could internalise the peptide and undergo a conformational change in which it no longer binds it. If this was the case then it might not be possible to find the protein by any binding studies, however if it was shown that CART peptide has such an interaction then a modified CART peptide in which internalisation was prohibited could be designed and the protein to which is binds could be identified.

It is possible that CART peptide does not have its effect by binding to a membrane protein, but rather by passing across the cell membrane and acting directly on an intracellular protein. Although this would represent a novel mechanism, there is some circumstantial evidence that this could occur: CART peptide passes freely across the blood-brain barrier and its rate of transfer is not self limiting suggesting it passes across by diffusion and not via an active transporter (Kastin and Akerstrom, 1999). CART peptide is predicted to have both positively and negatively charged areas on its surface, but this is was with only the core of the peptide and the free floating N-terminus could fold in such a way promote diffusion across a membrane (Ludvigsen et al., 2001).

The only identified protein to interact with CART is an intracellular protein associated with ATP generation in the mitochondrial (Mao et al., 2007); there are ion channels (examples ATP sensitive potassium channel; K_{ATP}) that respond to intracellular ATP and this could produce the observed increase in firing rate and decrease in membrane potential. K_{ATP} channels are found in Purkinje cells (Zhou et al., 1999b) and increases in ATP levels result in reduction of conductance of these channels, this has the effect of depolarising the cell. This does not fit with the observed decrease in membrane resistance after CART peptide application. Finally because the intracellular concentration of CART peptide required to effect SDHB was a hundred times lower than was used in my experiments only a small fraction of the CART peptide present would need to pass across the cell membrane to have its effects.

6.4 – General properties of Purkinje cells in the vestibular cerebellum

I observed that the Purkinje cells in lobe X (part of the vestibular cerebellum) had a median firing frequency of ~ 14 Hz and exhibited a number of different firing patterns. The firing frequency I observed is at the low end of the range that has been reported in literature (1-150 Hz) (Llinás and Sugimori, 1980a; Häusser and Clark, 1997; Womack and Khodakhah, 2002; Smith and Otis, 2003; Cerminara and Rawson, 2004; Loewenstein et al., 2005) and the different patterns I observed have also been reported for slice preparation, although none report observing the 7 patterns I outline in chapter 5.

It maybe that the firing rate/patterns in the vestibular cerebellum are slightly different from the rest of the cerebellum, and there is an indication of this from some

preliminary data. The median firing frequency outside lobe X was ~ 26 Hz which is significantly higher than in lobe X (14 Hz). This raises a number of interesting questions: Are the intrinsic properties of the Purkinje cells different in lobe X? Is there more synaptic inhibition in lobe X? What is the functional significance of the lower firing frequency? The first question could be addressed by recording the firing rates inside and outside of the lobe X in the presence of bicuculline to block GABAergic synapses.

The differences I observed between lobe X and the rest of the cerebellum maybe representative of the vestibular cerebellum in general, or may be particular to lobe X. It is difficult to make recordings from the other major part of the vestibular cerebellum, the paraflocculus, because its position makes it hard to remove without damaging and when removed the it is almost impossible to cut it in such as way as to not cut through the Purkinje cell dendrites.

My system of identifying firing patterns of Purkinje cells and grouping them into 7 different types (A, B1, B2, C1, C2, D and E) I think is the most comprehensive study of Purkinje cell firing patterns. Other investigators have used changes in firing patterns to show changes in Purkinje cell properties; a good example of this the *ducky* mutant (Barclay et al., 2001; Donato et al., 2006). Donato *et al* showed that a single or double copy of the mutant gene (an $\alpha 2\delta 2$ calcium channel subunit; is a model for absence epilepsy with spike-wave seizures and cerebellar ataxia) result in a decrease in the proportion of cells which show tonic firing, with no change in the proportion firing in bursts and an increase in the proportion of silent cells. They used 3 different classifications, including silent cells, but they do not look at the relative firing rates in the different firing patterns. I did occasionally have a silent Purkinje cell, and have tried to simulate them into firing by applying high potassium, but was never able to

stimulate them into firing. I believe that my classification system for firing rate is useful and that it is another tool to investigate how drugs or stimuli affect the firing of Purkinje cells. It is clear that different drugs can change the firing patterns as well as the firing rates. I believe that a single Purkinje cell cannot fire in all of the different firing patterns, meaning that the firing pattern do no just represent different degrees of depolarisation. However I did not do enough experiments to show how patterns are related to each other by increases or decreases in resting membrane potential. One way to investigate this would be to look at how the firing rate and firing pattern change using different concentration of extracellular potassium, some less than normal aSCF (hyperpolarising the membrane potential) and some higher (depolarising the membrane potential). This might be complicated by changes in synaptic input as well as direct changes to the Purkinje cell, but the experiment could be done in the presence and absence of synaptic blockers.

6.5 – Synaptic integration in the cerebellum.

The effect of blocking GABAergic transmission on the firing properties of the Purkinje cells is very pronounced, much more than blocking the glutamatergic inputs. This is not unexpected as the majority of the parallel fibres and all of the climbing fibres are cut in the parassagital slices. I believe that the large effect of the GABAergic interneurones on firing rate is more than just an artefact of the slice preparation, but suggest that it is the interneurones which relay the information from the granules cells to the Purkinje cells. In my experiments, I showed that decreasing the level of inhibition, using bicuculline, resulted in a large increase in the variance of

the firing rate of Purkinje cells, this is evidence that it is the activity of interneureones that sets the Purkinje cell firing rate within a narrow range. Increasing the level of inhibition, with zolpidem, did not result in a large change in the variance of firing rate, but significantly reduced the Purkinje cell firing rate. There are many more basket cells and stellate cells in the cerebellum than Purkinje cells, and they receive similar levels of synaptic inputs from the passing parallel fibres. If the interneurones respond to a similar degree to stimulation as the Purkinje cells do then activation of granules cells might be expected to create a net inhibition of Purkinje cells, this is not what is observed *in vivo* (Dunbar et al., 2004). However in order to see the typical beams of activation of parallel fibres a large stimulus has to be used and this may overcome the inhibition by interneurones. Also the *in vivo* experiments use calcium imaging (Dunbar et al., 2004) to visualise the activated Purkinje cells, however the calcium dyes only show changes in activity and this does not necessary have to come from parallel fibre-Purkinje cell activation, but could come from parallel fibre-interneurone activity.

This is of course just speculation, but the information coming into the cerebella cortex via the mossy fibres comes from very disparate nuclei in the CNS and is likely to result in a broad mild stimulation of parallel fibres rather than a focal stimulation. If Purkinje cells are both inhibited and excited by parallel fibres then when a single parallel fibre or group of parallel fibres are activated then they may not be a significantly net change in the level of Purkinje cell output along the axes of these parallel fibres. However the interneurones spread there axons and dendrites across several row and columns of Purkinje cells, so activation of multiple different parallel fibres could serves as way of addressing specific Purkinje cells by summing indirect inhibition from different parallel fibres. In addition if the normal function of the

Purkinje cell is to inhibit the neurones of the DCN then if mossy fibres provide an inhibitory rather than excitatory drive to Purkinje cells, this would result in a reduction of inhibition of neurones of the DCN, this is more in keeping with the idea that the cerebellum adjusts the motor movements to give a smooth and correct execution.

This is a difficult problem to address experimentally, but I believe that is can be investigated with some of the techniques I have used to investigate firing frequency. A key experiment which I did not have time to do was to look at the effect on firing by first blocking glutamate receptors with kynurenic acid, then block GABA receptors with bicuculline. This would give a measure of the relative importance of excitation of interneurones relative to the very low levels of direct excitation of Purkinje cells. I suspect that on its own kynurenic acid would have a small effect on the firing rate of Purkinje cells, much lower that effect of blocking inhibition, suggesting that the levels of parallel fibre activity are low and that the interneurone connection is a stronger connection. This could be further investigated by recording cell attached Purkinje cell activity with stimulation of granules cells to increase the baseline activity of parallel fibres, and then repeating the same drug application to see if during granule cell activation the relative importance of the direct excitation and indirect inhibition is the same. It would also be interesting to see record from Purkinje cells *in vivo* with the drug applications.

In investigating the effect of bicuculline as a positive control for my whole cell current clamp experiment investigating the current voltage relationship of Purkinje cells holding the membrane down at -75 mV, I believe I have found a new way of identifying the current carrying a change in neuronal behaviour using the firing rate against injected current. To my knowledge no-one else has used this method to look

for the reversal potential of the current causing a change in the firing properties, and certainly not in Purkinje cells where current clamp current voltage relationships are often difficult to interpret because of the multiple different channels open at the typical resting membrane potential of a Purkinje cell. If I had had time I would have liked to see if this technique could be used to identify the ions channels being affected by other drugs with known targets, such as zolpidem (chloride), ω-conotoxin (N-type calcium channels), ZD 7288 (I_h current block) and oubain (a sodium/potassium pump inhibitor).

6.5 – Importance of observations on CNQX.

CNQX has been used by many investigators to selectively block the AMPA receptors in the cerebellum. However, if experiments are done using current clamp, cell attached or field recording methods, the excitatory effects of CNQX on Purkinje cells could interfere with the interpretation of the experimental data. I was a little surprised that no-one has previously reported that CNQX has direct effects on Purkinje cells. Given that CNQX has been shown, in a number different areas of the brain, to directly excite cells (McBain et al., 1992; Brickley et al., 2001; Maccaferri and Dingledine, 2002; Hashimoto et al., 2004) if would seem that other blockers of glutamate receptor maybe more appropriate. If seems to me that for voltage clamp experiments, looking for example at EPSCs recorded in Purkinje cells, then CNQX is probably still an appropriate drug to use to show these events are glutamatergic. In experiments looking at intrinsic properties of Purkinje cells, CNQX is no longer an appropriate drug to use as it directly excites the Purkinje cell. If would be interesting to see if the

increase in Purkinje cell firing was also observed with other members of the CNQX family of drugs: 6,7-Dinitroquinoxaline-2,3-dione (DNQX) and 2,3-dihydroxy-6-nitro-7-sulfamoyl-benzo[f]quinoxaline-2,3-dione (NBQX). When trying to identify which channel CNQX is affecting I would have liked to have used the same method as I used to show the direct effect of CART peptide, only of course I would need first to block the glutamate receptors with kynurenic acid.

McBain *et al* (1992) showed that CNQX increases the spontaneous firing of CA3 hippocampal interneurones. The calculated the current voltage relationship of this current and showed that it had a reversal near to 0 mV, suggesting that the CNQX effect is caused by a mixed cation conductance. They also showed that both DNQX and NBQX that similar effects, but kynurenic acid did not have any effect. The concentrations of CNQX they used to show effects were an order of magnitude higher than I used, suggesting that I might have been applying the CNQX below its maximal effective concentration. It would be interesting to produce a concentration-response curve for CNQX on Purkinje cell firing rate.

References:

Aja S, Robinson BM, Mills KJ, Ladenheim EE, Moran TH (2002) Fourth ventricular CART reduces food and water intake and produces a conditioned taste aversion in rats. Behavioral neuroscience 116:918-921.

Armstrong DM, Rawson JA (1979) Activity patterns of cerebellar cortical neurones and climbing fibre afferents in the awake cat. The Journal of Physiology 289:425-448.

Asnicar MA, Smith DP, Yang DD, Heiman ML, Fox N, Chen Y-F, Hsiung HM, Köster A (2001) Absence of cocaine- and amphetamine-regulated transcript results in obesity in mice fed a high caloric diet. Endocrinology 142:4394-4400.

Atluri PP, Regehr WG (1996) Determinants of the Time Course of Facilitation at the Granule Cell to Purkinje Cell Synapse. The Journal of Neuroscience 16:5661-5671.

Bal T, McCormick DA (1997) Synchronized Oscillations in the Inferior Olive Are Controlled by the Hyperpolarization-Activated Cation Current Ih. The Journal of Neurophysiology 77:3145-3156.

Barbour B (1993) Synaptic currents evoked in purkinje cells by stimulating individual granule cells. Neuron 11:759-769.

Barclay J, Balaguero N, Mione M, Ackerman SL, Letts VA, Brodbeck J, Canti C, Meir A, Page KM, Kusumi K, PerezReyes E, Lander ES, Frankel WN, Gardiner RM, Dolphin AC, Rees M (2001) Ducky mouse phenotype of epilepsy and ataxia is associated with mutations in the Cacna2d2 gene and decreased calcium channel current in cerebellar Purkinje cells. The Journal of Neuroscience 21:6095-6104.

Barker RA, Barasi S (2003) Neuroscience at a Glance: Blackwell Publishing.

Barmack NH, Shojaku H (1992) Vestibularly induced slow oscillations in climbing fiber responses of Purkinje cells in the cerebellar nodulus of the rabbit. Neuroscience 50:1-5.

Barmack NH, Baughman RW, Eckenstein FP (1992a) Cholinergic innervation of the cerebellum of rat, rabbit, cat, and monkey as revealed by choline acetyltransferase activity and immunohistochemistry. The Journal of Comparative Neurology 317:233 - 249.

Barmack NH, Baughman RW, Eckenstein FP, Shojaku H (1992b) Secondary vestibular cholinergic projection to the cerebellum of rabbit and rat as revealed by choline acetyltransferase immunohistochemistry, retrograde and orthograde tracers. The Journal of Comparative Neurology 317:250 - 270.

Bear MF, Connors BW, Paradiso MA (2007) Neuroscience: Exploring the brain, 3 Edition: Lippincott William & Wilkins.

Bird GS, Putney Jr. JW (2006) Calcium. In: Basic Neurochemistry, 7 Edition (Siegel GJ, Albers RW, Brady ST, Price DL, eds), pp 379-390: Elsevier Academic Press.

Brenowitz SD, Regehr WG (2003) Calcium Dependence of Retrograde Inhibition by Endocannabinoids at Synapses onto Purkinje Cells. The Journal of Neuroscience 23:6373-6384.

Brickley SG, Farrant M, Swanson GT, Cull-Candy SG (2001) CNQX increases GABA-mediated synaptic transmission in the cerebellum by an

AMPA/kainate receptor-independent mechanism. Neuropharmacology 41:730-736.

Brown SP, Brenowitz SD, Regehr WG (2003) Brief presynaptic bursts evoke synapse-specific retrograde inhibition mediated by endogenous cannabinoids. Nature Neuroscience 6:1048-1057.

Campbell RC (1989) Statistics for Biologists, 3 Edition. Cambridge: Cambrige Univerisity Press.

Campuzano V, Montermini L, Molto MD, Pianese L, Cossee M, Cavalcanti F, Monros E, Rodius F, Duclos F, Monticelli A, Zara F, Canizares J, Koutnikova H, Bidichandani SI, Gellera C, Brice A, Trouillas P, de Michele G, Filla A, de Frutos R, Palau F, Patel PI, di Donato S, Mandel J-L, Cocozza S, Koenig M, Pandolfo M (1996) Friedreich's Ataxia: Autosomal Recessive Disease Caused by an Intronic GAA Triplet Repeat Expansion. Science 271:1423-1427.

Cavalcante JC, Bittencourt JC, Elias CF (2006) Female odors stimulate CART neurons in the ventral premammillary nucleus fo the male rat. Physiology and Behaviour 88:160-166.

Cerminara NL, Rawson JA (2004) Evidence that Climbing Fibers Control an Intrinsic Spike Generator in Cerebellar Purkinje Cells. The Journal of Neuroscience 24:4510-4517.

Chaki S, Kawashima N, Suzuki Y, Shimazaki T, Okuyama S (2003) Cocaine- and amphetamine-regulated transcript peptide produces anxiety-like behavior in rodents. European Journal of Pharmacology 464:49-54.

Chen Y, Brunson KL, Müller MB, Cariaga W, Baram TZ (2000) Immunocytochemical distribution of corticotropin-releasing hormone receptor type-1 (CRF1)-like immunoreactivity in the mouse brain: Light microscopy analysis using an antibody directed against the C-terminus. The Journal of Comparative Neurology 420:305 - 323.

Couceryro PR, Fitz T (2003) Production of recombinant CART peptides in *Escherichia coli.* with agonist and antagonist effects on food intake in rats. Protein Expression and Purification 32:185-193.

Couceyro PR, Koylu EO, Kuhar MJ (1997) Further studies on the anatomical distribution of CART by in situ hybridization. Journal of Chemical Neuroanatomy 12:229-241.

Couceyro PR, Evans C, McKinzie A, Mitchell D, Dube M, Hagshenas L, White FJ, Douglass J, Richards WG, Bannon AW (2005) Cocaine- and Amphetamine-Regulated Transcript (CART) Peptides Modulate the Locomotor and Motivational Properties of Psychostimulants. Journal of Pharmacology And Experimental Therapeutics 315:1091-1100.

Cummings SL (1989) Distribution of corticotropin-releasing factor in the cerebellum and precerebellar nuclei of the cat. The Journal of Comparative Neurology 289:657-675.

Dallvechia-Adams S, Smith Y, Kuhar MJ (2001) CART peptide-immunoreactive projection from the nucleus accumbens targets substantia nigra pars reticulata neurons in the rat. The Journal of Comparative Neurology 434:29-39.

Dallvechia-Adams S, Kuhar MJ, Smith Y (2002) Cocaine- and amphetamine-regulated transcript peptide projections in the ventral midbrain: Colocalization with gamma-aminobutyric acid, melanin-concentrating hormone, dynorphin, and synaptic interactions with dopamine neurons. The Journal of Comparative Neurology 448:360 - 372.

Damaj MI, Hunter RG, Martin BR, Kuhar MJ (2004) Intrathecal CART (55-102) enhances the spinal analgesic action of morphine in mice. Brain Research 1024:146-149.

Daniel H, Levenes C, Crépel F (1998) Cellular mechanisms of cerebellar LTD. Cerebellum 21:401-407.

Debiec J (2005) Peptides of love and fear: vasopressin and oxytocin modulate the integration of information in the amygdala. BioEssays 27:869 - 873.

Dey A, Xhu X, Carroll R, Turck CW, Stein J, Steiner DF (2003) Biological processing of the cocaine and amphetamine-regulated transcript precursors by prohormone convertase, PC2 and PC1/3. The Journal of Biological Chemistry 278:15007-15014.

Diana MA, Marty A (2004) Endocannabinoid-mediated short-term synaptic plasticity: depolarization-induced suppression of inhibition (DSI) and depolarization-induced suppression of excitation (DSE). British Journal of Pharmacology 142:9-19.

DiFrancesco D, Tortora P (1991) Direct activation of cardiac pacemaker channels by intracellular cyclic AMP. Nature 351:145 - 147.

Dolphin AC (2003) G Protein Modulation of Voltage-Gated Calcium Channels. Pharmacological Review 55:607-627.

Domingez G, Kuhar MJ (2004) Transcriptional regulation of the CART promoter in CATH.a cells. Brain Research Molecular Brain Research 126:22-29.

Dominguez G (2006) The CART gene: Structure and regulation. Peptide 27:1913-1918.

Dominguez G, Lakatos A, Kuhar MJ (2002) Characterization of the cocaine- and amphetamine-regulated transcript (CART) peptide gene promoter and its activation by a cyclic AMP-dependent signaling pathway in GH3 cells. Journal of Neurochemistry 80:885-893.

Donato R, Page KM, Koch D, Nieto-Rostro M, Foucault I, Davies A, Wilkinson T, Rees M, Edwards FA, Dolphin AC (2006) The ducky2J Mutation in Cacna2d2 Results in Reduced Spontaneous Purkinje Cell Activity and Altered Gene Expression. The Journal of Neuroscience 26:12576-12586.

Douglass J, Daoud S (1996) Characterization of the human cDNA and genomic DNA encoding CART: a cocaine- and amphetamine-regulated transcript. Gene 1996:241-245.

Douglass J, McKinzie AA, Couceyro P (1995) PCR differential display identifies a rat brain mRNA that is transcriptionally regulated by cocaine and amphetamine. The Journal of Neuroscience 15:2471-2481.

Duguid IC, Smart TG (2004) Retrograde activation of presynaptic NMDA receptors enhances GABA release at cerebellar interneuron–Purkinje cell synapses. Nature Neuroscience 7:525-533.

Dun SL, Chianca Jr. DA, Yang NJ, Chang J-K (2000) Differential expression of cocaine- and amphetamine-regulated transcript-immunoreactivity in the rat spinal preganglionic nuclei. Neuroscience Letters 294:143-146.

Dun SL, Castellino SJ, Yang J, Chang JK, Dun NJ (2001) Cocaine- and amphetamine-regulated transcript peptide-immunoreactivity in dorsal motor nucleus of the vagus neurons of immature rats. Developmental Brain Research 131:93-102.

Dun SL, Brailoiu GC, Yang J, Chang JK, Dun NJ (2006) Cocaine- and amphetamine-regulated transcript peptide and sympatho-adrenal axis. Peptide 27:1949-1955.

Dunbar RL, Chena G, Gao W, Reinert KC, Feddersen R, Ebner TJ (2004) Imaging parallel fiber and climbing fiber responses and their short-term interactions in the mouse cerebellar cortex in vivo. Neuroscience 126:213-227.

Dylag T, Kotlinska J, Rafalski P, Pachuta A, Silberring J (2006) The activity of CART peptide fragments. Peptide 27:1926-1933.

Ekblad E (2006) CART in the enteric nervous system. Peptide 27:2024-2030.

Fiez JA (1996) Cerebellar Contributions to Cognition. Neuron 16:13-15.

FitzGerald MJT, Folan-Curran J (2002) Clinical Neuroantatomy, 4th Edition: Saunders Ltd.

Fox EA, Gruol DL (1993) Corticotropin-releasing factor suppresses the afterhyperpolarization in cerebellar Purkinje neurons. 149 1.

Fushiki H, Barmack NH (1997) Topography and Reciprocal Activity of Cerebellar Purkinje Cells in the Uvula-Nodulus Modulated by Vestibular Stimulation. Journal of Physiology 78:3083-3094.

Hartell NA (2002) Parallel fiber plasticity. The Cerebellum 1:3-18.

Hashimoto K, Kano M (1998) Presynaptic origin of paired-pulse depression at climbing fibre-Purkinje cell synapses in the rat cerebellum. Journal of Physiology 506:391-405.

Hashimoto Y, Miyakawa H, Kudo Y, Inoue M (2004) 6-Cyan-7-Nitroquinoxaline-2,3-dione (CNQX) increase $GABA_A$ receptor-mediated spontaneous postsynaptic currents in the dentate granule cell of rat hippocampal slices. Neuroscience Letters 358:33-36.

Häusser M, Clark BA (1997) Tonic Synaptic Inhibition Modulates Neuronal Output Pattern and Spatiotemporal Synaptic Integration. Neuron 19:665-678.

Hille B (2001) Ion Channels of Excitable Membranes, 3 Edition: Sinauer Associates, Inc.

Hioki H, Fujiyama F, Taki K, Tomioka R, Furuta T, Tamamaki N, Kaneko T (2003) Differential distribution of vesicular glutamate transporters in the rat cerebellar cortex. Neuroscience 117:1-6.

Hubert GW, Kuhar MJ (2005) Colocalization of CART with substance P but not enkephalin in the rat nucleus accumbens. Brain Research 1050:8-14.

Hunter RG, Vicentic A, Rogge G, Kuhar MJ (2005) The effects of cocaine on CART expression in the rat nucleus accumbens: A possible role for corticosterone. European Journal of Pharmacology 517:45-50.

Hunter RG, Bellani R, Bloss E, Costa A, Romeo RD, McEwen BS (2007) Regulation of CART mRNA by stress and corticosteroids in the hippocampus and amygdala. Brain Research 1152:234-240.

Ito M (2000) Mechanisms of motor learning in the cerebellum. Brain Research 886:237-245.

Jaarsma D, Ruigrok TJ, Caffé R, Cozzari C, Levey AI, Mugnaini E, Voogd J (1997) Cholinergic innervation and receptors in the cerebellum. Progress in brain research 114:67-96.

Jaeger D, Bower JM (1994) Prolonged responses in rat cerebellar Purkinje cells following activation of the granule cell layer: an intracellular in vitro and in vivo investigation. Experiment Brain Research 100:200-214.

Jaeger D, Bower JM (1999) Synaptic Control of Spiking in Cerebellar Purkinje Cells: Dynamic Current Clamp Based on Model Conductances. The Journal of Neuroscience 19:6090-6101.

Jaworski JN, Kozel MA, Philpot KB, Kuhar MJ (2003) Intra-Accumbal Injection of CART (Cocaine-Amphetamine Regulated Transcript) Peptide Reduces

Cocaine-Induced Locomotor Activity. Journal of Pharmacology And Experimental Therapeutics 307:1038-1044.

Jones DC, Kuhar MJ (2005) CART expression in the rat nucleus accumbens is regulated by adenylyl cyclase and the cyclic-AMP/PKA second messenger system. Journal of Pharmacology and Experimental Therapeutics 317:454-461.

Kano M, Kano M, Maekawa K (1991) Binocular interaction and signal components of optokinetic responses of climbing fiber afferents in the cerebellar flocculus and nodulus of the pigmented rabbit. Neuroscience Research 12.

Kastin AJ, Akerstrom V (1999) Entry of CART into brain is rapid but not inhibited by excess CART or leptin. American Journal of Physiological - Endocrinology and Metabolism 277:E901-E904.

Keller PA, Compan V, Bockaert J, Giacobino J-P, Charnay Y, Bouras C, Assimacopoulos-Jeannet F (2005) Characterization and localization of cocaine- and amphetamine-regulated transcript (CART) binding sites. Peptide 27:1328-1334.

Khaliq ZM, Raman IM (2005) Axonal Propagation of Simple and Complex Spikes in Cerebellar Purkinje Neurons. The Journal of Neuroscience 25:454-463.

Kimmel HL, Gong W, Vechia SD, Hunter RG, Kuhar MJ (2000) Intra-Ventral Tegmental Area Injection of Rat Cocaine and Amphetamine-Regulated Transcript Peptide 55-102 Induces Locomotor Activity and Promotes Conditioned Place Preference. Journal of Pharmacology and Experimental Therapeutics 294:784-792.

Kimura S, Uchiyama S, Takahashi HE, Shibuki K (1998) cAMP-Dependent Long-Term Potentiation of Nitric Oxide Release from Cerebellar Parallel Fibers in Rats. The Journal of Neuroscience 18:8551-8558.

Kimura T, Sugimori M, Llinás RR (2005) Purkinje cell long-term depression is prevented by T-588, a neuroprotective compound that reduces cytosolic calcium release from intracellular stores. Proceedings of the National Academy of Sciences of the United States of America 102:17160-17165.

Kishimoto Y, Kano M (2006) Endogenous Cannabinoid Signaling through the CB1 Receptor Is Essential for Cerebellum-Dependent Discrete Motor Learning. The Journal of Neuroscience 26:8829-8837.

Koylu EO, Couceryro PR, Lambert PD, Kuhar MJ (1998) Cocaine- and amphetamine-regulated transcript peptide immunohistochemical localization in the rat brain. The Journal of Comparative Neurology 391:115-132.

Kreitzer AC, Regehr WG (2001) Retrograde Inhibition of Presynaptic Calcium Influx by Endogenous Cannabinoids at Excitatory Synapses onto Purkinje Cells. Neuron 29:717-727.

Kristensen P, Judge ME, Thim L, Ribel U, Christjansen KN, Wulff BS, Clausen JS, .Jensen PB, Madsen OD, Vrang N, Larsen PJ, Hastrup S (1998) Hypothalamic CART is a new anorectic peptide regulated by leptin. Nature 393:72-76.

Kuhar MJ, Jaworski JN, Hubert GW, Philpot KB, Dominguez G (2005) Cocaine- and Amphetamine-Regulated Transcript Peptides Play a Role in Drug Abuse and Are Potential Therapeutic Targets. American Association of Pharmaceutical Scientists Journal 7:259-265.

Kulik Á, Nakadate K, Nyíri G, Notomi T, Malitschek B, Bettler B, Shigemoto R (2002) Distinct localization of GABAB receptors relative to synaptic sites in the rat cerebellum and ventrobasal thalamus. European Journal of Neuroscience 15:291–307.

Lakatos A, Domingez G, Kuhar MJ (2002) CART promotor CRE site binds phosphorylated CREB. Molecular Brain Research 104:81-85.

Lakatos A, Prinster S, Vicentic A, Hall RA, Kuhar MJ (2005) Cocaine- and amphetamine-regulated transcript (CART) peptide activates the extracellular signal-regulated kinase (ERK) pathway in AtT20 cells via putative G-protein coupled receptors. Neuroscience Letters 384:198-202.

Lansman JB, Hess P, Tsien RW (1986) Blockade of current through single calcium channels by Cd2+, Mg2+, and Ca2+. Voltage and concentration dependence of calcium entry into the pore. The Journal of General Physiology 88:321-347.

Larsen P, Mikkelsen JD, Mau S, Saermark T (1989) Binding and internalization of a iodinated substance P analog by cultured anterior pituitary cells. Molecular and cellular endocrinology 65:91-101.

Larsen PJ, Vrang N, Petersen PC, Kristensen P (2000) Chronic Intracerebroventricular Administration of Recombinant CART(42–89) Peptide Inhibits Food Intake and Causes Weight Loss in Lean and Obese Zucker (fa/fa) Rats. Obesity 8:590-596.

Laurie DJ, Seeburg PH, Wisden W (1992) The distribution of 13 GABAA receptor subunit mRNAs in the rat brain. II. Olfactory bulb and cerebellum. The Journal of Neuroscience 12:1063-1076.

Lebrethon MC, Vandersmissen E, Gérard A, Parent AS, Bourguignon JP (2000) Cocaine and amphetamine-regulated-transcript peptide mediation of leptin stimulatory effect on the rat gonadotropin-releasing hormone pulse generator in vitro. Journal of Neuroendocrinology 12:383-385.

Leclerc N, Schwarting GA, Herrup K, Hawkes R, Yamamoto M (1992) Compartmentation in Mammalian Cerebellum: Zebrin II and P-Path Antibodies Define Three Classes of Sagittally Organized Bands of Purkinje Cells. Proceedings of the National Academy of Sciences of the United States of America 89:5006-5010.

Li C, Kim K, Nelson LS (1999) FMRFamide-related neuropeptide gene family in Caenorhabditis elegans. Brain Research 848:26-34.

Liang P, Pardee AB (1992) Differential display of eukaryotic messenger RNA by means of the polymerase chain reaction. Science 257:967-971.

Llano I, Leresche N, Marty A (1991a) Calcium entry increases the sensitivity of cerebellar Purkinje cells to applied GABA and decreases inhibitory synaptic currents. Neuron 6:565-574.

Llano I, Marty A, Armstrong CM, Konnerth A (1991b) Synaptic- and agonist-induced excitatory currents of Purkinje cells in rat cerebellar slices. The Journal of Physiology 434.

Llinás R, Sugimori M (1980a) Electrophysiological properties of in vitro Purkinje cell somata in mammalian cerebellar slices. Journal of Physiology 305:171-195.

Llinás R, Sugimori M (1980b) Electrophysiological properties of in vitro Purkinje cell dendrites in mammalian cerebellar slices. The Journal of Physiology 305:197-203.

Llinás RR, Lang EJ, Welch JB (1997) The cerebellum, LTD, and memory: alternative views. Learning and Memory 3:445-455.

Llinás RR, Walton KD, Lang EJ (2004) Cerebellum. In: The Synaptic Organization of the Brain, 5th Edition (Shepherd GM, ed), pp 271-309. Oxford: Oxford Univerisity Press.

Loewenstein Y, Mahon S, Chadderton P, Kitamura K, Sompolinsky H, Yarom Y, Häusser M (2005) Bistability of cerebellar Purkinje cells modulated by sensory stimulation. Nature Neuroscience 8:202-211.

Ludvigsen S, Thim L, Blom AM, Wulff BS (2001) Solution Structure of the Satiety Factor, CART, Reveals New Functionality of a Well-Known Fold. Biochemistry 40:9082 -9088.

Maccaferri G, Dingledine R (2002) Complex effect of CNQX on CA1 interneurons of the developing rat hippocampus. Neuropharmacology 43:523-529.

Macdonald RL, Olsen RW (1994) Gabaa Receptor Channels. Annual review of neuroscience 17:569-602.

Maejima T, Hashimoto K, Yoshida T, Aiba A, Kano M (2001) Presynaptic Inhibition Caused by Retrograde Signal from Metabotropic Glutamate to Cannabinoid Receptors. Neuron 31:463-475.

Maejima T, Oka S, Hashimotodani Y, Ohno-Shosaku T, Aiba A, Wu D, Waku K, Sugiura T, Kano M (2005) Synaptically Driven Endocannabinoid Release Requires Ca2+-Assisted Metabotropic Glutamate Receptor Subtype 1 to Phospholipase C {beta}4 Signaling Cascade in the Cerebellum. The Journal of Neuroscience 25:6826-6835.

Mains RE, Eipper BA (2006) Peptides. In: Basic Neurochemistry, 7 Edition (Siegel GJ, Albers RW, Brady ST, Price DL, eds), pp 317-332: Elsevier Academic Press.

Mao P, Ardeshiri A, Jacks R, Yang S, Hurn PD, Alkayed NJ (2007) Mitochondrial mechanism of neuroprotection by CART. European Journal of Neuroscience 26:624-632.

Mariani J, Changeux JP (1981) Ontogenesis of olivocerebellar relationships. I. Studies by intracellular recordings of the multiple innervation of Purkinje cells by climbing fibers in the developing rat cerebellum. Journal of Neuroscience 1:696-702.

Marie-Claire C, Laurendeau I, Canestrelli C, Cindie Courtina MV, Roques B, Noble F (2003) Fos but not Cart (cocaine and amphetamine regulated transcript) is overexpressed by several drugs of abuse: a comparative study using real-time quantitative polymerase chain reaction in rat brain. Neuroscience Letters 345:77-80.

Matsumura K, Tsuchihashi T, Abe I (2001) Central Human Cocaine- and Amphetamine-Regulated Transcript Peptide 55–102 Increases Arterial Pressure in Conscious Rabbits. Hypertension 38:1096-1100.

McBain CJ, Eaton JV, Brown T, Dingledine R (1992) CNQX increases spontaneous inhibitory inputs to CA3 pyramidal neurones in neonatal rat hippocamplal slices. Brain Research 592:255-260.

McKay BE, Engbers JDT, Mehaffey WH, Gordon GRJ, Molineux ML, Bains JS, Turner RW (2007) Climbing Fiber Discharge Regulates Cerebellar Functions by Controlling the Intrinsic Characteristics of Purkinje Cell Output. The Journal of Neurophysiology 97:2590-2604.

Menyhért J, Wittmann G, Lechan RM, Keller É, Liposits Z, Fekete C (2007) Cocaine- and Amphetamine-Regulated Transcript (CART) Is Colocalized with the Orexigenic Neuropeptide Y and Agouti-Related Protein and Absent from the Anorexigenic alpha-Melanocyte-Stimulating Hormone Neurons in the Infundibular Nucleus of the Human Hypothalamus. Endocrinology 148:4276-4281.

Millen KJ, Hui CC, Joyner AL (1995) A role for En-2 and other murine homologues of Drosophila segment polarity genes in regulating positional information in the developing cerebellum. Development 121:3935-3945.

Miraglia del Giudice E, Santoro N, Fiumani P, Dominguez G, Kuhar MJ, Perrone L (2006) Adolescents carrying a missense mutation in the CART gene exhibit increased anxiety and depression. Depression and Anxiety 23:90 - 92.

Mittmann W, Häusser M (2007) Linking Synaptic Plasticity and Spike Output at Excitatory and Inhibitory Synapses onto Cerebellar Purkinje Cells. The Journal of Neuroscience 27:5559-5570.

Mittmann W, Koch U, Häusser M (2005) Feed-forward inhibition shapes the spike output of cerebellar Purkinje cells. The Journal of Physiology 563:369-378.

Miyata M, Okada D, Kano KH, Ito M (1999) Corticotropin-Releasing Factor Plays a Permissive Role in Cerebellar Long-Term Depression. Neuron 22:763-775.

Moffett M, Stanek L, Harley J, Rogge G, Asnicar M, Hsiung H, Kuhar M (2006) Studies of cocaine- and amphetamine-regulated transcript (CART) knockout mice. Peptide 27:2037-2045.

O'Hearn E, Molliver ME (1993) Degeneration of purkinje cells in parasagittal zones of the cerebellar vermis after treatment with ibogaine or harmaline. Neuroscience 55:303-310.

Oberdick J, Baader SL, Schilling K (1998) From zebra stripes to postal zones: deciphering patterns of gene expression in the cerebellum. Cerebellum 21:383-390.

Ohsawa M, Dun SL, Tseng LF, Chang J-K, Dun NJ (2000) Decrease of hindpaw withdrawal latency by cocaine- and amphetamine-regulated transcript peptide to the mouse spinal cord. European Journal of Pharmacology 399:165-169.

Olschowka JA, O'Donohue TL, Mueller GP, Jacobowitz DM (1982) The distribution of corticotropin releasing factor-like immunoreactive neurons in rat brain. Peptide 3:995-1015.

Paxinos G (2004) The Rat Nervous System, 3rd Edition. New York: Acedemic Press.

Pearce JMS (2004) Friedreich's ataxia. Journal of Neurology Neurosurgery and Psychiatry 75.

Perkel DJ, Hestrin S, Sah P, Nicoll RA (1990) Excitatory Synaptic Currents in Purkinje Cells. Proceedings Biological sciences / The Royal Society 241:116-121.

Philpot KB, Smith Y (2006) CART peptide and the mesolimbic dopamine system. Peptide 27:1987-1992.

Playfair JHL, Chain B (2005) Immunology at a Glance (At a Glance), 8th rev Edition: Blackwell Publishing.

Primus RJ, Yevich E, Baltazar C, Gallager DW (1997) Autoradiographic Localization of CRF1 and CRF2 Binding Sites in Adult Rat Brain. Neuropsychopharmacology 17:308-316.

Raman IM, Bean BP (1997) Resurgent Sodium Current and Action Potential Formation in Dissociated Cerebellar Purkinje Neurons. The Journal of Neuroscience 17:4517-4526.

Raman IM, Bean BP (1999) Ionic Currents Underlying Spontaneous Action Potentials in Isolated Cerebellar Purkinje Neurons. The Journal of Neuroscience 19:1663-1674.

Risold PY, Bernard-Franchi G, Collard C, Jacquemard C, La Roche A, Griffond B (2006) Ontogenetic expression of CART-peptides in the central nervous system and the periphery: A possible neurotrophic role? Peptide 27:1938-1941.

Robinson FR (1995) Role of the cerebellum in movement control and adaptation. Current Opinion in Neurobiology 5:755-762.

Schmolesky MT, Ruiter MMD, Zeeuw CID, Hansel C (2007) The neuropeptide corticotropin-releasing factor regulates excitatory transmission and plasticity at the climbing fibre-Purkinje cell synapse. European Journal of Neuroscience 25:1460-1466.

Seidah NG, Chrétien M (1999) Proprotein and prohormone convertases: a family of subtilases generating diverse bioactive polypeptides. Brain Research 848:45-62.

Smith SL, Otis TS (2003) Persistent Changes in Spontaneous Firing of Purkinje Neurons Triggered by the Nitric Oxide Signaling Cascade. The Journal of Neuroscience 23:367-372.

Smith SM, Vaughan JM, Donaldson CJ, Ferandez RE, Li C, Chen A, Vale WW (2006) Cocaine- and amphetamine-regulated transcript is localized in pituitary lactotropes and is regulated during lactation. Endocrinology 147:1213-1223.

Smith Y, Koylu EO, Couceyro P, Kuhar MJ (1997) Ultrastructural localization of CART (cocaine- and amphetamine-regulated transcript) peptides in the nucleus accumbens of monkeys. Synapse 27:90 - 94.

Spiess J, Villarreal J, Vale W (1981) Isolation and sequence analysis of a somatostatin-like polypeptide from ovine hypothalamus. Biochemistry 20:1982-1988.

Stanek LM (2006) Cocaine- and amphetamine regulated transcript (CART) and anxiety. Peptide 27:2005-2011.

Stanley SA, Murphy KG, Bewick GA, Kong WM, Opacka-Juffry J, Gardiner JV, Ghatei M, Small CJ, Bloom SR (2004) Regulation of rat pituitary cocaine- and amphetamine-regulated transcript (CART) by CRH and glucocorticoids. American Journal of Physiological - Endocrinology and Metabolism 287.

Stanley SA, Small CJ, Murphy KG, Rayes E, Abbott CR, Seal LJ, Morgan DGA, Sunter D, Dakin CL, Kim MS, Hunter R, Kuhar M, Ghatei MA, Bloom SR (2001) Actions of cocaine- and amphetamine-regulated transcript (CART) peptide on regulation of appetite and hypothalamo–pituitary axes in vitro and in vivo in male rats. Brain Research 893:186-194.

Steen H, Mann M (2004) The abc's (and xyz's) of peptide sequencing. Nature Reviews Molecular Cell Biology 5:699-711.

Stjärne L (1989) Basic mechanisms and local modulation of nerve impulse-induced secretion of neurotransmitters from individual sympathetic nerve varicosities. Reviews of physiology, biochemistry and pharmacology 112:1-137.

Swensen AM, Bean BP (2003) Ionic Mechanisms of Burst Firing in Dissociated Purkinje Neurons. The Journal of Neuroscience 23:9650-9663.

Takayasu Y, Iino M, Ozawa S (2004) Roles of glutamate transporters in shaping excitatory synaptic currents in cerebellar Purkinje cells. European Journal of Neuroscience 19:1285-1295.

Takayasu Y, Iino M, Furuya N, Ozawa S (2003) Muscarine-Induced Increase in Frequency of Spontaneous EPSCs in Purkinje Cells in the Vestibulo-Cerebellum of the Rat. The Journal of Neuroscience 23:6200-6208.

Tang W-X, Fasulo WH, Mash DC, Hemby SE (2003) Molecular profiling of midbrain dopamine regions in cocaine overdose victims. Journal of Neurochemistry 85:911-924.

Thim L, Neilson PF, Judge ME, Anderson AS, Diers I, Egel-Mitani M, Hastrup S (1998) Purification and characterisation of a new hypothalamic satiety peptide,

cocaine and amphetamine regulated transcript (CART), produced in yeast. FEBS letters 428:263-268.

Udo M, Matsukawa K, Kamei H, Minoda K, Oda Y (1981) Simple and complex spike activities of purkinje cells during locomotion in the cerebellar vermal zones of decerebrate cats. Experiment Brain Research 41:292-300.

van den Dungen HM, Groenewegan HJ, Tilders FJH, Schoemaker J (1988) Immunoreactive Corticotropin Releasing Factor in Adult and Developing Rat Cerebellum: its Presence in Climbing and Mossy Fibres. Journal of Chemical Neuroanatomy 1:339-349.

Vicentic A (2006) CART peptide diurnal variations in blood and brain. Peptide 27:1942-1948.

Vicentic A, Lakatos A, Kuhar MJ (2005) CART (cocaine- and amphetamine-regulated transcript) peptide receptors: Specific binding in AtT20 cells. European Journal of Pharmacology 528:188-189.

Vicentic A, Lakatos A, Jones D (2006) The CART receptors: Background and recent advances. Peptide 27:1934-1937.

Vicentic A, Dominguez G, Hunter RG, Philpot K, Wilson M, Kuhar MJ (2004) Cocaine- and Amphetamine-Regulated Transcript Peptide Levels in Blood Exhibit a Diurnal Rhythm: Regulation by Glucocorticoids. Endocrinology 145:4119-4124.

Vrang N, Tang-Christensen M, Larsen PJ, Kristensen P (1999) Recombinant CART peptide induces c-Fos expression in central areas involved in control of feeding behaviour. Brain Research 818:499-509.

Vrang N, Larsen PJ, Kristensen P, Tang-Christensen M (2000) Central Administration of Cocaine-Amphetamine-Regulated Transcript Activates Hypothalamic Neuroendocrine Neurons in the Rat. Endocrinology 141:794-801.

Vrang NC, Larsen PJ, Kristensen P (2002) Cocaine-amphetamine regulated transcript (CART) expression is not regulated by amphetamine. NeuroReport 13:1215-1218.

Wall MJ (2005) Alterations in GABAA receptor occupancy occur during the postnatal development of rat Purkinje cell but not granule cell synapses. Neuropharmacology 49:596-609.

Wall MJ, Spanswick D (2004) Heterogeneous actions of cocaine and amphetamine regulated transcript (CART) peptides on rat sympathetic preganglionic neurones in vitro. In: The Physiology Society Meeting. King's College, London.

Wierup N, Sundler F (2006) CART is a novel islet reguatory peptide. Peptide 27:2031-2036.

Wierup N, Kuhar M, Nilsson BO, Mulder H, Ekblad E, Sundler F (2004) Cocaine- and Amphetamine-regulated Transcript (CART) Is Expressed in Several Islet Cell Types During Rat Development. Journal of Histochemistry and Cytochemistry 52:169-177.

Wierup N, Richards WG, Bannon AW, Kuhar MJ, Ahrén B, Sundler F (2005) CART knock out mice have impaired insulin secretion and glucose intolerance, altered beta cell morphology and increased body weight. Regulatory Peptides 129:203-211.

Williams SR, Christensen SR, Stuart GJ, Häusser M (2002) Membrane potential bistability is controlled by the hyperpolarization-activated current IH in rat cerebellar Purkinje neurons in vitro. Journal of Physiology 539:469-483.

Wilson RI, Nicoll RA (2002) Endocannabinoid Signaling in the Brain. Science 296:678-682.

Wiser AK, Andreasen NC, O'Leary DS, Watkins GL, Boles Ponto LL, Hichwa R (1998) Dysfunctional cortico-cerebellar circuits cause 'cognitive dysmetria' in schizophrenia. NeuroReport 9:1895-1899.

Womack M, Khodakhah K (2002) Active Contribution of Dendrites to the Tonic and Trimodal Patterns of Activity in Cerebellar Purkinje Neurons. The Journal of Neuroscience 22:10603-10612.

Womack MD, Khodakhah K (2004) Dendritic Control of Spontaneous Bursting in Cerebellar Purkinje Cells. The Journal of Neuroscience 24:3511-3521.

Xiong G, Matsushita M (2000) Connections of Purkinje cell axons of lobule X with vestibulocerebellar neurons projecting to lobule X or IX in the rat. Experiment Brain Research 133:219-228.

Xu Y, Zhang W, Klaus J, Young J, Koerner I, Sheldahl LC, Hurn PD, Martínez-Murillo F, Alkayed NJ (2006) Role of cocaine- and amphetamine-regulated transcript in estradiol-mediated neuroprotection. Proceedings of the National Academy of Sciences of the United States of America 103:14489-14494.

Yanik T, Dominguez G, Kuhar MJ, Giudice EMD, Loh YP (2006) The Leu34Phe ProCART mutation leads to cocaine- and amphetamine-regulated transcript (CART) deficiency: A possible cause for obesity in humans. Endocrinology 147:39-43.

Yermolaieva O, Chen J, Couceryro PR, Hoshi T (2001) Cocaine- and amphetamine-regulated transcript peptide modulation of voltage-gated Ca^{2+} signaling in hippocampal neurons. The Journal of Neuroscience 21:7474-7480.

Yi BA, Minor Jr. DL, Lin Y-F, Jan YN, Jan LY (2001) Controlling potassium channel activities: Interplay between the membrane and intracellular factors. Proceedings of the National Academy of Sciences of the United States of America 98:11016-11023.

Yoshida T, Hashimoto K, Zimmer A, Maejima T, Araishi K, Kano M (2002) The Cannabinoid CB1 Receptor Mediates Retrograde Signals for Depolarization-Induced Suppression of Inhibition in Cerebellar Purkinje Cells. The Journal of Neuroscience 22:1690-1697.

Zhou A, Webb G, Zhu X, Steiner DF (1999a) Proteolytic Processing in the Secretory Pathway. Journal of Biological Chemistry 274:20745-20748.

Zhou M, Tanaka O, Sekiguchi M, Sakabe K, Anzai M, Izumida I, Inoue T, Kawahara K, Abe H (1999b) Localization of the ATP-sensitive potassium channel subunit (Kir6.1/uKATP-1) in rat brain. Molecular Brain Research 74:15-25.

Appendix 1 – Worked example of Wilcoxen t-test

Data taken from section 4.2.3; change of median instantaneous firing frequency with application of 100 nM CART peptide at room temperature.

control	CART
32.47	35.21
4.13	4.71
6.79	7.43
4.90	4.69
13.89	19.08
3.43	3.75
7.58	8.91
3.35	2.73
2.52	3.06
13.51	15.15

25%	3.61	3.99
median	5.85	6.07
75%	12.03	13.59

A	B	B-A	R(+)	R(-)
3.349	2.734	-0.614		5
4.902	4.690	-0.212		1
3.429	3.751	0.322	2	
2.519	3.063	0.544	3	
4.132	4.706	0.574	4	
6.793	7.429	0.636	6	
7.576	8.909	1.333	7	
13.514	15.152	1.638	8	
32.468	35.211	2.744	9	
13.889	19.084	5.195	10	
		sum=	49	6

n=	10
5% significance level	8
z=	2.1915

The smallest sum of ranks was 6 which is less than the 5 % confidence level, therefore the null hypothesis (groups A and B are the same) is rejected. Alternatively using the z value; the 5 % confidence level is $z>1.960$, 1 % confidence level is $z>2.576$, therefore $p<0.05$ that groups A and B are the same.